LOCKHEED MARTIN ENERGY RESEARCH LIBRARIES

3 4456 0515109 1

ORNL-5021

Cy 79

Theoretical and Experimental Stress Analyses of ORNL Thin-Shell Cylinder-to-Cylinder Model 2

R. C. Gwaltney
S. E. Bolt
J. W. Bryson

OAK RIDGE NATIONAL LABORATORY
CENTRAL RESEARCH LIBRARY
DOCUMENT COLLECTION
LIBRARY LOAN COPY
DO NOT TRANSFER TO ANOTHER PERSON
If you wish someone else to see this document, send in name with document and the library will arrange a loan.

OAK RIDGE NATIONAL LABORATORY
OPERATED BY UNION CARBIDE CORPORATION • FOR THE U.S. ATOMIC ENERGY COMMISSION

Printed in the United States of America. Available from
National Technical Information Service
U.S. Department of Commerce
5285 Port Royal Road, Springfield, Virginia 22161
Price: Printed Copy $7.60; Microfiche $2.25

This report was prepared as an account of work sponsored by the United States Government. Neither the United States nor the Energy Research and Development Administration, nor any of their employees, nor any of their contractors, subcontractors, or their employees, makes any warranty, express or implied, or assumes any legal liability or responsibility for the accuracy, completeness or usefulness of any information, apparatus, product or process disclosed, or represents that its use would not infringe privately owned rights.

ORNL-5021
NRC-1, -5

Contract No. W-7405-eng-26

Reactor Division

THEORETICAL AND EXPERIMENTAL STRESS ANALYSES OF ORNL THIN-SHELL CYLINDER-TO-CYLINDER MODEL 2

R. C. Gwaltney S. E. Bolt
J. W. Bryson

OCTOBER 1975

OAK RIDGE NATIONAL LABORATORY
Oak Ridge, Tennessee 37830
operated by
UNION CARBIDE CORPORATION
for the
U.S. ENERGY RESEARCH AND DEVELOPMENT ADMINISTRATION

LOCKHEED MARTIN ENERGY RESEARCH LIBRARIES
3 4456 0515109 1

CONTENTS

Page

ABSTRACT 1
1. INTRODUCTION 2
2. EXPERIMENTAL ANALYSIS 5
2.1 Model Construction 6
2.2 Strain-Gage Layout 6
2.3 Test Description 8
2.4 Data Acquisition and Reduction 12
3. FINITE-ELEMENT ANALYSIS 12
3.1 Background 12
3.2 Finite-Element Method 14
3.3 Finite-Element Idealization of Model 19
4. COMPARISON OF THEORY AND EXPERIMENT 21
4.1 Internal Pressure 22
4.2 Out-of-Plane Moment Loading, M_{XN}, on Nozzle 26
4.3 Torsional Moment Loading, M_{YN}, on Nozzle 28
4.4 In-Plane Moment Loading, M_{ZN}, on Nozzle 28
4.5 In-Plane Force, F_{XN}, on Nozzle 37
4.6 Axial Force, F_{YN}, on Nozzle 37
4.7 Out-of-Plane Force, F_{ZN}, on Nozzle 44
4.8 Torsional Moment Loading, M_{XC}, on Cylinder 44
4.9 Out-of-Plane Moment Loading, M_{YC}, on Cylinder 44
4.10 In-Plane Moment Loading, M_{ZC}, on Cylinder 54
4.11 Axial Force, F_{XC}, on Cylinder 54
4.12 In-Plane Force, F_{YC}, on Cylinder 54
4.13 Out-of-Plane Force, F_{ZC}, on Cylinder 64
4.14 Out-of-Plane Moment, M_{XN}, on Nozzle with Restraints 64
4.15 In-Plane Moment, M_{ZN}, on Nozzle with Restraints ... 71
4.16 Axial Force, F_{YN}, on Nozzle with Restraints 71
5. CONCLUSIONS 71
ACKNOWLEDGMENTS 80
REFERENCES 80
APPENDIX. TABULATION OF EXPERIMENTAL DATA 83

THEORETICAL AND EXPERIMENTAL STRESS ANALYSES OF ORNL THIN-SHELL CYLINDER-TO-CYLINDER MODEL 2*

R. C. Gwaltney S. E. Bolt
J. W. Bryson

ABSTRACT

Model 2 in a series of four thin-shell cylinder-to-cylinder models was tested, and the experimentally determined elastic stress distributions were compared with theoretical predictions obtained from a thin-shell finite-element analysis. The models in the series are idealized thin-shell structures consisting of two circular cylindrical shells intersecting at right angles. There are no transitions, reinforcements, or fillets in the junction region. The series of model tests serves two basic purposes: (1) the experimental data provide design information directly applicable to nozzles in cylindrical vessels, and (2) the idealized models serve a basic need for test results for use in developing and evaluating theoretical analyses applicable to nozzles in cylindrical vessels and to thin piping tees.

Both the cylinder and the nozzle of model 2 had outside diameters of 10 in., giving a d_o/D_o ratio of 1.0, and both had outside diameter/thickness ratios of 100. Sixteen separate loading cases in which one end of the cylinder was rigidly held were analyzed. An internal pressure loading, three mutually perpendicular force components, and three mutually perpendicular moment components were individually applied at the free end of the cylinder and at the end of the nozzle. In addition to these 13 loadings, 3 additional loads were applied to the nozzle (in-plane bending moment, out-of-plane bending moment, and axial force) with the free end of the cylinder restrained. The experimental stress distributions for each of the 16 loadings were obtained using 152 three-gage strain rosettes located on the inner and outer surfaces.

All the 16 loading cases were also analyzed theoretically using a finite-element shell analysis developed at the University of California, Berkeley. The analysis used flat-plate elements and considered five degrees of freedom per node in the final assembled equations. The comparisons between theory and experiment show reasonably good general agreement, and it is felt that the analysis would be satisfactory for most engineering purposes.

---

*Work on this program was initiated under ERDA sponsorship and ultimately completed under NRC sponsorship.

1. INTRODUCTION

Intersecting cylindrical shells are common configurations in structural components for nuclear reactor systems. Piping tees and nozzles in cylindrical vessels are specific examples. However, despite their common occurrence, proven elastic stress analysis methods for such configurations have not been generally available, and only recently have potential analyses, both analytical and numerical, been developed. This is true even for the case of an idealized configuration consisting of two thin-shell normally intersecting cylinders with no transitions, reinforcements, or fillets in the junction region.

To meet the need for experimental data obtained from carefully machined models, Oak Ridge National Laboratory (ORNL) has tested a series of four thin-shell cylinder-to-cylinder models. In addition to serving a basic need for test results for use in developing and evaluating potential analytical techniques, the models in the series provide design information directly applicable to nozzles in cylindrical vessels and to a class of thin piping tees as well. The test results are particularly applicable to liquid-metal fast breeder reactor components in which relatively low internal pressures and high thermal transients dictate thin-walled structures.

Model 2 is shown in Fig. 1 along with the significant dimensions of the four models in the series. The test results for all four models have been compared with typical elastic finite-element predictions. This report describes the tests and analyses of model 2; similar results have been reported for model 1 (Refs. 1 and 2), model 3 (Refs. 2 and 3), and model 4 (Ref. 4). As the figure indicates, these models are truly idealized shell structures. There are no transitions, fillets, or reinforcing in the junction region. The outside diameter D_o of the cylinder of model 2 was 10 in. and the outside diameter d_o of the nozzle was 10 in., giving a d_o/D_o of 1.0. The cylinder and the nozzle were 0.1 in. thick; thus the outside diameter/thickness ratio of the cylinder and the nozzle was 100.

The cylinders for the remaining three models had outside diameters of 10 in. In model 1 the outside diameter of the nozzle was 5 in., giving a d_o/D_o ratio of 0.5. Model 3 had a nozzle outside diameter of 1.29 in.,

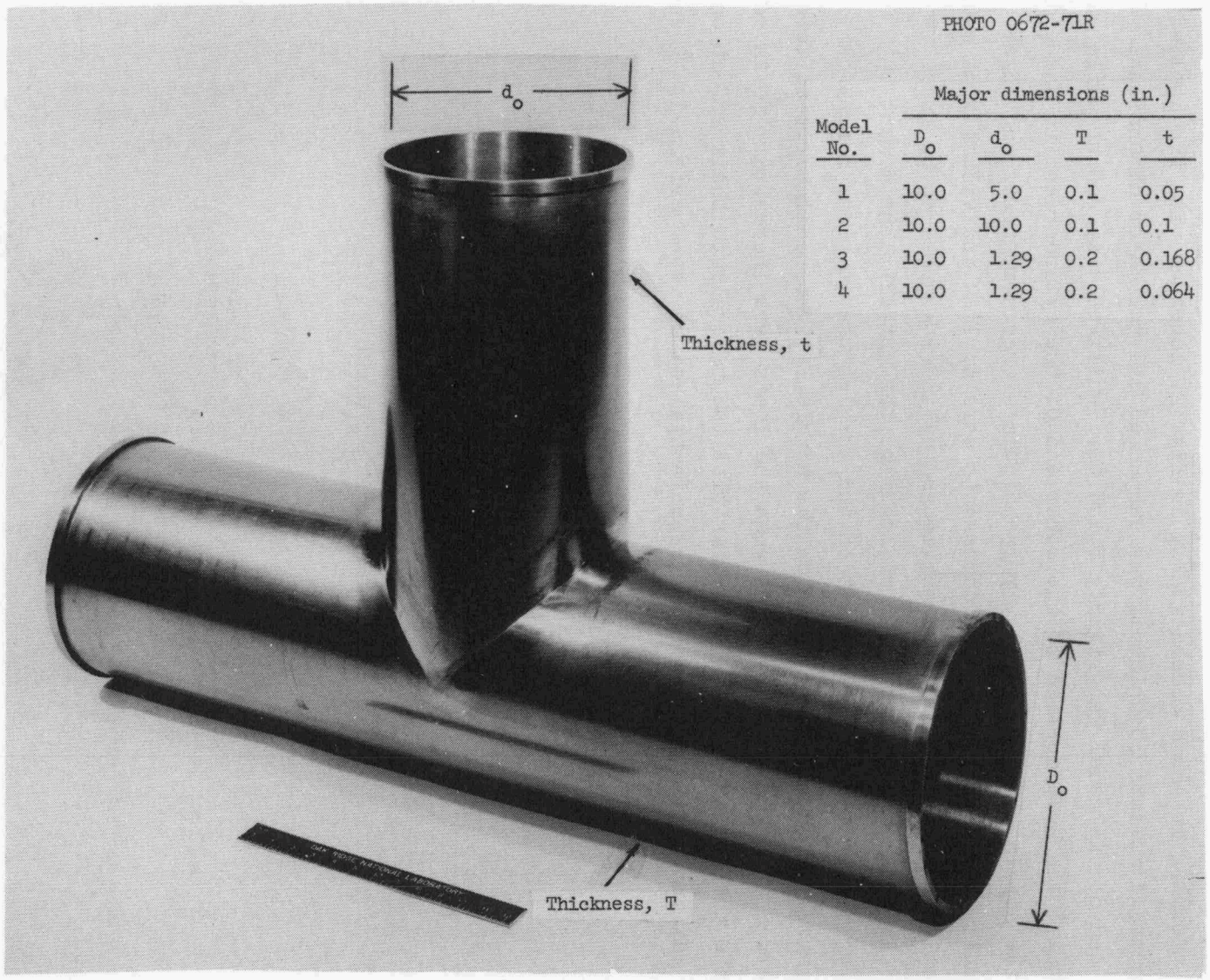

Model No.	Major dimensions (in.)			
	D_o	d_o	T	t
1	10.0	5.0	0.1	0.05
2	10.0	10.0	0.1	0.1
3	10.0	1.29	0.2	0.168
4	10.0	1.29	0.2	0.064

Fig. 1. Thin-shell cylinder-to-cylinder model 2 and table showing dimensions of all four models in the test series.

giving a d_o/D_o ratio of 0.129. The nozzle of model 4, which was obtained from the third by boring out the nozzle to provide a thinner wall thickness, had an outside diameter of 1.29.

Model 2 is shown schematically in Fig. 2, together with the applied forces and moments to which it was subjected and the major dimensions. One end of the model was rigidly fixed, or "built-in," as shown, while external loads were applied to the other end of the cylinder and to the end of the nozzle. Three mutually perpendicular force components and three mutually perpendicular moment components were applied individually at each location with the ends of the nozzle and cylinder assumed to be free.

In the cases of the pressure loading, the out-of-plane moment on the nozzle, the torsional moment on the nozzle, the in-plane moment on the nozzle, and the axial force on the nozzle, slight nonlinearities were observed in the measured strains when the loads were increased. To investigate the source of these nonlinearities and to evaluate their effect on the maximum strains, three extra experimental cases were performed. These

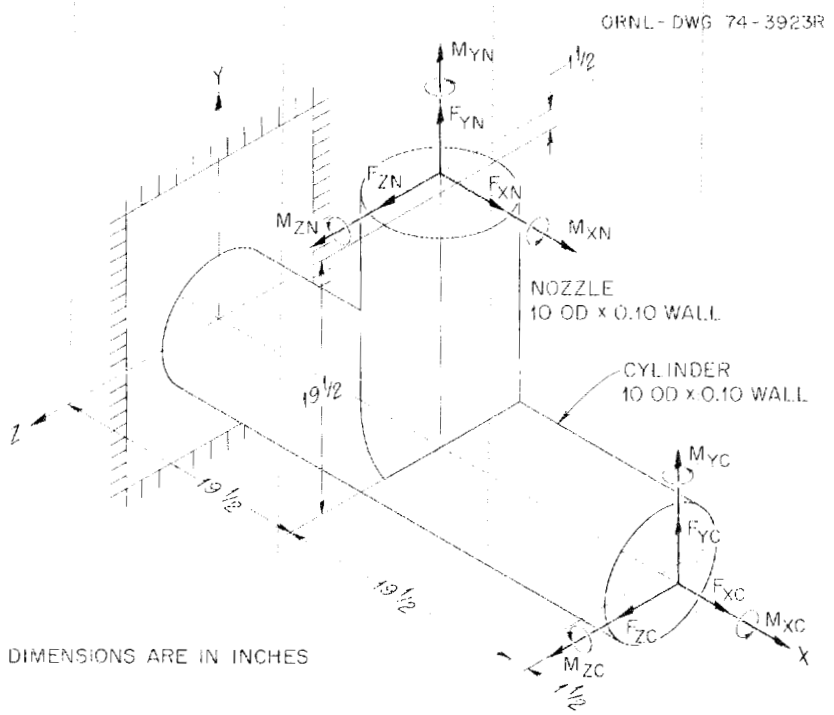

Fig. 2. Schematic of model 2 showing applied external loadings.

were the out-of-plane moment on the nozzle with the free end of the cylinder constrained to zero rotation about the x axis, the in-plane moment on the nozzle with the free end of the cylinder constrained to zero displacement in the y direction, and the axial force applied to the nozzle with the free end of the cylinder restrained as for the in-plane moment load. Thus, including internal pressure, there was a total of 16 loading cases. These loading cases were examined both experimentally and analytically, and the results were compared for each loading case.

Chapter 2 of this report describes the testing aspects of the experimental analysis and also the strain-gage data-acquisition and -reduction techniques used. Chapter 3 discusses the finite-element analysis, briefly describes the formulation used, and presents the specific element layout for the model. Complete comparisons of theory and experiment are presented and discussed in Chap. 4 for all 16 loading cases, and Chap. 5 contains a concise summary of the conclusions drawn from the study of this thin-shell cylinder-to-cylinder configuration. For the benefit of the reader who wishes to use the experimental data for comparisons with his own analyses, an appendix is included that gives a complete set of experimental data for each of the 16 loading cases.

2. EXPERIMENTAL ANALYSIS

Experimental investigations of thin-shell cylinder-to-cylinder pressure vessel configurations have used both strain-gage metal models and photoelastic models. Strain-gage studies for internal pressure and for external nozzle loadings have been carried out by Hardenbergh, Zamrik, and Edmondson,[5] by Hardenbergh and Zamrik,[6] and by Riley.[7] In the first two studies, contoured and reinforced outlets were used, while in the third, the model was fabricated from hot-rolled sheet steel by welding. Photoelastic studies have been carried out by Taylor and Lind[8] and by Leven.[9] In both cases, reinforced openings were examined. Thus, of the previous studies, only that of Riley[7] used a thin-shell idealized cylinder-to-cylinder metal model, and it was of welded construction rather than being carefully machined.

2.1 Model Construction

One of the primary objectives of the experimental analysis described in this report was to obtain experimental data on a carefully machined cylinder-to-cylinder model so that the effects of geometrical imperfections would be minimized.

The basic configuration was obtained by forging a billet of carbon steel into the basic shape of a tee and then annealing it. The forging was then bored out to the rough inside dimensions. The outside was then rough machined, and the structure was annealed a second time. To maintain the correct dimensions during annealing, tight-fitting graphite mandrels were machined and inserted in both the nozzle and the cylinder. The inside surfaces were then machined to the final dimensions by boring. The final machining on the outside surface was then done on a tracing-type milling machine using a carefully constructed mahogany wood pattern.

2.2 Strain-Gage Layout

The model was extensively instrumented with electric resistance strain gages on both the inside and outside surfaces. A sufficient number of gages was used on this model to provide a good description of the stress distributions for comparisons with predictions and for identifying the high-stress regions.

The strain-gage layout for model 2 is shown in Fig. 3. A total of 152 three-gage strain-gage rosettes was used, making 456 individual strain gages. Half of these were on the outer surface, and half were on the inner surface; they were in all cases located "back-to-back" at the locations shown in the figure.

The gages were arranged along two lines running from the junction of the nozzle and cylinder and around the junction. One line of gages was along a longitudinal axis (0° plane) and the other was along a transverse axis (270° plane). The gages around the junction were spaced at 22.5° intervals, with the first gage on the 0° plane. The gages around the junction are as close to the junction as possible and are always within 1/8 in. of the junction.

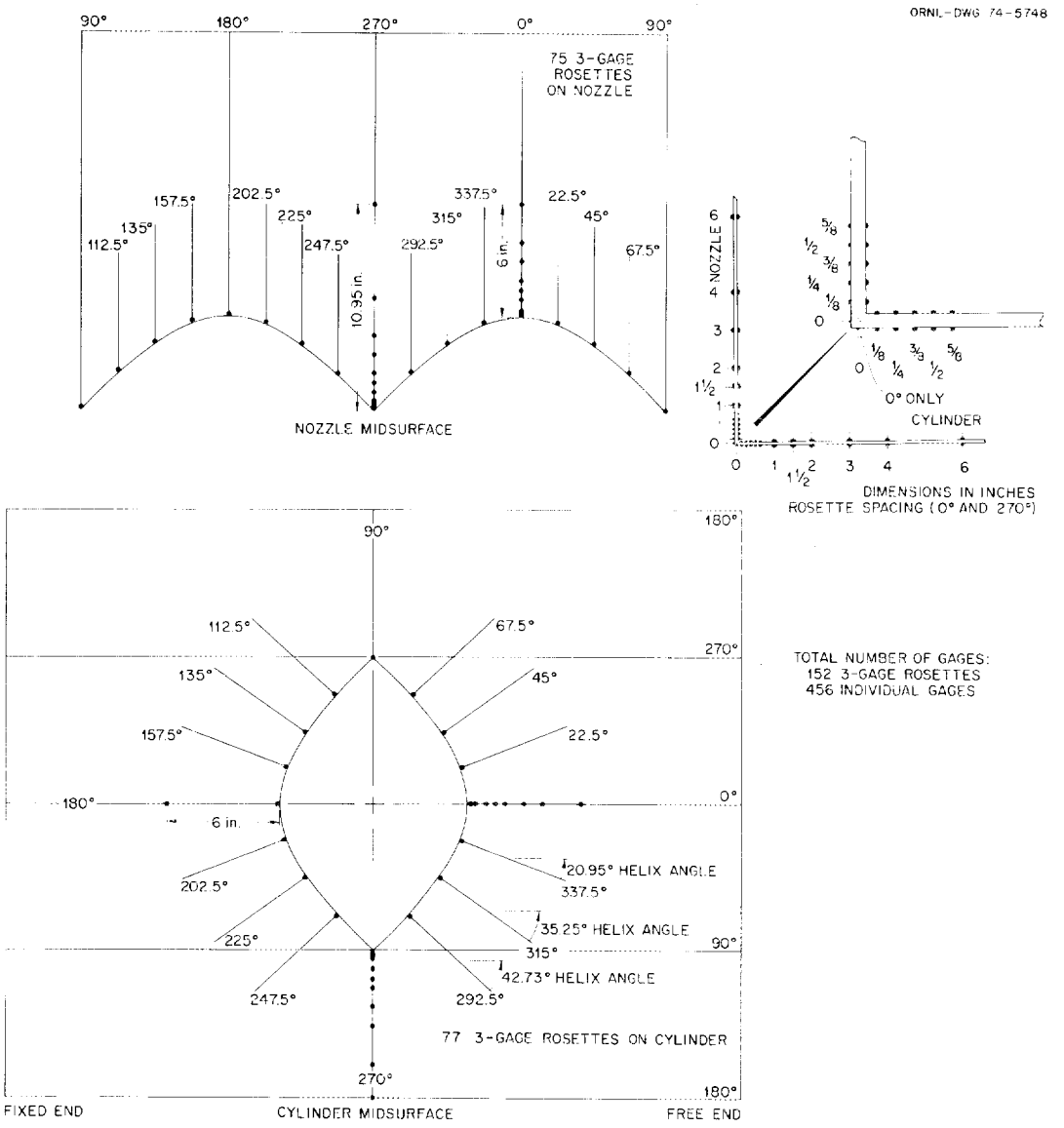

Fig. 3. Strain-gage layout.

The three-gage rosettes used were Micro-Measurements type EA-06-030YB-120, option SE, which is a very compact three-gage foil rosette. The three individual gages are arranged in a "Y" pattern and have an individual gage length of 0.030 in. As can be seen in the inset in the upper right-hand corner of Fig. 3, five complete rosettes were located along each gage line within the first 5/8 in. from the junction. These first five rosettes were supplied mounted on a common backing by the gage manufacturer. These

assemblies have the same designation as the single rosettes except that the option becomes B27. One of the five-rosette assemblies is shown in Fig. 4.

The rosettes were applied with an epoxy adhesive, BR-610, which is available from W. T. Bean, Inc. Curing times and temperatures ranged from 10 hr at 250°F to 24 hr at 200°F. Uninsulated 4-mil-diam wire was used to connect the gages to terminal tabs to which larger lead wires were connected. The strain-gage data were recorded by a Datum Computer-Controlled Data-Acquisition System (Sect. 2.4).

The junction region of the model is shown in Fig. 5 with the strain gages applied but not completely wired. The line of gages along the 0° plane can be clearly seen. Also, the gages along the junction can be seen from the 0° plane to the 270° plane.

2.3 Test Description

Figure 6 shows the instrumented model in a loading frame being subjected to a torsional moment on the cylinder. The right end of the cylinder was rigidly clamped to the heavy flat plate using a split ring arrangement acting over the flange on the end of the cylinder. The loading fixtures on the other end of the cylinder and on the end of the nozzle were attached in a similar manner. These heavy fixtures in effect constrained the end circles of the shell to remain plane circles. The end fixtures were counterbalanced by weights attached to the cables (Fig. 6).

The external loads were applied by hydraulic rams acting through load cells, and the loads were controlled by the load cell indications. The pressure loading was applied using a hydraulic fluid. To avoid undue straining of the model, weights were used to counterbalance the weight of the pressurizing fluid in the model.

For all 16 loading cases, data were taken in nine steps, usually at 0, 25, 50, 75, 100, 75, 50, 25, and 0% of full load. The procedure was then repeated, so that two complete sets of data were taken for each gage for every loading.

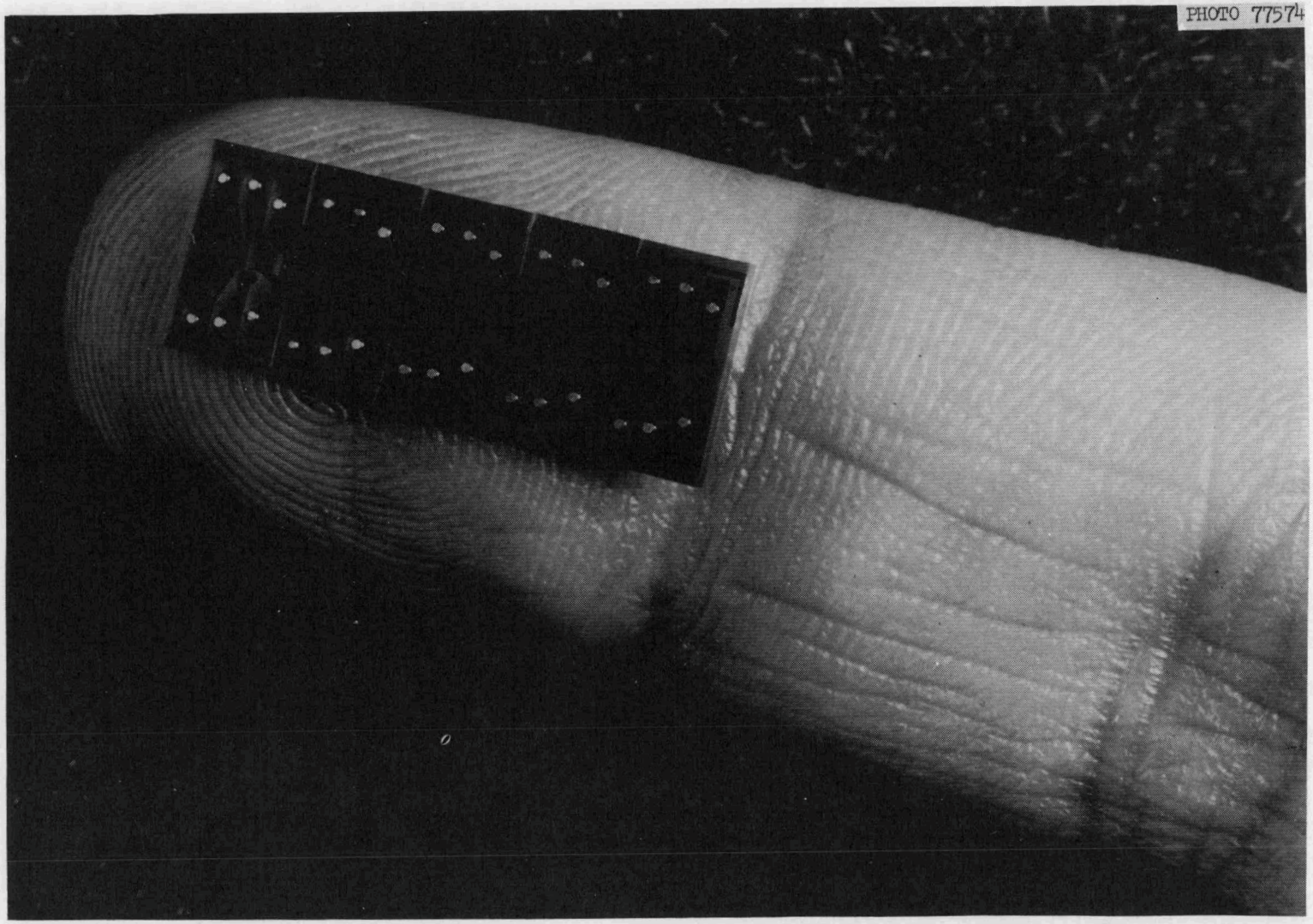

Fig. 4. Closeup of assembly of five strain-gage rosettes on a common foil backing.

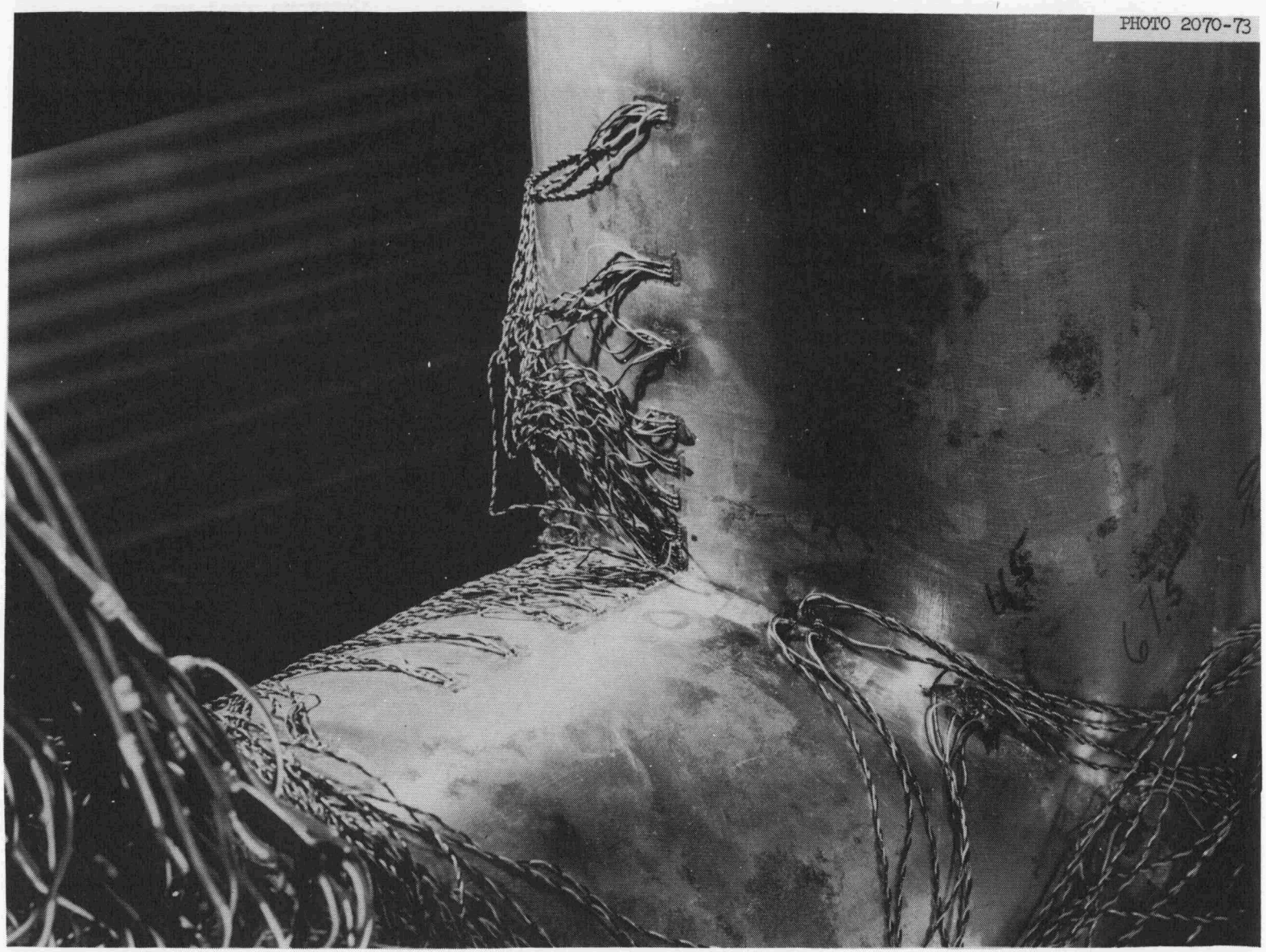

Fig. 5. Model during instrumentation.

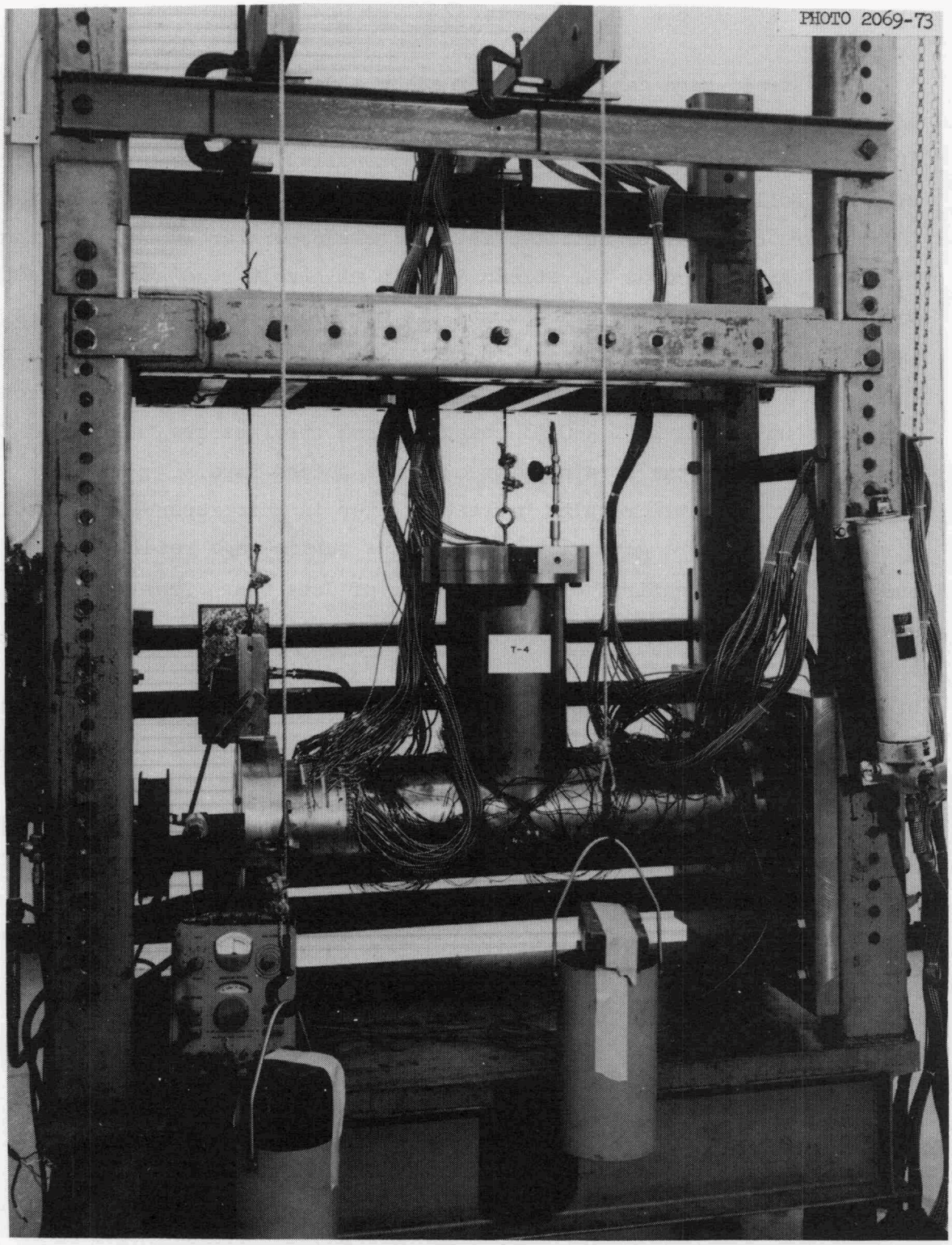

Fig. 6. Instrumented model in test frame being subjected to a torsional moment on the cylinder.

2.4 Data Acquisition and Reduction

The strain-gage data were recorded by a Datum Computer-Controlled Data Acquisition System (CCDAS). The system consists of a data-acquisition unit composed of a control module controlled by a PDP-8/I computer with the following capabilities: (1) magnetic tape input/output system, (2) in-core calculation ability, and (3) teletypewriter input and output.

The system records the strain data in millivolt readings on magnetic tape. The PDP-8/I computer converts the millivolt reading on the tape into engineering units (strains in this case) and stores them on a second tape which is compatible with the ORNL IBM 360/91 computer. This second tape is sent to the ORNL 360/91 computer, and stresses are calculated for each rosette from the strains stored on the second tape.

The experimental results presented later in this report, and tabulated in the appendix, are generally based on the strain-gage readings at maximum load and on the first of the two sets of data taken from each gage and loading. If the first set of data was questionable for some reason, the second set was used. The strain-gage readings at fractional values of the maximum load were used to check linearity and drift of the gages. In cases where nonlinearity or drift was excessive or where an individual gage or circuit was otherwise obviously malfunctioning, the rosette of which the gage was a part was not used in the final results for the specific loading case under consideration. In some instances, a gage that behaved erratically during one loading behaved normally during others. Thus, in the plots showing the experimental stresses, results from a given rosette may be included for some loadings but not for others.

Stresses were calculated from the experimental strains by using a modulus of elasticity value of 30×10^6 psi and a Poisson ratio of 0.3.

3. FINITE-ELEMENT ANALYSIS

3.1 Background

Thin-shell cylinder-to-cylinder intersection problems have, in recent years, been a favorite with the stress analyst. Their popularity stems

not only from the common occurrence of such configurations in practical design, but also from the challenge that they present as complex shell analysis problems. In addition to their use in piping and pressure vessel configurations, thin-shell cylinder-to-cylinder intersections occur in the petroleum industry, which uses tubular structural members extensively in off-shore oil-drilling towers. Much of the cylinder-to-cylinder intersection research, both experimental and theoretical, that has been done was motivated by the off-shore oil-drilling tower application. The literature associated with the latter application is reviewed in Ref. 10.

Both analytical and numerical analyses have been developed and applied to thin-shell cylinder-to-cylinder intersection problems. In 1961, Reidelbach[11] developed the first analytical solution for two perpendicularly intersecting cylindrical shells subjected to internal pressure. Eringen and his co-workers[12-15] corrected some errors and approximations in Reidelbach's solutions and formulated a solution in which the intersection curve was approximated by a circle. These solutions consisted of products of Krylov functions and Hankel functions of the first kind. A collocation method was used whereby the boundary conditions were satisfied in a least-squares sense at selected boundary points.

In 1969, Hansberry and Jones[16] used the method developed by Reidelbach and Eringen et al. to develop a solution for an in-plane bending moment applied to the nozzle of a nozzle-to-cylinder configuration. In 1970, Maye and Eringen[17] developed a solution using Fourier series involving Bessel functions in place of the Krylov functions. In 1973, Hansberry and Jones[18] expanded their solution to include the case of an axial force applied to the nozzle. However, as in the case of earlier solutions, the nozzle diameter was limited relative to the cylinder diameter.

In 1967, Bijlaard, Dohrmann, and Wang[19] formulated the problem to include the case where the nozzle and cylinder are of equal diameter. They indicated a solution in the form given by Flügge for closed cylindrical shells. In 1969, Pan and Beckett[20] developed a numerical solution to the differential equations of Flügge and Donnell that is applicable to the equal-diameter case. They compared their predictions with the experimental results obtained by Riley[7] for a nozzle-diameter/cylinder-diameter

ratio of 1/2. By careful choice of some of the factors used in the solution, they obtained predictions that agreed reasonably well with experiment.

In 1968, Herrmann and Campbell[21] presented a finite-element shell analysis formulation using flat-plate elements and the 1/2 diameter ratio model tested by Riley[7] as a sample problem. The limited comparisons shown were for internal pressure and indicated reasonably good agreement between theory and experiment. In 1969, Prince and Rashid[22] also presented a flat-plate finite-element shell analysis using the cylinder-to-cylinder intersection as a sample problem (ORNL model 1). Their shell analysis program was developed under subcontract to ORNL as a part of the ORNL Prestressed Concrete Reactor Vessel Program.

3.2 Finite-Element Method

The finite-element program used for the analysis of model 2 was chosen as being reasonably representative of currently available and widely used finite-element shell formulations. The program was developed at the University of California, Berkeley, under the direction of Professor R. W. Clough. The original program was written for general shell analyses by Johnson[23,24] and was later modified and adopted by Greste[10,25] for treating the "K" joints of cylindrical shells found in off-shore oil-drilling towers.

The basic elements used in the program are shown in Fig. 7. The elements are nonplanar quadrilaterals that are built up of an assemblage of four component triangles as shown. Within each component triangle, the in-plane displacements u and v are assumed to vary quadratically over the plane of the triangle except that they are constrained to vary linearly along the one exterior edge. The resulting membrane element, referred to as a constrained linear strain triangle (CLST), has two degrees of freedom (u and v) at each of the five nodes.

The plate bending portion of the component triangle elements has three degrees of freedom at each of the three corner nodes – two rotations about axes in the plane of the element and the transverse, or normal, displacement w. The displacement expansion for this element is due to Hsieh,

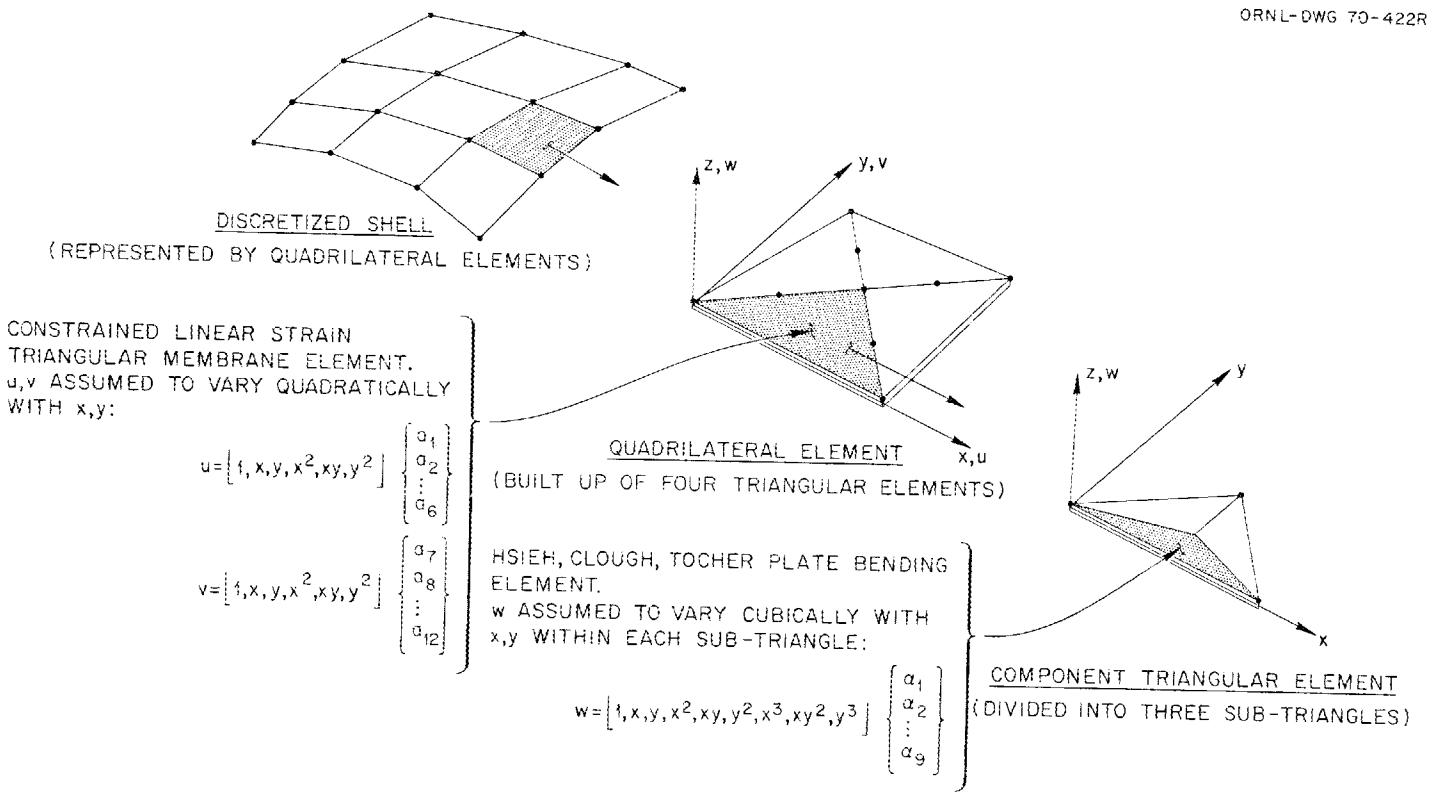

Fig. 7. Quadrilateral element and component triangles.

Clough, and Tocher,[26] and the element is referred to as the HCT triangle. Full compatibility of displacements and slopes between triangular element boundaries is achieved by dividing the element into three subtriangles and assuming an independent cubic variation for w within each subtriangle. One of the ten terms of the general cubic is neglected in each subtriangle, so that in the final assembled component triangle the normal slope varies linearly along each exterior edge. It is this feature that ensures slope compatibility in the resulting element system for plate bending problems. The 27 constants in the three cubic expressions for w within the triangular element are reduced to 9 (and related to the 9 nodal degrees of freedom) by internal compatibility considerations. With w varying as a cubic polynomial within each subtriangle, the three components of curvature, and hence the bending and twisting moments, vary linearly.

The total stiffness (membrane plus bending) of the triangular elements that form the components of the quadrilateral is obtained by superposition of the plate bending element and the membrane elements. The membrane plus bending stresses vary piecewise linearly over the surface of the resulting triangular element.

The quadrilateral element stiffness is obtained from that of the four component triangles. In general, due to the curvature of the shell that is being discretized, an arbitrary quadrilateral will be nonplanar. This introduces a complication in the transformation of the triangular element stiffness, because on the element level only two bending rotations per node are defined. When transformed from the element coordinates to some other coordinate system, a third bending rotation quantity is introduced, and in the transformed system three rotational degrees of freedom should be considered at each node. This consideration regarding the third rotational degree of freedom also arises in the subsequent assembly of the quadrilateral elements into the total structural stiffness, since adjacent elements are in general not coplanar. In his formulation, Johnson[23] chose to retain only two rotations per node in the total element assemblage. He argued that since the element plane in a sufficiently fine mesh lies close to the shell tangent plane at each node, the rotations could be transformed from the element coordinates (in the plane of the element) to coordinates in the shell tangent plane and the small transformed component of bending

rotation about the normal to the shell could be neglected. This is perhaps a reasonable assumption everywhere except at the junction of intersecting shells.

The stiffness formulation for the quadrilateral element, as well as for the CLST membrane element and the HCT plate bending element, is summarized by Greste.[10] The quadrilateral element has five degrees of freedom at each node: u, v, w, and the two rotations. In the final assembled structure the five degrees of freedom per node are u, v, w, and the two rotations about the shell tangent coordinates at each node.

The task of the finite-element method is to determine the unknown coefficients of the assumed element displacement functions for u, v, and w. This is done by connecting the quadrilateral elements together at discrete points, the corner nodes, and requiring compatibility of displacements and rotations and equilibrium of forces and moments at these nodes. Unfortunately, when the elements are assembled into a curved-shell structure, compatibility and equilibrium are not completely achieved along the element interfaces. Thus there are inherent small errors involved. However, studies by Johnson[23] have shown that these errors are not too significant provided a sufficiently fine element mesh is used.

There is an error in intersecting shell problems which is not diminished by mesh refinement. This error arises from the aforementioned neglect of the rotation about the shell normal. At the junction nodes in the cylinder-to-cylinder intersection, there are three nonzero rotational components, only two of which can be retained as nodal degrees of freedom. Greste[10] chose to define the tangent plane, and hence the two rotational degrees of freedom, at the junction nodes as the cylinder tangent plane. The manner in which he treated the junction nodes thus constrained the normal rotation about the cylindrical shell normal to be zero at the junction. This rotational constraint unrealistically constrains the bending deformation of the adjacent nozzle elements.

The most severe case of this situation is illustrated in Fig. 8. In this case, the rotation of the nozzle elements (adjacent to node A) about the normal to the cylinder at A is completely constrained. Thus, if in the actual structure the nozzle deforms into the shape shown, the constraint on the idealized structure prevents the rotation θ at A. Greste

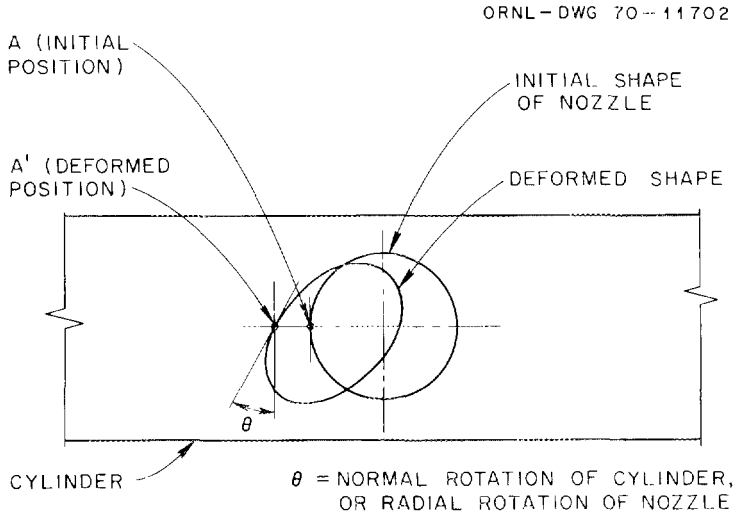

Fig. 8. Constraint at junction nodes.

considered two factors in estimating the magnitude of the constrained rotation and its effects: rigid body displacements and membrane deformations in the cylinder. Because of the relatively small length-to-diameter ratios that are generally considered for the cylinder, Greste reasoned that the rigid body displacements which produce rotations of the type shown in Fig. 8 are small compared with the bending rotations associated with straining of the structure. Therefore, essentially all the rotation of the type in Fig. 8 can be assumed to be produced by the membrane deformations of the cylinder wall. Greste then further reasoned that in oil-drilling towers the membrane stiffness of the cylinder is very large and the circumferential bending stiffness of the nozzle, or branch as he calls it, is relatively small. Thus the cylinder normal rotations, when applied as circumferential bending rotations to the nozzle, would be expected to generate only small forces and moments in the nozzle wall. That is, if the rotation θ of Fig. 8 were allowed to take place in the nozzle wall, relatively small additional stresses would be generated.

This argument may be valid for structural joints in off-shore oil-drilling towers, but it does not necessarily remain so for pressure vessel and piping cylinder-to-cylinder configurations in which the nozzle and

the cylinder may be nearly equivalent in stiffness. For these configurations there is, unfortunately, little justification for choosing the cylinder tangent plane as the reference plane for junction nodes. A better choice might have been some average or mean tangent plane at junction nodes giving partial bending constraint to both nozzle and cylinder. Johnson[23] used this latter approach to analyze a folded-plate structure and found that the results agreed well with an elasticity solution.

In conclusion, the error introduced in the junction region by the neglect of the sixth degree of freedom at the junction nodes and by the associated constraint on the bending deformations of the element adjacent to those nodes is not believed to be a large factor, but it is present and it is not reduced by mesh refinement.

3.3 Finite-Element Idealization of Model

The finite-element representation chosen for the model is depicted in Fig. 9, which shows developed views of one-half of the nozzle, cylinder, and end plates. It was necessary to consider only one-half of the structure because of symmetry considerations. This mesh layout was developed manually and was arranged so that lines of nodes corresponded to the lines of strain gages in the experimental model. There were 993 nodes, resulting in approximately 4500 linear algebraic simultaneous equations to be solved for the unknown displacement parameters. There were 27 nodes along the (half) junction line between the nozzle and cylinder. All 16 loading cases considered experimentally were analyzed using this mesh, and the theoretical predictions were compared with the experimentally determined stresses and are given in Chap. 4.

Nine of the 16 loadings – pressure, axial forces on the cylinder and the nozzle, and in-plane moment and forces on the cylinder and nozzle – produce behavior that is theoretically symmetric about the longitudinal plane of symmetry of the model. For these symmetric loadings, it is correct to consider just one-half of the model in the finite-element representation. The boundary conditions on nodal displacements and rotations are those commonly associated with symmetry conditions.

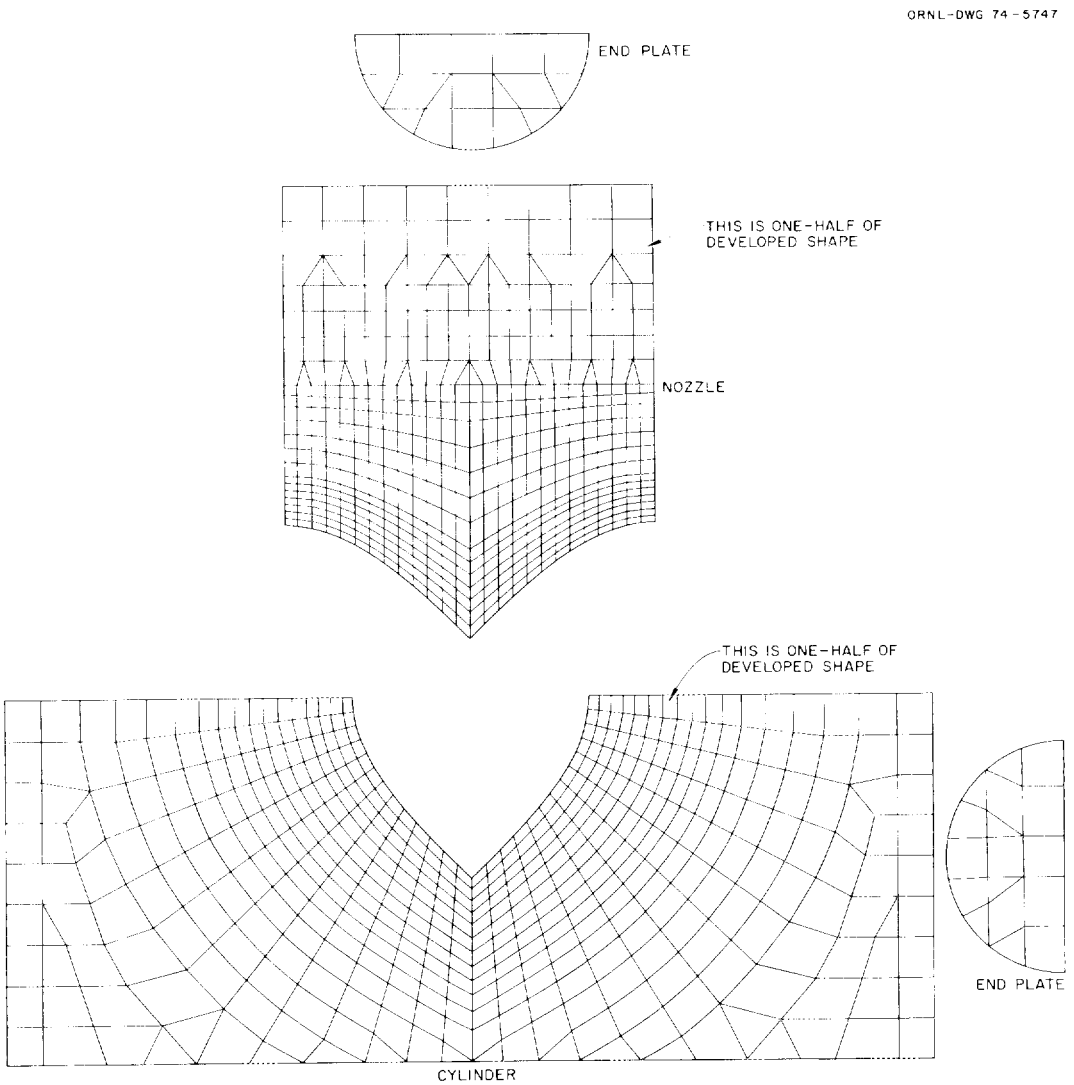

Fig. 9. Finite-element idealization of the model.

For the remaining seven loadings — out-of-plane moments and forces on the cylinder and nozzle and torsional moments on the cylinder and nozzle — asymmetric conditions exist; and to consider just one-half of the model in the finite-element representation requires assumptions, or approximations, in establishing nodal displacement and rotational boundary conditions. Basically, the boundary conditions used were based on the assumption that the projection on the X-Y plane (see Fig. 2) of the boundary remained fixed in the X-Y plane. In other words, the displacements in the X and Y directions and the rotation about the Z axis were assumed to be zero for the nodes along the boundary in the X-Y plane. Although

these conditions are obviously not strictly correct, they nonetheless seem to be reasonable assumptions that are useful for reducing the size of the problem to be solved.

4. COMPARISON OF THEORY AND EXPERIMENT

The theoretical predictions, based on the finite-element layout shown in Fig. 9, are compared in this chapter with experimentally determined distributions for all 16 loading cases. For each loading, the theoretical and experimental stress distributions along two gage lines on the cylinder and nozzle (see Fig. 3) and around the crotch are presented. The stresses shown are always those parallel (longitudinal) to the gage lines and those perpendicular (transverse) to the gage lines. The gages around the crotch are on gage lines of one gage each at the angles shown in Fig. 3. The theoretical stresses at the crotch are plotted at the position of the strain gage near the crotch, since the strain gages could not be placed exactly on the crotch (see Fig. 3).

To examine the stresses, the plots were drawn using stress ratios which were determined by dividing the stresses at a point by a nominal membrane stress value. The membrane hoop stress in the cylinder, and nozzle, was used as the nominal stress level for the pressure loading. For the moment loadings on the nozzle, or cylinder, the maximum membrane bending stresses (computed by Mc/I) or the membrane shear stress (computed by Tc/J and equal to the maximum normal stress) in the nozzle, or cylinder, were used as the nominal stresses. For the axial forces on the nozzle and the cylinder, the axial membrane stress (calculated by P/A) was used. For the in-plane and out-of-plane forces on the nozzle, the nominal stress was somewhat arbitrarily chosen as the maximum bending stress in the nozzle (calculated by Mc/I) at the level of the top of the cylinder. Finally, for the in-plane and out-of-plane forces on the cylinder, the nominal stress was arbitrarily chosen as the maximum bending stress in the cylinder at its midlength (at the center line of the nozzle).

The applied loads used in the experimental analyses are given in Table 1, together with the nominal membrane stress levels calculated by the above procedures.

Table 1. Applied loads and nominal stress levels

Loading case	Load level	Nominal membrane stress (psi)
Internal pressure	60 psi	2970
Out-of-plane moment, M_{XN}	10,000 in.-lb	1300
Torsional moment, M_{YN}	16,000 in.-lb	1040
In-plane moment, M_{ZN}	15,000 in.-lb	1950
In-plane force, F_{XN}	1200 lb	2260
Axial force, F_{YN}	4000 lb	1290
Out-of-plane force, F_{ZN}	600 lb	1330
Torsional moment, M_{XC}	20,000 in.-lb	1300
Out-of-plane moment, M_{YC}	60,000 in.-lb	7800
In-plane moment, M_{ZC}	24,000 in.-lb	3120
Axial force, F_{XC}	8000 lb	2570
In-plane force, F_{YC}	1000 lb	2530
Out-of-plane force, F_{ZC}	1200 lb	3040
Out-of-plane moment with restraints, M_{XN}	10,000 in.-lb	1300
In-plane moment with restraints, M_{ZN}	15,000 in.-lb	1950
Axial force with restraints, F_{YN}	4000 lb	1290

4.1 Internal Pressure

The measured and predicted stress distributions determined for an internal pressure of 60 psi applied to the model are shown in Figs. 10 through 12. Figure 10 shows the measured and predicted stress distributions on the outside and inside surfaces of the cylinder and the nozzle along the 0° gage line, which is the longitudinal plane of symmetry (see Fig. 3). The stresses are shown as a function of distance from the junction of the nozzle and cylinder midsurfaces. The heavy lines are the

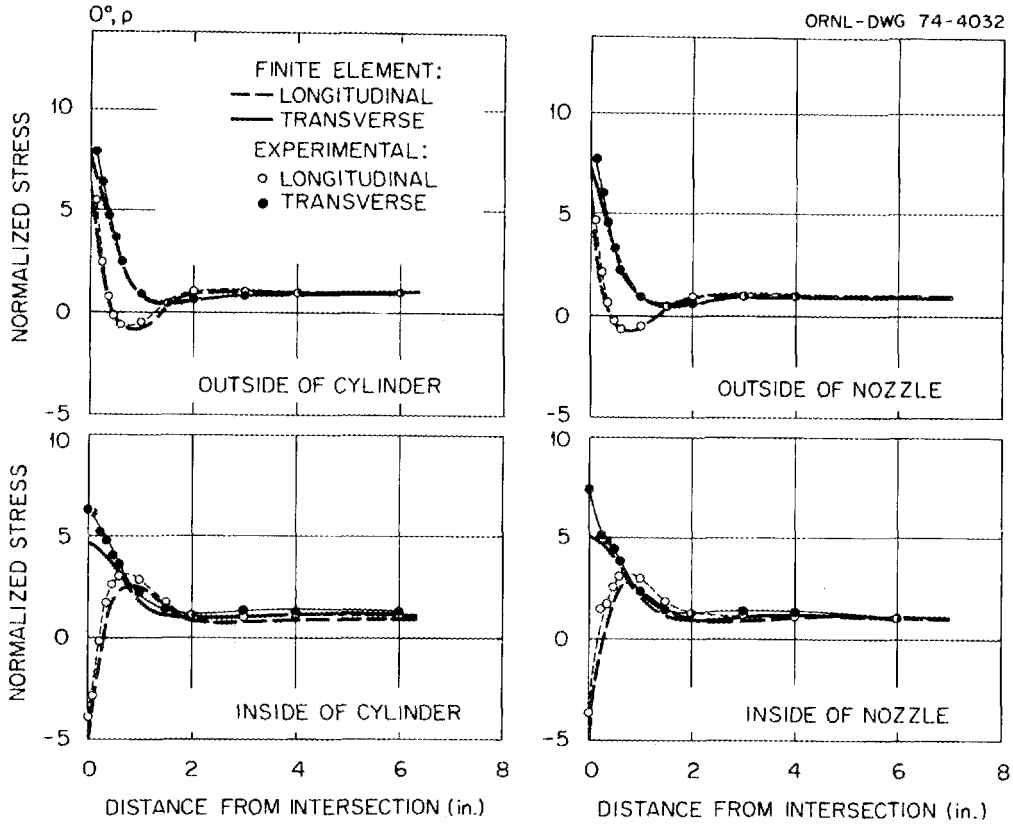

Fig. 10. Measured and predicted stress distributions at 0° for an internal pressure of 60 psi.

predicted stresses, while the fine lines through the experimental points show the measured distribution. The solid lines in each case represent the transverse stresses, which are perpendicular to the gage lines; the dashed lines represent the longitudinal stresses, which are parallel to the gage lines. Thus one can compare the solid lines with each other and the dashed lines with each other. All the stresses in the figures are normalized by the nominal membrane stresses given in Table 1.

The agreement between theory and experiment is excellent in Fig. 10, except that the stresses at the inside surface are somewhat underestimated by the finite-element predictions. The general shape and distribution of the stresses are well predicted by the theory.

Figure 11 shows the stresses along the 270° gage line, which is the transverse plane of symmetry. Here the agreement between theory and experiment is also excellent, and the shape and distribution of the stresses are again well predicted by the theory.

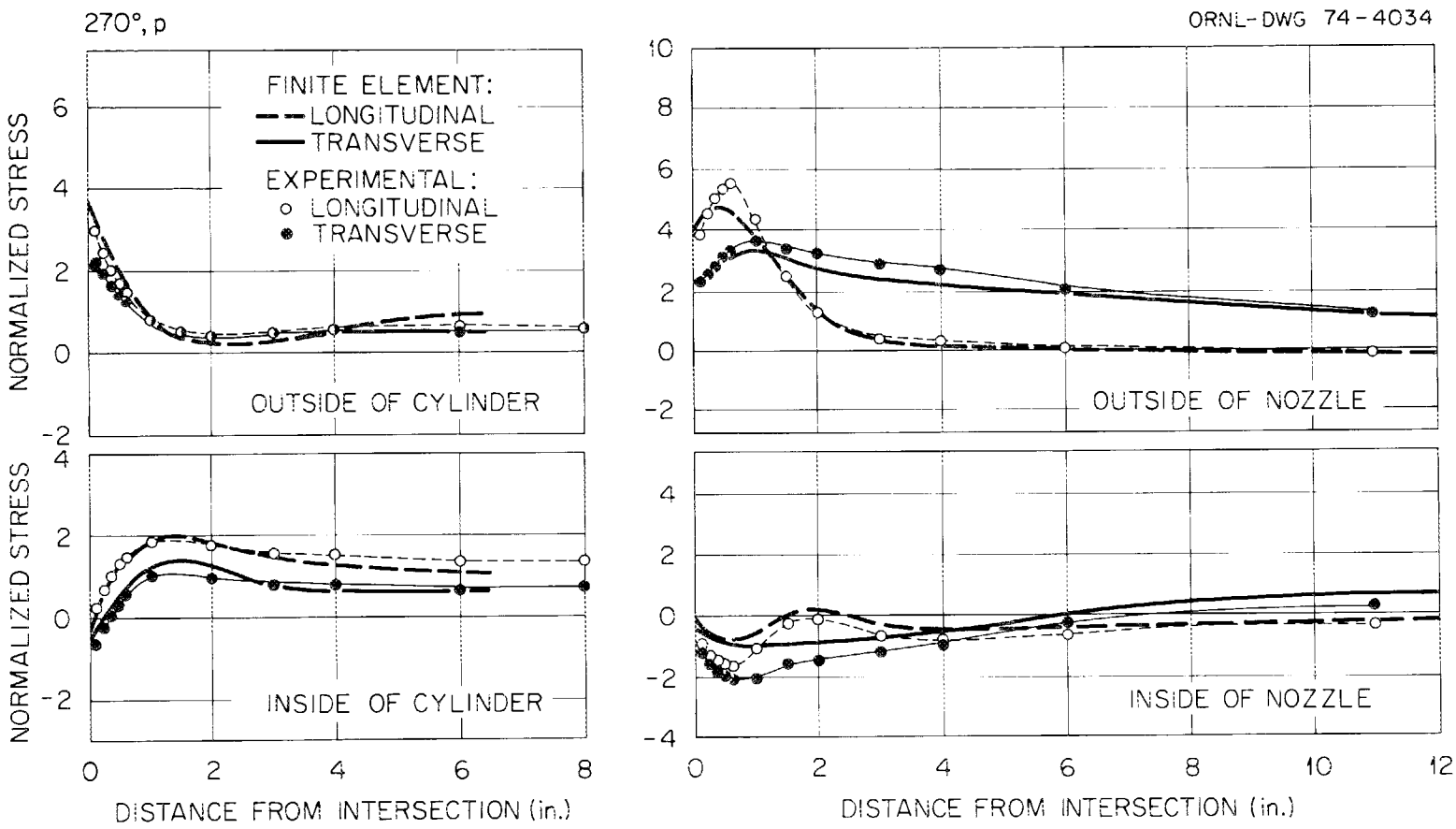

Fig. 11. Measured and predicted stress distributions at 270° for an internal pressure of 60 psi.

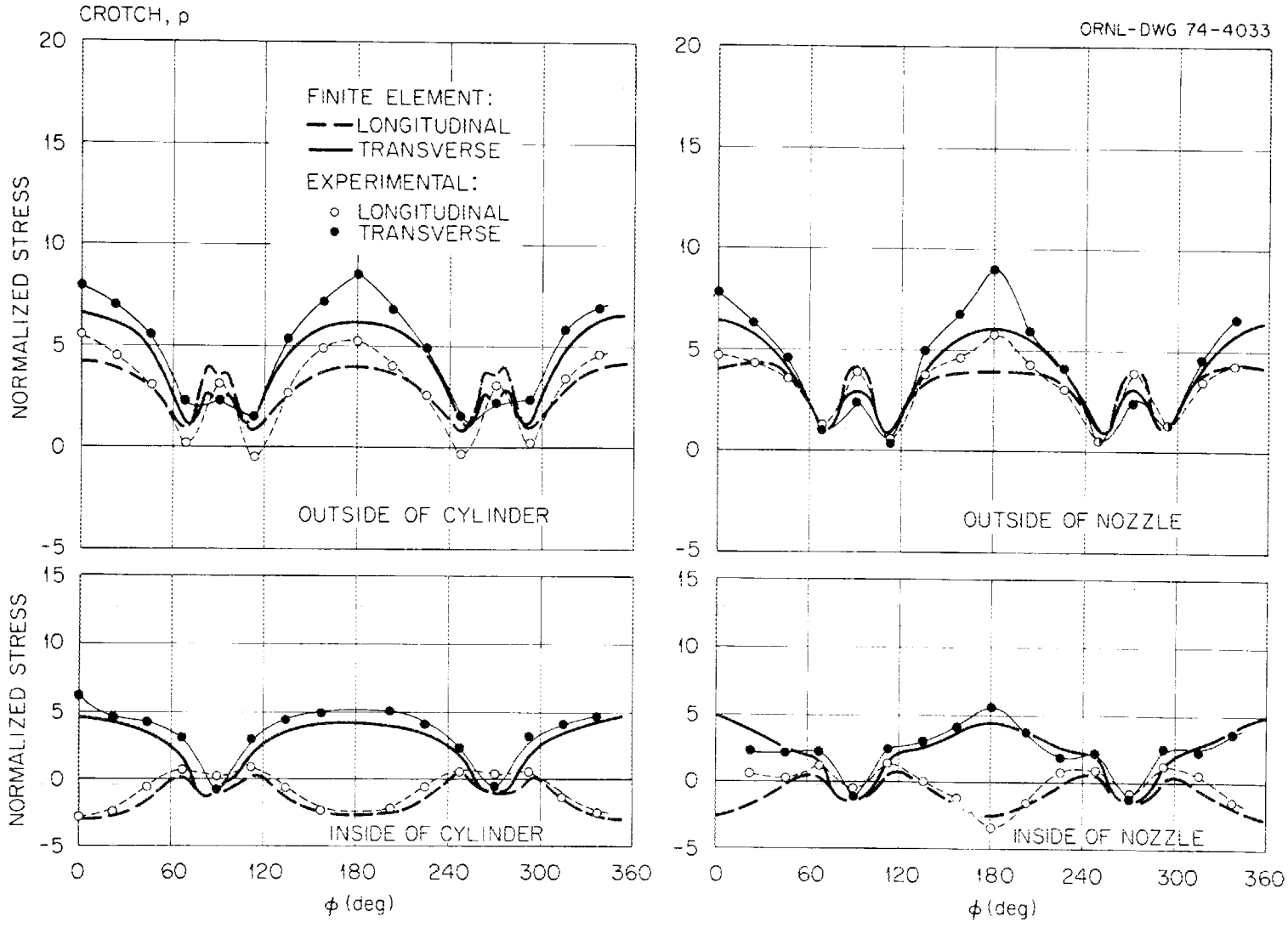

Fig. 12. Measured and predicted stress distributions around the nozzle-cylinder junction for an internal pressure of 60 psi.

The variation of the stresses around the nozzle-cylinder junction is shown in Fig. 12, and the sharp and rapid variation of stresses around the junction, which indicates the very complex nature of the stress distribution in this region, can immediately be seen. The agreement between theory and experiment is excellent except around the 180° plane on the outside surface. However, the shape and distribution of the stresses are well predicted by the theory.

To examine the maximum stresses, stress ratios were determined by dividing the maximum absolute principal stress* value at a point by a nominal membrane stress value (listed in Table 1). These maximum stress ratios were calculated for both experimental and theoretical stresses. The experimental stress ratios were extrapolated along the 0 and 270° gage lines to the junction where necessary, but the stress ratios around the crotch were calculated where they occurred. However, it should be emphasized that the maximum experimental stress estimates are based on a consideration of the stresses along the gage lines and on the string of gages around the crotch only; this does not preclude the existence of slightly higher ratios at locations away from gage lines. The theoretical maximums were calculated where they occurred.

The maximum experimentally determined stress occurred on the outside surface of the nozzle at 180°, and the maximum stress ratio was 9.0. The theoretical maximum stress was on the outer surface of the cylinder at 0°; the maximum stress ratio was 7.7.

4.2 Out-of-Plane Moment Loading, M_{XN}, on Nozzle

The measured and predicted stress distributions for an out-of-plane moment loading of 10,000 in.-lb applied to the nozzle are shown in Figs. 13 through 15. The results in Fig. 13 are for the 0° plane, the longitudinal plane of symmetry. As expected, the stresses are small, since this plane is analogous to the neutral axis of a beam in bending.

---

*Principal stress values are given in the appendix in terms of psi for the indicated value of the loading actually applied.

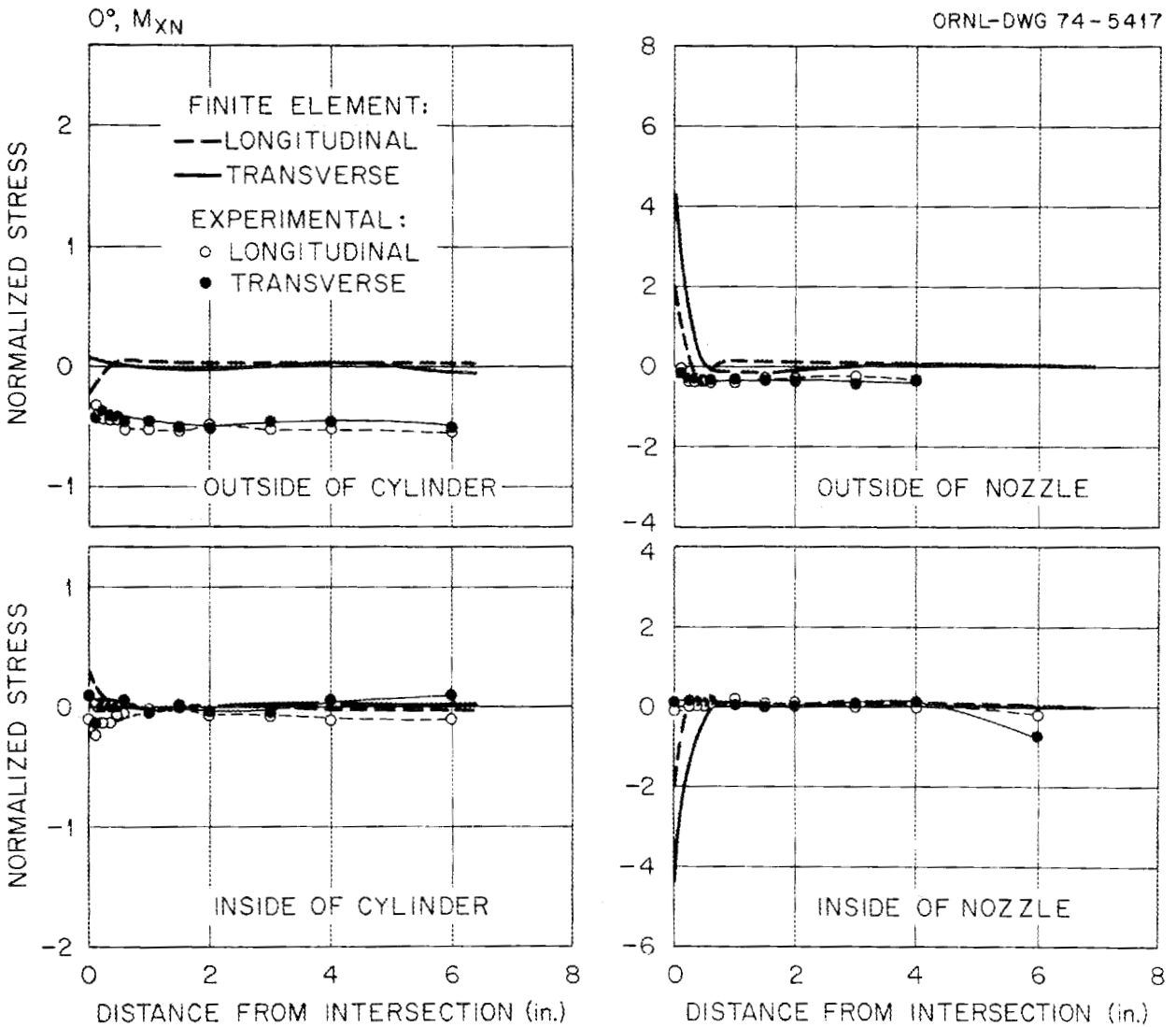

Fig. 13. Measured and predicted stress distributions at 0° for an out-of-plane moment, M_{XN}, on the nozzle.

The results for the 270° gage line, which is the transverse plane of symmetry, are shown in Fig. 14. Here, the stresses are a maximum and the agreement between theory and experiment is excellent except for the transverse stress on the inside surface of the nozzle.

The variation of the stresses around the junction is shown in Fig. 15, where again the complex variation of the stresses can be seen. The comparisons of the results are good, particularly on the inside surfaces.

The maximum experimentally determined principal stress ratio was 15.8, with the maximum stress occurring on the inside surface of the cylinder at the junction at 247°. The theoretical maximum stress was on the inside surface of the nozzle at the junction at 249°, and the ratio was 17.8.

4.3 Torsional Moment Loading, M_{YN}, on Nozzle

The measured and predicted stress distributions for a torsional moment loading of 16,000 in.-lb applied to the nozzle are shown in Figs. 16 through 18. Here the stresses in the longitudinal and transverse planes of symmetry are low and rise to their maximum levels on approximately the 70, 110, 250, and 290° planes (see Fig. 18). In general, the distributions show poor quantitative agreement except for the distribution around the crotch; here the agreement is good on the inside surfaces.

The maximum experimentally determined principal stress ratio was 31.3, with the maximum stress located on the inside surface of the cylinder at 247°. The maximum theoretical stress was on the outside surface of the cylinder at 256°, and the maximum principal stress ratio was 37.5.

4.4 In-Plane Moment Loading, M_{ZN}, on Nozzle

The measured and predicted stress distributions for an in-plane moment of 15,000 in.-lb applied to the nozzle are shown in Figs. 19 through 21. Here the stresses agree well on the longitudinal plane of symmetry, as shown in Fig. 19. The stresses along the transverse plane are larger than those along the longitudinal plane (Fig. 20). In general, the distributions show poor quantitative agreement between theory and experimental results. The agreement between the distributions around the crotch is

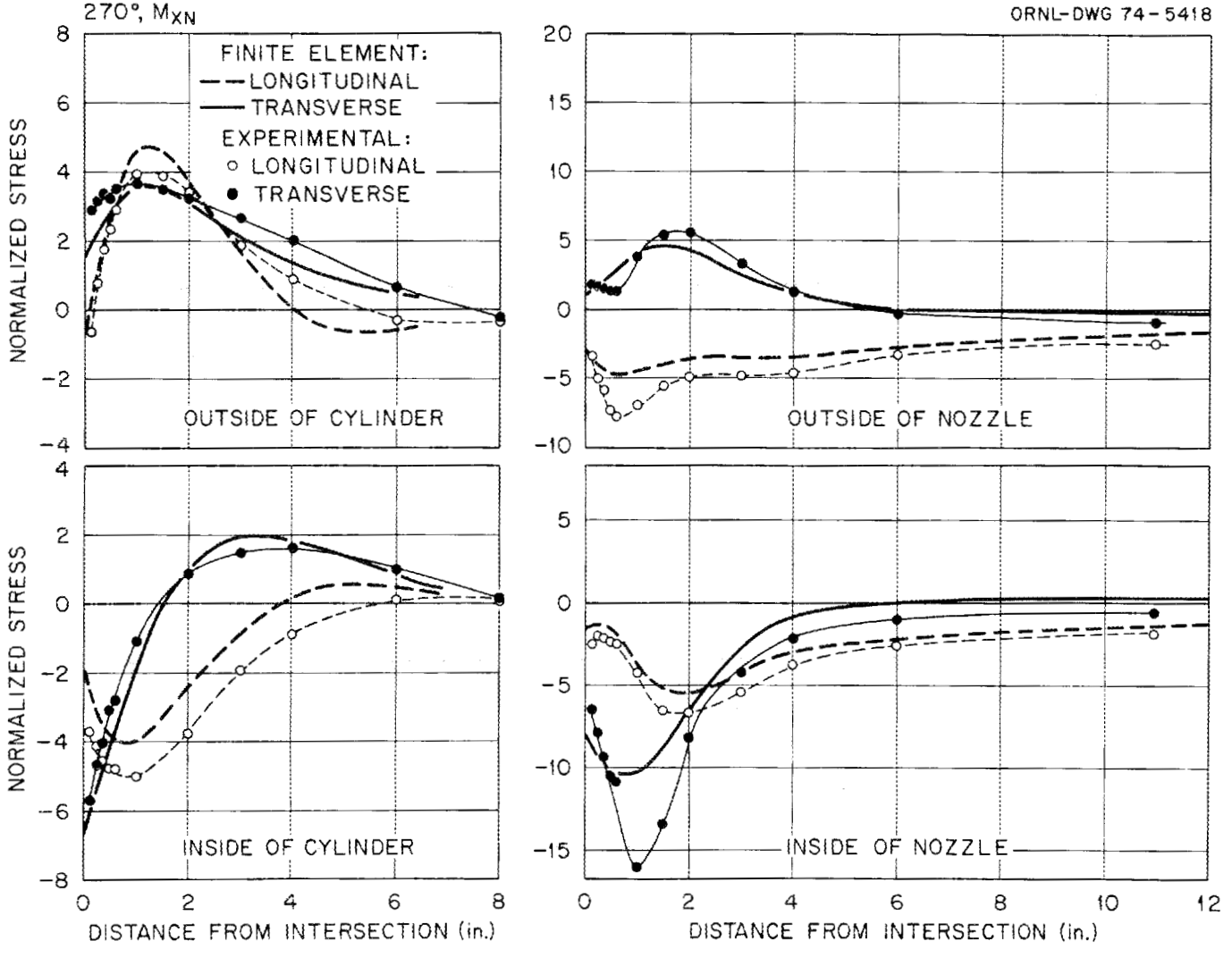

Fig. 14. Measured and predicted stress distributions at 270° for an out-of-plane moment, M_{XN}, on the nozzle.

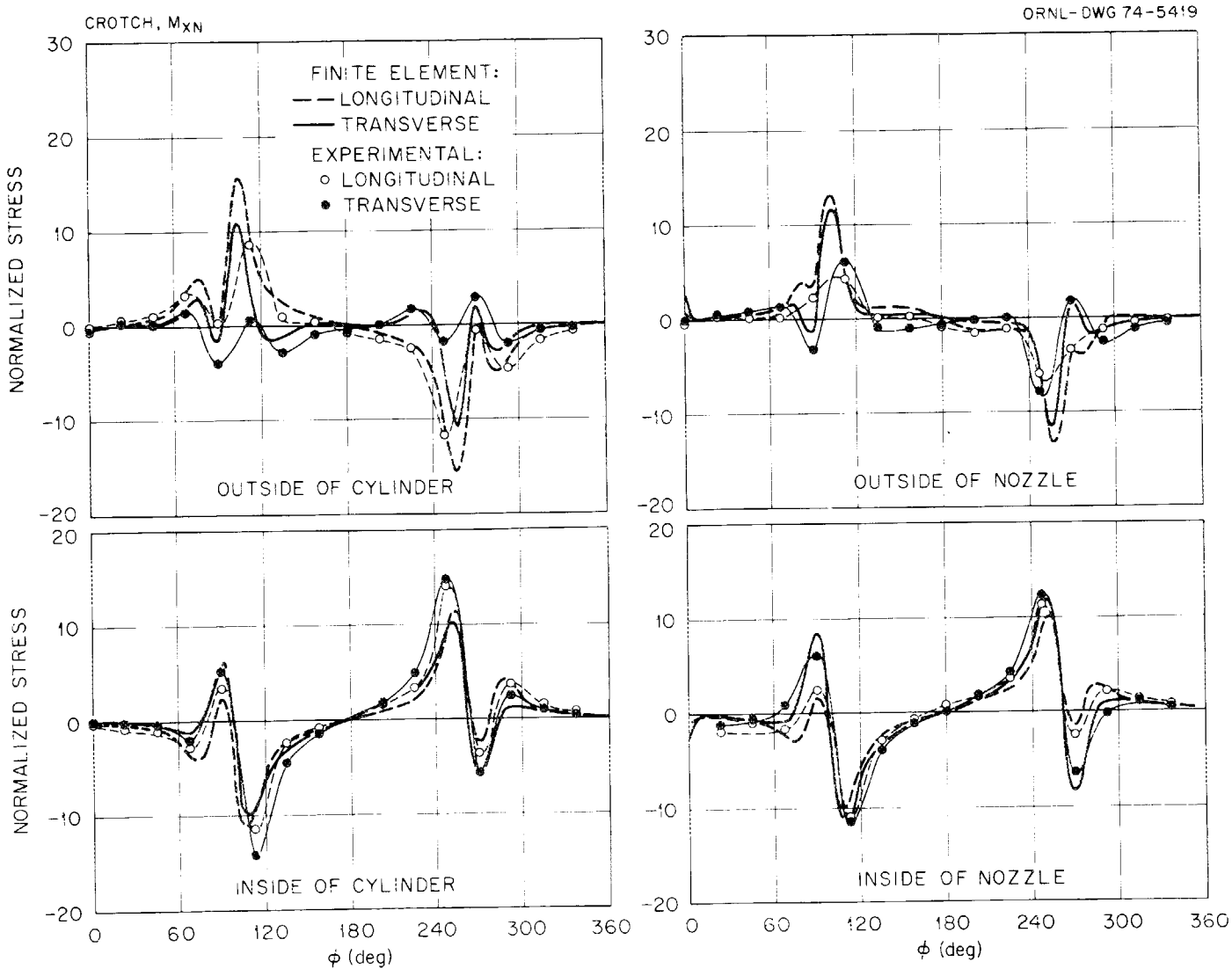

Fig. 15. Measured and predicted stress distributions around the nozzle-cylinder juntion for an out-of-plane moment, M_{XN}, on the nozzle.

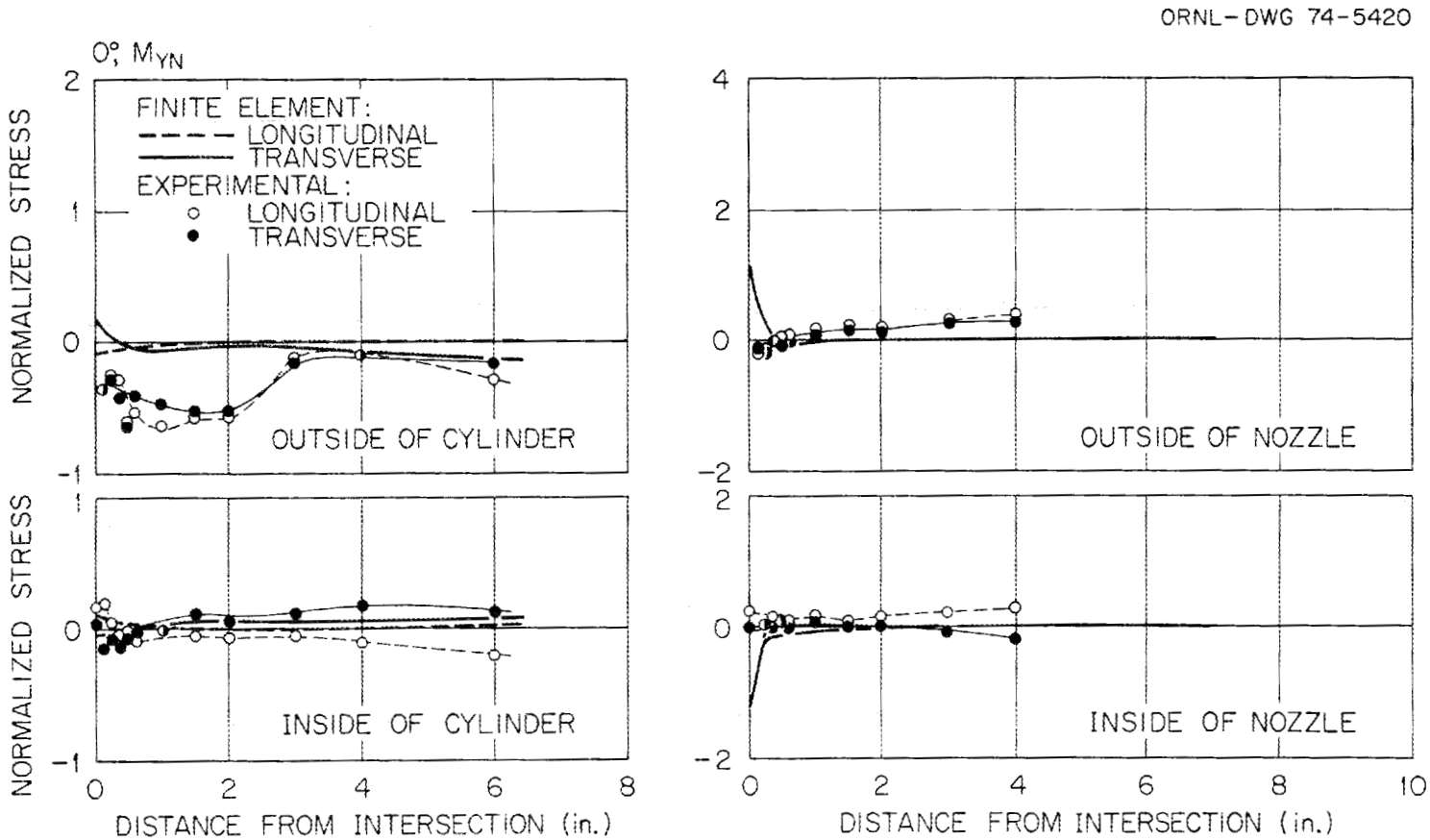

Fig. 16. Measured and predicted stress distributions at 0° for a torsional moment, M_{YN}, on the nozzle.

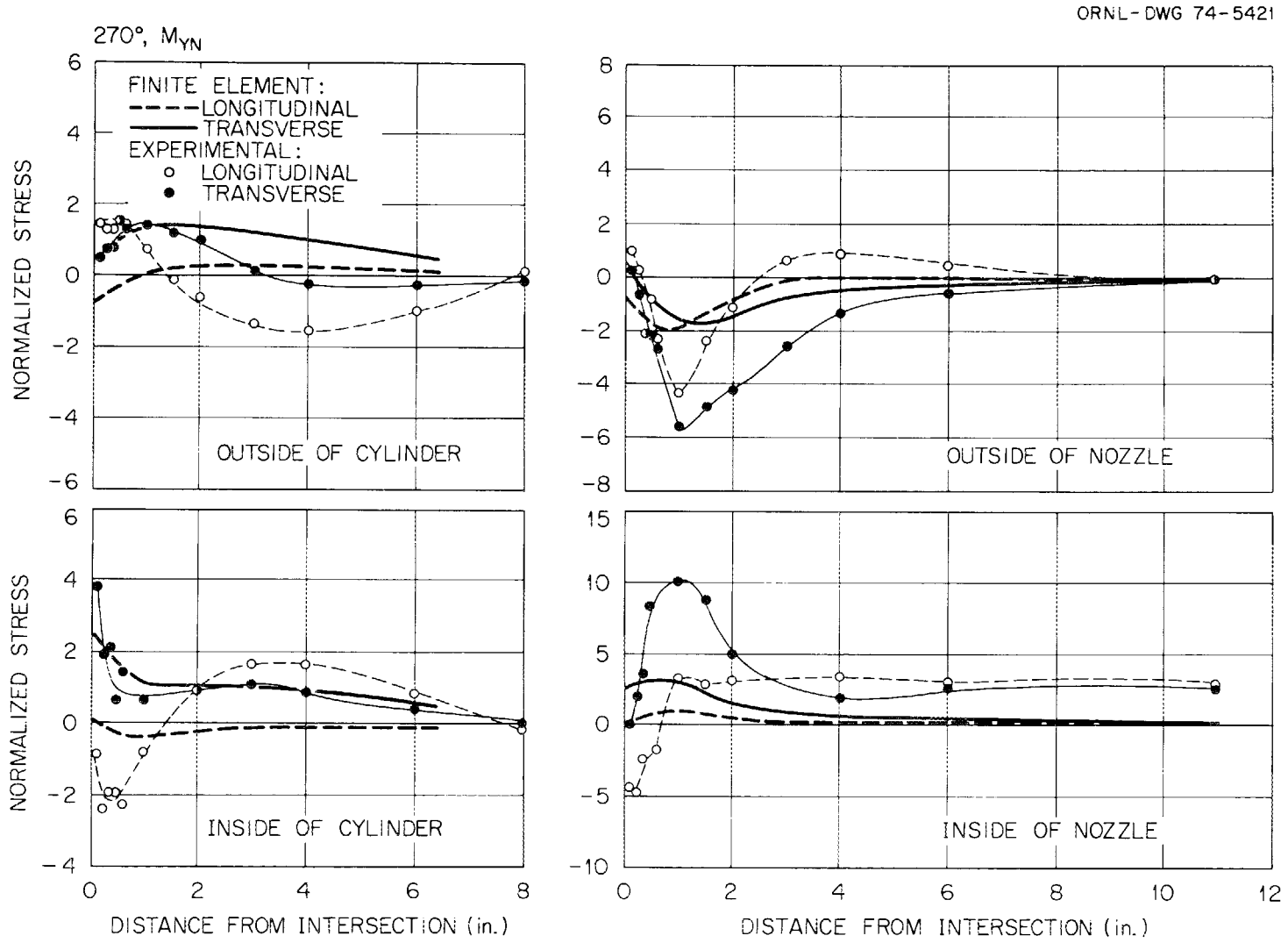

Fig. 17. Measured and predicted stress distributions at 270° for a torsional moment, M_{YN}, on the nozzle.

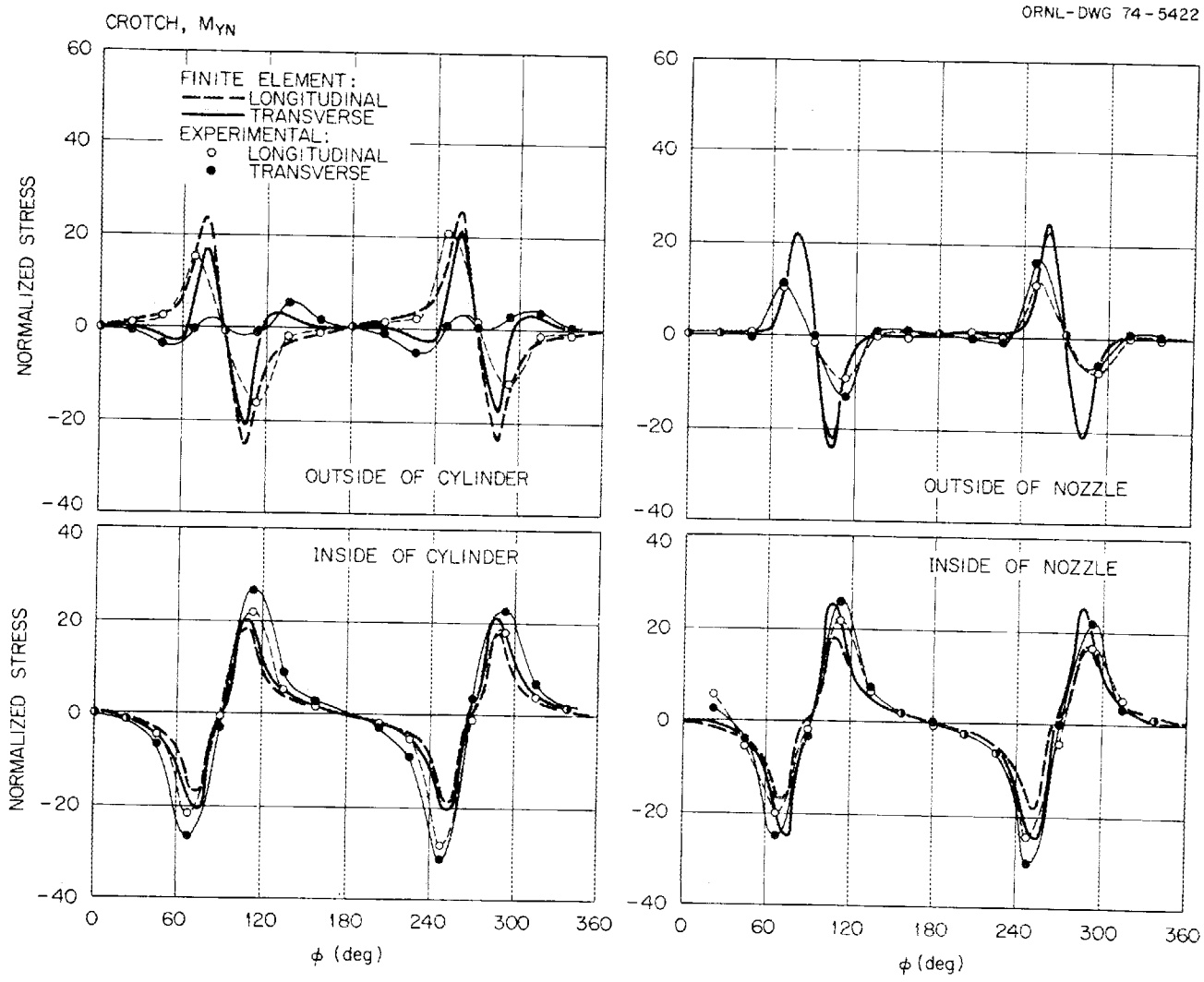

Fig. 18. Measured and predicted stress distributions around the nozzle-cylinder junction for a torsional moment, M_{YN}, on the nozzle.

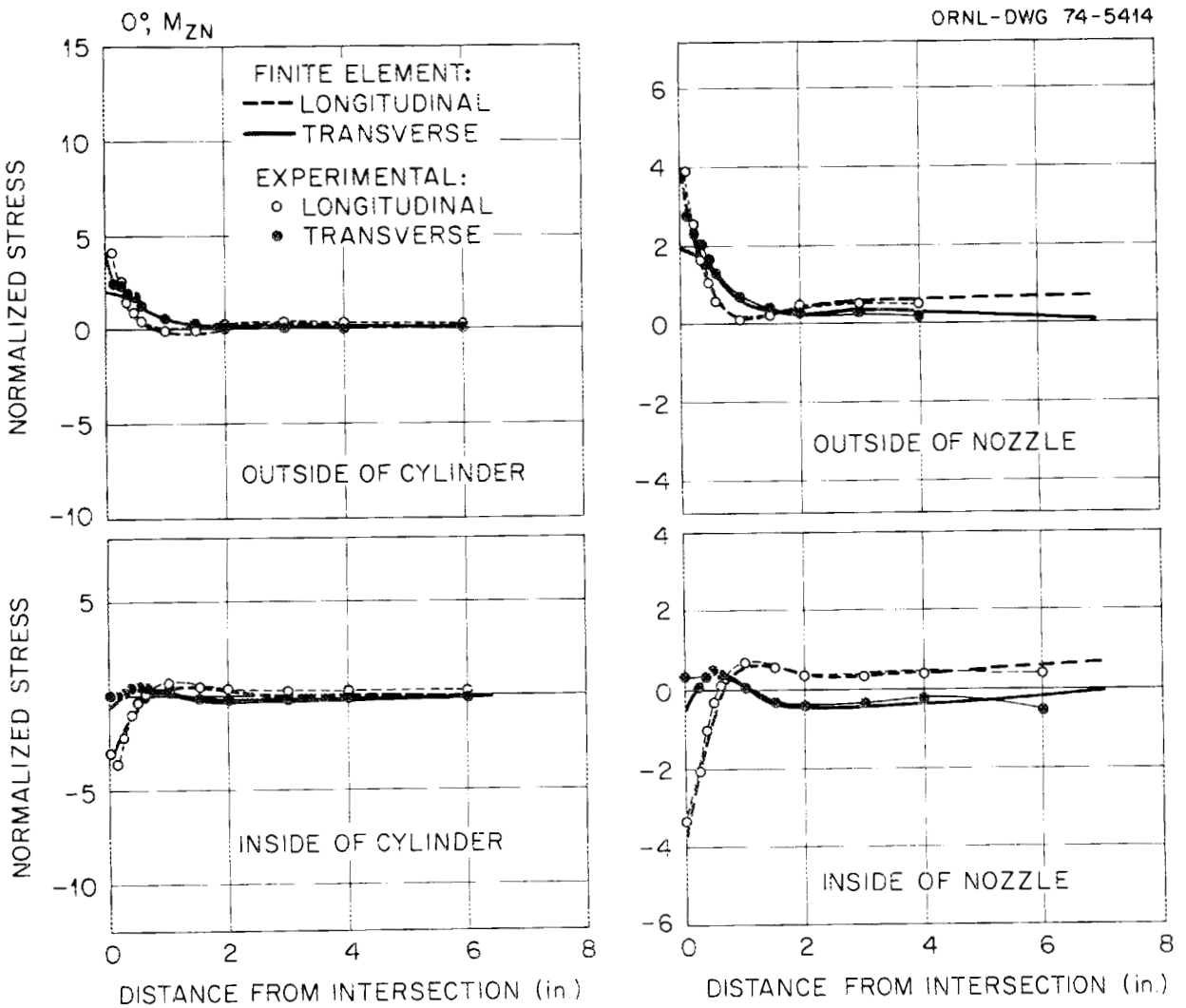

Fig. 19. Measured and predicted stress distributions at 0° for an in-plane moment, M_{ZN}, on the nozzle.

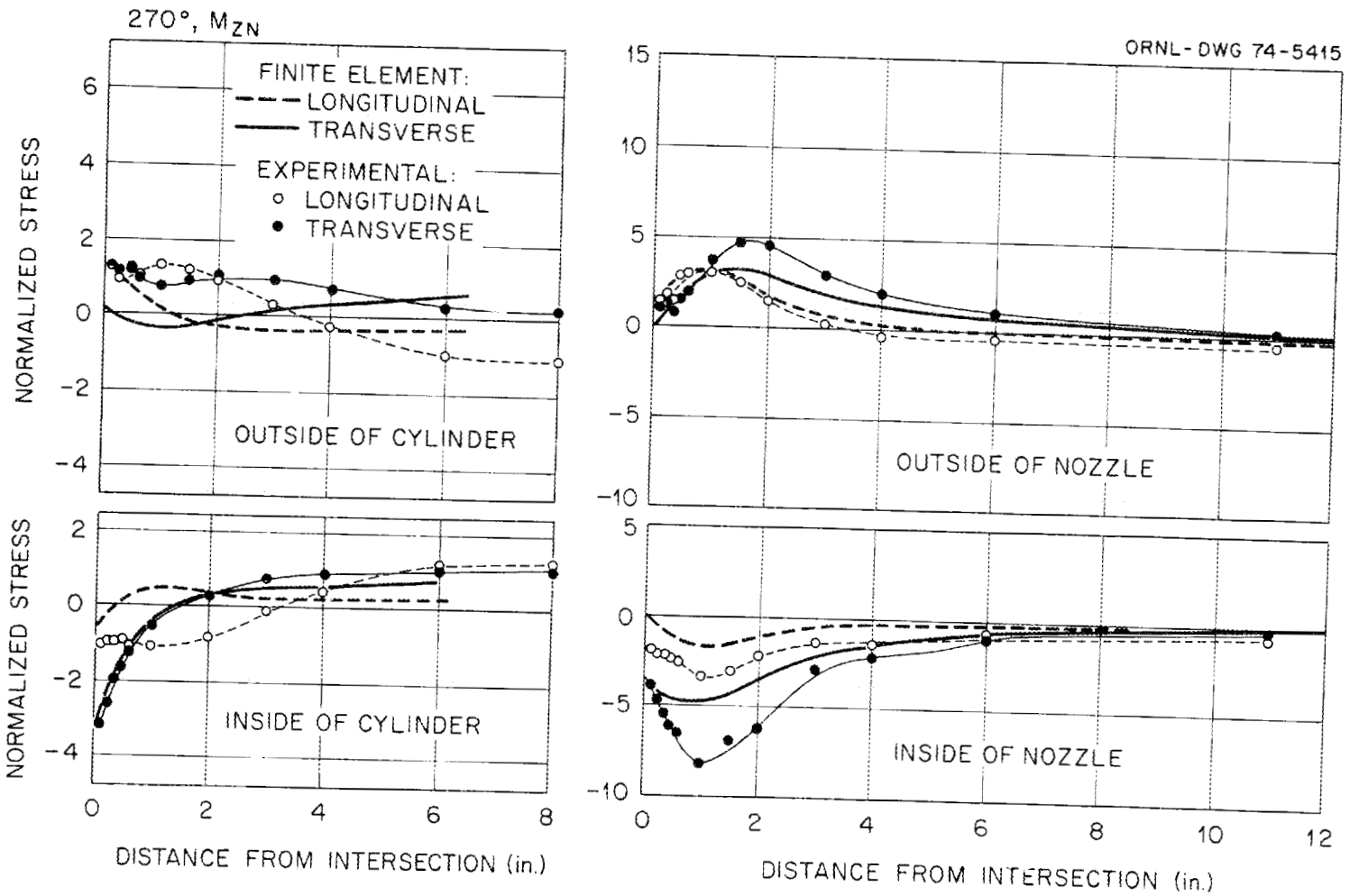

Fig. 20. Measured and predicted stress distributions at 270° for an in-plane moment, M_{ZN}, on the nozzle.

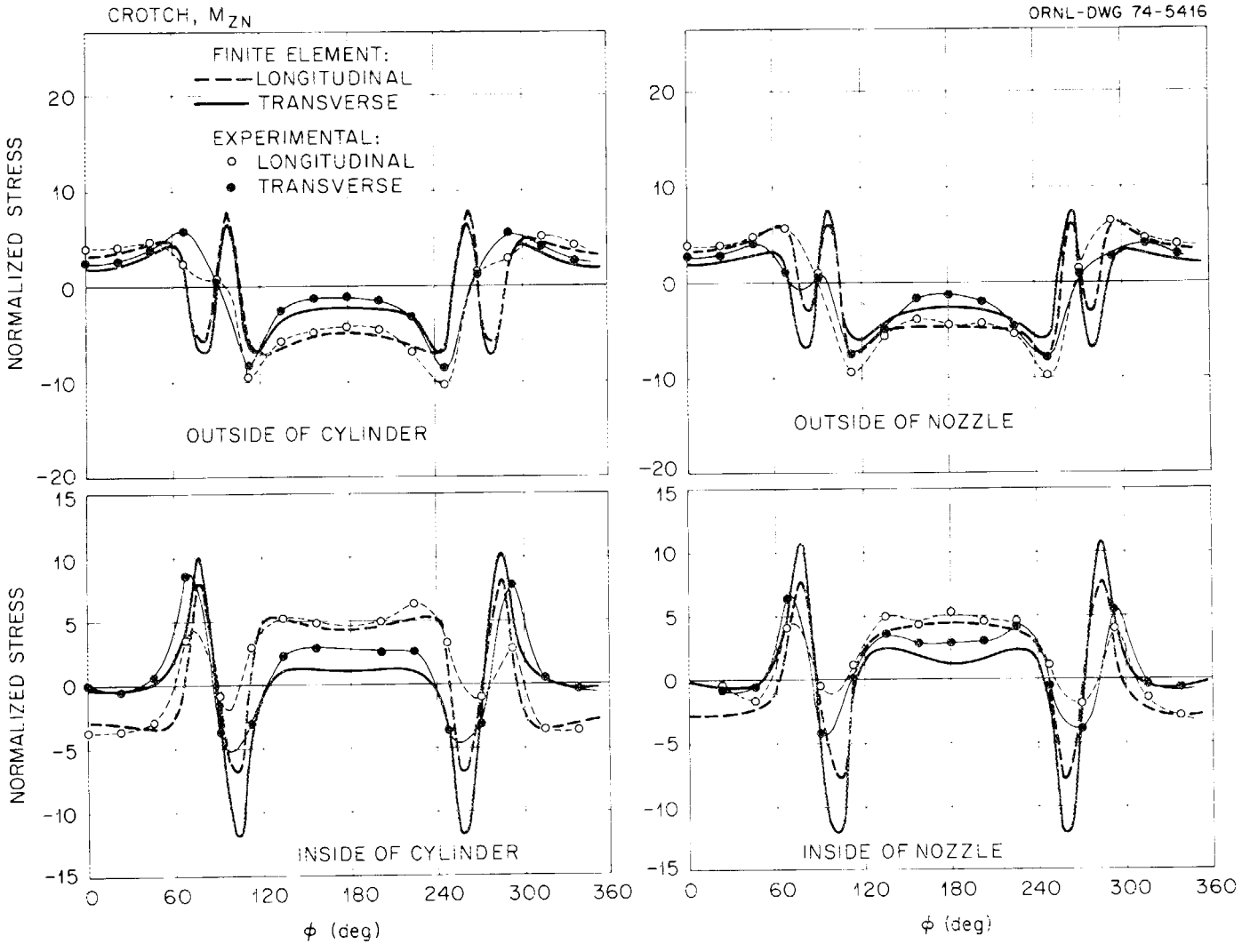

Fig. 21. Measured and predicted stress distributions around the nozzle-cylinder junction for an in-plane moment, M_{ZN}, on the nozzle.

excellent and again shows the complex state of stress with no neutral axis similar to the neutral axis of a beam.

The maximum experimentally determined principal stress ratio was 11.0, with the maximum stress occurring on the outside surface of the nozzle at about 1/2 in. from the junction along the 270° gage line. The maximum theoretical stress occurred on the inside surface of the nozzle at the junction at 265°; the principal stress ratio was 15.2.

4.5 In-Plane Force, F_{XN}, on Nozzle

The comparisons of theory and experiment for an in-plane force of 1200 lb applied to the nozzle are shown in Figs. 22 through 24. The results here are very similar to those for the in-plane bending moment on the nozzle, and overall agreement is excellent except on the inside surface of the nozzle along the 270° gage line.

The maximum experimentally determined principal stress ratio was 13.4, with the maximum stress occurring on the inside surface of the nozzle about 1.0 in. from the junction along the 270° gage line. The maximum theoretical stress occurred on the inside surface of the nozzle at the junction along the 256° plane; the ratio was 17.8.

4.6 Axial Force, F_{YN}, on Nozzle

The comparisons of theory and experiment for an axial force of 4000 lb applied to the nozzle are presented in Figs. 25 through 27. The agreement is excellent along the longitudinal plane (0° gage line). In general the agreement between the distributions along the transverse plane and around the crotch show poor quantitative agreement between theory and experiment.

The experimentally determined maximum principal stress ratio was 13.4, with the maximum stress occurring on the outside surface of the nozzle on the 180° plane at the junction. The theoretically determined maximum stress occurred on the inside surface of the cylinder on the 256° plane at the junction; the ratio was 17.2.

ORNL-DWG 74-4039

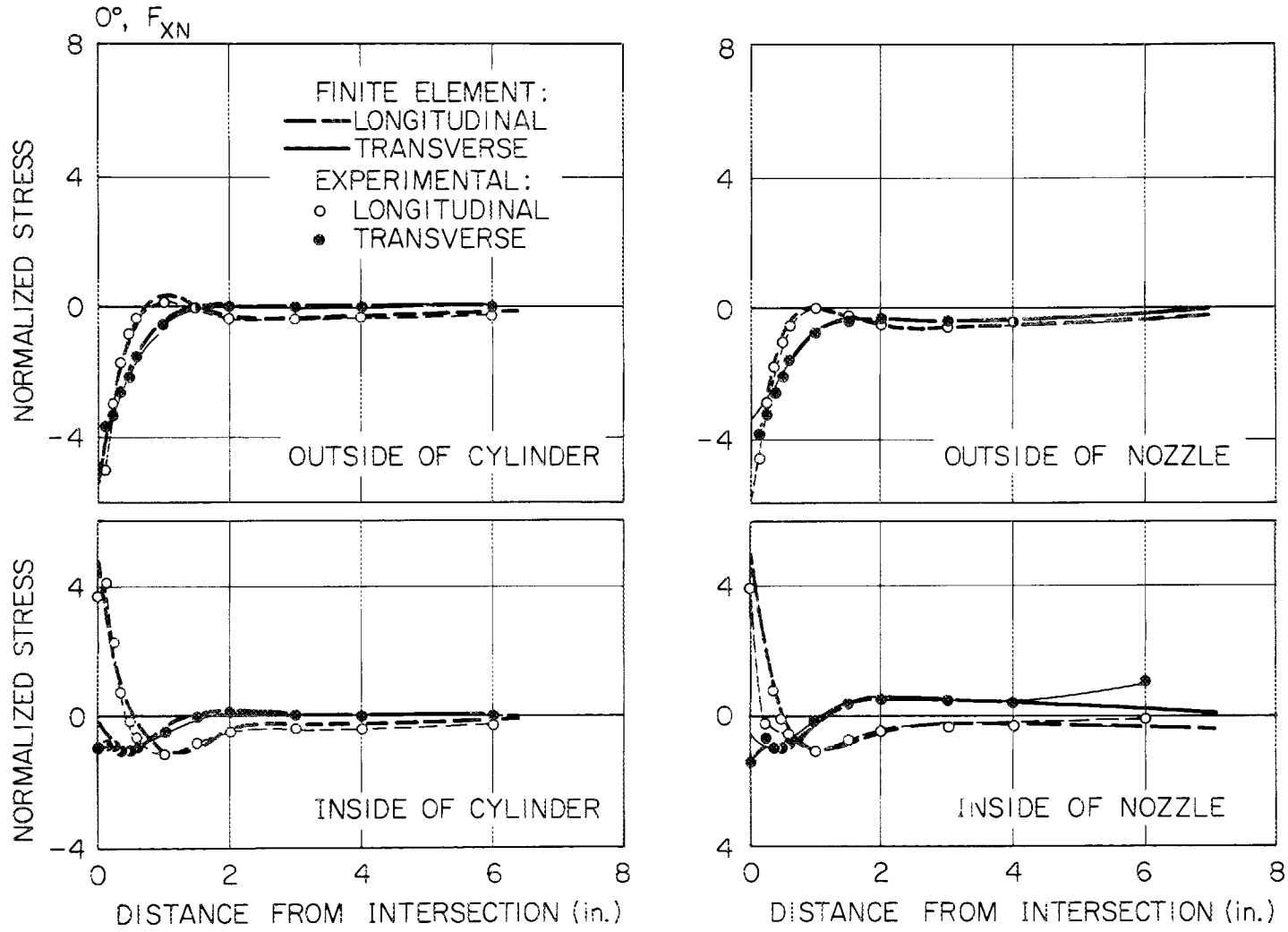

Fig. 22. Measured and predicted stress distributions at 0° for an in-plane force, F_{XN}, on the nozzle.

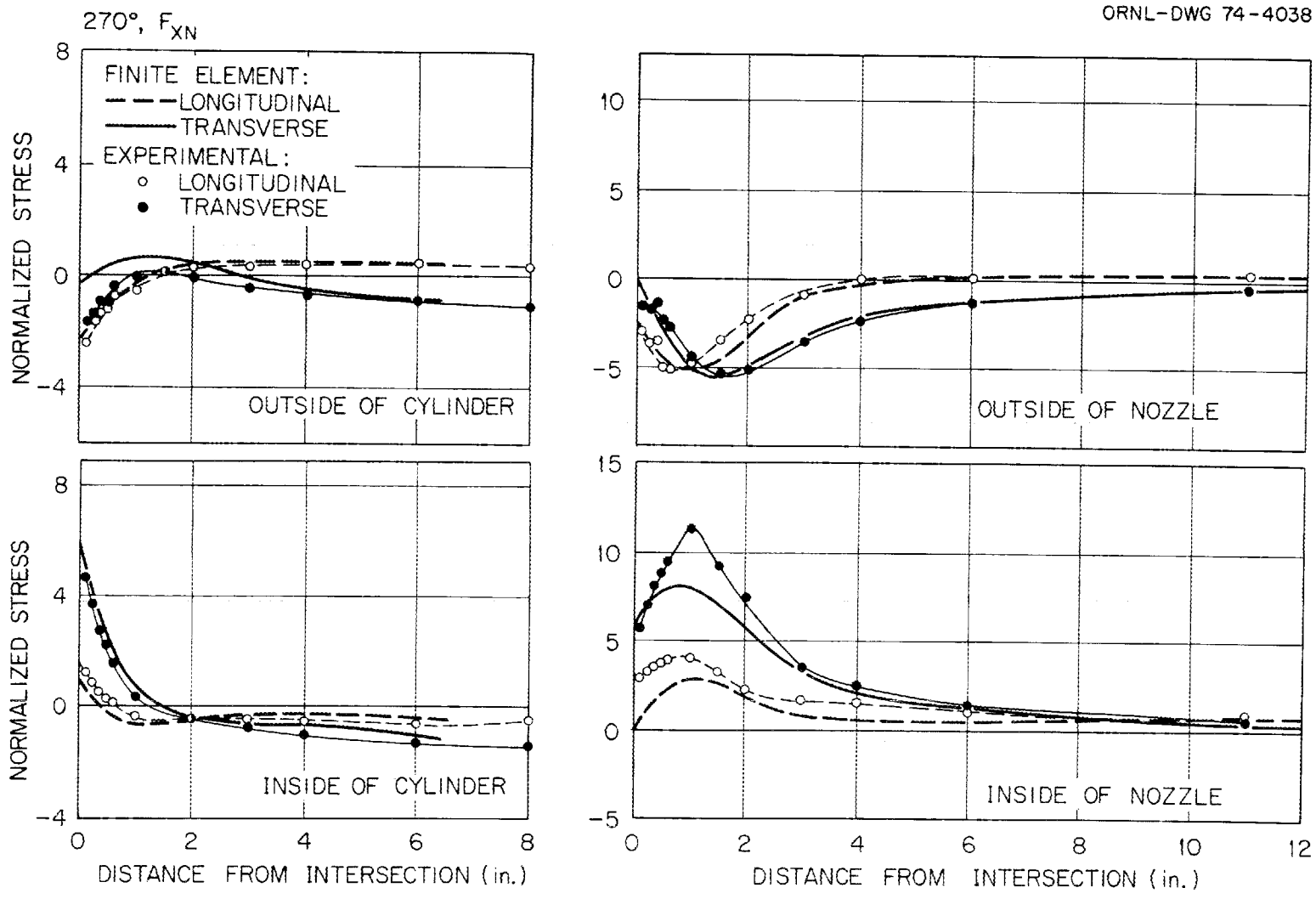

Fig. 23. Measured and predicted stress distributions at 270° for an in-plane force, F_{XN}, on the nozzle.

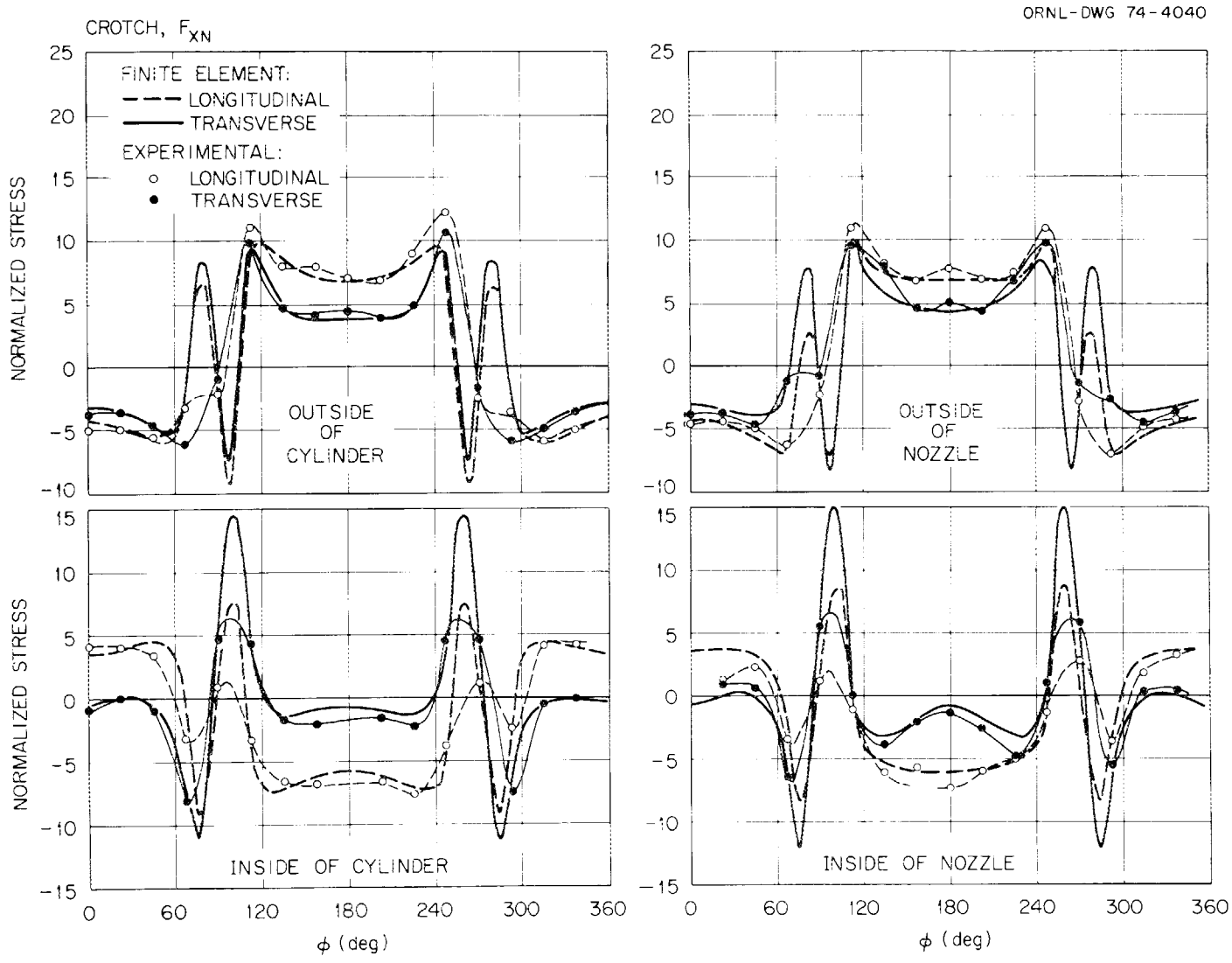

Fig. 24. Measured and predicted stress distributions around the nozzle-cylinder junction for an in-plane force, F_{XN}, on the nozzle.

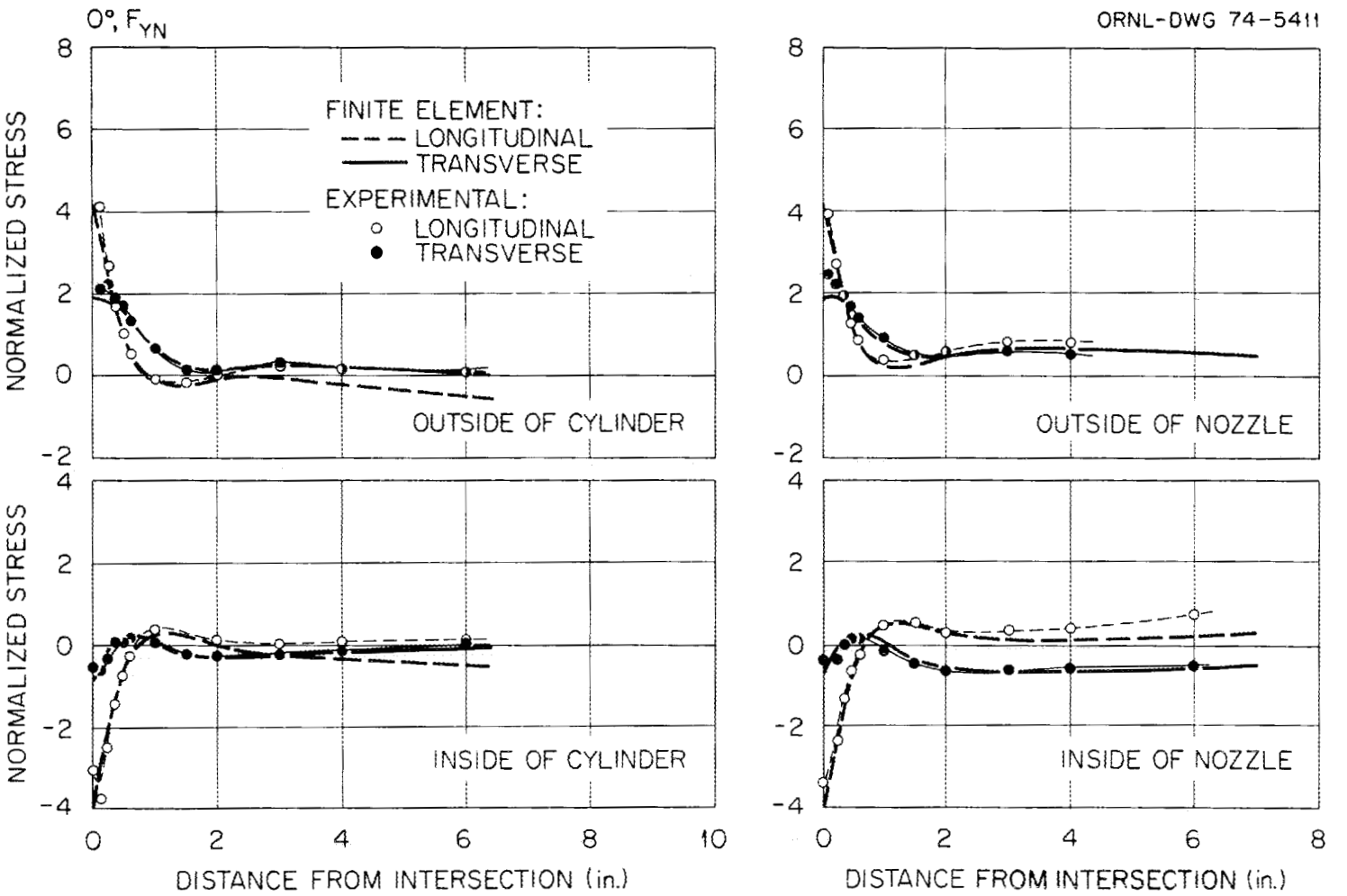

Fig. 25. Measured and predicted stress distributions at 0° for an axial force, F_{YN}, on the nozzle.

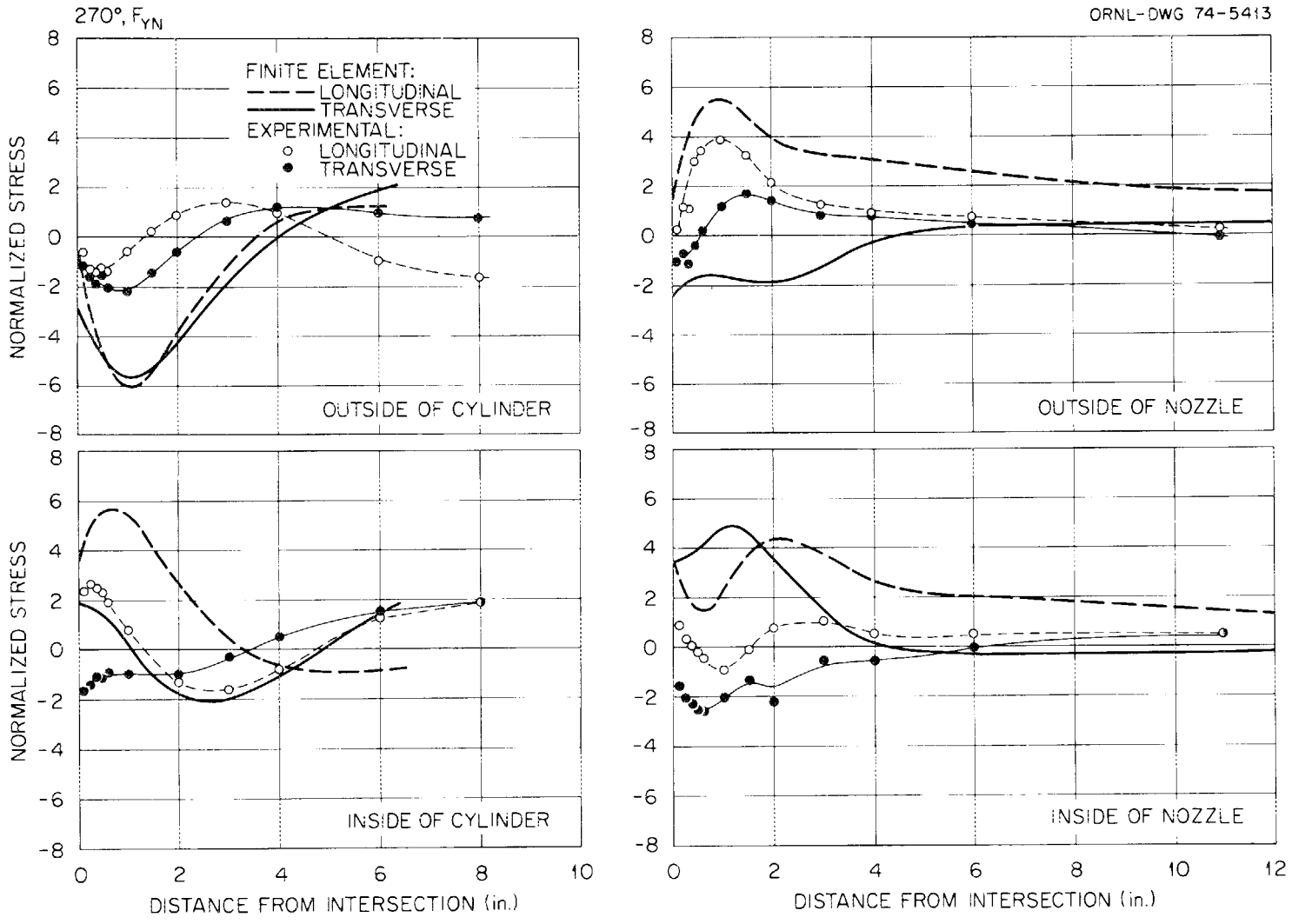

Fig. 26. Measured and predicted stress distributions at 270° for an axial force, F_{YN}, on the nozzle.

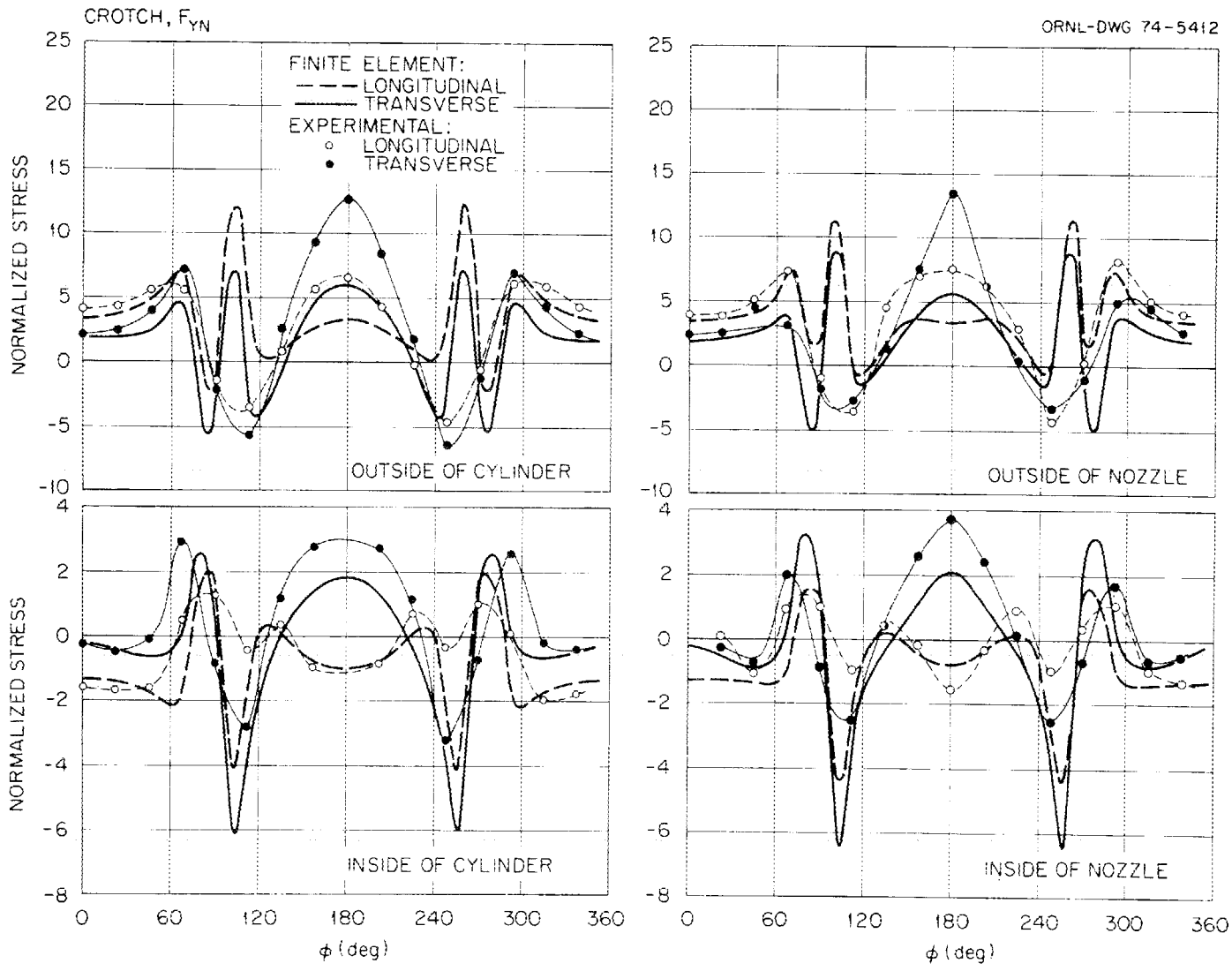

Fig. 27. Measured and predicted stress distributions around the nozzle-cylinder junction for an axial force, F_{YN}, on the nozzle.

4.7 Out-of-Plane Force, F_{ZN}, on Nozzle

The comparisons of theory and experimental data for an out-of-plane force of 600 lb applied to the nozzle are presented in Figs. 28 through 30. The results are very similar to those for an out-of-plane moment on the nozzle, and the overall agreement between theory and experiment is again very good.

The experimentally determined maximum principal stress (ratio 15.9) occurred on the inside surface of the cylinder on the 247° plane at the junction. The theoretically determined maximum stress (ratio 24.3) occurred on the outer surface of the cylinder on the 256° plane at the junction.

4.8 Torsional Moment Loading, M_{XC}, on Cylinder

The comparisons of theory and experiment for a torsional moment of 20,000 in.-lb applied to the cylinder are presented in Figs. 31 through 33. The experimental stresses are low in the longitudinal and transverse planes of symmetry and rise to their maximum levels on approximately the 67, 112, 247, and 292° planes. The agreement between theory and experiment is excellent along the crotch line. The sharp rise in the stresses at the junction of the nozzle is probably caused by neglecting the sixth degree of freedom.

The experimentally determined maximum stress (ratio 24.2) occurred on the inside surface of the nozzle on the 292° plane at the junction. The theoretically determined maximum stress (ratio 37.5) occurred on the outside surface of the cylinder on the 284° plane at the junction.

4.9 Out-of-Plane Moment Loading, M_{YC}, on Cylinder

The comparisons of theory and experiment for an out-of-plane moment loading of 60,000 in.-lb applied to the cylinder are presented in Figs. 34 through 36. The stress comparisons along the longitudinal plane (0° plane) seem to be poor, while the agreement between theory and experiment along the transverse plane is good and is excellent around the crotch. The experimentally determined maximum principal stress (ratio 4.5) occurred on the inside

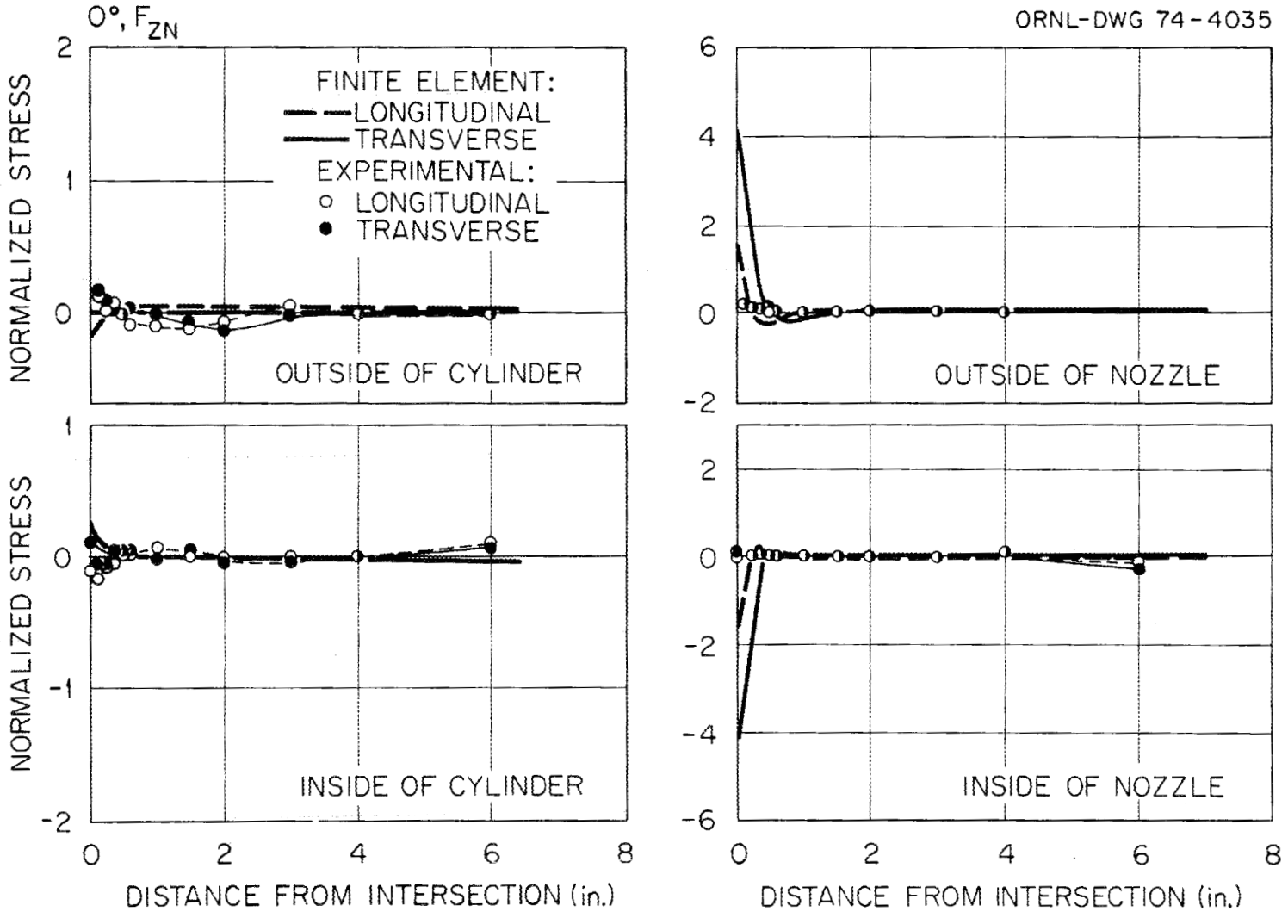

Fig. 28. Measured and predicted stress distributions at 0° for an out-of-plane force, F_{ZN}, on the nozzle.

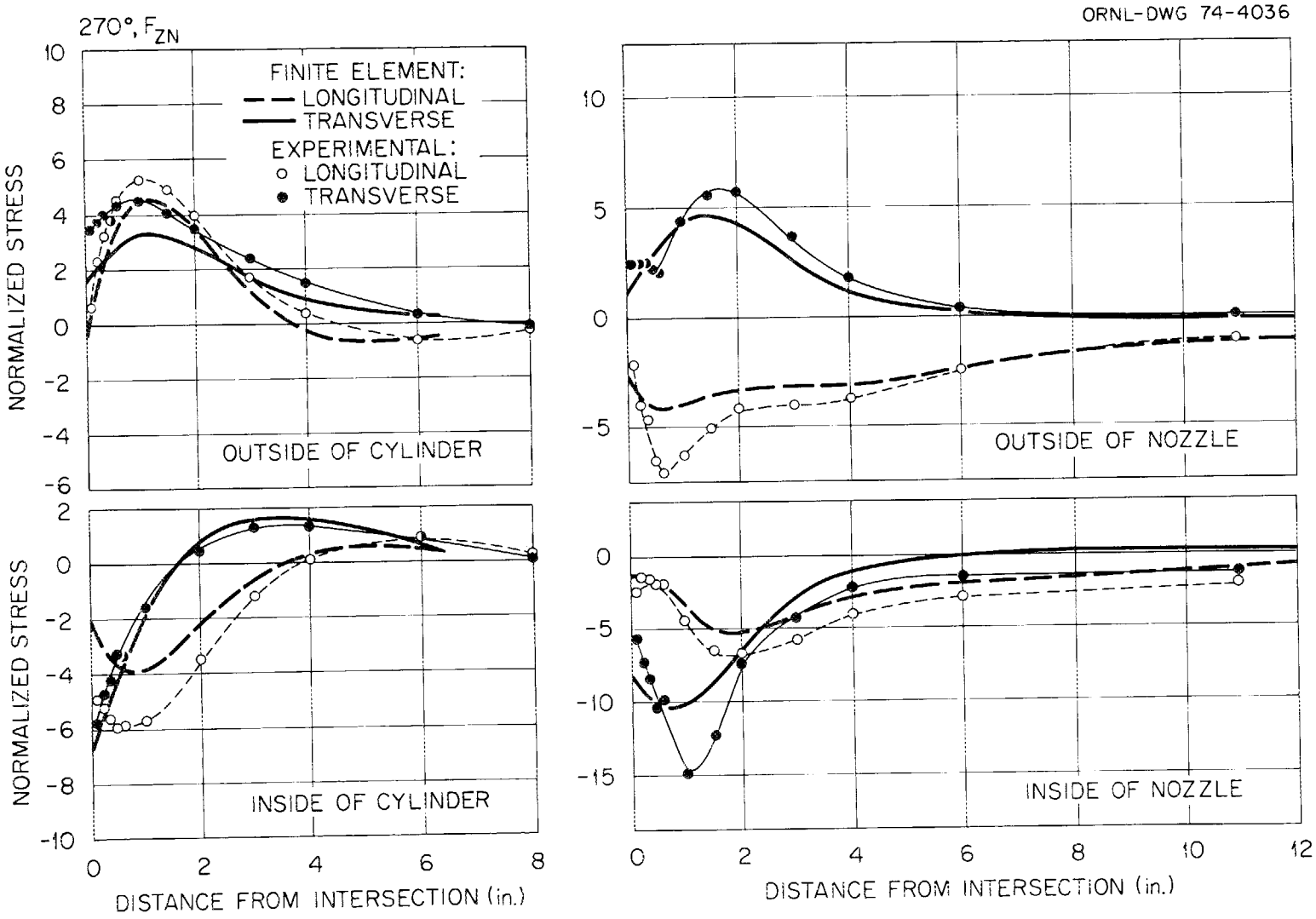

Fig. 29. Measured and predicted stress distributions at 270° for an out-of-plane force, F_{ZN}, on the nozzle.

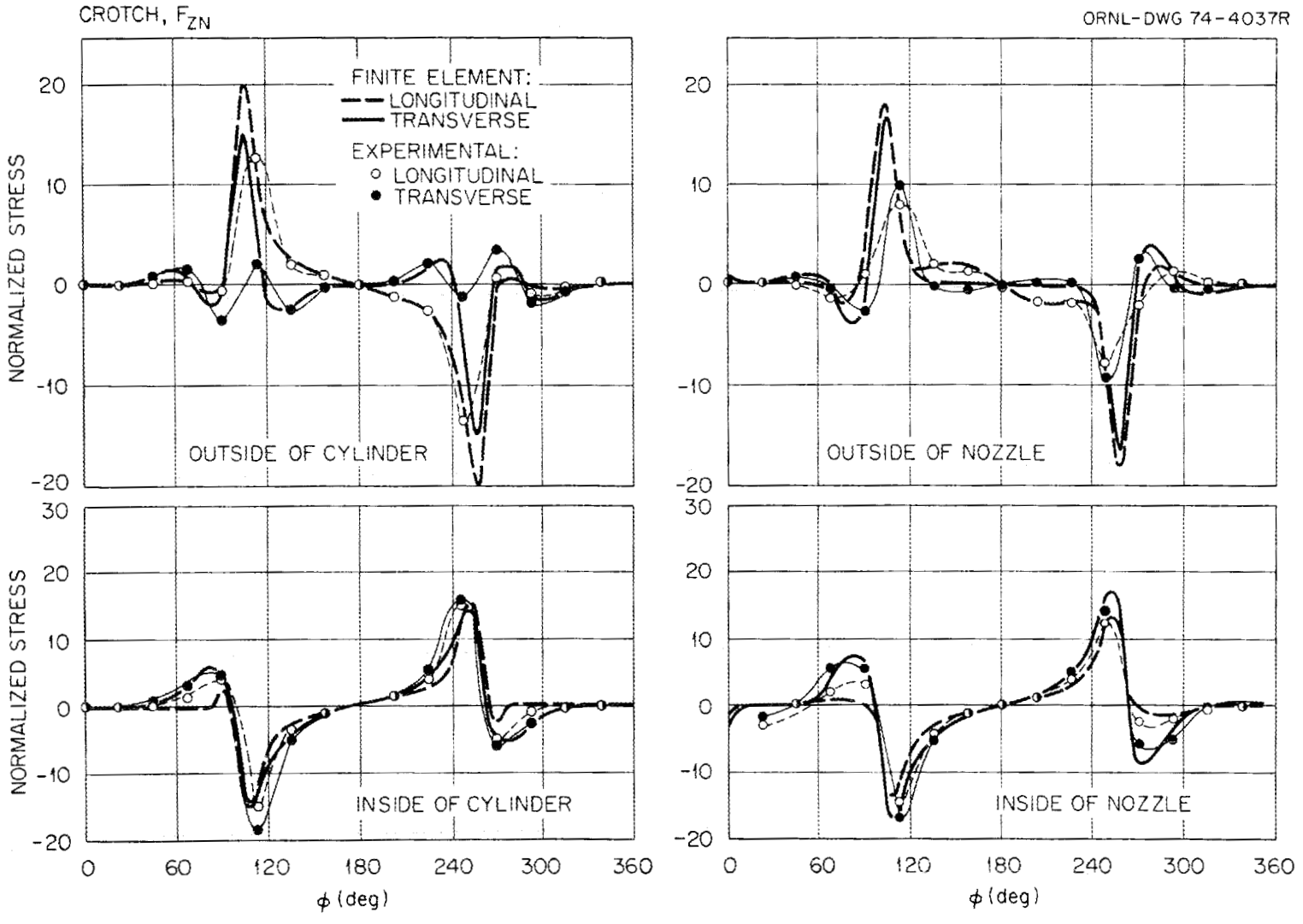

Fig. 30. Measured and predicted stress distributions around the nozzle-cylinder junction for an out-of-plane force, F_{ZN}, on the nozzle.

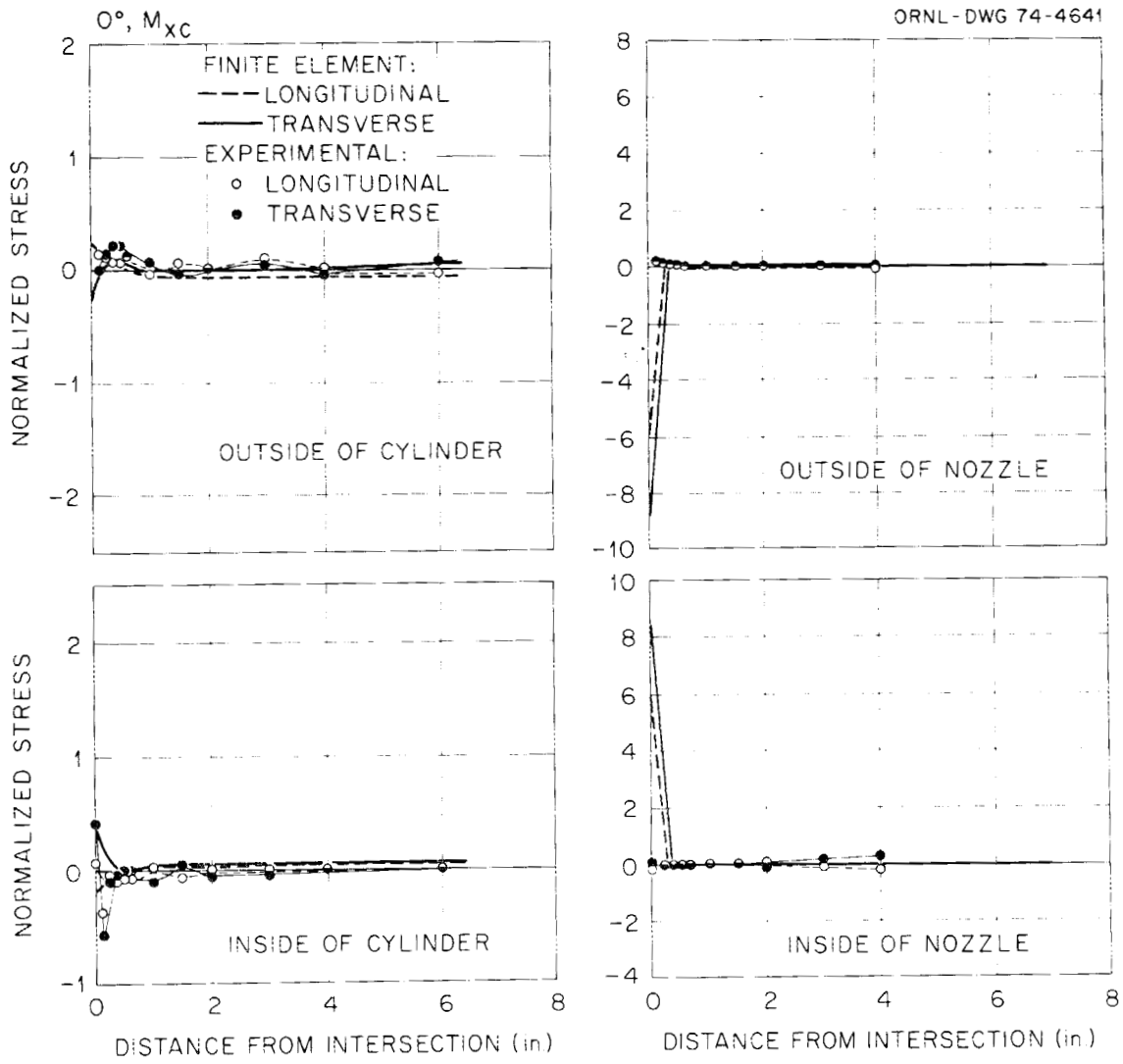

Fig. 31. Measured and predicted stress distributions at 0° for a torsional moment, M_{XC}, on the cylinder.

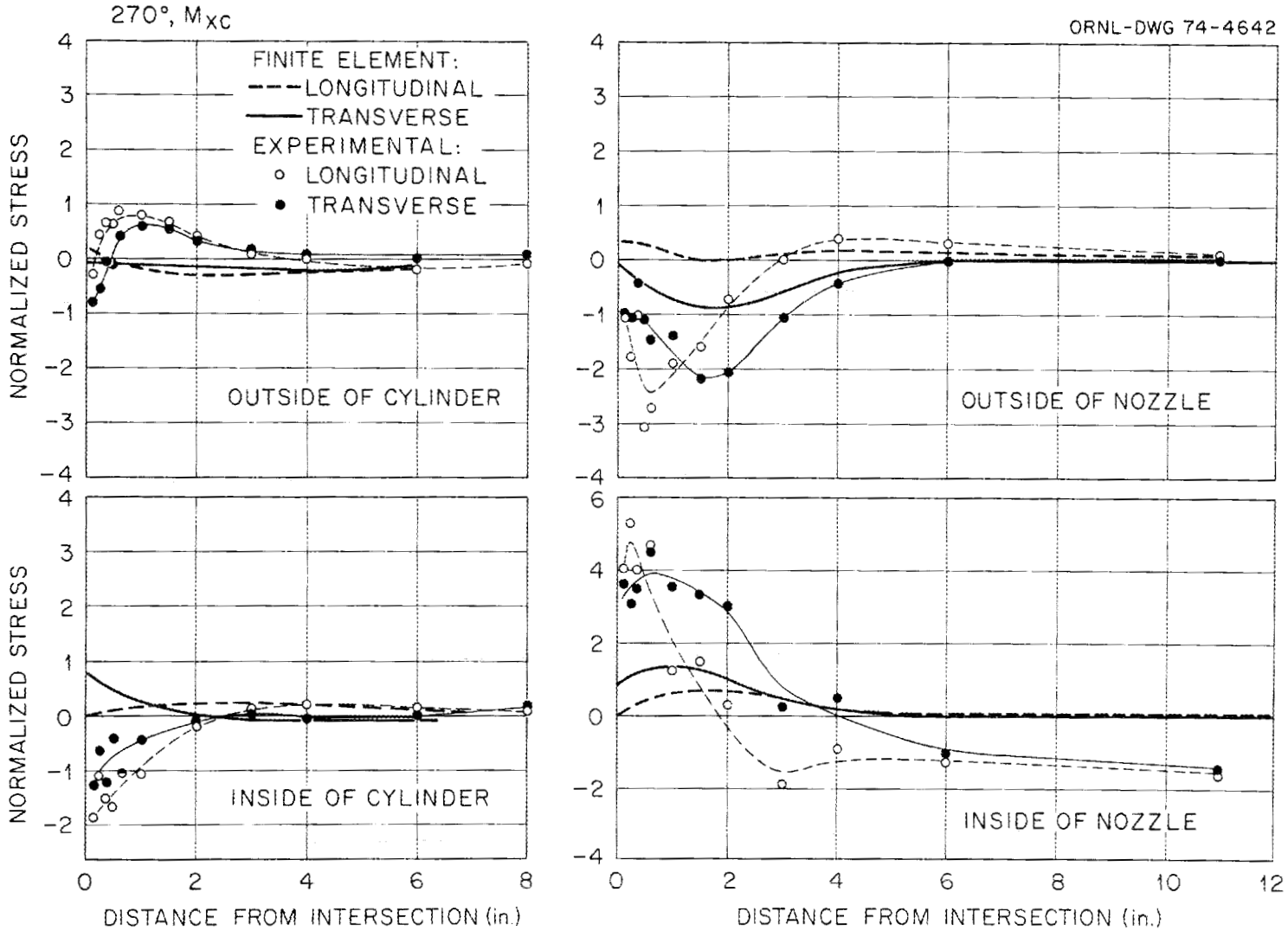

Fig. 32. Measured and predicted stress distributions at 270° for a torsional moment, M_{XC}, on the cylinder.

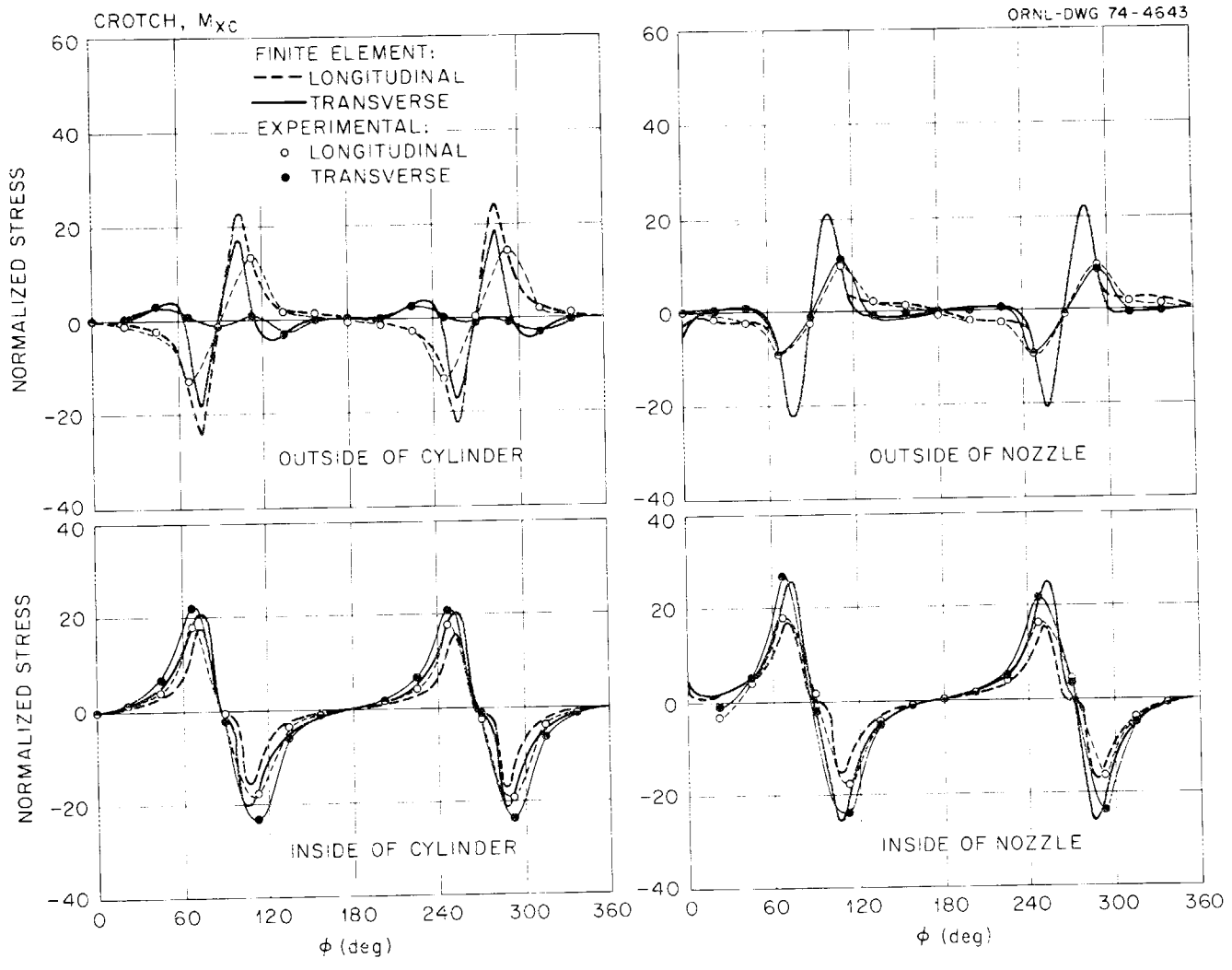

Fig. 33. Measured and predicted stress distributions around the nozzle-cylinder junction for a torsional moment, M_{XC}, on the cylinder.

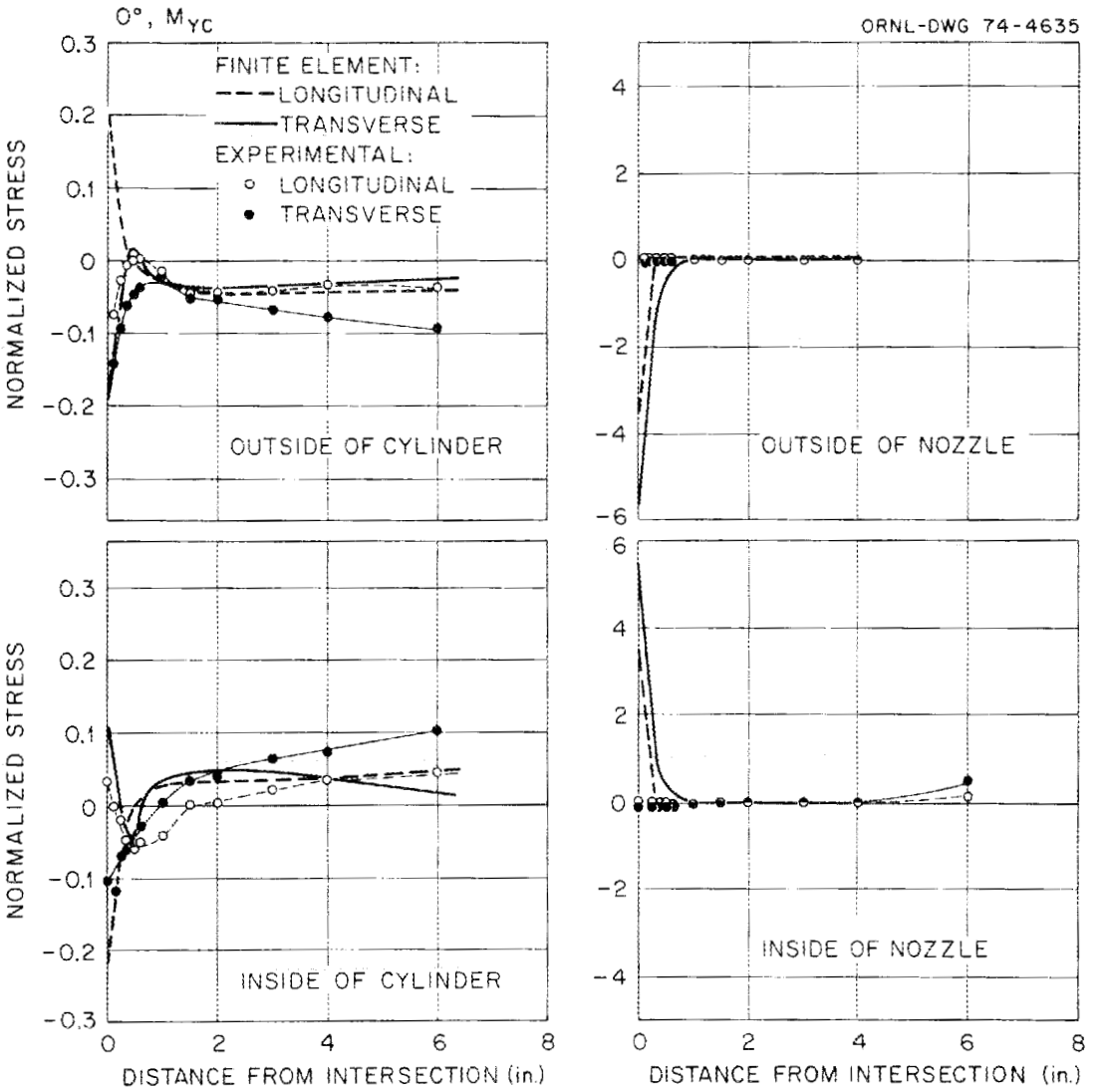

Fig. 34. Measured and predicted stress distributions at 0° for an out-of-plane moment, M_{YC}, on the cylinder.

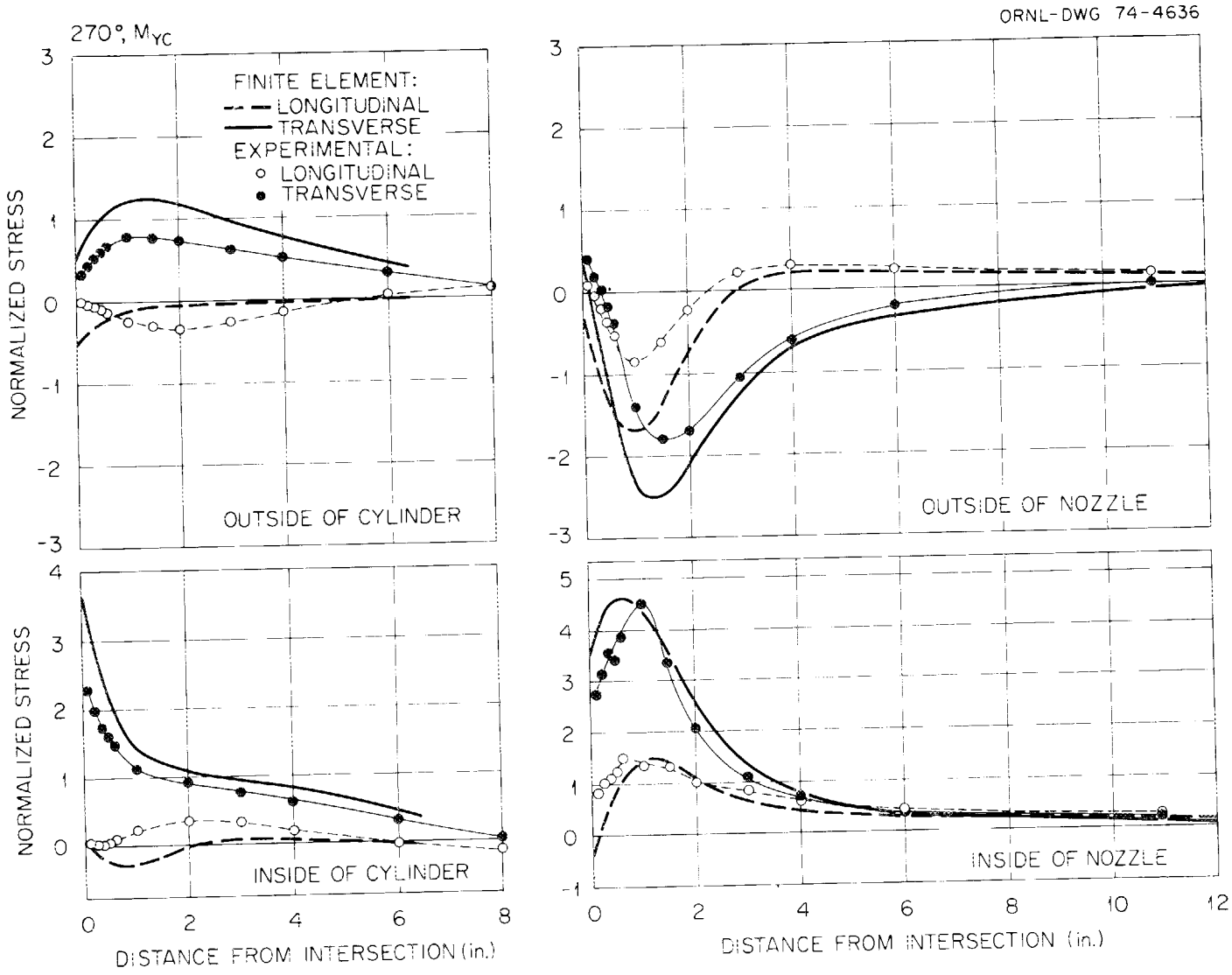

Fig. 35. Measured and predicted stress distributions at 270° for an out-of-plane moment, M_{YC}, on the cylinder.

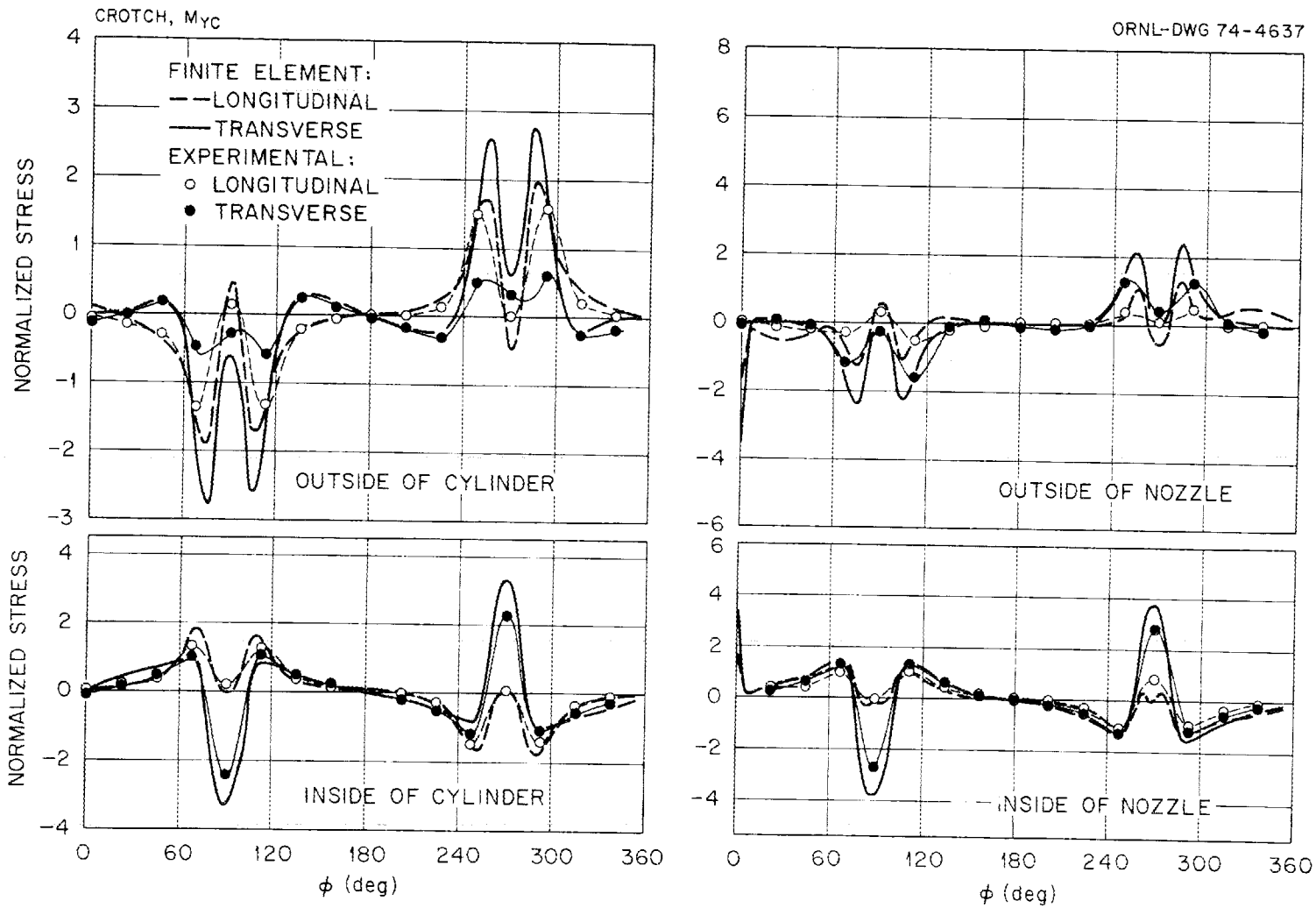

Fig. 36. Measured and predicted stress distributions around the nozzle-cylinder junction for an out-of-plane moment, M_{YC}, on the cylinder.

surface of the nozzle along the 270° plane at about 1.0 in. from the junction. The theoretically determined stress occurred on the outside surface of the nozzle along the 0° plane at the junction; the ratio was 5.9.

4.10 In-Plane Moment Loading, M_{ZC}, on Cylinder

The comparisons of theory and experiment for an in-plane moment loading of 24,000 in.-lb applied to the cylinder are presented in Figs. 37 through 39. Here the stress levels are a maximum in the transverse plane of symmetry, as shown in Figs. 38 and 39, and the comparisons between theory and experiment are excellent except for the inside surface of the nozzle along the 270° plane.

The experimentally and theoretically determined maximum stresses occurred on the inside surface of the nozzle along the 270° plane about 1.0 in. from the junction. The experimental maximum ratio was 14.9, while the theoretical maximum was 10.1.

4.11 Axial Force, F_{XC}, on Cylinder

The comparisons of theory and experiment for an axial force of 8000 lb applied to the cylinder are presented in Figs. 40 through 42. In general, the agreement between theory and experiment is very good, and along the 0° plane the agreement is excellent.

The experimentally and theoretically determined maximum stresses occurred on the inside surface of the nozzle along the 270° plane at about 1.0 in. from the junction. The experimental maximum was 14.4, while the theoretical maximum was 14.7.

4.12 In-Plane Force, F_{YC}, on Cylinder

The comparisons of theory and experiment for an in-plane force of 1000 lb applied to the cylinder are shown in Figs. 43 through 45. The agreement is very good except on the inside surface of the nozzle along the 270° plane.

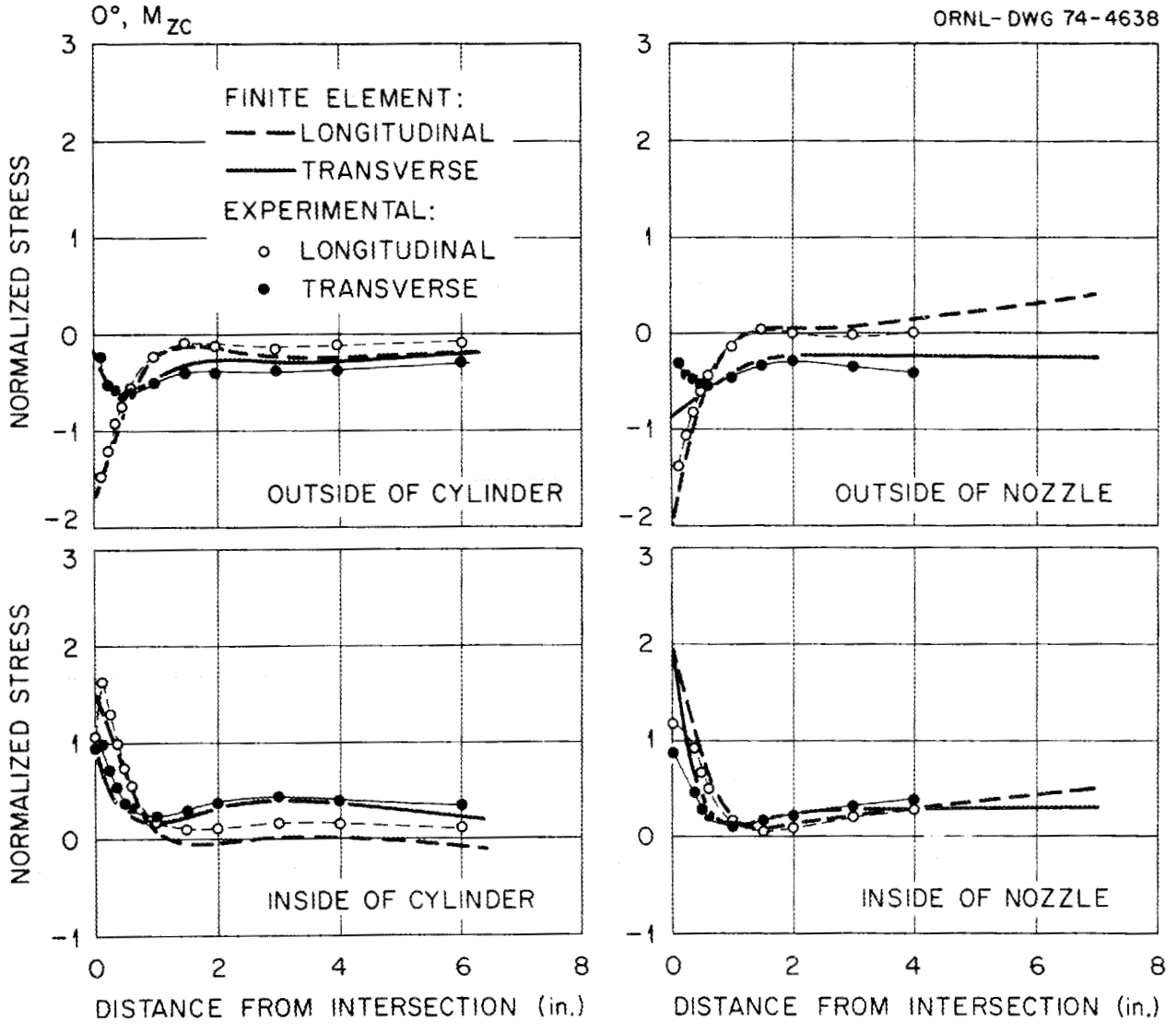

Fig. 37. Measured and predicted stress distributions at 0° for an in-plane moment, M_{ZC}, on the cylinder.

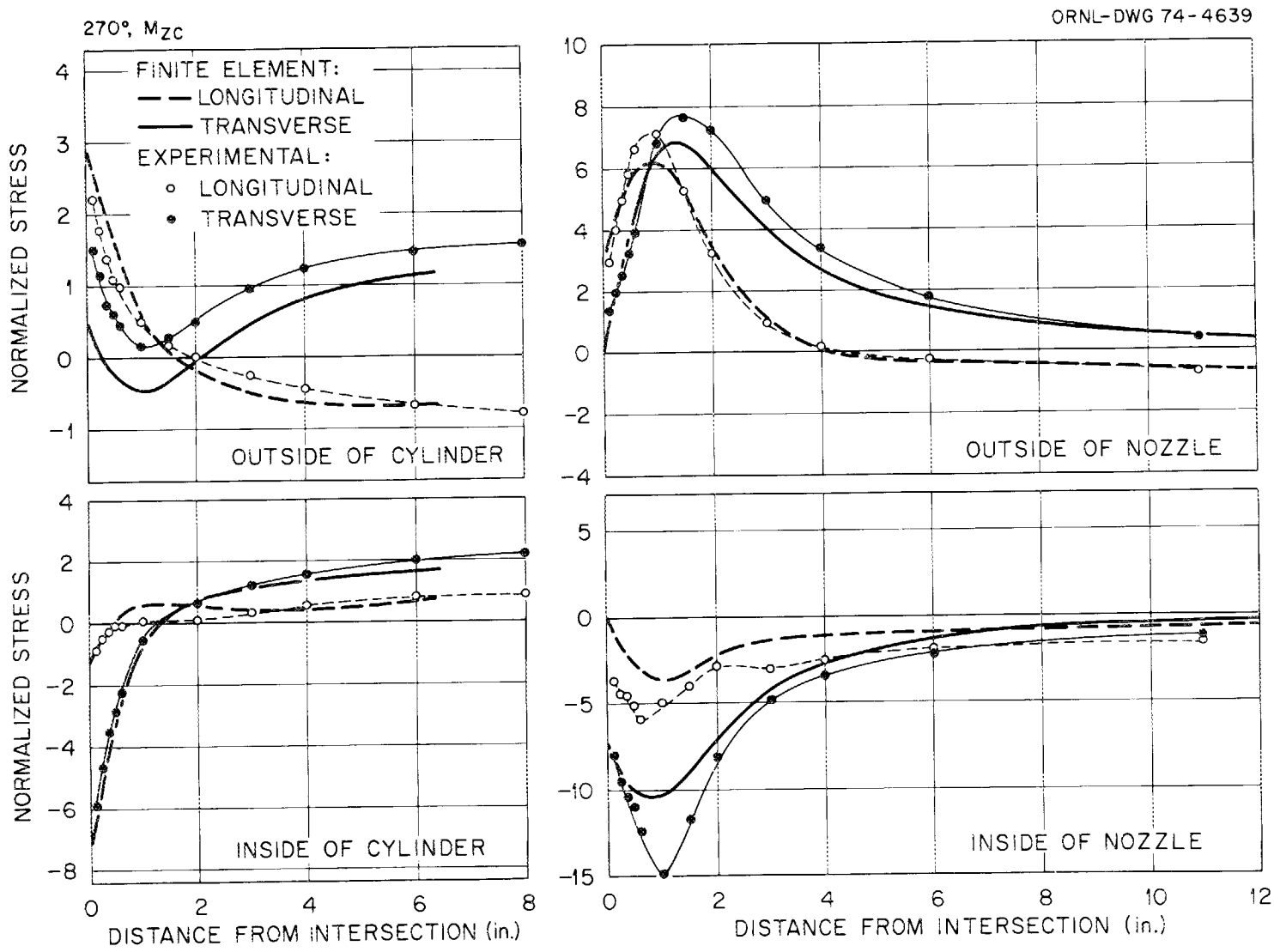

Fig. 38. Measured and predicted stress distributions at 270° for an in-plane moment, M_{ZC}, on the cylinder.

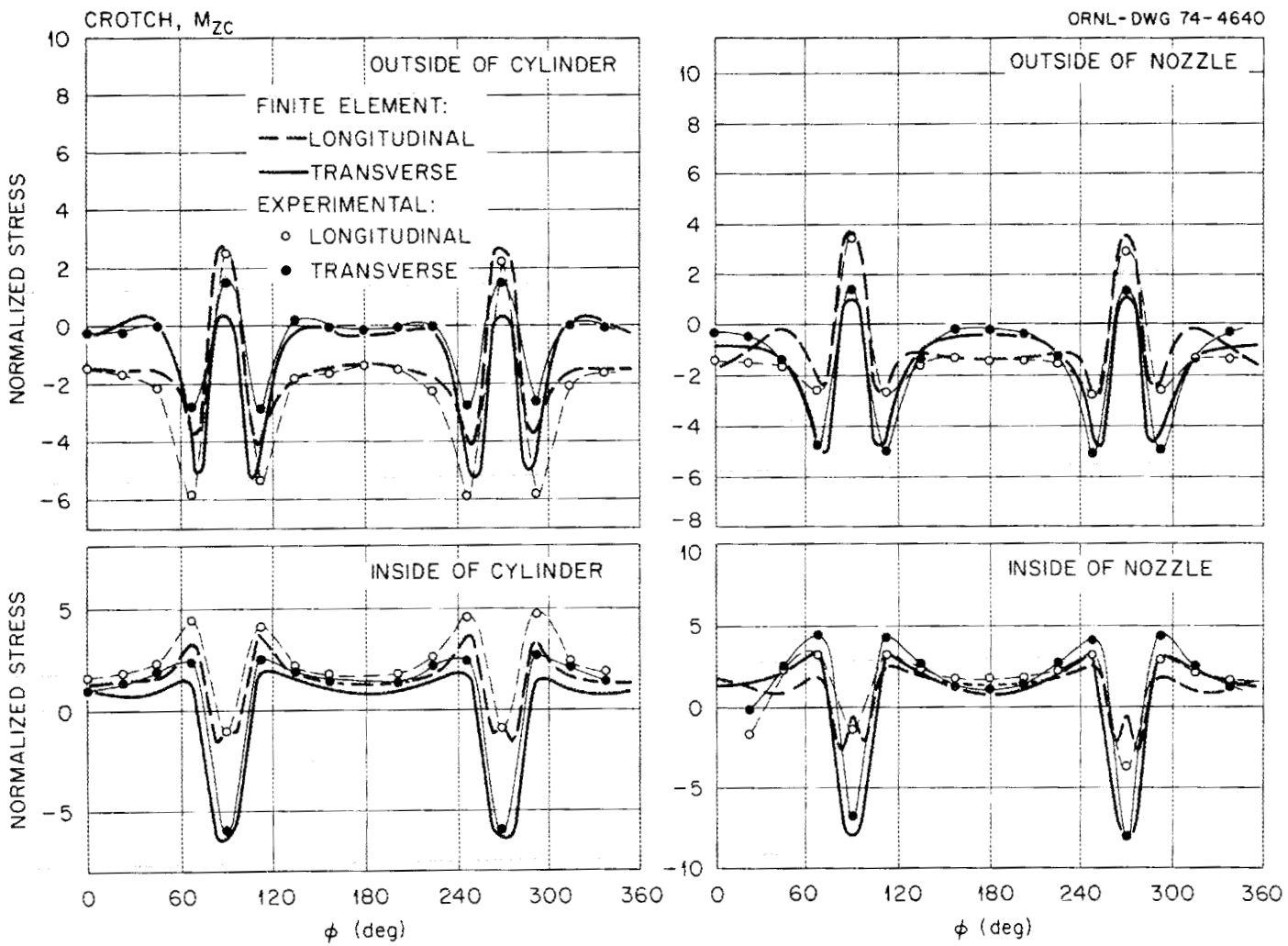

Fig. 39. Measured and predicted stress distributions around the nozzle-cylinder junction for an in-plane moment, M_{ZC}, on the cylinder.

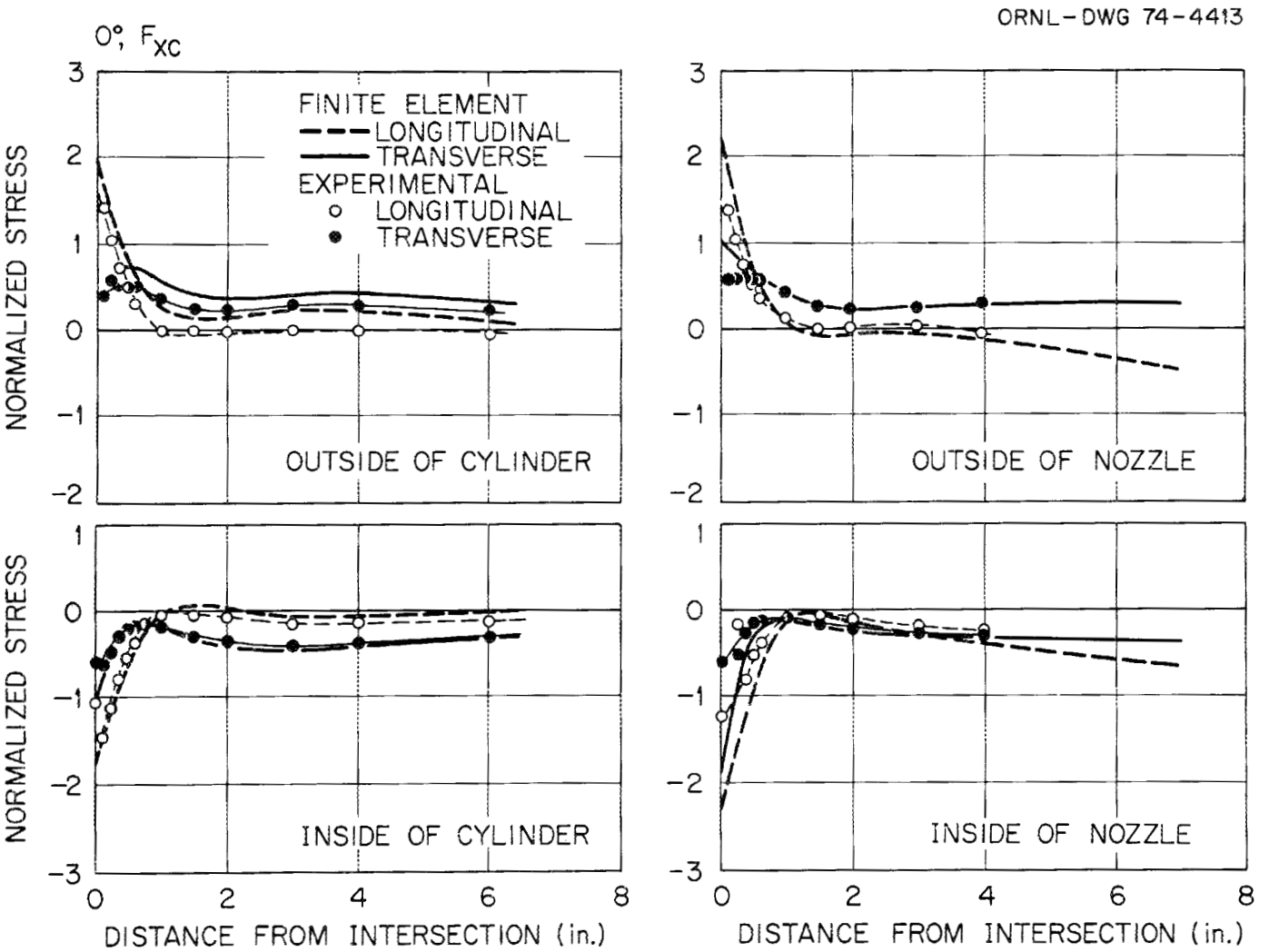

Fig. 40. Measured and predicted stress distributions at 0° for an axial force, F_{XC}, on the cylinder.

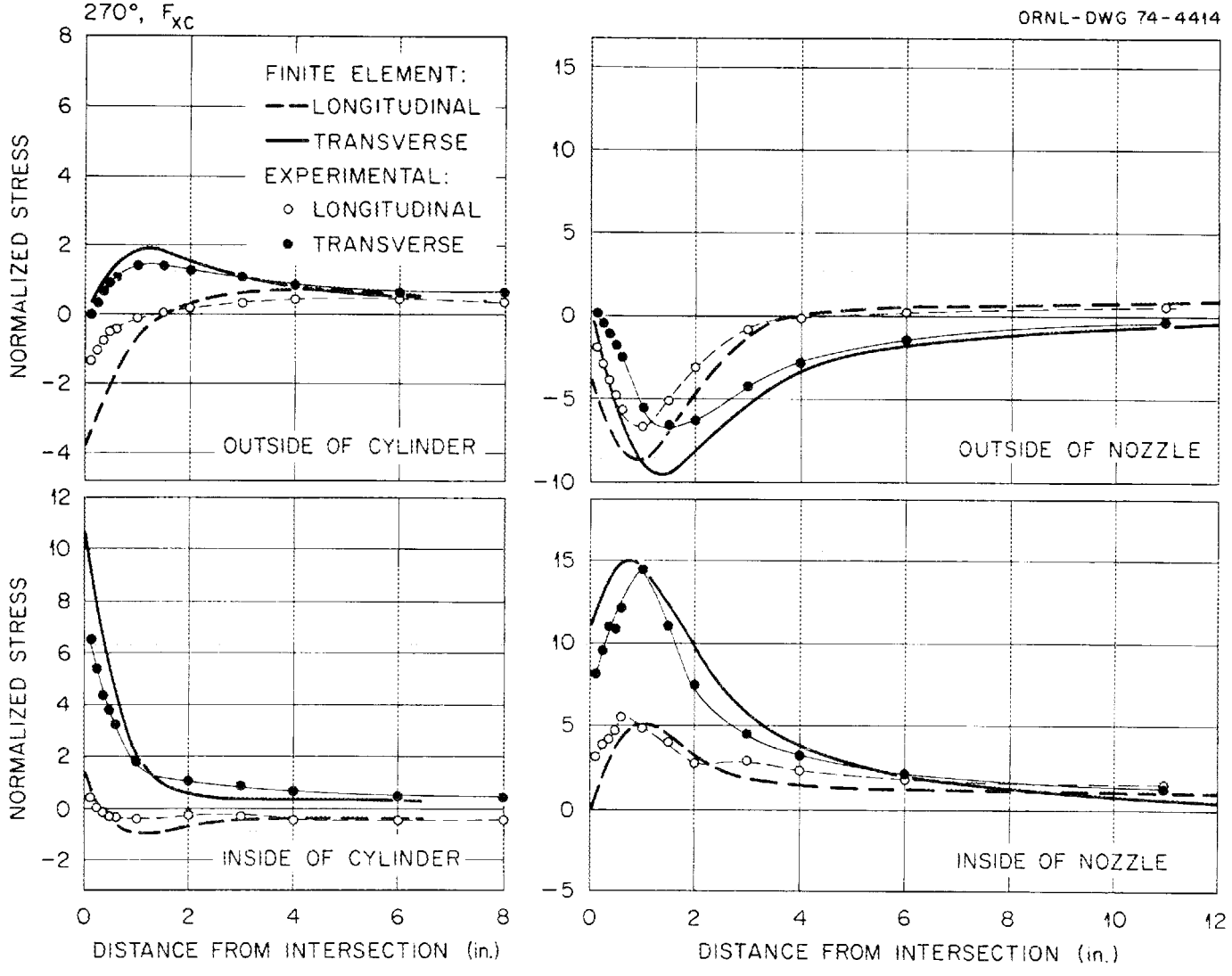

Fig. 41. Measured and predicted stress distributions at 270° for an axial force, F_{XC}, on the cylinder.

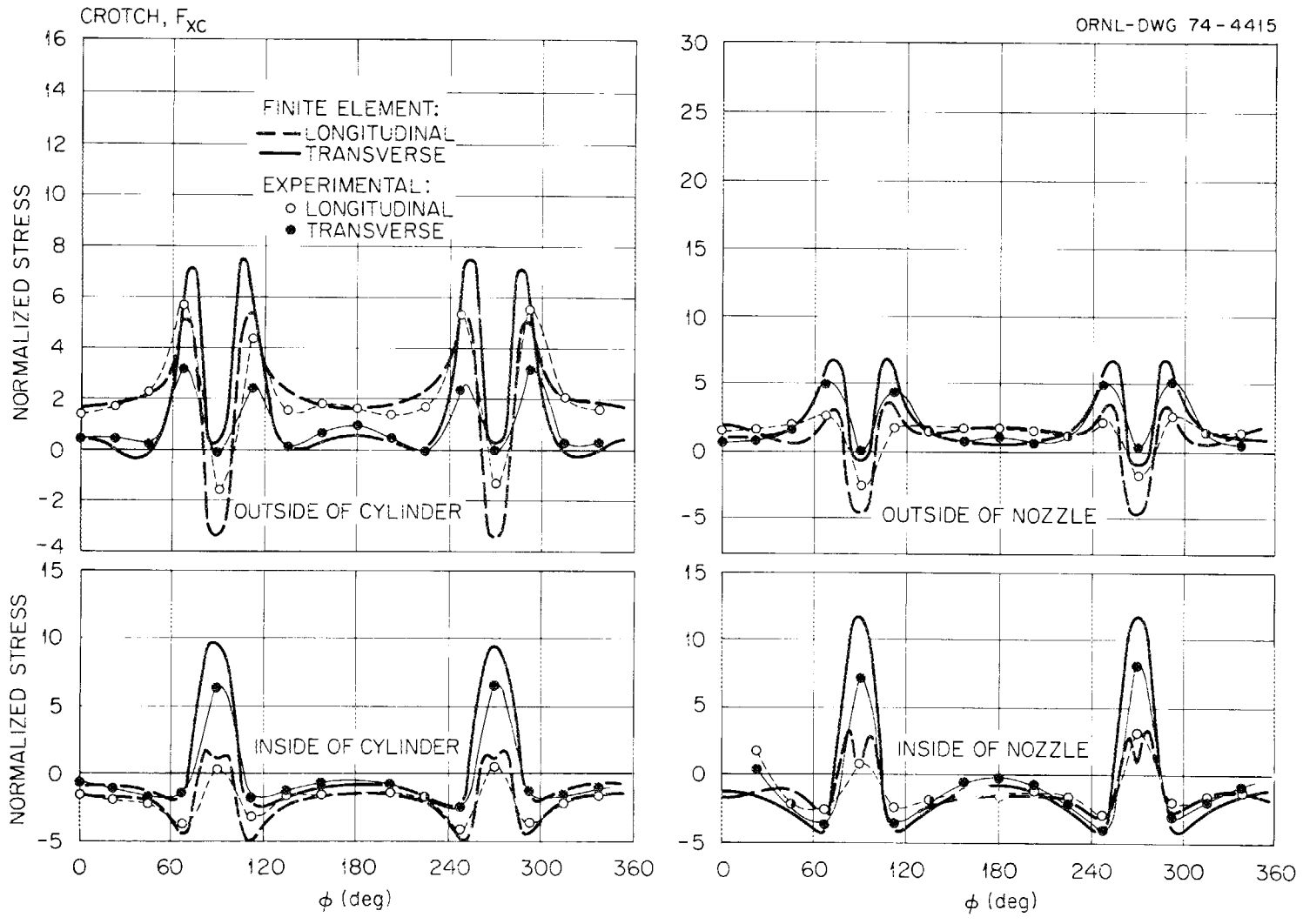

Fig. 42. Measured and predicted stress distributions around the nozzle-cylinder junction for an axial force, F_{XC}, on the cylinder.

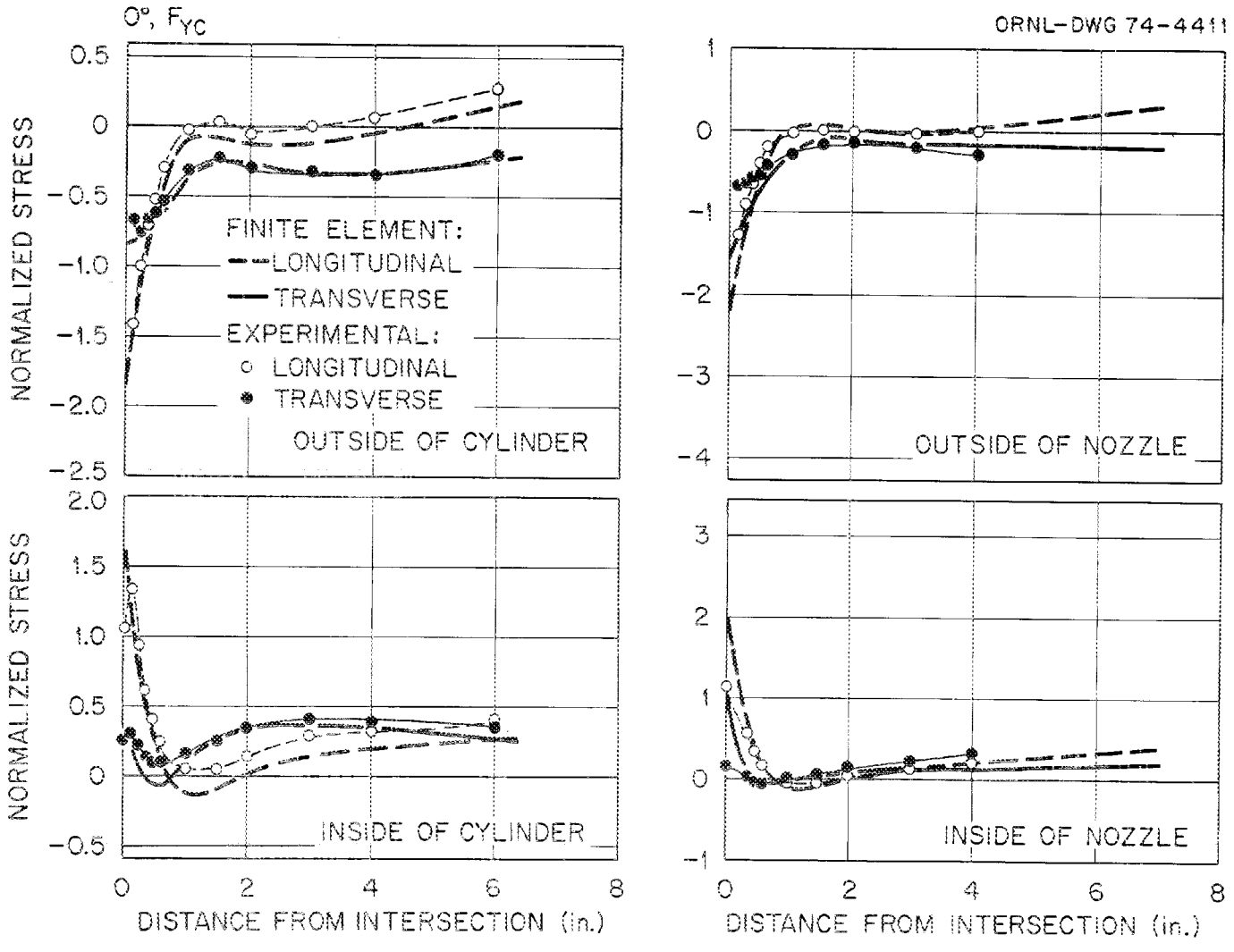

Fig. 43. Measured and predicted stress distributions at 0° for an in-plane force, F_{YC}, on the cylinder.

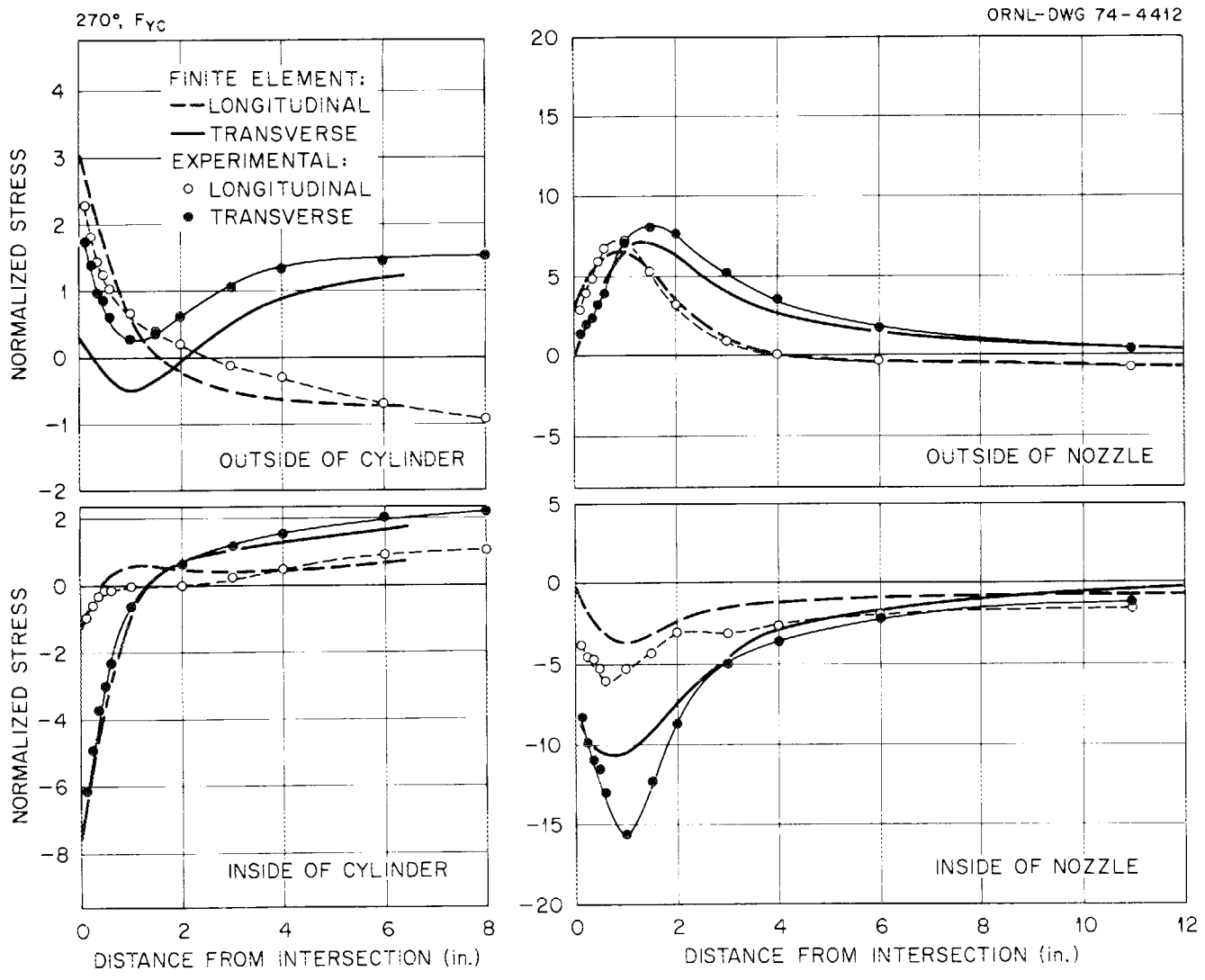

Fig. 44. Measured and predicted stress distributions at 270° for an in-plane force, F_{YC}, on the cylinder.

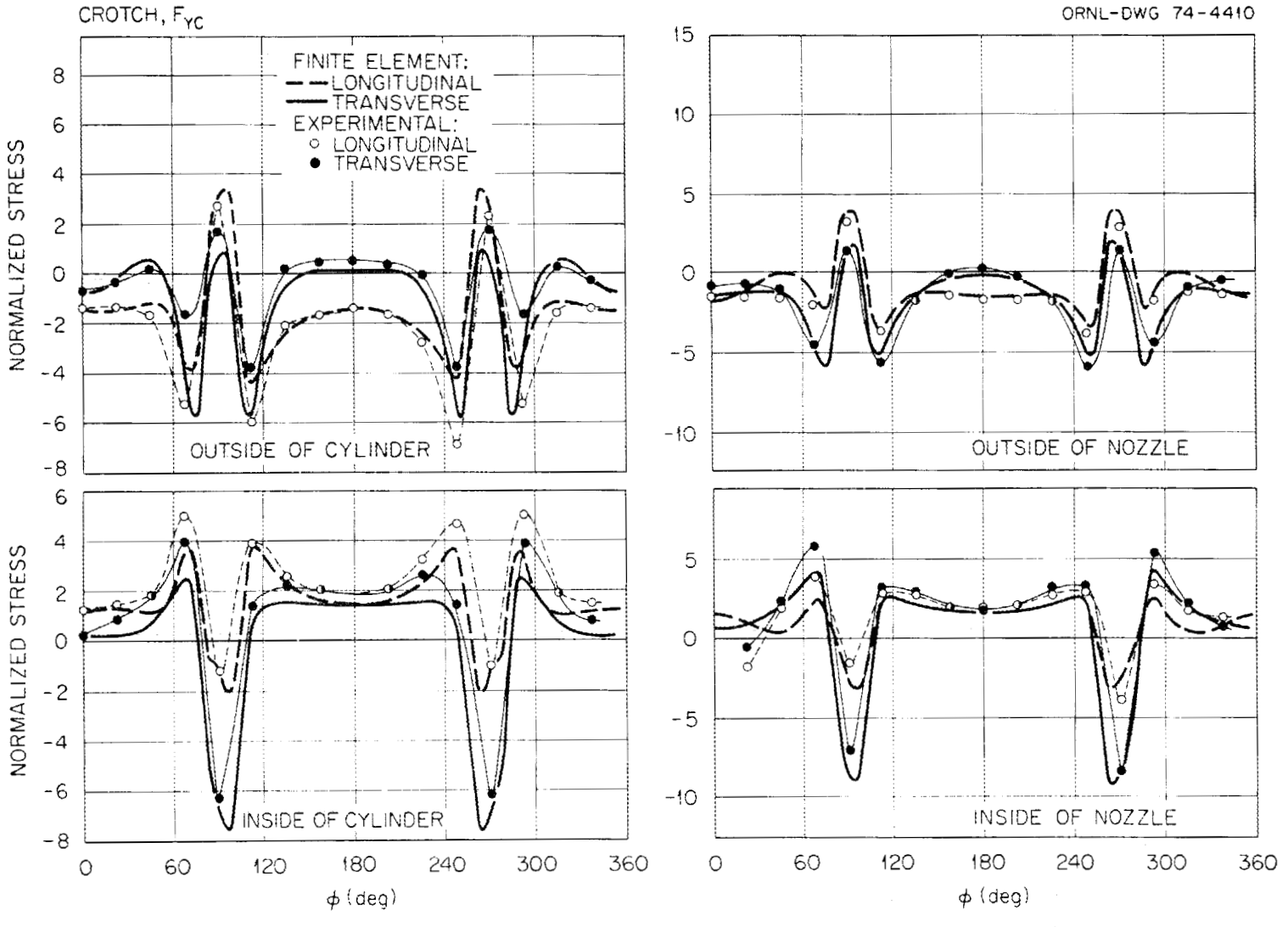

Fig. 45. Measured and predicted stress distributions around the nozzle-cylinder junction for an in-plane force, F_{YC}, on the cylinder.

Both the experimentally and theoretically determined maximum stresses occurred on the inside surface of the nozzle along the 270° plane at about 1.0 in. from the junction. The experimental maximum was 15.7, while the theoretical maximum was 10.7.

4.13 Out-of-Plane Force, F_{ZC}, on Cylinder

The comparisons of theory and experiment for an out-of-plane force of 1200 lb applied to the cylinder are shown in Figs. 46 through 48. The stress comparisons along the longitudinal plane (0° plane) seem to be excellent, while the agreement between theory and experiment along the transverse plane and around the crotch is poor. The sharp rise in the stress at the junction is probably caused by neglecting the sixth degree of freedom.

The experimentally determined maximum stress (ratio 6.9) occurred on the inside surface of the nozzle along the 270° plane at about 1.0 in. from the junction. The theoretically determined maximum stress (ratio 9.9) occurred on the outside surface of the cylinder along the 256° plane at the junction.

4.14 Out-of-Plane Moment, M_{XN}, on Nozzle with Restraints

The measured and predicted stress distributions for an out-of-plane moment loading of 10,000 in.-lb applied to the nozzle are shown in Figs. 49 through 51. The results here are very similar to those for the out-of-plane bending moment on the nozzle, and the overall agreement is very good except for the transverse stress on the inside surface of the nozzle along the 270° plane.

The maximum experimentally determined stress ratio (14.9) occurred on the inside surface of the nozzle along the 270° plane about 1.0 in. from the junction. The maximum theoretically determined stress ratio (11.8) occurred on the outside surface of the cylinder along either the 256 or 284° plane at the junction.

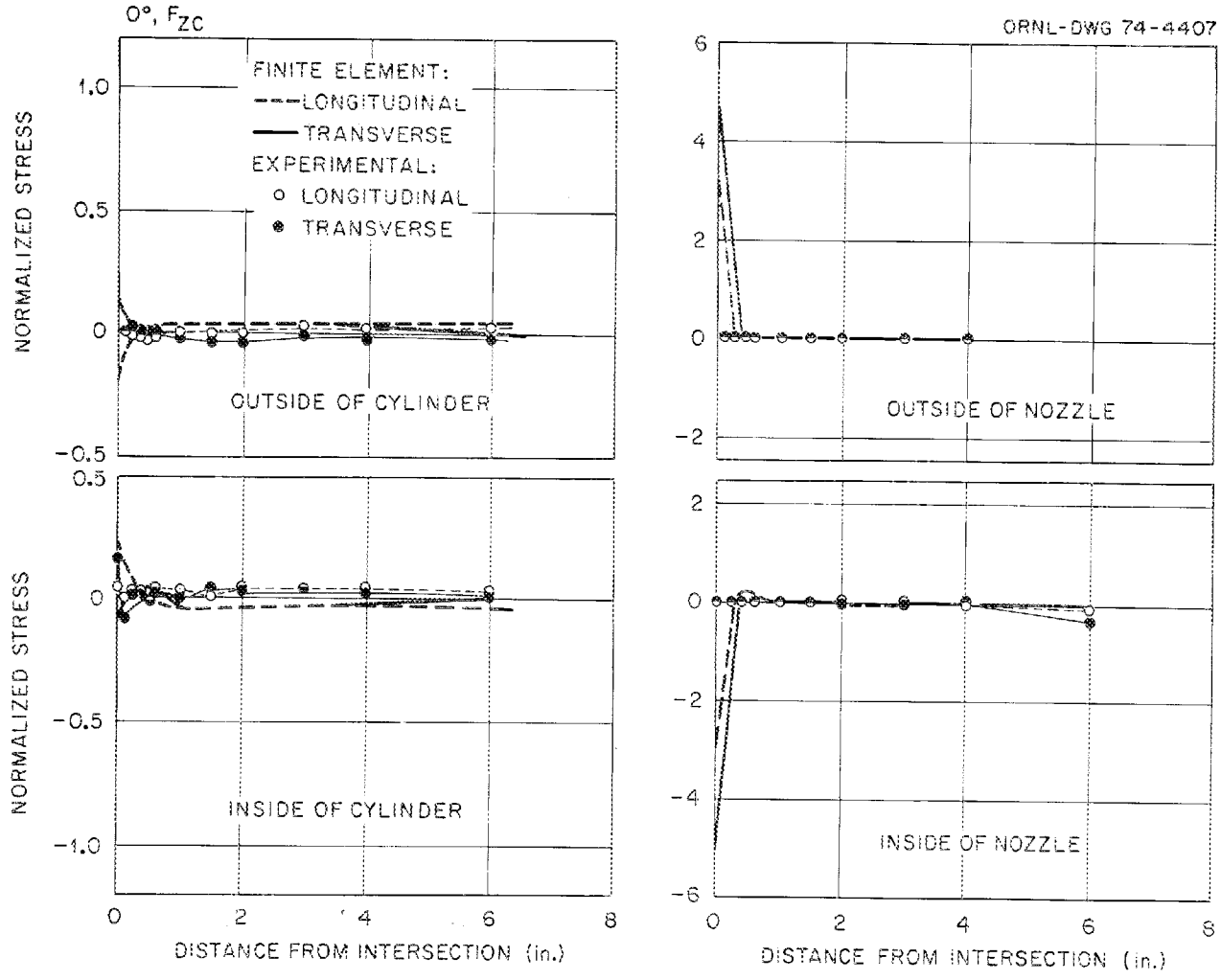

Fig. 46. Measured and predicted stress distributions at 0° for an out-of-plane force, F_{ZC}, on the cylinder.

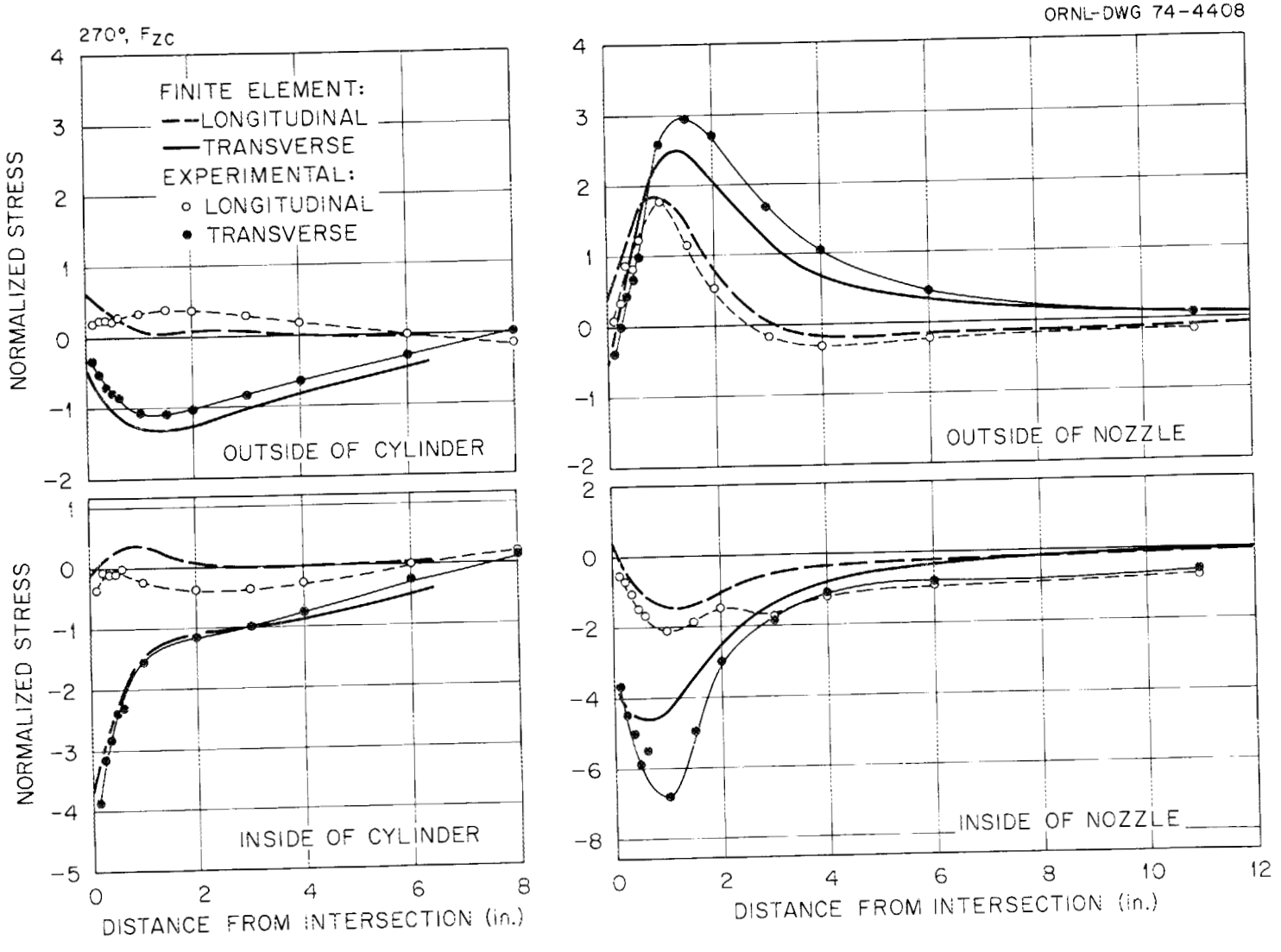

Fig. 47. Measured and predicted stress distributions at 270° for an out-of-plane force, F_{ZC}, on the cylinder.

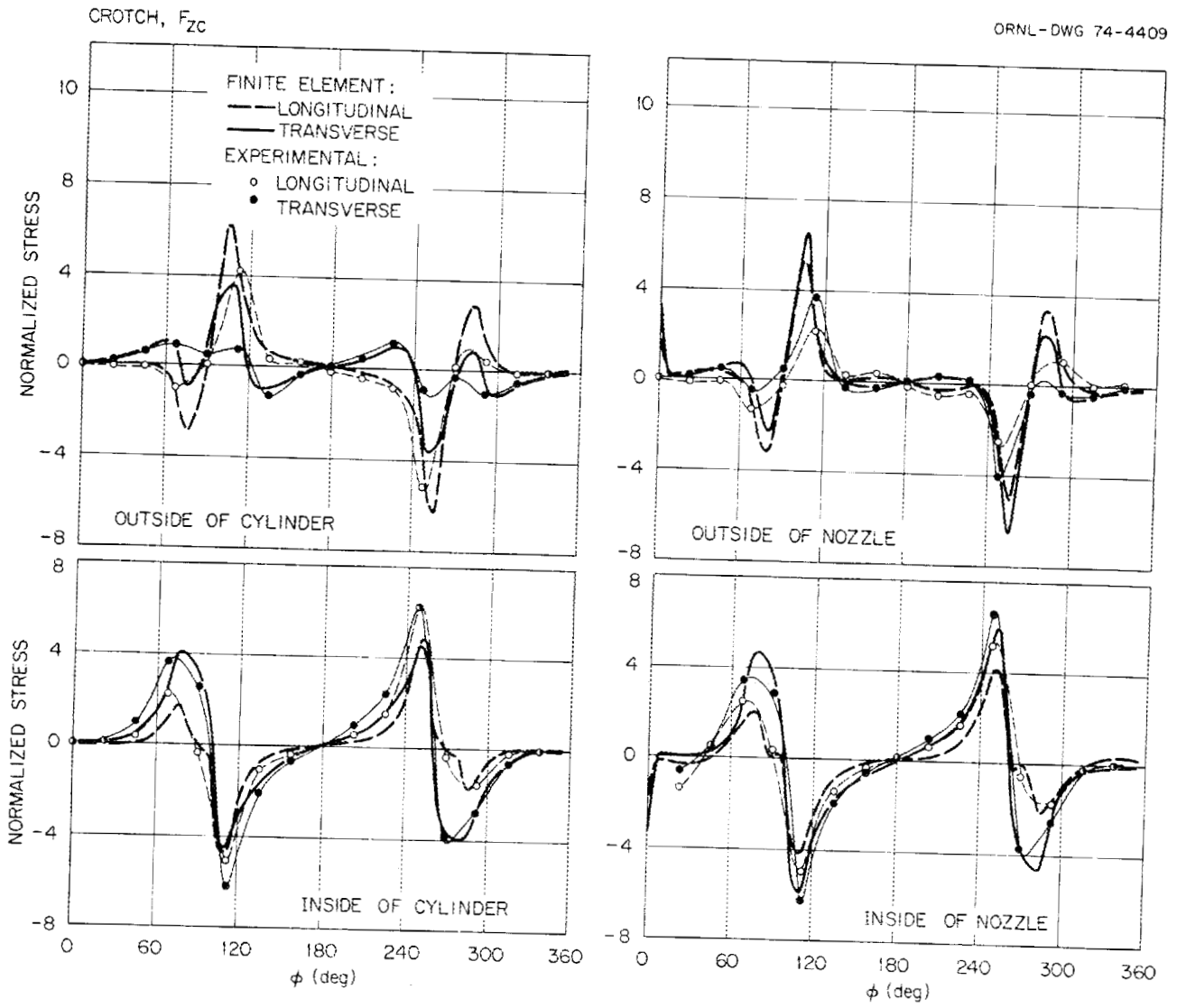

Fig. 48. Measured and predicted stress distributions around the nozzle-cylinder junction for an out-of-plane force, F_{ZC}, on the cylinder.

ORNL-DWG 74-5752

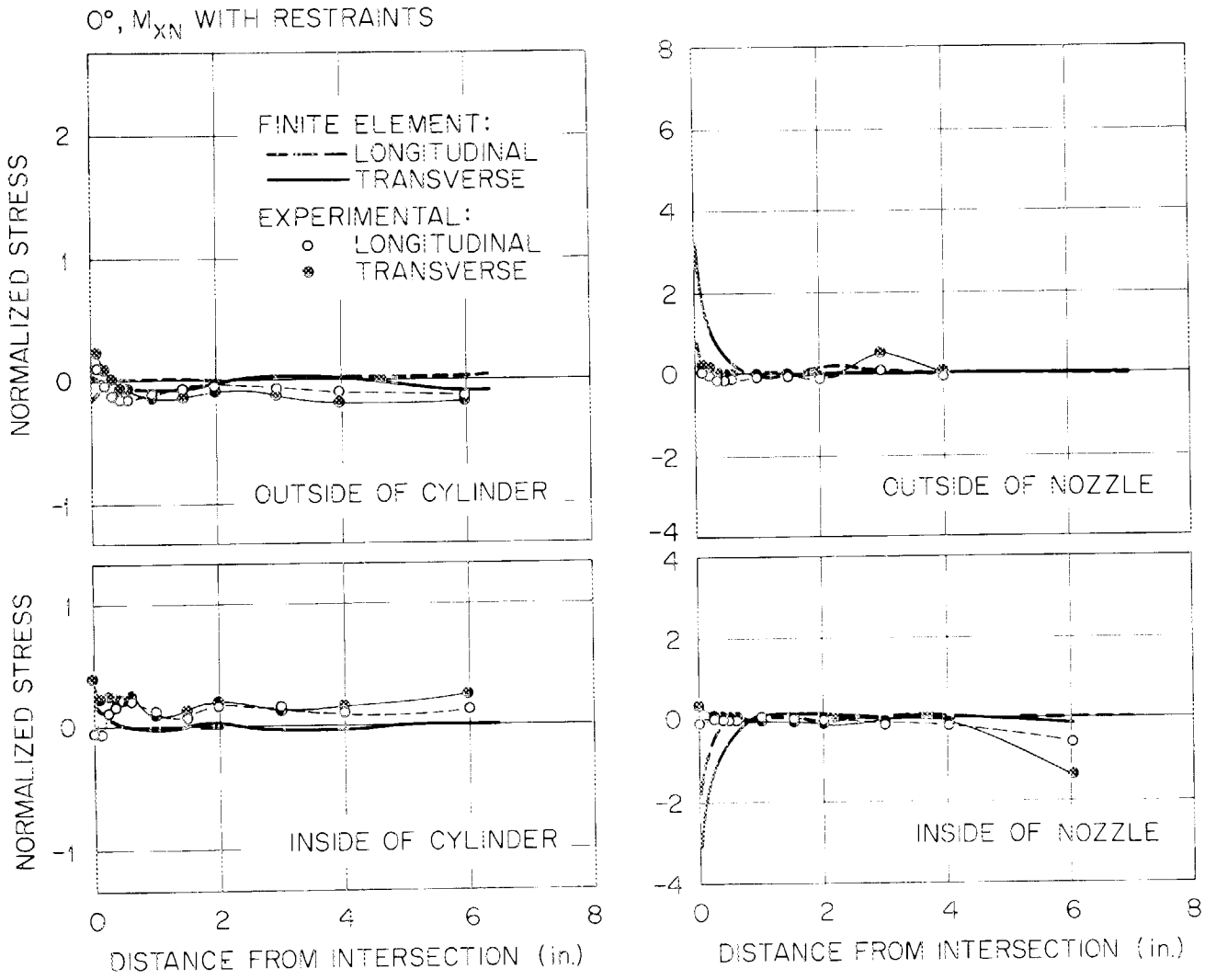

Fig. 49. Measured and predicted stress distributions at 0° for an out-of-plane moment, M_{XN}, on the nozzle with restraints.

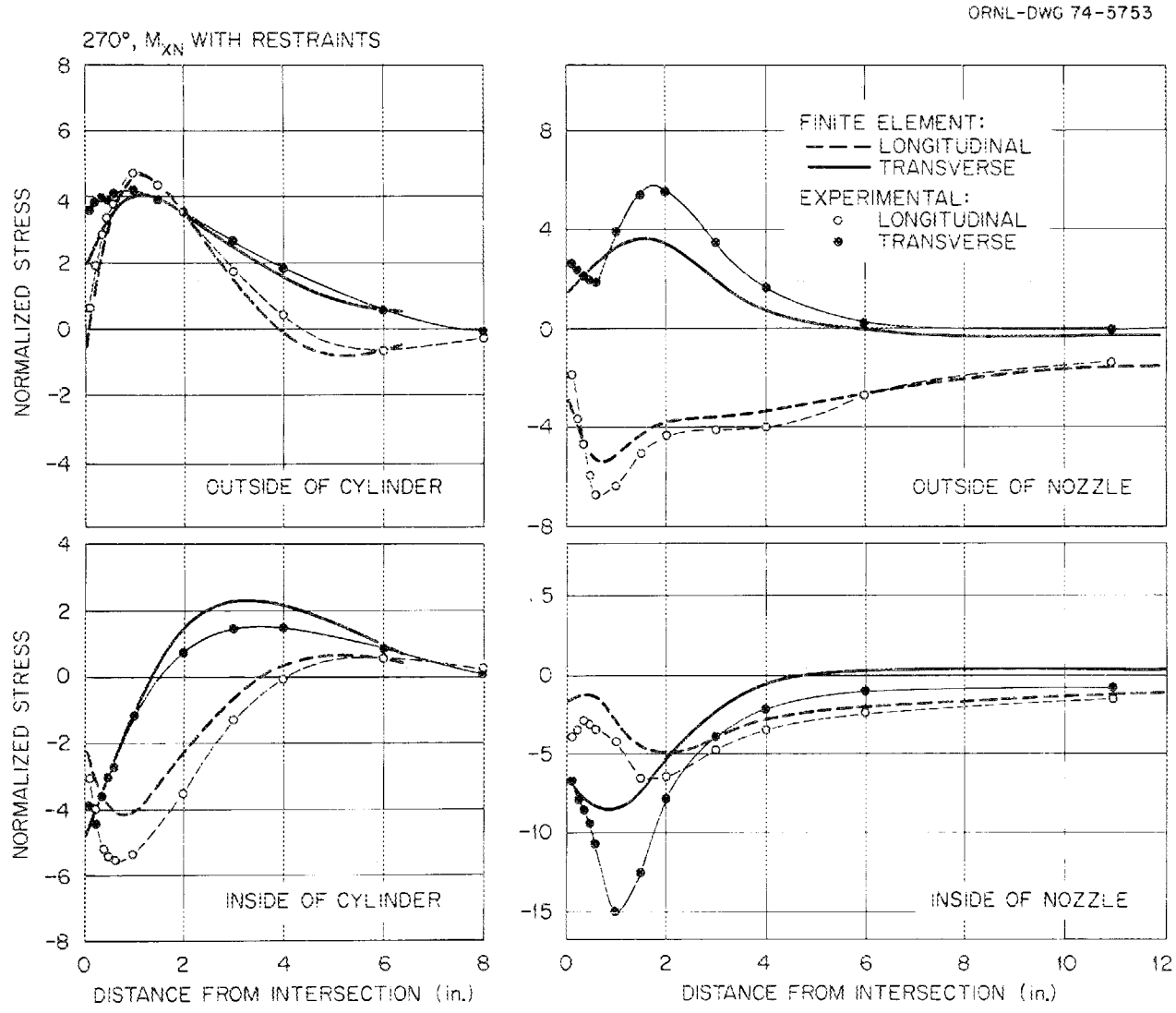

Fig. 50. Measured and predicted stress distributions at 270° for an out-of-plane moment, M_{XN}, on the nozzle with restraints.

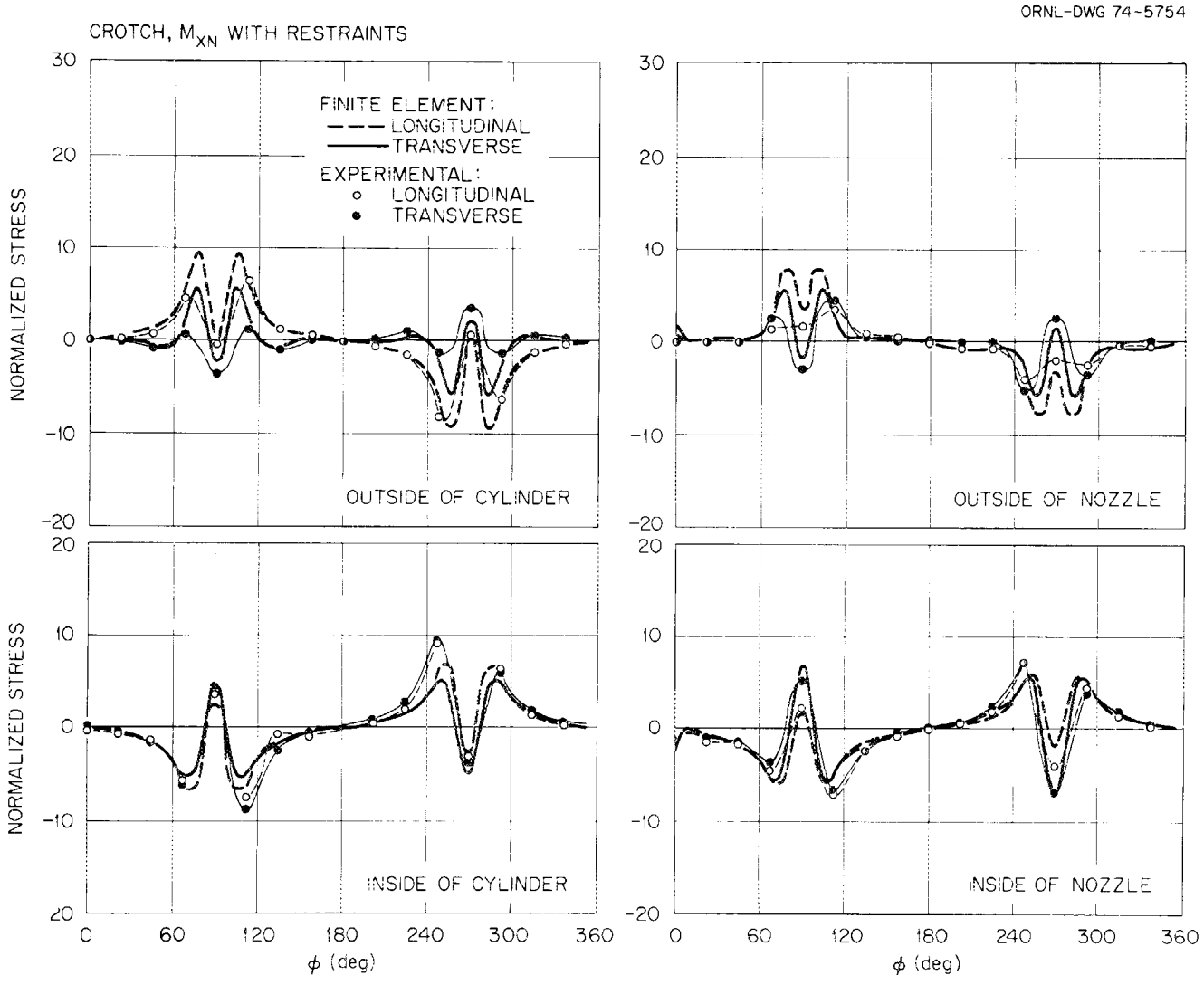

Fig. 51. Measured and predicted stress distributions around the nozzle-cylinder junction for an out-of-plane moment, M_{XN}, on the nozzle with restraints.

4.15 In-Plane Moment, M_{ZN}, on Nozzle with Restraints

The comparisons of theory and experiment for an in-plane moment of 15,000 in.-lb applied to the nozzle are presented in Figs. 52 through 54. The agreement between the theoretical and experimental distribution is excellent along the longitudinal plane and around the crotch. The stresses on the transverse plane are low, and the agreement is poorer than on the other plane.

The maximum experimentally determined principal stress ratio (8.0) occurred on the outside surface of the nozzle along the 270° plane at about 3/8 in. from the junction. The maximum theoretically determined stress ratio (12.5) occurred on the inside surface of the nozzle along the 284° plane at the junction.

4.16 Axial Force, F_{YN}, on Nozzle with Restraints

The comparisons of theory and experiment for an axial force of 4000 lb applied to the nozzle are presented in Figs. 55 through 57. The agreement is good along the longitudinal plane (0° plane). In general, the distributions along the transverse plane and around the crotch show poor quantitative agreement between theory and experiment.

The experimentally determined maximum stress ratio (31.0) occurred on the inside surface of the nozzle on the 270° plane about 1.0 in. from the junction. The theoretically determined maximum stress ratio (16.0) occurred on the inside surface of the nozzle on the 270° plane about 1.0 in. from the junction.

5. CONCLUSIONS

Table 2 represents an attempt to summarize concisely the principal findings of this study in terms of maximum principal stress ratios, locations of maximum principal stresses, and the relative overall agreement between theory and experiment for each loading case. The maximum experimental stress ratios are based on the stresses along two gage lines and the gage line around the crotch only, and were determined by dividing the

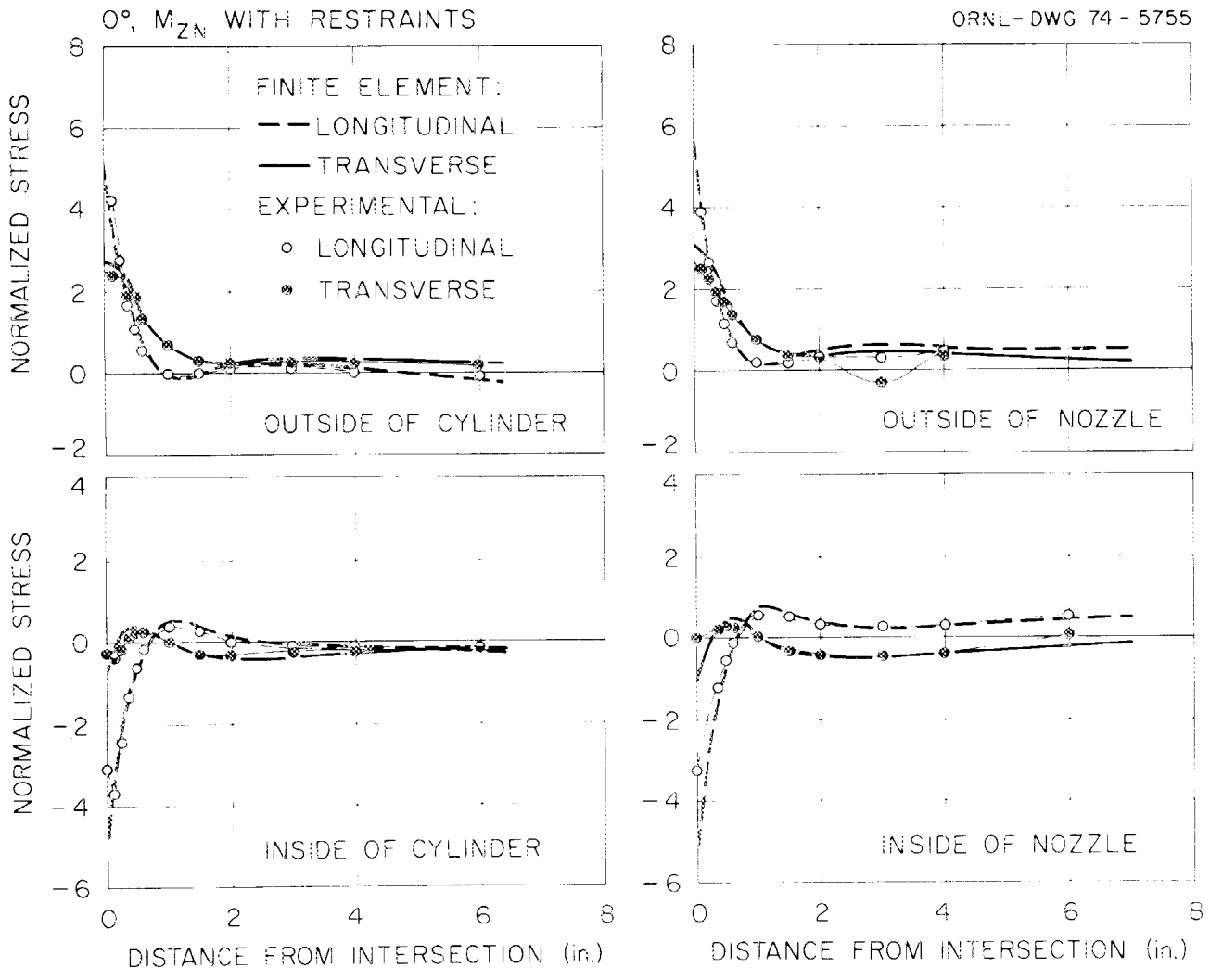

Fig. 52. Measured and predicted stress distributions at 0° for an in-plane moment, M_{ZN}, on the nozzle with restraints.

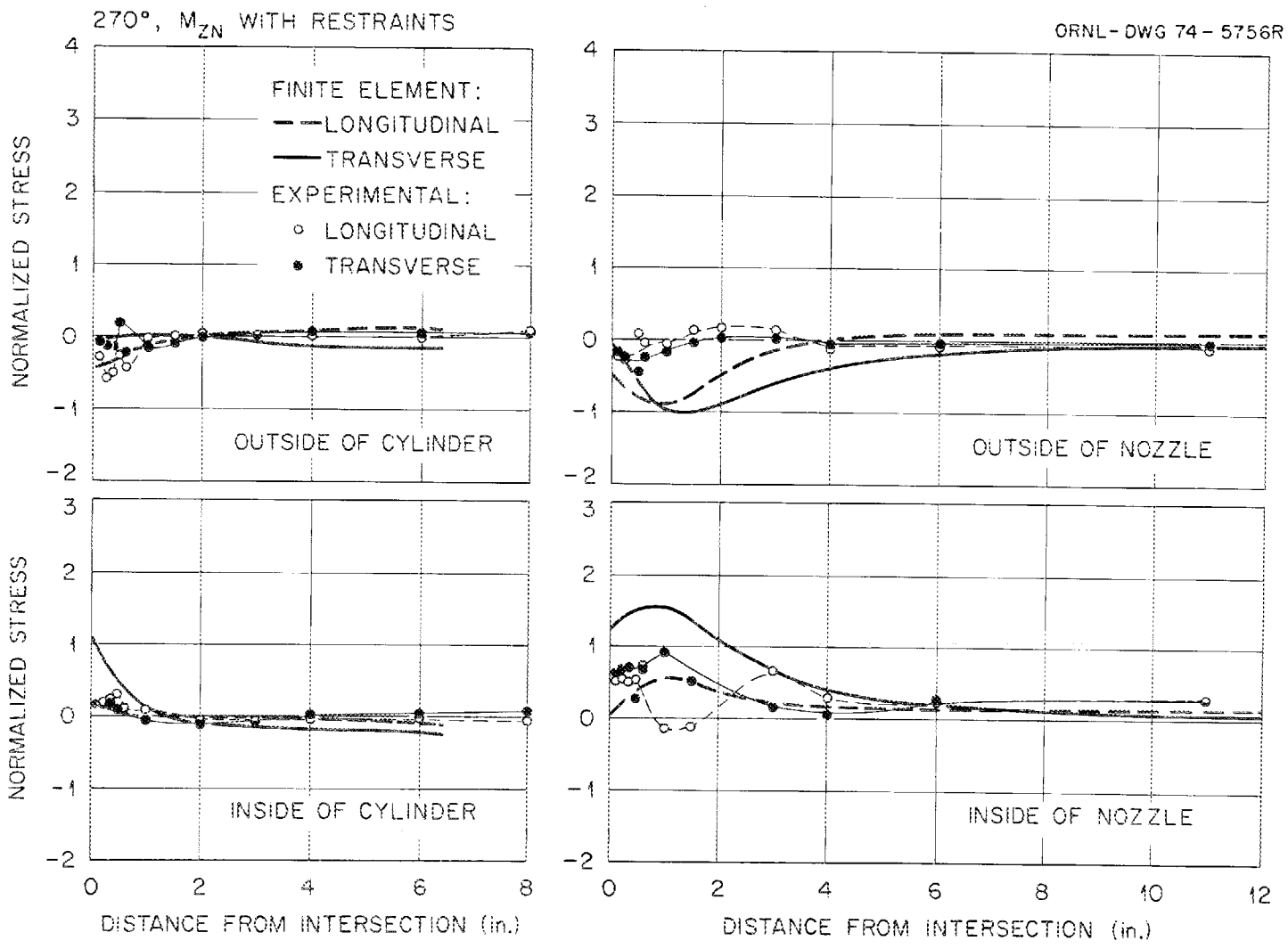

Fig. 53. Measured and predicted stress distributions at 270° for an in-plane moment, M_{ZN}, on the nozzle with restraints.

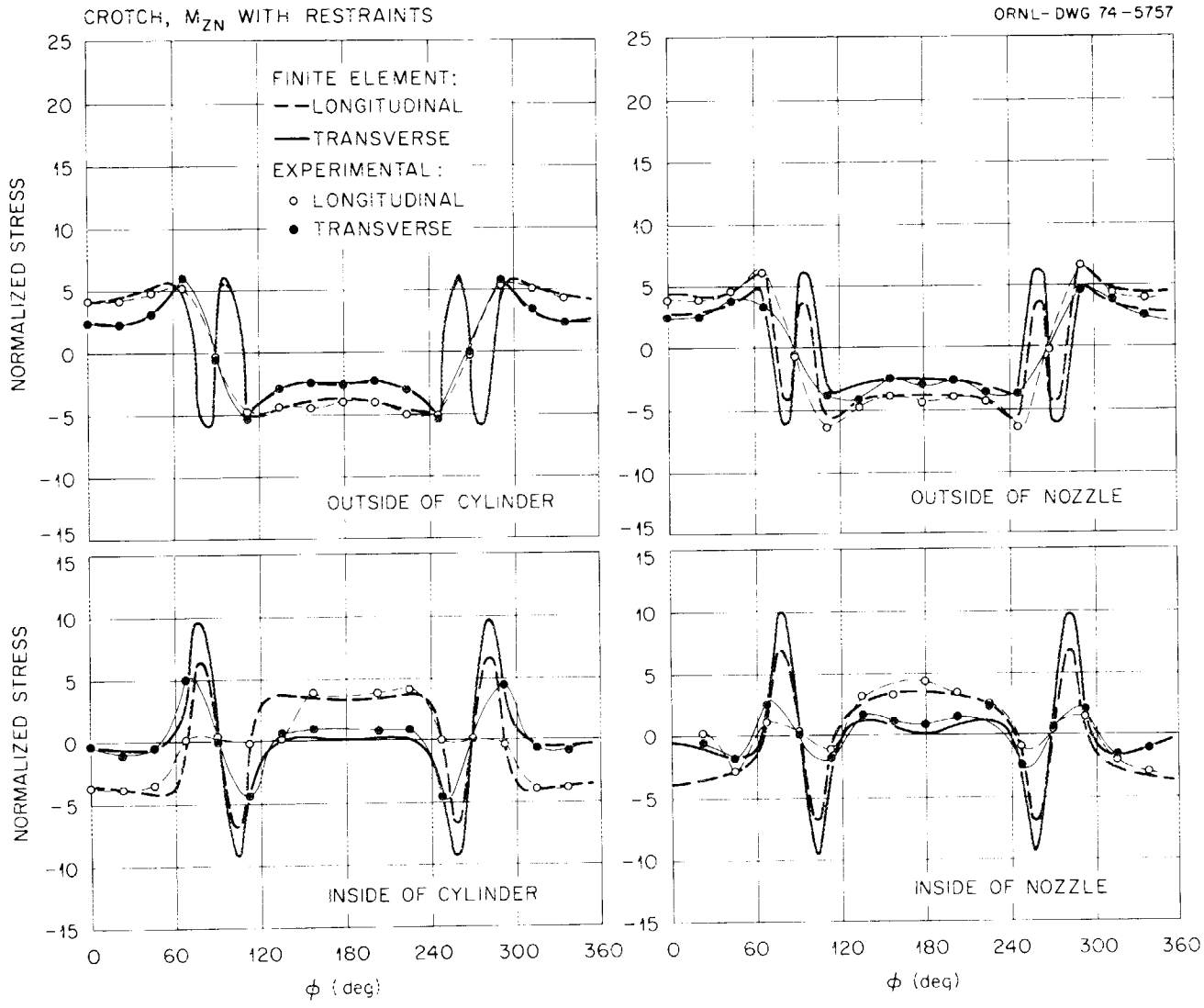

Fig. 54. Measured and predicted stress distributions around the nozzle-cylinder junction for an in-plane moment, M_{ZN}, on the nozzle with restraints.

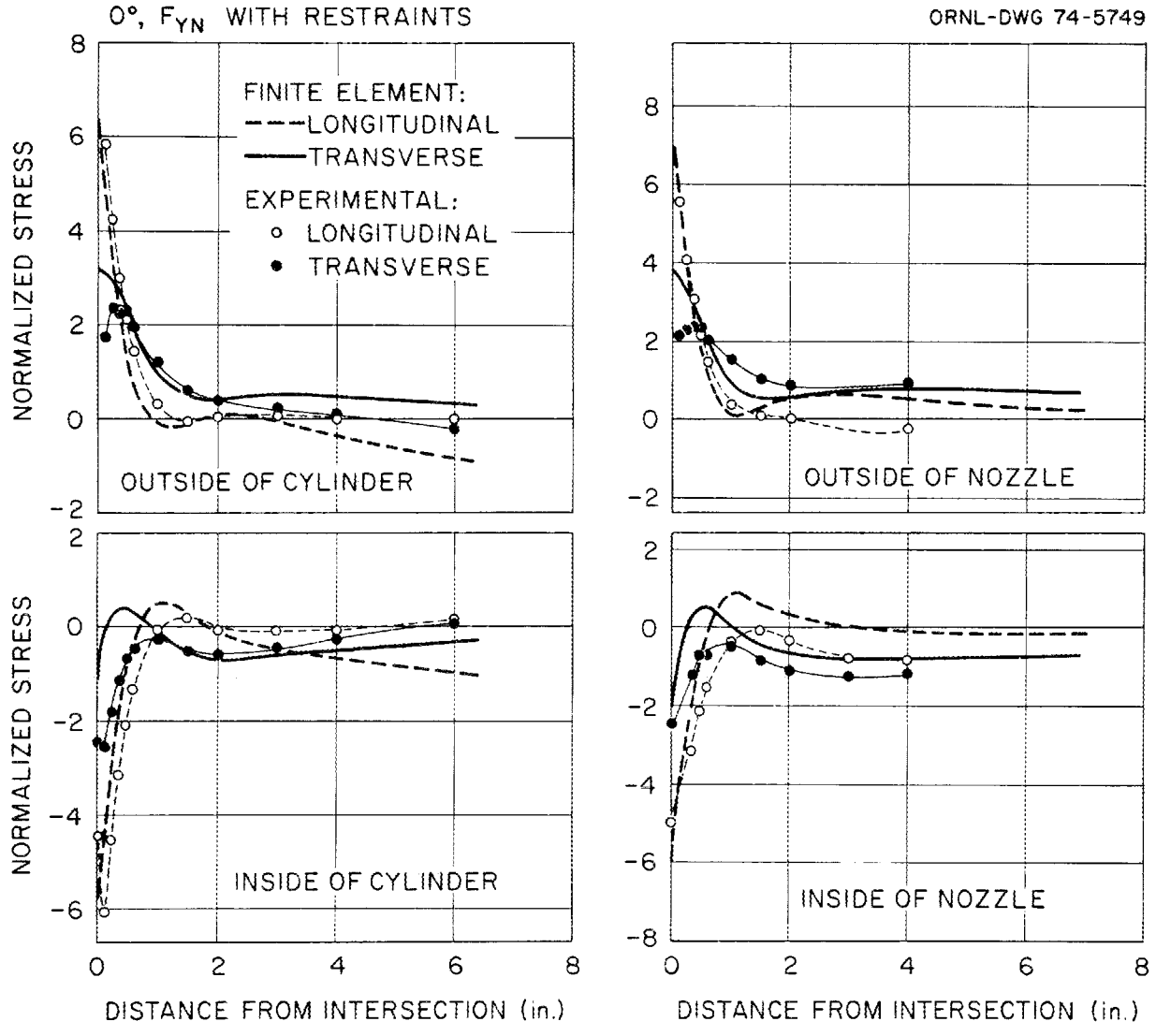

Fig. 55. Measured and predicted stress distributions at 0° for an axial force, F_{YN}, on the nozzle with restraints.

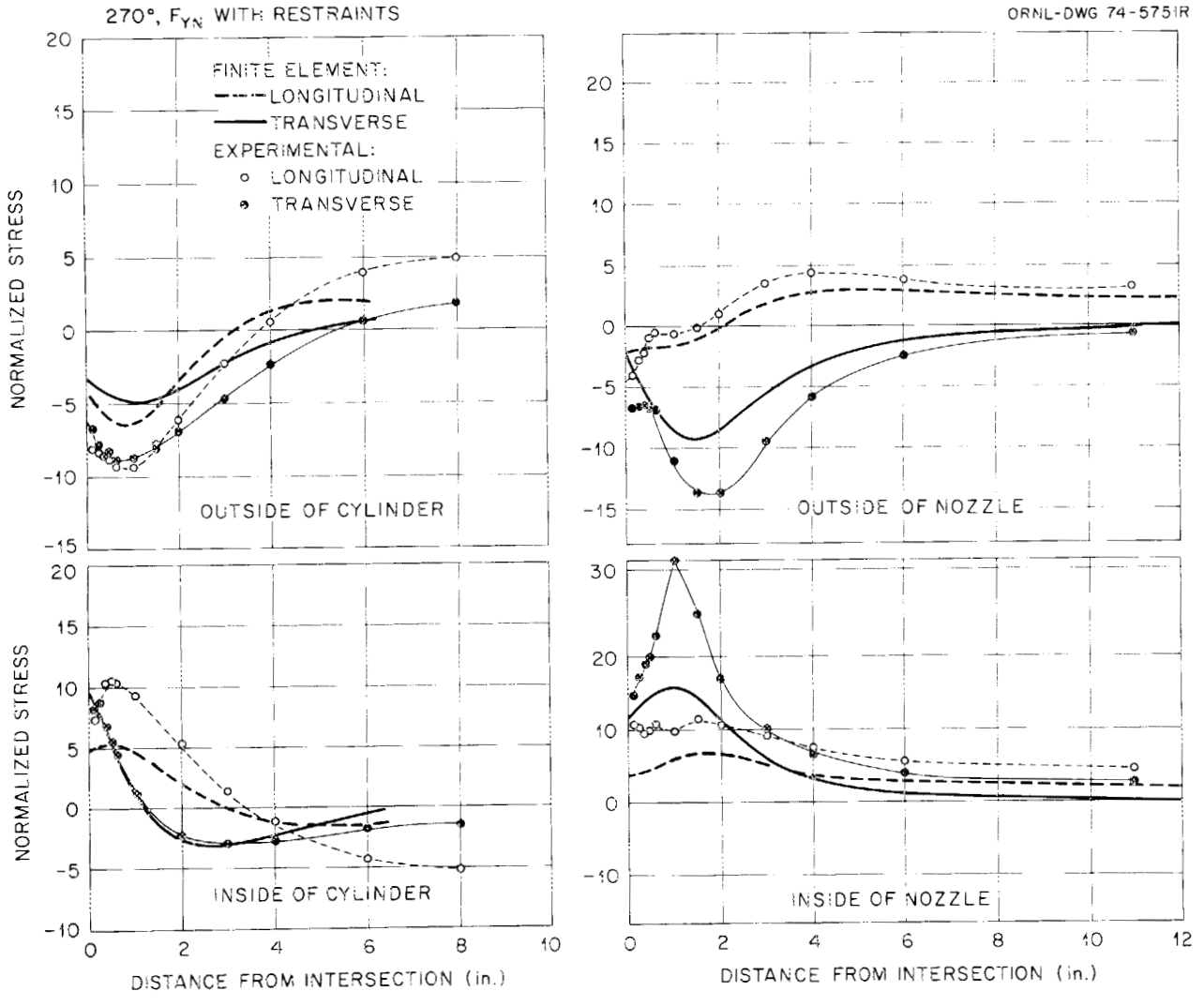

Fig. 56. Measured and predicted stress distributions at 270° for an axial force, F_{YN}, on the nozzle with restraints.

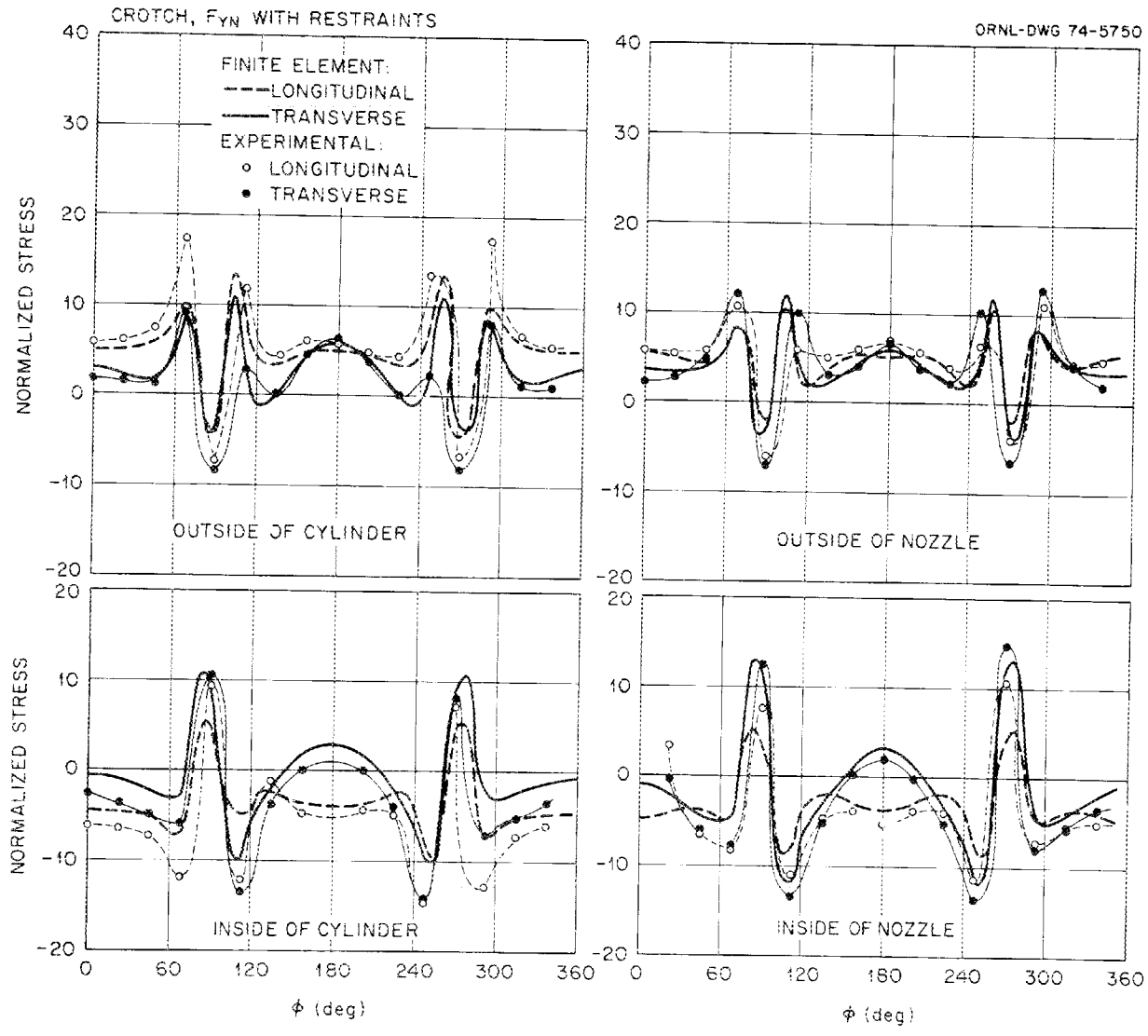

Fig. 57. Measured and predicted stress distributions around the nozzle-cylinder junction for an axial force, F_{YN}, on the nozzle with restraints.

Table 2. Summary of maximum principal stress ratios and locations

Loading case	Experimentally determined maximum stress		Theoretical maximum stress		Overall agreement between theory and experiment
	Stress ratio[a]	Location[b]	Stress ratio[a]	Location[b]	
Internal pressure	9.0	Outside nozzle, 180°	7.7	Outside cylinder, 0°	Excellent, excellent
M_{XN}, out-of-plane moment on nozzle	15.8	Inside cylinder, 247°	17.8	Inside nozzle, 249°	Excellent, good
M_{YN}, torsional moment on nozzle	31.3	Inside cylinder, 247°	37.5	Outside cylinder, 256°	Poor, good
M_{ZN}, in-plane moment on nozzle	11.0	Outside nozzle,[c] 270°	15.2	Inside nozzle, 256°	Good, excellent
F_{XN}, in-plane force on nozzle	13.4	Inside nozzle,[d] 270°	17.8	Inside nozzle, 256°	Excellent, excellent
F_{YN}, axial force on nozzle	13.4	Outside nozzle, 180°	17.2	Inside cylinder, 256°	Good, poor
F_{ZN}, out-of-plane force on nozzle	15.9	Inside cylinder, 247°	24.3	Outside cylinder, 256°	Good, excellent
M_{XC}, torsional moment on cylinder	24.2	Inside nozzle, 292°	37.5	Outside cylinder, 284°	Poor, excellent
M_{YC}, out-of-plane moment on cylinder	4.5	Inside nozzle,[d] 270°	5.9	Outside nozzle, 0°	Fair, excellent
M_{ZC}, in-plane moment on cylinder	14.9	Inside nozzle,[d] 270°	10.1	Inside nozzle,[d] 270°	Good, excellent
F_{XC}, axial force on cylinder	14.4	Inside nozzle,[d] 270°	14.7	Inside nozzle,[d] 270°	Good, good
F_{YC}, in-plane force on cylinder	15.7	Inside nozzle,[d] 270°	10.7	Inside nozzle,[d] 270°	Good, excellent
F_{ZC}, out-of-plane force on cylinder	6.9	Inside nozzle,[d] 270°	9.9	Outside cylinder, 256°	Fair, good
M_{XN}, out-of-plane moment on nozzle with restraints	14.9	Inside nozzle,[d] 270°	11.8	Outside cylinder, 284 and 256°	Good, excellent
M_{ZN}, in-plane moment on nozzle with restraints	8.0	Outside nozzle,[e] 270°	12.5	Inside nozzle, 284°	Excellent, excellent
F_{YN}, axial force on nozzle with restraints	31.0	Inside nozzle,[d] 270°	16.0	Inside nozzle,[d] 270°	Good, poor

[a]Ratio of maximum absolute principal stress value to nominal stress value.

[b]Maximums all occurred at the junction, except where noted.

[c]Maximums not at junction, at approximately 1/2 in. from junction on transverse plane.

[d]Maximums not at junction, at approximately 1.0 in. from junction on transverse plane.

[e]Maximums not at junction, at approximately 3/8 in. from junction on transverse plane.

maximum absolute principal stress value by a nominal membrane stress value as previously described. The maximum theoretical stress ratios were calculated where they occurred. The maximum experimental principal stresses occurred at the junction in only six cases; the other ten occurred on the 270° gage line at about 1.0 in. from the junction.

The relative overall agreement between the finite-element predictions and the experimental results is rated in Table 2 as excellent, good, fair, or poor. These ratings are, of course, a matter of opinion, but an attempt was made to make an unbiased evaluation by basing them both on the overall qualitative agreement along the gage lines and on the quantitative agreement in areas where the stresses were relatively high. In each case two ratings are given; the first rating is for the gage lines (0, 270° planes) and the second is for the crotch gage line.

Table 2 indicates that generally the experimentally determined maximum stress ratios and those based on finite-element predictions are in fair agreement. Furthermore, the degree of agreement between the stress ratios generally correlates well with relative ratings of the overall agreement between theory and experiment. Generally, the agreement was best for those cases involving loadings on the nozzle, except for the torsional moment and the axial force loadings.

In 14 cases, the maximum stress ratios occurred on or close to the transverse plane of symmetry for both the experimental and theoretical analysis. For the axial force applied to the nozzle, the experimental stress ratio occurred on the longitudinal plane, while the theoretical stress ratio occurred near the transverse plane (256° plane). The out-of-plane moment applied to the cylinder produced a maximum experimental stress ratio on the transverse plane, while the theoretical stress ratio occurred on the longitudinal plane (0° plane).

Finally, it should be pointed out that, as would be expected, the out-of-plane moment and force loadings produced quite similar results, and the in-plane moments and forces produced similar results. The stress distributions were very similar for each pair. The loadings on the nozzle with restraints applied to the free end of the cylinder compared favorably with unrestrained loadings on the nozzle except for the maximum experimental

stress ratio. The results from the three loadings with restraints indicated that the nonlinearities observed in the corresponding cases without restraints were reduced. However, the maximum stresses and stress distributions were similar, which indicates that the observed small nonlinearities had little effect on the measured maximum stresses that are reported.

In conclusion, the comparison of these particular finite-element predictions with the experimental results shows reasonably good general agreement. It is felt that this analysis would be satisfactory for most engineering purposes.

ACKNOWLEDGMENTS

The planning and execution of the analytical and experimental study reported herein would not have been possible without the assistance and cooperation of many individuals, both within ORNL and outside. The authors are deeply indebted to these people for their contributions.

Special thanks is due J. P. Rudd for the instrumentation of the model, which was a very painstaking task.

The finite-element computer program used in the analysis was developed at the University of California, Berkeley.

REFERENCES

1. J. M. Corum et al., Theoretical and Experimental Stress Analysis of ORNL Thin-Shell Cylinder-to-Cylinder Model No. 1, ORNL-4553 (October 1972).

2. J. M. Corum and W. L. Greenstreet, "Experimental Elastic Stress Analyses of Cylinder-to-Cylinder Shell Models and Comparisons with Theoretical Predictions," Paper G2/5, First International Conference on Structural Mechanics in Reactor Technology, Berlin, Sept. 20–24, 1971.

3. R. C. Gwaltney et al., Theoretical and Experimental Stress Analysis of ORNL Thin-Shell Cylinder-to-Cylinder Model 3, ORNL-5020 (June 1975).

4. R. C. Gwaltney, S. E. Bolt, and J. W. Bryson, Theoretical and Experimental Stress Analyses of ORNL Thin-Shell Cylinder-to-Cylinder Model 4, ORNL-5019 (June 1975).

5. D. E. Hardenbergh, S. Y. Zamrik, and A. J. Edmondson, "Experimental Investigation of Stresses in Nozzles in Cylindrical Pressure Vessels," Welding Research Council Bulletin 89, July 1963.

6. D. E. Hardenbergh and S. Y. Zamrik, "Effects of External Loadings on Large Outlets in a Cylindrical Pressure Vessel," Welding Research Council Bulletin 96, May 1964.

7. W. F. Riley, Experimental Determination of Stress Distributions in Thin Walled Cylindrical and Spherical Pressure Vessels with Circular Nozzles, IIT Research Institute Report M6053 (March 1965).

8. C. E. Taylor and N. C. Lind, "Photoelastic Study of the Stresses near Openings in Pressure Vessels," Welding Research Council Bulletin 113, April 1966.

9. M. M. Leven, "Photoelastic Determination of Stresses in Reinforced Openings in Pressure Vessels," Welding Research Council Bulletin 113, April 1966.

10. Ojars Greste, Finite Element Analysis of Tubular K Joints, Report UCSESM 70-11, University of California, Berkeley (June 1970).

11. W. Reidelbach, "The State of Stress at the Perpendicular Intersection of Two Right Circular Tubes," Ingenieur-Archiv. 30(5), 293–316 (1961).

12. A. C. Eringen, A. K. Naghdi, and C. C. Thiel, "State of Stress in a Circular Cylindrical Shell with a Circular Hole," Welding Research Council Bulletin 102, January 1965.

13. A. K. Naghdi and A. C. Eringen, "Stress Distribution in a Circular Cylindrical Shell with a Circular Cut-Out," Ingenieur-Archiv. 34(3), 161–72 (1965).

14. A. C. Eringen and E. S. Suhubi, "Stress Distribution at Two Normally Intersecting Shells," Nucl. Struct. Eng. 2(3), 253–70 (1965).

15. A. C. Eringen et al., "Stress Concentrations in Two Normally Intersecting Cylindrical Shells Subject to Internal Pressure," Welding Research Council Bulletin 139, April 1969.

16. J. W. Hansberry and N. Jones, "A Theoretical Study of the Elastic Behavior of Two Normally Intersecting Cylindrical Shells," Trans. ASME, J. Eng. Ind. 91B(3), 563–72 (1969).

17. R. F. Maye and A. C. Eringen, "Further Analysis of Two Normally Intersecting Cylindrical Shells Subjected to Internal Pressure," Nucl. Eng. Des. 12(3), 457–74 (1970).

18. J. W. Hansberry and N. Jones, "Elastic Stresses Due to Axial Loads on a Nozzle Which Intersects a Cylindrical Shell," Proceedings of the Second International Conference on Pressure Vessel Technology, Part I. Design and Analysis, pp. 129–54, October 1973.

19. P. P. Bijlaard, R. J. Dohrmann, and I. C. Wang, "Stresses in Junction of Nozzle to Cylinder Pressure Vessel for Equal Diameter of Vessel and Nozzle," Nucl. Eng. Des. 5(3), 349–66 (1967).

20. K. C. Pan and R. E. Beckett, "Stress and Displacement Analysis of a Shell Intersection," Trans. ASME, J. Eng. Ind. 92B(3), 303–8 (May 1970).

21. L. R. Herrmann and D. M. Campbell, "A Finite-Element Analysis for Thin Shells," AIAA J. 6(10), 1842–47 (1968).

22. N. Prince and Y. R. Rashid, "Structural Analysis of Shell Intersections," presented at First International Conference on Pressure Vessels and Piping, Sept. 29–Oct. 2, 1969, Delft, The Netherlands.

23. C. P. Johnson, The Analysis of Thin Shells by a Finite Element Procedure, Report 67-22, Department of Civil Engineering, University of California, Berkeley (September 1967).

24. C. P. Johnson and P. G. Smith, A Computer Program for the Analysis of Thin Shells, Report 69-5, Department of Civil Engineering, University of California, Berkeley (August 1967).

25. Ojars Greste, A Computer Program for the Analysis of Tubular K Joints, Report 69-19, Department of Civil Engineering, University of California, Berkeley (November 1969).

26. R. W. Clough and J. L. Tocher, "Finite Element Stiffness Matrices for the Analysis of Plate Bending," Proceedings of Conference on Matrix Methods in Structural Mechanics, Report AFFDL-TR-66-80, Wright-Patterson Air Force Base (November 1966).

Appendix

TABULATION OF EXPERIMENTAL DATA

For the benefit of the reader who may wish to use the experimental data presented herein for comparison with his own analysis techniques, the experimental data on which the various plots in this report were based are given in Tables A.1 through A.16. For each loading case, a set of data is tabulated for each operable rosette. These data were obtained from the several sets of data taken in each case by the procedures described in Sect. 2.4.

The rosette listings are grouped according to gage lines. For each rosette, the three strain readings are first listed, followed by the normal stress transverse (perpendicular) to the gage line, the normal stress longitudinal (parallel) to the gage line, the shear stress (referred to the gage line as a coordinate axis), and finally the maximum and minimum principal stresses. The strains are given in microinches per inch, and the stresses are in pounds per square inch.

The nomenclature used to identify and locate each rosette can be explained by considering the following sample designation:

$$\underline{I}\ \underline{270}\ \underline{N} - \underline{E}\ .$$

The letter I designates that the rosette is located on the inner surface of the nozzle or cylinder (O denotes an outside rosette). The number 270 indicates that the rosette is located on the 270° gage line (see Fig. 3 for the gage line designations). The letter N indicates that the rosette is on the nozzle (C designates a rosette on the cylinder), and E designates the location of the rosette along the gage line according to the following convention:

Rosette designation	Distance from nozzle-cylinder intersection (see Fig. 3) (in.)
*	≈0
A	1/8
B	1/4
C	3/8

Rosette designation	Distance from nozzle-cylinder intersection (see Fig. 3) (in.)
D	1/2
E	5/8
F	1
G	1 1/2
H	2
J	3
K	4
L	6
M	8
N	10.95

In every case, the rosettes were positioned on the gage lines so that the leg of the Y lay along the gage line and pointed away from the nozzle-cylinder junction. The convention used can be understood by referring to Fig. 5. The leg of the Y is designated as gage 1 in the tabulations, with gages 2 and 3 being numbered from 1 in the counterclockwise direction.

Finally, in those cases where nonlinearity or drift was excessive, or where an individual gage or circuit was otherwise obviously malfunctioning, the rosette of which the gage was a part was not used in the final results plotted in this report for the specific loading under consideration. Nonetheless, these data are listed in the tabulations, but they are marked by a double asterisk beside the rosette number.

Table A.1. Internal pressure

INTERNAL PRESSURE (60 PSI)

	MICRO-STRAIN			STRESSES			PRIN STRESSES	
ROSETTE	GAGE1	GAGE2	GAGE3	TRANS	LONG	SHEAR	SIGMX	SIGMN
I-0-C-A	-462	320	486	18226	-8379	-2212	18408	-8562
I-0-C-B	-172	351	345	15495	-509	77	15496	-510
I-0-C-C	30	320	329	14228	5183	-111	14229	5182
I-0-C-D	137	264	295	12128	7760	-411	12166	7722
I-0-C-E	191	244	258	10841	8976	-187	10859	8957
I-0-C-F	213	160	154	6666	8400	74	8403	6663
I-0-C-G	129	92	106	4222	5132	-188	5169	4185
I-0-C-H	78	86	75	3466	3381	149	3578	3268
I-0-C-J	64	86	92	3851	3078	-74	3858	3071
I-0-C-K	75	89	89	3838	3408	0	3838	3408
I-0-C-L	70	89	86	3781	3223	38	3784	3221
O-0-C-A	308	534	548	23447	16278	-189	23452	16273
O-0-C-B	51	442	425	19015	7234	225	19020	7229
O-0-C-C	-63	322	308	13925	2277	193	13928	2274
O-0-C-D	-129	237	251	10861	-612	-192	10864	-615
O-0-C-E	-132	157	168	7284	-1773	-155	7286	-1776
O-0-C-F	-75	54	62	2637	-1448	-114	2641	-1451
O-0-C-G	31	31	28	1263	1309	38	1330	1242
O-0-C-H	79	45	48	1967	2971	-37	2973	1966
O-0-C-J	77	60	57	2491	3060	38	3063	2489
O-0-C-K	74	60	60	2552	2994	0	2994	2552
O-0-C-L	74	63	66	2739	3048	-38	3053	2735

Table A.1 (continued)

INTERNAL PRESSURE (60 PSI)

	MICRO-STRAIN			STRESSES			PRIN STRESSES	
ROSETTE	GAGE1	GAGE2	GAGE3	TRANS	LONG	SHEAR	SIGMX	SIGMN
I-0-N-B	0	337	354	15195	4559	-232	15200	4554
I-0-N-C	26	322	340	14527	5143	-232	14533	5137
I-0-N-D	122	311	299	13274	7643	156	13278	7638
I-0-N-E	189	273	264	11604	9147	117	11610	9141
I-0-N-F	224	168	157	6903	8781	155	8794	6891
I-0-N-G	139	102	99	4251	5459	39	5460	4250
I-0-N-H	84	84	90	3737	3648	-78	3782	3603
I-0-N-J	73	93	93	4023	3389	0	4023	3389
I-0-N-K	70	87	94	3898	3267	-84	3909	3256
I-0-N-L	76	93	35	2735	3101	778	3718	2119
O-0-N-A	236	523	541	23123	14015	-228	23129	14009
O-0-N-B	40	398	421	17959	6573	-304	17967	6565
O-0-N-C	-71	319	304	13774	2015	195	13777	2011
O-0-N-D	-123	216	228	9903	-727	-156	9905	-730
O-0-N-E	-135	146	155	6766	-2018	-117	6767	-2019
O-0-N-F	-79	61	64	2843	-1529	-39	2844	-1530
O-0-N-G	29	35	35	1497	1314	-1	1497	1314
O-0-N-H	73	43	43	1824	2724	3	2724	1824
O-0-N-J	76	61	61	2605	3057	0	3057	2605
O-0-N-K	70	61	61	2619	2880	0	2880	2619

Table A.1 (continued)

INTERNAL PRESSURE (60 PSI)

	MICRO-STRAIN			STRESSES			PRIN STRESSES	
ROSETTE	GAGE1	GAGE2	GAGE3	TRANS	LONG	SHEAR	SIGMX	SIGMN
I270C-A	42	-25	-59	-1889	685	446	760	-1964
I270C-B	75	8	-36	-701	2045	595	2168	-825
I270C-C	98	31	-17	197	2985	632	3121	60
I270C-D	123	45	0	843	3932	594	4042	732
I270C-E	128	63	20	1675	4355	571	4471	1558
I270C-F	154	94	51	3027	5532	570	5655	2903
I270C-H	148	80	57	2846	5306	304	5343	2809
I270C-J	131	68	51	2488	4684	229	4707	2464
I270C-K	128	57	57	2366	4562	0	4562	2366
I270C-L	114	51	51	2130	4063	0	4063	2130
I270C-M	114	54	54	2256	4101	0	4101	2256
O270C-A	231	211	97	6514	8879	1517	9619	5773
O270C-B	185	174	94	5688	7267	1063	7802	5154
O270C-C	148	148	80	4851	5904	910	6429	4326
O270C-D	123	131	69	4257	4960	832	5512	3706
O270C-E	106	117	60	3775	4304	759	4843	3236
O270C-F	60	60	40	2125	2432	266	2586	1971
O270C-G	40	34	28	1332	1595	76	1615	1312
O270C-H	37	23	28	1085	1436	-76	1452	1069
O270C-J	37	26	37	1335	1510	-152	1598	1247
O270C-K	46	31	40	1515	1822	-114	1860	1478
O270C-L	51	34	37	1507	1990	-38	1993	1504
O270C-M	51	40	37	1634	2027	38	2031	1630

Table A.1 (continued)

INTERNAL PRESSURE (60 PSI)

	MICRO-STRAIN			STRESSES			PRIN STRESSES	
ROSETTE	GAGE1	GAGE2	GAGE3	TRANS	LONG	SHEAR	SIGMX	SIGMN
I270N-A	-53	-68	-97	-3554	-2656	391	-2510	-3700
I270N-B	-79	-97	-114	-4550	-3742	235	-3679	-4613
I270N-C	-88	-117	-135	-5445	-4274	232	-4230	-5490
I270N-D	-97	-138	-129	-5753	-4631	-116	-4619	-5765
I270N-E	-100	-147	-138	-6139	-4835	-117	-4824	-6149
I270N-F	-41	-159	-118	-6045	-3055	-550	-2957	-6143
I270N-G	23	-130	-77	-4563	-665	-707	-541	-4687
I270N-H	32	-112	-80	-4249	-306	-431	-260	-4296
I270N-J	-30	-77	-80	-3403	-1908	39	-1907	-3404
I270N-K	-50	-62	-59	-2604	-2287	-39	-2282	-2609
I270N-L	-47	-18	-12	-599	-1597	-78	-593	-1603
I270N-N	-35	21	23	1007	-761	-39	1008	-762
O270N-A	313	224	109	6973	11486	1534	11959	6501
O270N-B	379	235	132	7658	13674	1380	13975	7356
O270N-C	414	259	141	8317	14908	1572	15264	7962
O270N-D	434	276	172	9372	15828	1379	16110	9089
O270N-E	448	282	192	9924	16423	1186	16633	9715
O270N-F	319	273	233	10766	12798	536	12931	10633
O270N-G	149	244	221	10062	7496	305	10098	7461
O270N-H	31	221	218	9627	3832	39	9627	3832
O270N-J	-38	181	210	8649	1463	-385	8669	1442
O270N-K	-41	178	187	8075	1204	-115	8077	1202
O270N-L	-44	141	135	6119	529	77	6120	527
O270N-N	-44	78	83	3583	-231	-77	3585	-233

Table A.1 (continued)

INTERNAL PRESSURE (60 PSI)

	MICRO-STRAIN			STRESSES			PRIN STRESSES	
ROSETTE	GAGE1	GAGE2	GAGE3	TRANS	LONG	SHEAR	SIGMX	SIGMN
I-0-C-*	-566	495	323	18590	-11389	2289	18764	-11562
I-22C-A	-375	295	304	13569	-7191	-115	13569	-7192
I-45C-A	-186	289	275	12605	-1807	191	12608	-1810
I-67C-A	-29	229	180	9032	1849	649	9090	1790
I-90C-A	34	-40	-72	-2496	281	420	343	-2558
I112C-A	3	172	218	8557	2651	-611	8620	2589
I135C-A	-192	292	284	12863	-1902	114	12864	-1903
I157C-A	-378	292	338	14264	-7068	-611	14282	-7086
I202C-A	-370	341	306	14634	-6710	462	14644	-6720
I225C-A	-182	263	277	12077	-1841	-193	12079	-1843
I247C-A	-17	173	121	6497	1428	693	6590	1335
I292C-A	-38	188	225	9123	1609	-501	9157	1575
I315C-A	-252	257	275	11963	-3957	-231	11966	-3960
I337C-A	-382	312	292	13694	-7340	269	13697	-7343
I180C-L	38	90	78	3641	2222	154	3657	2206
O-22C-A	237	462	488	20620	13290	-341	20636	13274
O-45C-A	136	382	368	16330	8993	185	16335	8989
O-67C-A	-53	117	184	6671	406	-892	6795	281
O-90C-A	237	137	184	6782	9140	-631	9298	6624
O112C-A	-101	70	120	4272	-1735	-669	4345	-1809
O135C-A	103	379	348	15877	7854	408	15898	7834
O157C-A	268	507	471	21210	14390	483	21244	14356
O180C-A	262	566	597	25262	15438	-410	25279	15421
O202C-A	192	452	471	20065	11784	-260	20073	11776
O225C-A	105	313	347	14385	7464	-453	14414	7435
O247C-A	-80	77	125	4515	-1046	-644	4589	-1120
O292C-A	-43	185	125	6858	777	797	6960	674
O315C-A	165	393	398	17198	10102	-74	17198	10101
O337C-A	245	464	481	20489	13482	-227	20496	13475
O180C-L	31	54	62	2523	1689	-114	2538	1674

Table A.1 (continued)

INTERNAL PRESSURE (60 PSI)

	MICRO-STRAIN			STRESSES			PRIN STRESSES	
ROSETTE	GAGE1	GAGE2	GAGE3	TRANS	LONG	SHEAR	SIGMX	SIGMN
I-0-N-*	-578	491	477	21913	-10771	193	21914	-10772
I-22N-A	-15	259	38	6553	1521	2945	7910	164
I-45N-A	-46	419	-144	6090	446	7508	11289	-4753
I-67N-A	50	292	6	6507	3464	3808	9087	884
I-90N-A	-20	-59	-91	-3274	-1589	431	-1485	-3378
I112N-A	68	36	286	7002	4142	-3341	9206	1937
I135N-A	-91	-71	463	8734	-115	-7115	12688	-4069
I157N-A	-242	21	520	12141	-3609	-6645	14570	-6038
I180N-A	-510	461	260	16392	-10390	2674	16657	-10654
I202N-A	-268	508	-23	10945	-4760	7080	13665	-7480
I225N-A	14	391	-152	5233	2003	7224	11020	-3785
I247N-A	23	251	38	6311	2590	2836	7842	1059
I292N-A	58	3	329	7236	3916	-4350	10233	920
I315N-A	-21	-105	414	6808	1427	-6913	11537	-3301
I337N-A	-248	6	469	10709	-4225	-6176	12932	-6448
O-22N-A	239	363	495	18600	12749	-1767	19092	12257
O-45N-A	216	236	395	13621	10561	-2113	14700	9482
O-67N-A	92	-23	164	2985	3655	-2496	5838	801
O-90N-A	314	141	190	6925	11490	-653	11582	6833
O112N-A	43	136	-85	1074	1601	2956	4305	-1630
O135N-A	227	427	245	14499	11174	2426	15777	9896
O157N-A	256	540	378	19907	13650	2160	20580	12976
O180N-A	307	620	614	26787	17249	76	26787	17249
O202N-A	247	350	460	17522	12677	-1467	17932	12268
O225N-A	179	190	367	12052	8988	-2350	13325	7715
O247N-A	34	-60	131	1522	1478	-2539	4039	-1040
O292N-A	91	205	-31	3706	3838	3146	6918	626
O315N-A	208	393	222	13293	10224	2284	14510	9007
O337N-A	225	503	388	19326	12540	1537	19658	12208
O-0-N-L	70	56	59	2452	2840	-38	2844	2449

Table A.2. Out-of-plane moment loading, M_{XN}, on nozzle

OUT-OF-PLANE MOMENT LOADING, MXN, ON NOZZLE (10000 IN-LB)

	MICRO-STRAIN			STRESSES			PRIN STRESSES	
ROSETTE	GAGE1	GAGE2	GAGE3	TRANS	LONG	SHEAR	SIGMX	SIGMN
I-O-C-A	-9	-12	3	-189	-318	-188	-55	-452
I-O-C-B	-6	-14	14	-9	-180	-373	288	-478
I-O-C-C	-6	-14	14	-4	-180	-374	292	-476
I-O-C-D	-3	-14	14	-11	-96	-374	322	-430
I-O-C-E	-3	-14	17	56	-77	-412	407	-428
I-O-C-F	0	-17	14	-77	-32	-413	358	-468
I-O-C-G	0	-14	14	-18	-18	-375	358	-393
I-O-C-H	-3	-17	14	-68	-110	-408	320	-497
I-O-C-J	-3	-14	11	-62	-106	-335	252	-419
I-O-C-K	-6	-11	14	62	-158	-334	304	-400
I-O-C-L	-6	-11	16	118	-141	-370	381	-403
O-O-C-A	-8	-6	-20	-553	-419	190	-285	-687
O-O-C-B	-14	-6	-17	-482	-569	153	-367	-685
O-O-C-C	-14	-8	-17	-544	-588	113	-450	-682
O-O-C-D	-14	-11	-14	-545	-589	39	-523	-611
O-O-C-E	-17	-11	-17	-604	-691	77	-560	-736
O-O-C-F	-17	-11	-17	-604	-693	76	-560	-736
O-O-C-G	-17	-11	-20	-666	-711	114	-572	-805
O-O-C-H	-14	-11	-20	-671	-625	114	-531	-764
O-O-C-J	-17	-6	-23	-601	-689	227	-414	-877
O-O-C-K	-17	-8	-20	-604	-689	152	-489	-804
O-O-C-L	-17	-8	-23	-666	-709	190	-497	-879

Table A.2 (continued)

OUT-OF-PLANE MOMENT LOADING, MXN, CN NOZZLE (10000 IN-LB)

	MICRO-STRAIN			STRESSES			PRIN STRESSES	
ROSETTE	GAGE1	GAGE2	GAGE3	TRANS	LONG	SHEAR	SIGMX	SIGMN
I-C-N-B	0	-3	12	191	57	-193	329	-80
I-C-N-C	0	0	9	191	57	-116	259	-10
I-C-N-D	0	-3	9	128	38	-155	244	-78
I-C-N-E	3	0	9	188	144	-116	284	48
I-C-N-F	6	0	3	57	192	-39	202	47
I-C-N-G	3	-3	3	-3	86	-77	131	-48
I-C-N-H	3	0	6	124	124	-77	202	47
I-C-N-J	0	0	3	73	33	-39	97	9
I-C-N-K	0	0	6	136	49	-71	175	9
I-C-N-L	0	-3	-44	-1020	-309	546	-13	-1316
O-C-N-A	-6	-3	-14	-371	-284	151	-170	-485
O-C-N-B	-11	-3	-17	-427	-471	189	-258	-640
O-C-N-C	-12	-6	-15	-441	-487	117	-345	-583
O-C-N-D	-12	-3	-18	-442	-487	195	-269	-661
O-C-N-E	-12	-6	-18	-505	-505	157	-349	-662
O-C-N-F	-12	-3	-18	-441	-487	195	-268	-661
O-C-N-G	-9	-3	-18	-446	-403	195	-228	-621
O-C-N-H	-9	0	-21	-452	-408	275	-154	-705
O-C-N-J	-6	-3	-24	-578	-351	274	-168	-761
O-C-N-K	-12	0	-23	-503	-507	312	-193	-818

Table A.2 (continued)

OUT-OF-PLANE MOMENT LOADING, MXN, ON NOZZLE (10000 IN-LB)

	MICRO-STRAIN			STRESSES			PRIN STRESSES	
ROSETTE	GAGE1	GAGE2	GAGE3	TRANS	LONG	SHEAR	SIGMX	SIGMN
I270C-A	-87	-354	14	-7391	-4822	-4904	-1037	-11176
I270C-B	-118	-315	33	-6077	-5348	-4645	-1054	-10372
I270C-C	-145	-282	36	-5240	-5932	-4236	-1336	-9837
I270C-D	-168	-237	47	-3992	-6225	-3792	-1155	-9062
I270C-E	-171	-217	43	-3638	-6229	-3461	-1238	-8629
I270C-F	-203	-103	29	-1408	-6502	-1749	-865	-7045
I270C-H	-174	23	20	1132	-4883	38	1132	-4884
I270C-J	-103	57	26	1932	-2503	418	1971	-2542
I270C-K	-60	63	29	2073	-1176	456	2136	-1239
I270C-L	-9	43	14	1264	122	380	1379	7
I270C-M	3	17	-9	185	141	342	506	-180
O270C-A	-65	-37	205	3767	-830	-3223	5428	-2490
O270C-B	-8	-8	196	4143	992	-2730	5719	-584
O270C-C	31	17	185	4411	2267	-2237	5820	858
O270C-D	60	31	162	4194	3057	-1746	5461	1789
O270C-E	80	60	154	4609	3780	-1251	5513	2876
O270C-F	123	100	123	4773	5127	-305	5302	4598
O270C-G	123	120	95	4584	5070	342	5246	4407
O270C-H	106	109	89	4225	4446	268	4625	4046
O270C-J	46	83	78	3479	2427	75	3484	2421
O270C-K	12	54	66	2632	1141	-154	2647	1125
O270C-L	-22	6	32	858	-413	-342	944	-499
O270C-M	-11	-20	6	-287	-412	-342	-2	-698

Table A.2 (continued)

OUT-OF-PLANE MOMENT LOADING, MXN, ON NOZZLE (10000 IN-LB)

	MICRO-STRAIN			STRESSES			PRIN STRESSES	
ROSETTE	GAGE1	GAGE2	GAGE3	TRANS	LONG	SHEAR	SIGMX	SIGMN
I270N-A	-26	-333	-52	-8438	-3310	-3740	-1340	-10408
I270N-B	15	-368	-99	-10285	-2638	-3584	-1221	-11702
I270N-C	30	-394	-158	-12157	-2762	-3152	-1802	-13117
I270N-D	35	-403	-216	-13646	-3032	-2493	-2476	-14202
I270N-E	32	-412	-231	-14153	-3272	-2414	-2760	-14665
I270N-F	23	-522	-428	-20891	-5564	-1257	-5461	-20993
I270N-G	-109	-398	-401	-17441	-8509	39	-8509	-17442
I270N-H	-183	-245	-251	-10688	-8694	79	-8691	-10691
I270N-J	-180	-97	-162	-5507	-7050	864	-5120	-7437
I270N-K	-136	-47	-89	-2835	-4922	550	-2699	-5058
I270N-L	-100	-24	-44	-1383	-3425	275	-1347	-3461
I270N-N	-74	-15	-27	-829	-2463	157	-814	-2478
O270N-A	-170	-95	192	2319	-4409	-3831	4054	-6143
O270N-B	-239	-130	218	2203	-6520	-4638	4208	-8525
O270N-C	-274	-164	241	1991	-7617	-5404	4418	-10043
O270N-D	-334	-176	239	1744	-9504	-5521	4001	-11760
O270N-E	-354	-193	253	1703	-10123	-5945	4174	-12595
O270N-F	-351	-78	288	4994	-9044	-4869	6518	-10567
O270N-G	-311	31	276	7093	-7206	-3261	7801	-7915
O270N-H	-285	95	221	7259	-6375	-1686	7464	-6580
O270N-J	-251	84	98	4268	-6248	-192	4271	-6252
O270N-K	-216	46	17	1630	-6001	384	1649	-6021
O270N-L	-139	6	-32	-421	-4281	499	-357	-4345
O270N-N	-98	-26	-38	-1289	-3331	153	-1278	-3343

Table A.2 (continued)

OUT-OF-PLANE MOMENT LOADING, MXN, ON NOZZLE (10000 IN-LB)

	MICRO-STRAIN			STRESSES			PRIN STRESSES	
ROSETTE	GAGE1	GAGE2	GAGE3	TRANS	LONG	SHEAR	SIGMX	SIGMN
I-0-C-*	-6	-3	8	119	-138	-148	186	-205
I-22C-A	-32	-9	-6	-280	-1029	-38	-278	-1031
I-45C-A	-40	-14	-14	-585	-1379	0	-585	-1379
I-67C-A	-95	-166	40	-2666	-3635	-2748	-360	-5941
I-90C-A	80	-32	344	6773	4438	-4999	10739	472
I112C-A	-312	-392	-464	-18478	-14910	954	-14671	-18717
I135C-A	-46	-160	-106	-5804	-3116	-725	-2933	-5987
I157C-A	-17	-54	-32	-1869	-1076	-305	-973	-1973
I202C-A	52	35	64	2102	2191	-385	2534	1759
I225C-A	81	121	173	6389	4344	-693	6602	4131
I247C-A	413	514	381	19233	18168	1771	20550	16851
I292C-A	127	-20	170	3163	4763	-2541	6627	1299
I315C-A	49	29	29	1216	1839	0	1839	1216
I337C-A	26	6	14	416	905	-116	931	390
I180C-L	-46	3	0	114	-1353	39	115	-1354
O-22C-A	23	12	7	379	813	71	824	367
O-45C-A	47	28	-17	195	1483	595	1715	-38
O-67C-A	123	73	17	1829	4233	744	4444	1618
O-90C-A	64	-265	36	-5097	397	-4015	2515	-7215
O112C-A	366	25	28	766	11197	-37	11197	766
O135C-A	75	-81	-84	-3698	1151	37	1152	-3699
O157C-A	25	-11	-45	-1252	379	446	493	-1366
O180C-A	-25	0	-39	-829	-1001	520	-388	-1442
O202C-A	-67	20	-17	136	-1968	483	242	-2073
O225C-A	-128	46	46	2143	-3204	0	2143	-3204
O247C-A	-484	-57	-71	-2286	-15213	190	-2284	-15216
O292C-A	-177	-34	-94	-2622	-6082	797	-2448	-6257
O315C-A	-66	3	-46	-867	-2227	645	-610	-2484
O337C-A	-26	-6	-17	-473	-912	152	-426	-960
O180C-L	3	20	-26	-129	46	607	572	-655

Table A.2 (continued)

OUT-OF-PLANE MOMENT LOADING, MXN, ON NOZZLE (10000 IN-LB)

	MICRO-STRAIN			STRESSES			PRIN STRESSES	
ROSETTE	GAGE1	GAGE2	GAGE3	TRANS	LONG	SHEAR	SIGMX	SIGMN
I-0-N-*	-6	0	9	197	-114	-116	235	-153
I-22N-A	-68	-35	-38	-1549	-2502	39	-1548	-2503
I-45N-A	-30	-18	-27	-945	-1188	118	-897	-1236
I-67N-A	-86	24	26	1190	-2214	-37	1190	-2215
I-90N-A	26	-9	369	7880	3154	-5033	11077	-43
I112N-A	-331	-304	-396	-15015	-14426	1219	-13466	-15975
I135N-A	-77	-95	-145	-5175	-3859	669	-3579	-5455
I157N-A	-18	-33	-39	-1542	-997	79	-986	-1554
I180N-A	29	3	3	92	911	-1	911	92
I202N-A	53	44	59	2204	2250	-198	2427	2027
I225N-A	99	154	96	5399	4590	777	5871	4119
I247N-A	329	411	335	16042	14698	1011	16583	14156
I292N-A	93	3	-12	-298	2707	194	2719	-310
I315N-A	32	38	29	1434	1390	117	1531	1293
I337N-A	20	14	12	549	773	39	779	543
O-22N-A	14	23	0	488	577	307	843	222
O-45N-A	-3	52	-3	1078	234	730	1499	-187
O-67N-A	-9	52	26	1716	254	346	1794	177
O-90N-A	138	-260	78	-4149	2905	-4496	5093	-6336
O112N-A	105	8	356	7884	5523	-4624	11475	1931
O135N-A	17	-111	57	-1206	150	-2236	1808	-2865
O157N-A	20	-40	-20	-1334	196	-265	241	-1379
O180N-A	-28	-11	-37	-1033	-1164	341	-751	-1446
O202N-A	-68	-23	5	-316	-2144	-370	-244	-2216
O225N-A	-51	-85	80	-70	-1557	-2198	1507	-3134
O247N-A	-159	-410	-63	-10201	-7839	-4624	-4248	-13792
O292N-A	-20	-48	-105	-3356	-1606	757	-1324	-3638
O315N-A	-12	-6	-65	-1549	-814	786	-314	-2049
O337N-A	-17	0	-23	-500	-667	307	-266	-901
O-0-N-L	-9	0	-23	-492	-410	298	-150	-752

Table A.3. Torsional moment loading, M_{YN}, on nozzle

TORSIONAL MOMENT LOADING, MYN, ON NOZZLE (16000 IN-LB)

	MICRO-STRAIN			STRESSES			PRIN STRESSES	
ROSETTE	GAGE1	GAGE2	GAGE3	TRANS	LONG	SHEAR	SIGMX	SIGMN
I-0-C-A	8	3	-8	-133	213	150	269	-189
I-0-C-B	3	0	-3	-65	65	37	75	-75
I-0-C-C	0	-3	-3	-124	-37	0	-37	-124
I-0-C-D	0	-3	0	-62	-19	-37	3	-83
I-0-C-E	-3	-6	6	3	-83	-150	116	-196
I-0-C-F	0	-8	8	0	0	-225	225	-225
I-0-C-G	-3	-8	14	127	-46	-300	352	-272
I-0-C-H	-3	-11	14	64	-64	-334	341	-341
I-0-C-J	-3	-11	17	126	-46	-372	421	-342
I-0-C-K	-6	-11	20	190	-110	-409	475	-396
I-0-C-L	-8	-14	20	132	-211	-446	438	-518
O-0-C-A	-9	9	-26	-367	-367	457	90	-824
O-0-C-B	-6	3	-17	-308	-265	265	-20	-553
O-0-C-C	-6	3	-23	-434	-302	343	-19	-717
O-0-C-D	-14	-9	-23	-675	-631	190	-462	-844
O-0-C-E	-14	-11	-9	-425	-557	-38	-414	-567
O-0-C-F	-17	-6	-17	-484	-659	152	-396	-747
O-0-C-G	-14	-9	-17	-550	-594	114	-456	-688
O-0-C-H	-14	-9	-17	-550	-595	114	-456	-689
O-0-C-J	-3	-3	-5	-170	-127	38	-105	-191
O-0-C-K	-2	-3	-3	-113	-108	0	-107	-113
O-0-C-L	-8	-8	0	-169	-298	-114	-103	-364

Table A.3 (continued)

TORSIONAL MOMENT LOADING, MYN, ON NOZZLE (16000 IN-LB)

	MICRO-STRAIN			STRESSES			PRIN STRESSES	
ROSETTE	GAGE1	GAGE2	GAGE3	TRANS	LONG	SHEAR	SIGMX	SIGMN
I-0-N-B	0	3	0	57	17	39	81	-7
I-0-N-C	6	3	-3	-11	166	77	195	-40
I-0-N-D	3	6	-3	54	100	115	194	-40
I-0-N-E	3	6	-6	-10	79	154	195	-126
I-0-N-F	6	6	-3	54	188	117	255	-13
I-0-N-G	3	6	-6	-7	82	154	198	-123
I-0-N-H	6	6	-6	-9	168	155	258	-99
I-0-N-J	9	6	-9	-77	236	195	330	-170
I-0-N-K	12	3	-12	-209	285	193	352	-275
I-0-N-L**	15	6	-108	-2267	-242	1518	571	-3079
O-0-N-A	-6	17	-23	-137	-227	531	351	-714
O-0-N-B	-3	17	-26	-204	-162	568	386	-752
O-0-N-C	-1	23	-24	-23	-27	625	600	-650
O-0-N-D	2	23	-27	-95	42	663	640	-693
O-0-N-E	2	26	-27	-26	66	703	724	-684
O-0-N-F	5	29	-24	99	185	702	846	-562
O-0-N-G	5	31	-24	157	198	741	919	-563
O-0-N-H	5	31	-25	142	186	745	909	-581
O-0-N-J	8	32	-18	285	331	664	972	-356
O-0-N-K	11	32	-18	293	414	663	1020	-313

Table A.3 (continued)

TORSIONAL MOMENT LOADING, MYN, ON NOZZLE (16000 IN-LB)

	MICRO-STRAIN			STRESSES			PRIN STRESSES	
ROSETTE	GAGE1	GAGE2	GAGE3	TRANS	LONG	SHEAR	SIGMX	SIGMN
I270C-A	-70	742	-563	3999	-892	17389	19114	-16007
I270C-B	-103	667	-580	2013	-2491	16609	16522	-17000
I270C-C	-89	622	-524	2243	-2004	15271	15538	-15299
I270C-D	-75	530	-502	695	-2050	13748	13139	-14494
I270C-E	-94	505	-442	1478	-2386	12625	12317	-13226
I270C-F	-34	288	-260	662	-834	7301	7253	-7425
I270C-H	23	71	-29	912	956	1331	2265	-397
I270C-J	46	8	46	1133	1706	-496	1992	847
I270C-K	48	3	40	884	1718	-494	1948	654
I270C-L	26	8	11	406	888	-38	891	403
I270C-M	-6	3	-3	2	-173	76	30	-202
O270C-A	46	433	-406	526	1532	11181	12222	-10163
O270C-B	37	373	-335	787	1358	9440	10516	-8371
O270C-C	37	302	-264	784	1355	7542	8617	-6478
O270C-D	37	253	-182	1538	1584	5797	7358	-4236
O270C-E	35	197	-133	1353	1444	4397	5795	-2998
O270C-F	11	40	28	1479	774	152	1510	743
O270C-G	-17	-37	94	1261	-146	-1748	2441	-1326
O270C-H	-32	-63	108	1026	-642	-2281	2621	-2236
O270C-J	-49	-46	51	164	-1416	-1291	887	-2139
O270C-K	-52	-26	11	-265	-1626	-493	-105	-1786
O270C-L	-32	-6	-9	-293	-1041	38	-291	-1043
O270C-M	5	0	-6	-141	114	76	135	-162

Table A.3 (continued)

TORSIONAL MOMENT LOADING, MYN, ON NOZZLE (16000 IN-LB)

	MICRO-STRAIN			STRESSES			PRIN STRESSES	
ROSETTE	GAGE1	GAGE2	GAGE3	TRANS	LONG	SHEAR	SIGMX	SIGMN
I270N-A	-152	488	-494	34	-4553	13085	11025	-15544
I270N-B	-184	506	-421	2062	-4908	12345	11404	-14251
I270N-C	-123	552	-386	3791	-2548	12500	13517	-12274
I270N-D	-129	473	-85	8680	-1257	7438	12657	-5233
I270N-E**	-102	447	-263	4154	-1826	9463	11088	-8760
I270N-F	9	389	88	10477	3409	4003	12283	1603
I270N-G	6	100	315	9121	2913	-2865	10241	1793
I270N-H	56	-97	339	5247	3253	-5809	10144	-1644
I270N-J**	156	-38	253	4554	6050	-3886	9259	1345
I270N-K	97	-32	127	1965	3506	-2119	4990	480
I270N-L	77	-21	147	2699	3108	-2237	5150	657
I270N-N	71	18	109	2706	2933	-1217	4041	1597
O270N-A	31	514	-501	250	1002	13535	14166	-12915
O270N-B	16	583	-614	-686	284	15948	15754	-16156
O270N-C	-50	644	-749	-2252	-2166	18555	16346	-20764
O270N-D	-7	690	-795	-2296	-886	19779	18201	-21383
O270N-E	-53	718	-849	-2814	-2426	20887	18268	-23508
O270N-F	-93	538	-806	-5796	-4521	17900	12753	-23070
O270N-G	-32	307	-539	-5052	-2487	11267	7570	-15108
O270N-H	5	92	-294	-4453	-1177	5138	2578	-8207
O270N-J	48	-41	-78	-2673	649	498	722	-2746
O270N-K	45	-44	-18	-1412	939	-345	989	-1462
O270N-L	22	-24	-3	-620	482	-269	544	-682
O270N-N	-4	17	-21	-89	-136	498	387	-611

Table A.3 (continued)

TORSIONAL MOMENT LOADING, MYN, ON NOZZLE (16000 IN-LB)

	MICRO-STRAIN			STRESSES			PRIN STRESSES	
ROSETTE	GAGE1	GAGE2	GAGE3	TRANS	LONG	SHEAR	SIGMX	SIGMN
I-0-C-*	6	6	-3	56	185	112	250	-9
I-22C-A	-32	-41	-32	-1558	-1425	-121	-1353	-1629
I-45C-A	-86	-172	-152	-7027	-4697	-266	-4667	-7057
I-67C-A	-476	-599	-679	-27564	-22548	1069	-22330	-27783
I-90C-A	14	601	-745	-3185	-535	17934	16123	-19842
I112C-A	486	661	624	27703	22904	492	27753	22854
I135C-A	83	220	200	9142	5221	270	9160	5203
I157C-A	31	63	68	2842	1780	-76	2847	1775
I202C-A	-41	-61	-72	-2882	-2083	153	-2054	-2910
I225C-A	-90	-199	-237	-9493	-5539	500	-5477	-9555
I247C-A	-653	-777	-728	-32373	-29309	-655	-29175	-32507
I292C-A	396	572	517	23499	18923	732	23613	18809
I315C-A	72	144	176	6967	4254	-423	7031	4189
I337C-A	43	26	52	1664	1796	-346	2083	1377
I180C-L	-9	-6	20	325	-186	-346	500	-360
0-22C-A	40	5	-35	-695	978	537	1135	-852
0-45C-A	122	-90	-81	-3890	2502	-112	2504	-3892
0-67C-A	535	-17	19	-544	15892	-483	15906	-558
0-90C-A	-42	424	-447	-460	-1409	11599	10675	-12543
0112C-A	-547	-59	-20	-1132	-16755	-522	-1114	-16772
0135C-A	-120	145	108	5695	-1903	482	5725	-1934
0157C-A	-51	44	30	1691	-1013	185	1704	-1026
0180C-A	14	13	16	642	598	-39	664	575
0202C-A	61	-20	-34	-1255	1446	186	1458	-1267
0225C-A	133	-94	-146	-5421	2373	685	2433	-5480
0247C-A	706	54	34	1144	21515	266	21519	1141
0292C-A	-436	11	96	2843	-12222	-1138	2928	-12307
0315C-A	-97	82	91	3908	-1747	-112	3910	-1749
0337C-A	-49	31	-15	413	-1342	607	602	-1531
0180C-L	-15	-20	11	-185	-494	-418	106	-785

Table A.3 (continued)

TORSIONAL MOMENT LOADING, MYN, ON NOZZLE (16000 IN-LB)

	MICRO-STRAIN			STRESSES			PRIN STRESSES	
ROSETTE	GAGE1	GAGE2	GAGE3	TRANS	LONG	SHEAR	SIGMX	SIGMN
I-0-N-*	9	6	-6	-14	254	154	325	-84
I-22N-A	177	65	56	2460	6040	118	6044	2456
I-45N-A	-142	-153	-53	-4382	-5562	-1336	-3511	-6432
I-67N-A	-434	-681	-522	-25968	-20798	-2122	-20039	-26728
I-90N-A	-38	584	-743	-3458	-2188	17684	14872	-20518
I112N-A	490	560	693	27009	22791	-1768	27652	22148
I135N-A	153	109	239	7480	6845	-1729	8920	5405
I157N-A	44	29	77	2285	2013	-629	2792	1505
I180N-A	-24	-9	12	91	-681	-275	179	-769
I202N-A	-56	-80	-44	-2661	-2479	-472	-2090	-3050
I225N-A	-163	-236	-82	-6802	-6937	-2058	-4810	-8928
I247N-A	-536	-804	-647	-31306	-25479	-2097	-24803	-31982
I292N-A	350	443	609	22736	17313	-2213	23525	16524
I315N-A	137	41	131	3628	5198	-1204	5850	2976
I337N-A	44	6	47	1105	1643	-544	1980	767
O-22N-A	5	40	-35	90	180	999	1134	-865
O-45N-A	16	80	-107	-620	308	2496	2382	-2695
O-67N-A	242	521	11	11417	10671	6800	17854	4234
O-90N-A	-50	469	-505	-740	-1720	12985	11764	-14224
O112N-A	-191	-28	-620	-14040	-9929	7882	-3839	-20130
O135N-A	-9	159	-117	947	28	3676	4192	-3217
O157N-A	-14	63	-17	1016	-122	1061	1651	-757
O180N-A	17	26	3	606	694	303	956	344
O202N-A	34	28	-48	-475	881	1023	1431	-1024
O225N-A	0	100	-159	-1312	-394	3448	2626	-4332
O247N-A	222	685	74	16443	11588	8147	22517	5515
O292N-A	-202	97	-398	-6403	-7979	6593	-551	-13831
O315N-A	-6	104	-70	747	56	2321	2748	-1945
O337N-A	-14	39	-39	15	-417	1048	870	-1271
O-0-N-L	11	28	-17	235	408	599	926	-284

Table A.4. In-plane moment loading, M_{ZN}, on nozzle

IN-PLANE MOMENT LOADING, MZN, ON NOZZLE (15000 IN-LB)

	MICRO-STRAIN			STRESSES			PRIN STRESSES	
ROSETTE	GAGE1	GAGE2	GAGE3	TRANS	LONG	SHEAR	SIGMX	SIGMN
I-0-C-A	-233	-25	11	-48	-7014	-487	-14	-7048
I-0-C-B	-143	0	6	286	-4214	-75	288	-4215
I-0-C-C	-76	17	17	829	-2026	0	829	-2026
I-0-C-D	-31	23	20	966	-635	37	967	-636
I-0-C-E	0	23	23	992	301	0	992	301
I-0-C-F	39	14	6	395	1303	113	1317	381
I-0-C-G	34	-5	-5	-278	933	0	933	-278
I-0-C-H	25	-6	-11	-402	628	75	634	-408
I-0-C-J	17	-6	-8	-328	400	37	402	-330
I-0-C-K	17	-3	-6	-207	434	37	436	-209
I-0-C-L	14	0	-6	-145	369	76	379	-156
O-0-C-A	220	109	126	4910	8076	-229	8092	4893
O-0-C-B	120	114	106	4707	5015	115	5054	4668
O-0-C-C	63	94	83	3829	3038	152	3857	3010
O-0-C-D	26	77	80	3429	1804	-38	3430	1803
O-0-C-E	6	57	57	2510	928	1	2510	928
O-0-C-F	-11	26	26	1147	4	0	1147	4
O-0-C-G	0	12	9	445	137	38	449	132
O-0-C-H	14	6	9	303	524	-38	531	296
O-0-C-J	15	9	6	319	537	37	543	312
O-0-C-K	15	6	3	184	499	37	504	179
O-0-C-L	9	3	3	127	306	0	306	127

Table A.4 (continued)

IN-PLANE MOMENT LOADING, MZN, ON NOZZLE (15000 IN-LB)

	MICRO-STRAIN			STRESSES			PRIN STRESSES	
ROSETTE	GAGE1	GAGE2	GAGE3	TRANS	LONG	SHEAR	SIGMX	SIGMN
I-0-N-B	-134	0	0	153	-3960	-1	153	-3960
I-0-N-C	-72	9	18	659	-1976	-116	664	-1981
I-0-N-D	-29	21	20	932	-588	1	932	-588
I-0-N-E	0	18	18	773	237	1	773	237
I-0-N-F	44	6	3	147	1354	38	1355	146
I-0-N-G	44	-12	-14	-619	1125	39	1126	-620
I-0-N-H	32	-14	-20	-798	722	77	726	-802
I-0-N-J	29	-15	-15	-680	666	0	666	-680
I-0-N-K	32	-12	-6	-425	832	-83	838	-430
I-0-N-L	38	6	-53	-1075	820	779	1099	-1354
O-0-N-A	200	123	132	5376	7615	-113	7621	5371
O-0-N-B	118	103	109	4530	4885	-75	4900	4515
O-0-N-C	68	94	88	3941	3224	78	3949	3216
O-0-N-D	36	74	77	3274	2055	-39	3275	2054
O-0-N-E	12	59	59	2585	1140	0	2585	1140
O-0-N-F	-5	30	33	1381	259	-38	1382	258
O-0-N-G	10	15	15	664	488	1	664	488
O-0-N-H	22	16	13	606	835	34	840	601
O-0-N-J	24	12	15	582	895	-40	900	577
O-0-N-K	27	9	9	371	930	0	930	371

Table A.4 (continued)

IN-PLANE MOMENT LOADING, MZN, ON NOZZLE (15000 IN-LB)

	MICRO-STRAIN			STRESSES			PRIN STRESSES	
ROSETTE	GAGE1	GAGE2	GAGE3	TRANS	LONG	SHEAR	SIGMX	SIGMN
I270C-A	-6	-25	-257	-6191	-2032	3085	-391	-7831
I270C-B	-14	50	-282	-5082	-1951	4422	1174	-8207
I270C-C	-25	106	-279	-3777	-1893	5128	2379	-8049
I270C-D	-28	134	-282	-3224	-1809	5535	3064	-8097
I270C-E	-46	166	-280	-2454	-2102	5934	3659	-8215
I270C-F	-60	174	-225	-1060	-2112	5326	3766	-6938
I270C-H	-60	103	-83	508	-1643	2473	2129	-3264
I270C-J	-23	49	14	1414	-257	458	1531	-374
I270C-K	12	31	46	1685	851	-190	1726	810
I270C-L	54	40	52	1953	2217	-152	2287	1884
I270C-M	60	46	49	2009	2404	-38	2408	2005
O270C-A	57	613	-498	2461	2460	14793	17254	-12333
O270C-B	38	576	-472	2234	1800	13962	15981	-11947
O270C-C	43	516	-435	1722	1814	12670	14438	-10902
O270C-D	49	476	-361	2475	2216	11147	13493	-8803
O270C-E	46	411	-333	1663	1889	9901	11677	-8125
O270C-F	72	237	-168	1444	2588	5400	7446	-3414
O270C-G	58	129	-45	1772	2258	2319	4347	-317
O270C-H	40	60	26	1852	1766	458	2269	1349
O270C-J	0	17	66	1837	564	-648	2108	293
O270C-K	-31	9	52	1362	-524	-572	1522	-684
O270C-L	-71	3	18	535	-1966	-190	549	-1980
O270C-M	-77	9	6	411	-2172	38	412	-2172

Table A.4 (continued)

IN-PLANE MOMENT LOADING, MZN, ON NOZZLE (15000 IN-LB)

	MICRO-STRAIN			STRESSES			PRIN STRESSES	
ROSETTE	GAGE1	GAGE2	GAGE3	TRANS	LONG	SHEAR	SIGMX	SIGMN
I270N-A	-50	-82	-269	-7664	-3798	2494	-2575	-8886
I270N-B	-50	-178	-243	-9204	-4258	858	-4114	-9348
I270N-C	-38	-261	-231	-10763	-4375	-391	-4351	-10787
I270N-D	-38	-331	-214	-11917	-4722	-1558	-4399	-12239
I270N-E	-41	-412	-173	-12815	-5080	-3195	-3931	-13964
I270N-F	-65	-693	-38	-15990	-6737	-8720	-1491	-21235
I270N-G	-65	-640	21	-13527	-5997	-8800	-191	-19334
I270N-H	-17	-501	-50	-12087	-4149	-6011	-914	-15322
I270N-J	-32	-180	-79	-5659	-2665	-1336	-2156	-6169
I270N-K	-53	-118	-76	-4210	-2849	-550	-2655	-4404
I270N-L	-47	-56	-35	-1951	-1994	-275	-1696	-2249
I270N-N	-35	-18	-23	-862	-1314	79	-848	-1328
O270N-A	69	717	-624	1960	2669	17862	20180	-15551
O270N-B	90	734	-621	2382	3403	18054	20954	-15169
O270N-C	75	728	-661	1384	2669	18514	20552	-16499
O270N-D	153	717	-581	2815	5429	17289	21460	-13216
O270N-E	150	694	-518	3703	5611	16140	20826	-11511
O270N-F	124	478	-152	7014	5824	8395	14835	-1997
O270N-G	69	285	130	9040	4792	2072	9883	3949
O270N-H	6	135	265	8789	2815	-1726	9252	2352
O270N-J	-43	-17	274	5704	430	-3879	7758	-1623
O270N-K	-66	-34	205	3840	-820	-3190	5460	-2440
O270N-L	-48	-23	110	1975	-857	-1767	2823	-1705
O270N-N	-40	-11	29	449	-1057	-536	621	-1228

Table A.4 (continued)

IN-PLANE MOMENT LOADING, MZN, ON NOZZLE (15000 IN-LB)

	MICRO-STRAIN			STRESSES			PRIN STRESSES	
ROSETTE	GAGE1	GAGE2	GAGE3	TRANS	LONG	SHEAR	SIGMX	SIGMN
I-0-C-*	-197	20	-25	96	-5875	599	156	-5934
I-22C-A	-223	-31	-26	-1009	-7004	-75	-1008	-7005
I-45C-A	-198	-11	63	1353	-5522	-993	1493	-5663
I-67C-A	69	321	450	16866	7127	-1718	17160	6833
I-90C-A	29	-292	-29	-7078	-1262	-3512	390	-8729
I112C-A	252	-252	-3	-5875	5805	-3320	6683	-6753
I135C-A	295	66	152	4466	10197	-1146	10417	4245
I157C-A	258	138	135	5703	9451	38	9452	5703
I202C-A	272	122	116	4916	9631	78	9632	4915
I225C-A	361	168	81	5069	12364	1156	12543	4890
I247C-A	283	-72	-237	-7103	6373	2195	6721	-7451
I292C-A	29	390	295	15030	5380	1271	15195	5216
I315C-A	-240	41	-20	711	-6981	809	795	-7065
I337C-A	-231	-23	-32	-950	-7219	115	-948	-7221
I180C-L	-45	9	0	243	-1291	115	252	-1300
O-22C-A	217	120	132	5309	8115	-157	8123	5300
O-45C-A	232	173	190	7734	9284	-222	9315	7703
O-67C-A	45	154	369	11436	4787	-2863	12499	3725
O-90C-A	45	-566	628	1316	1751	-15915	17450	-14382
O112C-A	-446	-373	-379	-16050	-18197	76	-16048	-18200
O135C-A	-318	-106	-136	-4969	-11021	411	-4941	-11048
O157C-A	-293	-50	-75	-2418	-9501	335	-2402	-9516
O180C-A	-253	-64	-44	-2094	-8231	-258	-2084	-8242
O202C-A	-264	-94	-47	-2810	-8774	-632	-2744	-8840
O225C-A	-389	-165	-136	-6181	-13535	-384	-6161	-13555
O247C-A	-501	-390	-392	-16631	-20005	36	-16631	-20005
O292C-A	80	319	186	11007	5696	1783	11550	5153
O315C-A	249	208	183	8325	9954	338	10021	8258
O337C-A	226	114	129	5094	8298	-189	8309	5083
O180C-L	-42	-11	-5	-311	-1359	-76	-306	-1364

Table A.4 (continued)

IN-PLANE MOMENT LOADING, MZN, ON NOZZLE (15000 IN-LB)

	MICRO-STRAIN			STRESSES			PRIN STRESSES	
ROSETTE	GAGE1	GAGE2	GAGE3	TRANS	LONG	SHEAR	SIGMX	SIGMN
I-0-N-*	-223	12	6	630	-6487	77	630	-6487
I-22N-A	-26	9	-79	-1517	-1246	1179	-195	-2568
I-45N-A	-99	118	-177	-1178	-3316	3933	1828	-6323
I-67N-A	139	526	48	12451	7905	6365	16937	3420
I-90N-A	48	-280	-85	-8086	-991	-2598	-141	-8935
I112N-A	71	290	-271	321	2227	7474	8808	-6260
I135N-A	254	298	30	6935	9707	3580	12160	4482
I157N-A	228	189	71	5470	8468	1571	9141	4798
I180N-A	284	118	142	5411	10131	-313	10151	5390
I202N-A	240	80	195	5793	8924	-1529	9547	5170
I225N-A	202	41	339	8120	8483	-3964	12269	4334
I247N-A	82	-286	239	-1105	2124	-6996	7689	-6671
I292N-A	149	-6	499	10674	7674	-6723	16062	2285
I315N-A	-84	-169	120	-988	-2828	-3848	2049	-5865
I337N-A	-175	-111	38	-1401	-5662	-1982	-622	-6441
O-22N-A	188	168	93	5525	7298	1000	7747	5075
O-45N-A	223	217	156	7959	9073	809	9498	7534
O-67N-A	347	-34	151	2192	11057	-2459	11693	1556
O-90N-A	27	-625	684	1268	1184	-17445	18671	-16218
O112N-A	-466	-281	-415	-14798	-18433	1782	-14070	-19160
O135N-A	-262	-88	-373	-9835	-10798	3790	-6497	-14137
O157N-A	-222	-8	-154	-3316	-7648	1933	-2579	-8385
O180N-A	-273	-74	-65	-2757	-9015	-114	-2755	-9017
O202N-A	-239	-173	-22	-4029	-8372	-2020	-3235	-9166
O225N-A	-262	-341	-85	-9085	-10572	-3411	-6337	-13320
O247N-A	-486	-441	-282	-15339	-19191	-2122	-14399	-20131
O292N-A	367	216	43	5292	12600	2312	13270	4622
O315N-A	214	152	217	7862	8771	-861	9290	7343
O337N-A	191	96	166	5542	7399	-938	7791	5151
O-0-N-L	34	0	0	-34	1005	0	1005	-34

Table A.5. In-plane force loading, F_{XN}, on nozzle

IN-PLANE FORCE LOADING, FXN, ON NOZZLE (1200 LB)

	MICRO-STRAIN			STRESSES			PRIN STRESSES	
ROSETTE	GAGE1	GAGE2	GAGE3	TRANS	LONG	SHEAR	SIGMX	SIGMN
I-0-C-A	329	0	-70	-1896	9299	936	9377	-1974
I-0-C-B	191	-36	-42	-1929	5160	74	5160	-1930
I-0-C-C	82	-48	-53	-2304	1760	75	1761	-2306
I-0-C-D	14	-50	-53	-2291	-260	37	-259	-2291
I-0-C-E	-25	-48	-48	-2065	-1371	0	-1371	-2065
I-0-C-F	-73	-28	-22	-1021	-2492	-75	-1017	-2496
I-0-C-G	-59	0	-5	-48	-1777	75	-44	-1780
I-0-C-H	-39	3	9	296	-1077	-75	300	-1081
I-0-C-J	-28	0	0	36	-821	0	36	-821
I-0-C-K	-28	0	-3	-24	-836	37	-23	-838
I-0-C-L	-16	-5	-3	-157	-541	-38	-153	-545
O-0-C-A	-291	-185	-205	-8269	-11209	265	-8246	-11233
O-0-C-B	-148	-180	-168	-7482	-6688	-150	-6661	-7509
O-0-C-C	-68	-140	-131	-5872	-3806	-116	-3800	-5878
O-0-C-D	-17	-108	-117	-4926	-1982	115	-1978	-4931
O-0-C-E	6	-80	-77	-3444	-850	-36	-850	-3445
O-0-C-F	23	-25	-28	-1204	332	38	333	-1205
O-0-C-G	-5	-5	-3	-167	-211	-38	-145	-233
O-0-C-H	-25	-3	-3	-85	-782	0	-85	-782
O-0-C-J	-25	-2	-2	-81	-782	0	-81	-782
O-0-C-K	-25	-3	0	-26	-764	-38	-24	-766
O-0-C-L	-20	0	3	93	-561	-38	95	-563

Table A.5 (continued)

IN-PLANE FORCE LOADING, FXN, ON NOZZLE (1200 LB)

	MICRO-STRAIN			STRESSES			PRIN STRESSES	
ROSETTE	GAGE1	GAGE2	GAGE3	TRANS	LONG	SHEAR	SIGMX	SIGMN
I-0-N-B	0	-32	-34	-1454	-436	37	-435	-1455
I-0-N-C	79	-40	-52	-2116	1726	155	1732	-2122
I-0-N-D	18	-46	-52	-2175	-122	78	-119	-2178
I-0-N-E	-23	-40	-43	-1811	-1230	39	-1227	-1814
I-0-N-F	-75	-11	-11	-420	-2384	-1	-420	-2384
I-0-N-G	-64	15	20	844	-1655	-76	846	-1658
I-0-N-H	-43	26	26	1203	-938	0	1203	-938
I-0-N-J	-35	26	24	1137	-703	39	1137	-704
I-0-N-K	-29	24	18	937	-589	81	942	-594
I-0-N-L	-29	9	99	2413	-151	-1206	2891	-629
O-0-N-A	-259	-199	-207	-8643	-10349	115	-8635	-10357
O-0-N-B	-145	-165	-170	-7202	-6499	77	-6490	-7211
O-0-N-C	-73	-140	-131	-5890	-3949	-118	-3941	-5897
O-0-N-D	-29	-108	-108	-4710	-2278	1	-2278	-4710
O-0-N-E	-3	-82	-82	-3585	-1152	0	-1152	-3585
O-0-N-F	15	-38	-38	-1672	-45	1	-45	-1672
O-0-N-G	-11	-20	-17	-799	-570	-38	-564	-806
O-0-N-H	-28	-20	-19	-828	-1096	-4	-828	-1096
O-0-N-J	-32	-23	-23	-971	-1244	-1	-971	-1244
O-0-N-K	-23	-23	-20	-929	-960	-39	-903	-986

Table A.5 (continued)

IN-PLANE FORCE LOADING, FXN, ON NOZZLE (1200 LB)

	MICRO-STRAIN			STRESSES			PRIN STRESSES	
ROSETTE	GAGE1	GAGE2	GAGE3	TRANS	LONG	SHEAR	SIGMX	SIGMN
I270C-A	-14	151	329	10556	2757	-2377	11224	2090
I270C-B	-19	36	340	8300	1913	-4048	10262	-49
I270C-C	-22	-42	321	6155	1185	-4827	9100	-1759
I270C-D	-28	-89	315	4999	670	-5383	8636	-2967
I270C-E	-25	-139	300	3551	306	-5852	8001	-4144
I270C-F	-34	-191	223	736	-794	-5509	5533	-5591
I270C-H	-23	-117	69	-1031	-986	-2469	1461	-3478
I270C-J	-17	-45	-37	-1780	-1037	-112	-1020	-1796
I270C-K	-17	-31	-77	-2353	-1211	608	-948	-2616
I270C-L	-17	-51	-82	-2914	-1378	418	-1272	-3021
I270C-M	-5	-71	-74	-3178	-1117	38	-1116	-3179
O270C-A	-145	-745	564	-3829	-5494	-17447	12806	-22129
O270C-B	-93	-694	544	-3196	-3763	-16497	13020	-19978
O270C-C	-82	-617	510	-2274	-3147	-15020	12316	-17736
O270C-D	-73	-563	456	-2277	-2888	-13582	11003	-16168
O270C-E	-51	-472	425	-990	-1817	-11947	10551	-13357
O270C-F	-40	-257	257	56	-1171	-6844	6314	-7429
O270C-G	0	-122	132	200	70	-3384	3520	-3250
O270C-H	20	-45	37	-200	548	-1101	1337	-989
O270C-J	37	-8	-31	-906	851	303	902	-956
O270C-K	49	-20	-45	-1488	1016	341	1061	-1533
O270C-L	57	-43	-45	-1994	1125	38	1125	-1994
O270C-M	55	-51	-54	-2370	928	38	928	-2370

Table A.5 (continued)

IN-PLANE FORCE LOADING, FXN, ON NOZZLE (1200 LB)

	MICRO-STRAIN			STRESSES			PRIN STRESSES	
ROSETTE	GAGE1	GAGE2	GAGE3	TRANS	LONG	SHEAR	SIGMX	SIGMN
I270N-A	85	219	374	12944	6432	-2063	13543	5834
I270N-B	88	348	368	15636	7326	-273	15645	7317
I270N-C	76	462	377	18347	7788	1130	18467	7669
I270N-D	79	543	365	19883	8337	2373	20351	7868
I270N-E	82	637	327	21101	8791	4125	22355	7537
I270N-F	48	961	210	25664	9129	10009	30379	4415
I270N-G	36	831	112	20694	7287	9577	25680	2301
I270N-H	-5	616	148	16794	4880	6238	19463	2211
I270N-J	48	221	148	8057	3846	981	8275	3629
I270N-K	62	148	115	5713	3584	432	5798	3500
I270N-L	56	62	77	2997	2592	-197	3077	2513
I270N-N	53	18	56	1577	2077	-510	2395	1260
O270N-A	-186	-865	706	-3298	-6574	-20933	16061	-25933
O270N-B	-229	-882	694	-3879	-8035	-21007	15152	-27067
O270N-C	-229	-880	726	-3127	-7814	-21392	16049	-26990
O270N-D	-316	-877	631	-5058	-10983	-20085	12281	-28323
O270N-E	-315	-851	556	-6135	-11299	-18739	10199	-27633
O270N-F	-244	-607	136	-10082	-10338	-9889	-320	-20099
O270N-G	-137	-379	-181	-12144	-7762	-2641	-6521	-13384
O270N-H	-54	-198	-333	-11613	-5109	1799	-4645	-12077
O270N-J	12	9	-357	-7666	-1941	4880	854	-10462
O270N-K	52	44	-279	-5230	2	4302	2421	-7649
O270N-L	38	38	-161	-2749	317	2651	1847	-4279
O270N-N	41	38	-66	-658	1030	1384	1807	-1435

Table A.5 (continued)

IN-PLANE FORCE LOADING, FXN, ON NOZZLE (1200 LB)

	MICRO-STRAIN			STRESSES			PRIN STRESSES	
ROSETTE	GAGE1	GAGE2	GAGE3	TRANS	LONG	SHEAR	SIGMX	SIGMN
I-0-C-*	301	-76	-3	-2051	8408	-975	8498	-2141
I-22C-A	312	9	9	47	9381	3	9381	47
I-45C-A	278	14	-91	-1996	7737	1410	7937	-2196
I-67C-A	-51	-317	-506	-18045	-6950	2516	-6406	-18589
I-90C-A	-43	358	121	10565	1888	3165	11596	856
I112C-A	-340	358	60	9569	-7337	3968	10454	-8222
I135C-A	-452	-60	-143	-3957	-14744	1104	-3845	-14856
I157C-A	-466	-129	-94	-4382	-15299	-458	-4362	-15318
I202C-A	-459	-83	-107	-3673	-14866	309	-3664	-14875
I225C-A	-519	-173	-84	-5070	-17105	-1192	-4953	-17222
I247C-A	-384	122	329	10333	-8410	-2770	10734	-8811
I292C-A	-17	-447	-314	-16719	-5528	-1770	-5254	-16992
I315C-A	327	-63	26	-1176	9443	-1193	9576	-1308
I337C-A	327	3	0	-287	9710	38	9710	-287
I180C-L	13	-14	-14	-641	197	-1	197	-641
O-22C-A	-282	-197	-185	-8073	-10887	-155	-8064	-10895
O-45C-A	-312	-248	-237	-10310	-12455	-148	-10300	-12465
O-67C-A	-106	-167	-460	-13663	-7267	3903	-5419	-15510
O-90C-A	-142	661	-761	-2039	-4866	18953	15554	-22458
O112C-A	608	547	494	22210	24917	707	25090	22036
O135C-A	494	221	274	10322	17920	-705	17985	10257
O157C-A	502	224	224	9273	17857	1	17857	9273
O180C-A	424	243	232	9970	15723	150	15727	9966
O202C-A	430	226	193	8744	15528	446	15557	8715
O225C-A	564	291	231	10852	20189	793	20256	10785
O247C-A	675	630	496	24000	27463	1782	28216	23247
O292C-A	-137	-401	-202	-13102	-8030	-2656	-6894	-14239
O315C-A	-335	-259	-259	-11001	-13362	-3	-11001	-13362
O337C-A	-298	-170	-210	-8040	-11365	532	-7958	-11448
O180C-L	3	9	12	449	233	-38	455	227

Table A.5 (continued)

IN-PLANE FORCE LOADING, FXN, ON NOZZLE (1200 LB)

	MICRO-STRAIN			STRESSES			PRIN STRESSES	
ROSETTE	GAGE1	GAGE2	GAGE3	TRANS	LONG	SHEAR	SIGMX	SIGMN
I-0-N-*	329	-66	-57	-3080	8956	-116	8958	-3081
I-22N-A	68	-14	109	2018	2650	-1648	4013	656
I-45N-A	160	-159	230	1389	5219	-5187	8833	-2225
I-67N-A	-115	-610	-47	-14317	-7741	-7508	-2832	-19225
I-90N-A	-38	360	201	12366	2568	2121	12805	2129
I112N-A	-88	-383	395	365	-2539	-10374	9388	-11563
I135N-A	-368	-457	36	-8854	-13710	-6562	-4285	-18279
I157N-A	-380	-265	39	-4565	-12777	-4049	-2905	-14437
I180N-A	-522	-44	-121	-3047	-16571	1023	-2970	-16648
I202N-A	-392	6	-283	-5650	-13454	3853	-4069	-15036
I225N-A	-268	-6	-495	-10712	-11249	6524	-4451	-17510
I247N-A	-122	402	-294	2515	-2911	9280	9471	-9866
I292N-A	-148	18	-591	-12447	-8185	8116	-1925	-18707
I315N-A	131	216	-163	1019	4247	5048	7932	-2667
I337N-A	239	149	-90	1029	7486	3184	8792	-277
O-22N-A	-245	-245	-149	-8389	-9855	-1267	-7658	-10586
O-45N-A	-265	-302	-201	-10775	-11171	-1343	-9616	-12331
O-67N-A	-446	12	-167	-2901	-14263	2382	-2422	-14742
O-90N-A	-155	724	-824	-2022	-5257	20630	17053	-24332
O112N-A	605	406	594	21314	24553	-2500	25913	19955
O135N-A	432	205	614	17509	18208	-5453	23322	12395
O157N-A	403	153	318	9922	15079	-2196	15888	9113
O180N-A	466	273	258	11158	17324	190	17330	11152
O202N-A	415	327	138	9749	15367	2519	16331	8785
O225N-A	395	531	173	15050	16361	4771	20522	10890
O247N-A	594	617	401	21702	24327	2877	26177	19852
O292N-A	-469	-242	-74	-6427	-16003	-2235	-5931	-16499
O315N-A	-261	-199	-297	-10625	-11015	1310	-9496	-12144
O337N-A	-247	-154	-247	-8540	-9969	1232	-7830	-10679
O-0-N-L	-22	-8	-8	-339	-769	1	-339	-769

Table A.6. Axial force loading, F_{YN}, on nozzle

AXIAL FORCE LOADING, FYN, ON NOZZLE (4000 LB)

	MICRO-STRAIN			STRESSES			PRIN STRESSES	
ROSETTE	GAGE1	GAGE2	GAGE3	TRANS	LONG	SHEAR	SIGMX	SIGMN
I-0-C-A	-152	-34	-8	-756	-4780	-337	-728	-4808
I-0-C-B	-101	-11	-14	-440	-3166	37	-439	-3167
I-0-C-C	-62	0	0	72	-1831	0	72	-1831
I-0-C-D	-34	3	0	104	-978	37	105	-979
I-0-C-E	-14	6	3	204	-357	37	206	-360
I-0-C-F	17	3	0	49	524	38	527	46
I-0-C-G	17	-8	-5	-321	414	-37	416	-323
I-0-C-H	8	-6	-11	-373	141	74	152	-384
I-0-C-J	3	-6	-8	-308	-7	37	-2	-312
I-0-C-K	6	-3	-6	-187	115	37	119	-192
I-0-C-L	6	3	-3	-2	170	74	197	-29
O-0-C-A	149	60	72	2728	5279	-153	5288	2719
O-0-C-B	86	69	66	2861	3433	39	3436	2858
O-0-C-C	49	60	52	2401	2181	113	2449	2133
O-0-C-D	23	49	52	2177	1342	-38	2178	1340
O-0-C-E	6	37	40	1694	684	-37	1695	682
O-0-C-F	-11	17	20	834	-90	-38	835	-92
O-0-C-G	-8	3	6	203	-193	-38	207	-196
O-0-C-H	0	3	3	130	44	0	130	44
O-0-C-J	6	9	9	391	302	-1	391	302
O-0-C-K	3	3	6	196	161	-39	221	136
O-0-C-L	0	3	3	136	53	0	136	53

Table A.6 (continued)

AXIAL FORCE LOADING, FYN, ON NOZZLE (4000 LB)

	MICRO-STRAIN			STRESSES			PRIN STRESSES	
ROSETTE	GAGE1	GAGE2	GAGE3	TRANS	LONG	SHEAR	SIGMX	SIGMN
I-0-N-B	-96	-14	-12	-468	-3014	-38	-468	-3015
I-0-N-C	-55	-3	0	-2	-1655	-39	-1	-1656
I-0-N-D	-29	3	3	160	-822	-1	160	-822
I-0-N-E	-12	3	6	203	-288	-39	206	-291
I-0-N-F	23	-6	0	-151	652	-78	660	-159
I-0-N-G	29	-15	-12	-605	690	-39	691	-606
I-0-N-H	20	-20	-17	-850	355	-38	356	-852
I-0-N-J	23	-18	-18	-795	462	0	462	-795
I-0-N-K	23	-20	-12	-730	482	-118	494	-742
I-0-N-L	38	-12	-15	-618	956	39	957	-619
O-0-N-A	136	74	77	3158	5041	-38	5041	3157
O-0-N-B	88	65	68	2835	3491	-38	3493	2832
O-0-N-C	56	62	56	2519	2430	78	2564	2384
O-0-N-D	32	50	50	2159	1618	0	2159	1618
O-0-N-E	18	41	41	1788	1066	0	1788	1066
O-0-N-F	3	26	26	1160	439	0	1160	439
O-0-N-G	12	15	15	636	547	0	636	547
O-0-N-H	18	15	15	633	723	-1	723	633
O-0-N-J	26	21	15	749	1019	78	1040	728
O-0-N-K	27	15	15	617	981	0	981	617

Table A.6 (continued)

AXIAL FORCE LOADING, FYN, ON NOZZLE (4000 LB)

	MICRO-STRAIN			STRESSES			PRIN STRESSES	
ROSETTE	GAGE1	GAGE2	GAGE3	TRANS	LONG	SHEAR	SIGMX	SIGMN
I270C-A	123	34	-123	-2093	3058	2081	3793	-2828
I270C-B	131	70	-145	-1793	3399	2861	4666	-3061
I270C-C	120	92	-148	-1355	3195	3196	4843	-3003
I270C-D	114	95	-156	-1471	2992	3345	4782	-3260
I270C-E	94	106	-154	-1166	2477	3460	4566	-3255
I270C-F	46	80	-134	-1239	1001	2851	2944	-3182
I270C-H	-43	11	-71	-1267	-1662	1103	-344	-2585
I270C-J	-66	-3	-20	-426	-2094	228	-396	-2124
I270C-K	-43	17	9	614	-1098	114	621	-1105
I270C-L	34	49	40	1909	1602	114	1947	1565
I270C-M	54	51	57	2326	2326	-76	2403	2250
O270C-A	-11	359	-427	-1468	-769	10469	9356	-11593
O270C-B	-36	328	-421	-2002	-1692	9979	8134	-11827
O270C-C	-36	282	-395	-2445	-1828	9028	6897	-11169
O270C-D	-33	251	-344	-2001	-1604	7923	6122	-9728
O270C-E	-33	203	-327	-2692	-1809	7056	4819	-9320
O270C-F	3	86	-214	-2809	-743	3993	2348	-5901
O270C-G	26	35	-117	-1832	235	2015	1466	-3063
O270C-H	46	15	-48	-789	1145	838	1458	-1102
O270C-J	52	23	18	839	1807	75	1812	834
O270C-K	26	37	32	1488	1226	74	1507	1206
O270C-L	-54	26	26	1206	-1251	0	1206	-1251
O270C-M	-79	20	20	979	-2087	0	979	-2087

Table A.6 (continued)

AXIAL FORCE LOADING, FYN, ON NOZZLE (4000 LB)

	MICRO-STRAIN			STRESSES			PRIN STRESSES	
ROSETTE	GAGE1	GAGE2	GAGE3	TRANS	LONG	SHEAR	SIGMX	SIGMN
I270N-A	56	23	-114	-2052	1051	1830	1898	-2899
I270N-B	38	-29	-91	-2673	337	818	545	-2881
I270N-C	32	-70	-64	-2990	67	-78	69	-2992
I270N-D	23	-102	-47	-3300	-289	-740	-117	-3472
I270N-E	15	-149	-3	-3355	-568	-1947	433	-4355
I270N-F	-15	-268	147	-2637	-1230	-5539	3650	-7517
I270N-G	12	-253	174	-1759	-170	-5696	4787	-6716
I270N-H	59	-206	77	-2911	899	-3772	3220	-5231
I270N-J	50	-59	27	-764	1277	-1139	1786	-1273
I270N-K	27	-35	0	-803	558	-471	705	-950
I270N-L	21	-6	3	-84	597	-118	616	-104
I270N-N	15	15	9	505	597	79	642	460
O270N-A	23	446	-506	-1348	289	12689	12186	-13245
O270N-B	58	466	-503	-880	1467	12919	13266	-12679
O270N-C	61	466	-529	-1453	1381	13264	13303	-13376
O270N-D	132	460	-478	-521	3818	12498	14333	-11036
O270N-E	144	455	-437	225	4388	11885	14373	-9759
O270N-F	150	276	-201	1482	4936	6364	9803	-3385
O270N-G	118	118	-14	2151	4188	1764	5206	1133
O270N-H	75	3	81	1755	2773	-1035	3418	1110
O270N-J	43	-72	121	1024	1599	-2575	3903	-1279
O270N-K	29	-61	106	973	1151	-2229	3292	-1169
O270N-L	23	-35	60	538	846	-1268	1970	-585
O270N-N	8	-20	11	-208	190	-423	459	-477

Table A.6 (continued)

AXIAL FORCE LOADING, FYN, ON NOZZLE (4000 LB)

	MICRO-STRAIN			STRESSES			PRIN STRESSES	
ROSETTE	GAGE1	GAGE2	GAGE3	TRANS	LONG	SHEAR	SIGMX	SIGMN
I-0-C-*	-124	-6	-31	-664	-3909	337	-629	-3944
I-22C-A	-154	-31	-40	-1387	-5043	120	-1383	-5047
I-45C-A	-160	-28	9	-255	-4876	-497	-202	-4929
I-67C-A	-37	135	267	8866	1557	-1756	9266	1157
I-90C-A	155	-134	29	-2478	3903	-2174	4573	-3149
I112C-A	43	-349	-43	-8650	-1294	-4079	521	-10465
I135C-A	0	-25	189	3604	1094	-2863	5475	-778
I157C-A	-180	132	241	8395	-2879	-1450	8578	-3062
I202C-A	-165	231	142	8371	-2427	1193	8502	-2557
I225C-A	38	182	-20	3516	2182	2694	5625	73
I247C-A	66	-104	-335	-9720	-922	3079	48	-10691
I292C-A	-66	231	124	7883	373	1424	8144	112
I315C-A	-191	-6	-32	-614	-5903	346	-591	-5925
I337C-A	-165	-38	-29	-1278	-5321	-115	-1274	-5325
I180C-L	-260	-23	-49	-1299	-8192	347	-1282	-8209
0-22C-A	152	66	84	3123	5490	-233	5512	3100
0-45C-A	187	117	120	5011	7116	-37	7117	5011
0-67C-A	148	159	271	9286	7227	-1487	10065	6447
0-90C-A	-31	-488	360	-2784	-1752	-11304	9047	-13584
0112C-A	-78	-190	-148	-7331	-4541	-557	-4434	-7438
0135C-A	6	173	-22	3309	1163	2603	5052	-579
0157C-A	123	388	159	11890	7254	3049	13402	5742
0180C-A	120	366	385	16369	8515	-260	16378	8506
0202C-A	76	140	357	10839	5517	-2900	12114	4242
0225C-A	-32	-49	156	2404	-227	-2731	4119	-1943
0247C-A	-114	-217	-163	-8210	-5889	-720	-5683	-8415
0292C-A	174	239	179	9003	7912	797	9423	7492
0315C-A	199	134	131	5593	7651	39	7651	5592
0337C-A	159	71	74	3009	5680	-38	5681	3009
0180C-L	-265	6	8	597	-7773	-38	597	-7773

Table A.6 (continued)

AXIAL FORCE LOADING, FYN, ON NOZZLE (4000 LB)

	MICRO-STRAIN			STRESSES			PRIN STRESSES	
ROSETTE	GAGE1	GAGE2	GAGE3	TRANS	LONG	SHEAR	SIGMX	SIGMN
I-0-N-*	-141	-14	-14	-478	-4388	0	-478	-4388
I-22N-A	18	15	-50	-793	295	864	772	-1270
I-45N-A	-85	50	-150	-2108	-3183	2675	83	-5374
I-67N-A	36	316	-38	6067	2886	4718	9455	-502
I-90N-A	130	-118	6	-2603	3123	-1653	3565	-3046
I112N-A	-21	-62	-283	-7564	-2887	2950	-1461	-8990
I135N-A	27	-94	154	1274	1183	-3304	4533	-2076
I157N-A	-97	12	343	7897	-550	-4406	9777	-2430
I180N-A	-272	284	219	11333	-4746	866	11380	-4792
I202N-A	-106	325	3	7327	-985	4289	9143	-2802
I225N-A	91	93	-70	418	2843	2177	4122	-862
I247N-A	-17	-280	-76	-7796	-2861	-2721	-1656	-9001
I292N-A	58	-67	303	5131	3294	-4936	9233	-808
I315N-A	-73	-149	56	-1967	-2775	-2721	380	-5121
I337N-A	-119	-93	15	-1594	-4062	-1438	-934	-4722
O-22N-A	132	106	49	3267	4954	768	5252	2970
O-45N-A	158	179	92	5774	6483	1152	7334	4923
O-67N-A	274	72	127	4059	9431	-730	9528	3962
O-90N-A	-20	-516	409	-2333	-1314	-12334	10521	-14169
O112N-A	-119	-131	-37	-3553	-4648	-1250	-2736	-5465
O135N-A	176	85	3	1747	5818	1099	6096	1470
O157N-A	205	336	111	9592	9025	2994	12315	6301
O180N-A	148	401	390	17220	9608	151	17223	9605
O202N-A	182	88	285	8011	7869	-2626	10566	5313
O225N-A	120	-43	71	498	3737	-1516	4336	-101
O247N-A	-142	-68	-134	-4278	-5547	872	-3835	-5991
O292N-A	287	174	131	6380	10537	569	10613	6303
O315N-A	155	96	180	5889	6408	-1123	7301	4996
O337N-A	138	54	107	3377	5148	-713	5400	3126
O-0-N-L	34	9	8	336	1116	0	1116	336

Table A.7. Out-of-plane force loading, F_{ZN}, on nozzle

OUT-OF-PLANE FORCE LOADING, FZN, CN NOZZLE (600 LB)

	MICRO-STRAIN			STRESSES			PRIN STRESSES	
ROSETTE	GAGE1	GAGE2	GAGE3	TRANS	LONG	SHEAR	SIGMX	SIGMN
I-0-C-A	-6	-9	5	-74	-202	-188	61	-336
I-0-C-B	-3	-12	8	-79	-120	-260	162	-361
I-0-C-C	-3	-6	8	50	-83	-186	181	-214
I-0-C-D	0	-6	8	42	0	-187	209	-167
I-0-C-E	0	-6	8	50	1	-187	214	-163
I-0-C-F	2	-6	5	-24	65	-150	177	-136
I-0-C-G	-1	-3	5	38	-5	-113	132	-98
I-0-C-H	0	-6	3	-65	-22	-111	70	-157
I-0-C-J	0	-6	3	-63	-21	-111	72	-155
I-0-C-K	0	-3	3	-3	-4	-74	71	-78
I-0-C-L	3	-3	5	54	97	-111	188	-37
O-0-C-A	2	5	2	171	119	40	193	97
O-0-C-B	-1	2	3	105	11	-5	105	11
O-0-C-C	2	2	-1	32	75	42	101	7
O-0-C-D	-1	-1	0	-22	-24	-3	-20	-26
O-0-C-E	-4	-1	2	42	-95	-41	53	-106
O-0-C-F	-3	-1	-1	-21	-106	1	-21	-106
O-0-C-G	-3	-1	-3	-87	-129	38	-65	-151
O-0-C-H	-1	-3	-3	-147	-70	1	-70	-147
O-0-C-J	2	-1	-1	-31	57	1	57	-31
O-0-C-K	-1	3	-3	-14	-27	77	56	-97
O-0-C-L	0	3	-3	-13	-19	76	60	-92

Table A.7 (continued)

OUT-OF-PLANE FORCE LOADING, FZN, CN NOZZLE (600 LB)

	MICRO-STRAIN			STRESSES			PRIN STRESSES	
ROSETTE	GAGE1	GAGE2	GAGE3	TRANS	LONG	SHEAR	SIGMX	SIGMN
I-0-N-B	0	-9	8	-26	-8	-229	212	-246
I-0-N-C	-1	-9	11	46	-6	-272	293	-254
I-0-N-D	0	-12	11	-26	-21	-313	290	-337
I-0-N-E	-1	-9	8	-28	-29	-235	206	-264
I-0-N-F	0	-9	8	-12	-14	-230	217	-244
I-0-N-G	0	-12	8	-78	-36	-273	216	-330
I-0-N-H	0	-9	6	-75	-35	-193	139	-249
I-0-N-J	-3	-9	8	-8	-105	-233	182	-295
I-0-N-K	0	-6	12	118	25	-243	319	-175
I-0-N-L	-3	-12	-6	-392	-203	-79	-174	-421
O-0-N-A	5	5	5	225	222	-1	225	222
O-0-N-B	2	2	5	164	118	-39	186	96
O-0-N-C	2	3	3	111	108	0	111	108
O-0-N-D	0	2	3	110	21	0	110	21
O-0-N-E	0	0	3	50	6	-39	72	-17
O-0-N-F	0	0	0	-15	-18	-1	-15	-18
O-0-N-G	-1	0	0	-20	-22	-1	-19	-22
O-0-N-H	-1	-1	2	33	-13	-37	53	-33
O-0-N-J	0	3	0	46	2	39	69	-21
O-0-N-K	-1	3	-3	-10	-20	78	63	-93

Table A.7 (continued)

OUT-OF-PLANE FORCE LOADING, FZN, CN NOZZLE (600 LB)

	MICRO-STRAIN			STRESSES			PRIN STRESSES	
ROSETTE	GAGE1	GAGE2	GAGE3	TRANS	LONG	SHEAR	SIGMX	SIGMN
I270C-A	-120	-432	128	-6551	-5567	-7468	1425	-13543
I270C-B	-142	-393	142	-5365	-5880	-7134	1516	-12761
I270C-C	-165	-357	131	-4786	-6375	-6502	970	-12131
I270C-D	-187	-307	131	-3659	-6706	-5834	847	-11212
I270C-E	-183	-286	105	-3771	-6628	-5209	202	-10601
I270C-F	-198	-146	57	-1740	-6448	-2700	-512	-7677
I270C-H	-137	11	5	514	-3967	76	515	-3968
I270C-J	-60	56	5	1413	-1390	680	1569	-1547
I270C-K	-12	51	14	1442	79	495	1603	-82
I270C-L	22	25	17	897	938	114	1033	802
I270C-M	8	0	2	37	256	-38	263	31
O270C-A	-15	-117	295	3926	734	-5494	8052	-3392
O270C-B	45	-78	273	4233	2609	-4666	8157	-1315
O270C-C	76	-40	250	4519	3639	-3866	7970	188
O270C-D	99	-12	215	4356	4264	-3024	7335	1286
O270C-E	118	25	204	4900	5020	-2388	7349	2572
O270C-F	148	99	139	5079	5954	-531	6205	4828
O270C-G	139	125	88	4527	5532	494	5734	4324
O270C-H	111	111	71	3871	4483	530	4788	3565
O270C-J	36	74	51	2693	1902	306	2798	1798
O270C-K	-3	34	42	1682	408	-112	1692	398
O270C-L	-29	-1	14	322	-778	-190	354	-810
O270C-M	-9	-12	2	-196	-338	-189	-64	-469

Table A.7 (continued)

OUT-OF-PLANE FORCE LOADING, FZN, CN NOZZLE (600 LB)

	MICRO-STRAIN			STRESSES			PRIN STRESSES	
ROSETTE	GAGE1	GAGE2	GAGE3	TRANS	LONG	SHEAR	SIGMX	SIGMN
I270N-A	-27	-360	67	-6410	-2726	-5684	1407	-10543
I270N-B	23	-389	17	-8194	-1769	-5412	1312	-11275
I270N-C	29	-404	-27	-9494	-1983	-5026	536	-12013
I270N-D	40	-395	-138	-11748	-2310	-3426	-1198	-12861
I270N-E	35	-395	-109	-11104	-2293	-3816	-870	-12527
I270N-F	0	-448	-322	-16919	-5089	-1689	-4853	-17156
I270N-G	-107	-286	-354	-13954	-7384	903	-7262	-14076
I270N-H	-171	-139	-251	-8380	-7658	1494	-6482	-9556
I270N-J	-171	-59	-171	-4879	-6604	1492	-4018	-7465
I270N-K	-127	-30	-95	-2598	-4593	864	-2276	-4915
I270N-L	-95	-18	-68	-1787	-3377	668	-1544	-3620
I270N-N	-65	-24	-50	-1561	-2425	353	-1435	-2551
O270N-A	-109	-190	311	2770	-2452	-6669	7321	-7002
O270N-B	-179	-230	348	2782	-4520	-7704	7656	-9394
O270N-C	-204	-273	391	2812	-5288	-8853	8498	-10974
O270N-D	-273	-296	394	2445	-7469	-9199	7938	-12961
O270N-E	-291	-317	406	2275	-8038	-9621	8034	-13798
O270N-F	-288	-184	394	4928	-7154	-7704	8677	-10903
O270N-G	-253	-40	313	6279	-5714	-4715	7911	-7345
O270N-H	-224	63	219	6439	-4802	-2069	6807	-5171
O270N-J	-194	86	89	4065	-4587	-39	4065	-4588
O270N-K	-162	60	20	1932	-4277	538	1978	-4323
O270N-L	-99	23	-15	283	-2871	499	360	-2948
O270N-N	-47	-3	-6	-157	-1445	38	-156	-1446

Table A.7 (continued)

OUT-OF-PLANE FORCE LOADING, FZN, CN NOZZLE (600 LB)

	MICRO-STRAIN			STRESSES			PRIN STRESSES	
ROSETTE	GAGE1	GAGE2	GAGE3	TRANS	LONG	SHEAR	SIGMX	SIGMN
I-0-C-*	-6	-3	8	115	-142	-147	181	-209
I-22C-A	0	5	0	107	20	70	146	-19
I-45C-A	-6	28	20	1067	137	116	1081	123
I-67C-A	20	3	163	3611	1669	-2136	4987	294
I-90C-A	91	-155	400	5290	4328	-7403	12228	-2610
I112C-A	-356	-482	-493	-21029	-16977	149	-16971	-21034
I135C-A	-69	-172	-98	-5859	-3833	-989	-3430	-6262
I157C-A	-29	-58	-9	-1435	-1307	-648	-719	-2022
I202C-A	34	14	66	1720	1539	-697	2332	927
I225C-A	86	107	179	6182	4440	-963	6610	4013
I247C-A	444	511	453	20698	19539	770	21082	19155
I292C-A	-1	-148	14	-2947	-899	-2156	463	-4309
I315C-A	5	-12	-23	-779	-74	155	-42	-812
I337C-A	-6	0	-3	-69	-207	39	-59	-217
I180C-L	-6	-20	14	-132	-218	-460	287	-636
O-22C-A	-3	2	2	91	-77	7	91	-78
O-45C-A	2	39	5	964	360	446	1200	124
O-67C-A	-6	69	11	1769	349	781	2114	4
O-90C-A	16	-274	94	-3955	-699	-4905	2841	-7495
O112C-A	454	55	72	2306	14322	-224	14327	2302
O135C-A	103	-37	-87	-2825	2237	668	2324	-2912
O157C-A	39	39	-48	-244	1086	1152	1751	-909
O180C-A	-9	44	-45	-6	-266	1188	1059	-1331
O202C-A	-42	47	-31	392	-1155	1041	915	-1678
O225C-A	-117	77	31	2488	-2774	610	2558	-2844
O247C-A	-499	-23	-63	-1352	-15370	532	-1332	-15390
O292C-A	-11	-15	-77	-2003	-945	835	-485	-2463
O315C-A	-3	3	-35	-703	-313	495	24	-1040
O337C-A	8	2	2	100	272	-1	272	100
O180C-L	5	45	-34	231	228	1062	1291	-833

Table A.7 (continued)

OUT-OF-PLANE FORCE LOADING, FZN, ON NOZZLE (600 LB)

	MICRO-STRAIN			STRESSES			PRIN STRESSES	
ROSETTE	GAGE1	GAGE2	GAGE3	TRANS	LONG	SHEAR	SIGMX	SIGMN
I-0-N-*	-3	-3	8	114	-60	-152	202	-148
I-22N-A	-92	-45	-42	-1795	-3290	-39	-1794	-3291
I-45N-A	15	14	-12	28	466	354	663	-169
I-67N-A	23	153	132	6237	2567	285	6259	2545
I-90N-A	61	-136	421	6203	3694	-7429	12483	-2586
I112N-A	-355	-411	-473	-19022	-16342	826	-16108	-19256
I135N-A	-95	-139	-130	-5820	-4595	-118	-4584	-5831
I157N-A	-21	-53	-9	-1359	-1041	-587	-592	-1808
I180N-A	6	-18	26	165	217	-593	784	-402
I202N-A	26	20	61	1753	1302	-558	2129	926
I225N-A	84	145	116	5658	4217	387	5756	4120
I247N-A	352	454	414	18690	16182	545	18803	16068
I292N-A	-15	-108	-152	-5699	-2164	582	-2070	-5792
I315N-A	-21	5	-6	4	-623	157	41	-660
I337N-A	-9	0	0	-10	-284	-1	-10	-284
O-22N-A	2	2	5	168	125	-39	191	102
O-45N-A	-9	20	23	940	6	-40	942	5
O-67N-A	-47	-53	28	-482	-1541	-1076	187	-2211
O-90N-A	71	-277	141	-3078	1221	-5570	5042	-6899
O112N-A	190	48	466	11087	9037	-5572	15728	4396
O135N-A	79	-88	82	-226	2309	-2274	3645	-1561
O157N-A	56	0	-23	-574	1522	304	1565	-618
O180N-A	-15	37	-43	-132	-482	1063	770	-1384
O202N-A	-66	14	-6	235	-1907	270	269	-1941
O225N-A	-72	-74	79	188	-2091	-2045	1390	-3293
O247N-A	-194	-447	-46	-10613	-8995	-5343	-4400	-15208
O292N-A	53	-49	28	-524	1445	-1024	1881	-959
O315N-A	11	-14	-11	-574	161	-38	163	-576
O337N-A	3	0	3	51	96	-35	115	31
O-0-N-L	0	6	-3	59	14	112	151	-78

Table A.8. Torsional moment loading, M_{XC}, on cylinder

TORSIONAL MOMENT LOADING, MXC, ON CYLINDER (20000 IN-LB)

	MICRO-STRAIN			STRESSES			PRIN STRESSES	
ROSETTE	GAGE1	GAGE2	GAGE3	TRANS	LONG	SHEAR	SIGMX	SIGMN
I-0-C-A	-9	-39	6	-736	-477	-599	7	-1219
I-0-C-B	0	-42	36	-129	-42	-1048	963	-1134
I-0-C-C	-3	-37	34	-63	-106	-936	851	-1020
I-0-C-D	-3	-34	34	-2	-88	-898	854	-944
I-0-C-E	-3	-34	34	0	-88	-898	855	-943
I-0-C-F	3	-34	28	-132	42	-824	783	-873
I-0-C-G	-3	-28	31	59	-71	-786	783	-795
I-0-C-H	0	-31	28	-65	-22	-779	736	-823
I-0-C-J	0	-28	25	-63	-21	-705	664	-748
I-0-C-K	0	-28	28	-3	-4	-743	739	-746
I-0-C-L	0	-31	31	-4	-5	-816	812	-820
O-0-C-A	6	49	-48	-1	177	1293	1384	-1207
O-0-C-B	3	49	-40	193	151	1181	1352	-1009
O-0-C-C	0	52	-40	261	86	1216	1392	-1046
O-0-C-D	0	52	-40	259	84	1218	1393	-1050
O-0-C-E	3	49	-43	131	133	1218	1350	-1086
O-0-C-F	-3	46	-43	75	-58	1179	1189	-1172
O-0-C-G	3	43	-45	-56	75	1179	1191	-1171
O-0-C-H	0	49	-48	8	12	1293	1303	-1283
O-0-C-J	3	51	-48	70	114	1327	1418	-1235
O-0-C-K	0	48	-51	-57	-9	1327	1294	-1359
O-0-C-L	-3	54	-51	71	-58	1403	1411	-1398

Table A.8 (continued)

TORSIONAL MOMENT LOADING, MXC, ON CYLINDER (20000 IN-LB)

	MICRO-STRAIN			STRESSES			PRIN STRESSES	
ROSETTE	GAGE1	GAGE2	GAGE3	TRANS	LONG	SHEAR	SIGMX	SIGMN
I-0-N-B	0	-47	40	-134	-40	-1160	1074	-1248
I-0-N-C	0	-47	43	-68	-26	-1200	1153	-1247
I-0-N-D	0	-47	43	-70	-24	-1200	1153	-1248
I-0-N-E	0	-50	46	-71	-27	-1277	1229	-1326
I-0-N-F	0	-49	52	61	16	-1354	1392	-1316
I-0-N-G	0	-55	55	-4	-4	-1470	1467	-1474
I-0-N-H	0	-58	52	-131	-42	-1470	1384	-1557
I-0-N-J	-3	-53	58	120	-66	-1479	1509	-1455
I-0-N-K	-12	-53	67	323	-264	-1605	1661	-1602
I-0-N-L**	-3	-62	199	3011	818	-3466	5550	-1721
O-0-N-A	5	51	-40	226	224	1213	1438	-988
O-0-N-B	2	39	-29	228	138	909	1093	-727
O-0-N-C	0	35	-30	117	25	858	931	-789
O-0-N-D	3	32	-27	111	112	780	891	-668
O-0-N-E	-3	29	-27	56	-78	741	733	-755
O-0-N-F	0	29	-27	52	5	741	770	-713
O-0-N-G	0	29	-30	-16	-17	780	763	-796
O-0-N-H	0	29	-27	44	-1	742	764	-721
O-0-N-J	0	29	-30	-15	-13	780	767	-794
O-0-N-K	-3	29	-29	-6	-102	780	728	-835

Table A.8 (continued)

TORSIONAL MOMENT LOADING, MXC, ON CYLINDER (20000 IN-LB)

	MICRO-STRAIN			STRESSES			PRIN STRESSES	
ROSETTE	GAGE1	GAGE2	GAGE3	TRANS	LONG	SHEAR	SIGMX	SIGMN
I270C-A	-64	-688	610	-1648	-2421	-17302	15272	-19341
I270C-B	-39	-638	599	-820	-1421	-16486	15368	-17609
I270C-C	-50	-596	521	-1601	-1989	-14889	13096	-16686
I270C-D	-67	-510	482	-542	-2172	-13219	11887	-14601
I270C-E	-32	-477	416	-1288	-1332	-11899	10589	-13209
I270C-F	-40	-240	211	-586	-1379	-6007	5037	-7003
I270C-H	-6	8	-17	-185	-230	342	135	-550
I270C-J	3	77	-74	51	97	2014	2088	-1940
I270C-K	8	60	-63	-75	231	1635	1720	-1564
I270C-L	6	34	-34	-11	164	912	993	-840
I270C-M	3	31	-23	181	137	722	882	-564
O270C-A	-3	-492	444	-1050	-394	-12472	11755	-13199
O270C-B	26	-412	381	-705	566	-10575	10525	-10664
O270C-C	29	-324	322	-85	836	-8605	8993	-8242
O270C-D	29	-259	254	-144	821	-6826	7181	-6505
O270C-E	32	-190	217	540	1112	-5421	6254	-4602
O270C-F	26	-23	60	795	1015	-1103	2013	-203
O270C-G	20	46	-11	738	827	760	1544	21
O270C-H	12	49	-28	433	478	1027	1483	-572
O270C-J	3	6	3	194	150	37	215	129
O270C-K	0	-31	34	68	25	-875	922	-829
O270C-L	-8	-45	46	18	-244	-1216	1110	-1337
O270C-M	-3	-43	49	135	-37	-1216	1269	-1170

Table A.8 (continued)

TORSIONAL MOMENT LOADING, MXC, ON CYLINDER (20000 IN-LB)

	MICRO-STRAIN			STRESSES			PRIN STRESSES	
ROSETTE	GAGE1	GAGE2	GAGE3	TRANS	LONG	SHEAR	SIGMX	SIGMN
I270N-A	128	-389	610	4722	5260	-13313	18307	-8325
I270N-B	187	-377	569	4021	6804	-12613	18102	-7277
I270N-C	128	-369	581	4524	5203	-12656	17524	-7797
I270N-D**	154	-293	266	-762	4404	-7435	9692	-6050
I270N-E	143	-243	514	5795	6021	-10083	15992	-4176
I270N-F	9	-73	282	4574	1640	-4733	8062	-1848
I270N-G	21	200	-3	4303	1911	2699	6059	155
I270N-H	-26	323	-147	3904	382	6258	8644	-4358
I270N-J	-85	141	-132	290	-2464	3638	2803	-4976
I270N-K	-47	88	-62	636	-1215	1995	1909	-2489
I270N-L	-41	41	-106	-1371	-1642	1956	454	-3467
I270N-N	-50	-9	-82	-1942	-2077	978	-1029	-2990
O270N-A	-32	-587	529	-1246	-1334	-14860	13570	-16150
O270N-B	-64	-685	620	-1339	-2313	-17389	15569	-19222
O270N-C	-38	-774	747	-544	-1297	-20261	19344	-21185
O270N-D	-118	-837	767	-1402	-3969	-21373	18726	-24097
O270N-E	-98	-886	796	-1866	-3507	-22409	19737	-25110
O270N-F	-64	-748	664	-1773	-2440	-18807	16703	-20916
O270N-G	-41	-501	371	-2814	-2063	-11607	9174	-14052
O270N-H	-3	-242	120	-2662	-894	-4825	3128	-6684
O270N-J	14	-20	-40	-1348	26	269	77	-1399
O270N-K	23	23	-46	-534	529	921	1061	-1066
O270N-L	14	35	-35	-19	426	921	1151	-744
O270N-N	3	6	0	121	121	77	198	44

Table A.8 (continued)

TORSIONAL MOMENT LOADING, MXC, ON CYLINDER (20000 IN-LB)

	MICRO-STRAIN			STRESSES			PRIN STRESSES	
ROSETTE	GAGE1	GAGE2	GAGE3	TRANS	LONG	SHEAR	SIGMX	SIGMN
I-0-C-*	-3	-8	34	555	80	-561	926	-292
I-22C-A	37	14	69	1779	1647	-726	2443	984
I-45C-A	92	155	235	8455	5283	-1068	8781	4957
I-67C-A	501	584	736	28453	23565	-2022	29181	22837
I-90C-A	6	-719	601	-2592	-608	-17587	16015	-19215
I112C-A	-464	-796	-610	-30391	-23037	-2481	-22279	-31150
I135C-A	-80	-215	-140	-7719	-4725	-991	-4426	-8017
I157C-A	-37	-63	-12	-1600	-1601	-687	-914	-2287
I202C-A	49	23	69	1972	2061	-617	2635	1398
I225C-A	101	156	219	8140	5472	-847	8386	5225
I247C-A	502	572	690	27185	23231	-1578	27738	22678
I292C-A	-526	-766	-659	-30727	-24995	-1424	-24661	-31061
I315C-A	-87	-220	-153	-8097	-5033	-885	-4795	-8334
I337C-A	-43	-67	-15	-1733	-1823	-693	-1084	-2472
I180C-L	2	-23	20	-69	43	-577	567	-592
O-22C-A	-45	60	-45	377	-1249	1404	1186	-2059
O-45C-A	-134	162	0	3698	-2909	2153	4337	-3549
O-67C-A	-572	36	-25	867	-16890	817	904	-16928
O-90C-A	-14	-510	449	-1338	-825	-12778	11699	-13862
O112C-A	563	11	78	1336	17291	-892	17341	1287
O135C-A	123	-39	-142	-4123	2439	1374	2715	-4399
O157C-A	53	50	-48	-3	1584	1300	2314	-733
O180C-A	-14	44	-48	-52	-438	1225	995	-1485
O202C-A	-59	47	-42	179	-1708	1189	753	-2282
O225C-A	-140	131	17	3387	-3183	1519	3721	-3517
O247C-A	-564	56	-66	410	-16794	1631	563	-16947
O292C-A	637	31	-52	-1151	18772	1100	18833	-1212
O315C-A	128	-26	-148	-3972	2634	1632	3015	-4354
O337C-A	54	42	-52	-262	1529	1251	2172	-905
O180C-L	2	51	-46	108	105	1289	1396	-1183

Table A.8 (continued)

TORSIONAL MOMENT LOADING, MXC, ON CYLINDER (20000 IN-LB)

	MICRO-STRAIN			STRESSES			PRIN STRESSES	
ROSETTE	GAGE1	GAGE2	GAGE3	TRANS	LONG	SHEAR	SIGMX	SIGMN
I-0-N-*	-6	-12	9	-61	-194	-269	150	-404
I-22N-A	-129	-56	-12	-1338	-4274	-587	-1225	-4387
I-45N-A	125	173	129	6507	5707	588	6818	5396
I-67N-A	429	714	893	34849	23324	-2384	35323	22851
I-90N-A	108	-709	588	-2778	2416	-17270	17284	-17645
I112N-A	-459	-656	-776	-30963	-23051	1606	-22738	-31277
I135N-A	-127	-147	-159	-6589	-5777	157	-5748	-6619
I157N-A	-27	-56	-3	-1272	-1182	-703	-522	-1932
I180N-A	9	-27	47	431	389	-980	1391	-570
I202N-A	47	26	70	2063	2020	-591	2633	1450
I225N-A	125	171	136	6620	5724	464	6817	5528
I247N-A	430	674	636	28304	21382	504	28340	21345
I292N-A	-404	-625	-802	-30901	-21391	2360	-20837	-31455
I315N-A	-119	-137	-145	-6070	-5399	117	-5380	-6089
I337N-A	-32	-55	-12	-1443	-1400	-581	-840	-2003
O-22N-A	-66	20	6	640	-1798	192	655	-1813
O-45N-A	-115	-61	115	1327	-3061	-2341	2342	-4075
O-67N-A	-277	-550	0	-11793	-11838	-7333	-4483	-19149
O-90N-A	-78	-582	496	-1817	-2881	-14359	12020	-16717
O112N-A	287	34	642	14528	12962	-8102	21885	5605
O135N-A	108	-122	79	-1068	2906	-2688	4261	-2423
O157N-A	65	0	-23	-583	1774	303	1812	-622
O180N-A	-20	36	-55	-376	-725	1213	676	-1776
O202N-A	-86	5	-12	-56	-2589	232	-34	-2610
O225N-A	-114	-66	99	858	-3166	-2195	1824	-4131
O247N-A	-287	-569	-15	-12497	-12367	-7382	-5050	-19814
O292N-A	298	-55	576	11133	12270	-8404	20124	3279
O315N-A	87	-110	76	-842	2355	-2470	3698	-2185
O337N-A	62	0	-23	-569	1679	301	1719	-609
O-0-N-L	-9	28	-31	-55	-273	785	629	-957

Table A.9. Out-of-plane moment loading, M_{YC}, on cylinder

OUT-OF-PLANE MOMENT LOADING, MYC, ON CYLINDER (60000 IN-LB)

	MICRO-STRAIN			STRESSES			PRIN STRESSES	
ROSETTE	GAGE1	GAGE2	GAGE3	TRANS	LONG	SHEAR	SIGMX	SIGMN
I-0-C-A	9	-14	-28	-926	-19	188	18	-964
I-0-C-B	0	-14	-11	-545	-157	-38	-154	-549
I-0-C-C	-8	-11	-11	-477	-389	0	-389	-477
I-0-C-D	-11	-11	-8	-410	-453	-38	-388	-475
I-0-C-E	-11	-5	-5	-228	-399	0	-228	-399
I-0-C-F	-11	-3	3	23	-324	-75	38	-339
I-0-C-G	-3	6	6	261	2	0	261	2
I-0-C-H	-3	6	9	318	17	-38	322	12
I-0-C-J	0	6	17	496	153	-148	551	98
I-0-C-K	3	3	22	555	257	-260	705	107
I-0-C-L	3	3	34	802	331	-409	1039	95
O-0-C-A	-8	-8	-43	-1110	-581	456	-318	-1373
O-0-C-B	0	3	-37	-741	-212	534	119	-1072
O-0-C-C	3	12	-34	-491	-52	607	374	-917
O-0-C-D	3	17	-34	-367	-16	685	516	-899
O-0-C-E	3	17	-31	-304	4	647	516	-815
O-0-C-F	-3	23	-31	-173	-130	722	571	-874
O-0-C-G	-8	17	-37	-415	-372	722	329	-1117
O-0-C-H	-8	17	-37	-418	-370	722	328	-1116
O-0-C-J	-5	12	-37	-541	-324	644	220	-1086
O-0-C-K	-2	12	-40	-613	-258	682	269	-1140
O-0-C-L	-3	3	-37	-738	-298	530	57	-1092

Table A.9 (continued)

OUT-OF-PLANE MOMENT LOADING, MYC, ON CYLINDER (60000 IN-LB)

	MICRO-STRAIN			STRESSES			PRIN STRESSES	
ROSETTE	GAGE1	GAGE2	GAGE3	TRANS	LONG	SHEAR	SIGMX	SIGMN
I-0-N-B	0	-11	-23	-746	-224	152	-183	-787
I-0-N-C	-8	-8	-20	-615	-431	156	-342	-703
I-0-N-D	-11	-8	-17	-542	-501	119	-401	-642
I-0-N-E	-14	-8	-14	-473	-562	79	-426	-608
I-0-N-F	-11	-9	-6	-297	-430	-40	-286	-441
I-0-N-G	-5	-6	0	-111	-198	-76	-67	-242
I-0-N-H	-3	-9	0	-180	-131	-116	-37	-274
I-0-N-J	-5	-9	0	-178	-217	-117	-79	-316
I-0-N-K	-6	-8	3	-115	-202	-149	-3	-313
I-0-N-L	-3	-9	187	3926	1088	-2606	5474	-461
O-0-N-A	3	-2	-28	-677	-104	342	56	-836
O-0-N-B	12	0	-17	-371	245	229	320	-446
O-0-N-C	12	0	-11	-256	288	156	329	-298
O-0-N-D	15	3	-5	-62	432	118	459	-89
O-0-N-E	12	9	0	194	418	117	468	144
O-0-N-F	6	9	6	330	288	40	354	265
O-0-N-G	3	9	9	403	225	1	403	225
O-0-N-H	1	9	10	420	152	-4	420	152
O-0-N-J	-3	6	6	279	7	0	279	7
O-0-N-K	-2	3	6	205	-9	-39	211	-15

Table A.9 (continued)

OUT-OF-PLANE MOMENT LOADING, MYC, ON CYLINDER (60000 IN-IB)

	MICRO-STRAIN			STRESSES			PRIN STRESSES	
ROSETTE	GAGE1	GAGE2	GAGE3	TRANS	LONG	SHEAR	SIGMX	SIGMN
I270C-A	-161	413	385	17700	470	371	17708	462
I270C-B	-145	346	351	15481	306	-74	15481	305
I270C-C	-125	312	293	13433	276	260	13438	271
I270C-D	-108	296	270	12560	514	335	12569	505
I270C-E	-88	266	254	11518	816	152	11520	814
I270C-F	-28	208	186	8688	1766	304	8702	1752
I270C-H	23	168	157	7128	2832	152	7134	2827
I270C-J	23	135	137	5953	2483	-35	5953	2482
I270C-K	-3	103	114	4776	1356	-152	4782	1349
I270C-L	-34	52	55	2370	-304	-38	2371	-304
I270C-M	-40	0	6	181	-1135	-76	186	-1139
O270C-A	-25	91	17	2417	-34	985	2763	-380
O270C-B	-42	106	43	3312	-274	835	3497	-459
O270C-C	-59	117	66	4078	-557	682	4176	-655
O270C-D	-74	123	86	4660	-808	491	4704	-851
O270C-E	-88	134	100	5238	-1061	455	5270	-1093
O270C-F	-128	149	123	6105	-2008	341	6119	-2022
O270C-G	-139	143	123	5992	-2384	266	6000	-2392
O270C-H	-145	129	126	5746	-2630	39	5747	-2630
O270C-J	-117	114	97	4778	-2064	227	4785	-2071
O270C-K	-77	89	89	3978	-1109	-1	3978	-1109
O270C-L	-14	57	54	2471	324	38	2472	323
O270C-M	26	23	12	733	1001	152	1070	665

Table A.9 (continued)

OUT-OF-PLANE MOMENT LOADING, MYC, ON CYLINDER (60000 IN-LB)

	MICRO-STRAIN			STRESSES			PRIN STRESSES	
ROSETTE	GAGE1	GAGE2	GAGE3	TRANS	LONG	SHEAR	SIGMX	SIGMN
I270N-A	3	488	485	21380	6513	38	21380	6513
I270N-B	24	564	555	24563	8080	116	24564	8079
I270N-C	9	611	652	27731	8591	-542	27746	8576
I270N-D	56	646	573	26712	9688	972	26767	9633
I270N-E	91	660	713	30078	11750	-700	30105	11724
I270N-F	3	777	819	35075	10608	-550	35087	10596
I270N-G	88	604	589	26113	10482	196	26115	10479
I270N-H	100	415	327	16196	7859	1178	16359	7696
I270N-J	132	185	209	8524	6531	-314	8573	6483
I270N-K	106	124	127	5382	4793	-39	5384	4790
I270N-L	79	65	65	2758	3211	0	3211	2758
I270N-N	53	38	35	1557	2055	39	2058	1554
O270N-A	-8	113	33	3202	723	1068	3599	326
O270N-B	-25	73	-8	1454	-312	1071	1959	-817
O270N-C	-51	38	-34	150	-1484	954	589	-1924
O270N-D	-80	-5	-63	-1403	-2813	766	-1067	-3149
O270N-E	-105	-42	-97	-2956	-4050	732	-2589	-4417
O270N-F	-112	-233	-270	-10926	-6624	498	-6567	-10982
O270N-G	-19	-313	-325	-13984	-4780	157	-4777	-13987
O270N-H	72	-299	-304	-13335	-1830	75	-1830	-13336
O270N-J	142	-181	-187	-8255	1771	78	1772	-8256
O270N-K	127	-115	-98	-4811	2374	-231	2381	-4819
O270N-L	75	-46	-29	-1718	1747	-230	1762	-1733
O270N-N	38	3	3	100	1168	1	1168	100

Table A.9 (continued)

OUT-OF-PLANE MOMENT LOADING, MYC, ON CYLINDER (60000 IN-LB)

	MICRO-STRAIN			STRESSES			PRIN STRESSES	
ROSETTE	GAGE1	GAGE2	GAGE3	TRANS	LONG	SHEAR	SIGMX	SIGMN
I-0-C-*	17	-20	-17	-813	266	-38	268	-814
I-22C-A	35	23	29	1108	1372	-72	1390	1090
I-45C-A	69	46	120	3579	3143	-992	4377	2345
I-67C-A	267	218	152	7834	10347	876	10622	7558
I-90C-A	243	-415	-443	-19118	1568	382	1575	-19125
I112C-A	246	172	218	8298	9883	-607	10089	8092
I135C-A	63	115	61	3781	3033	722	4221	2594
I157C-A	20	43	35	1690	1121	114	1712	1099
I202C-A	6	-31	-55	-1895	-383	311	-321	-1956
I225C-A	-34	-69	-121	-4143	-2271	693	-2043	-4372
I247C-A	-297	-280	-164	-9429	-11735	-1539	-8659	-12505
I292C-A	-285	-127	-274	-8487	-11110	1962	-7439	-12158
I315C-A	-49	-118	-75	-4189	-2719	-577	-2519	-4389
I337C-A	-3	-55	-37	-2018	-683	-231	-644	-2057
I180C-L	-3	23	-6	393	13	383	630	-224
O-22C-A	-40	26	-34	-128	-1226	796	290	-1644
O-45C-A	-92	20	36	1336	-2353	-223	1350	-2366
O-67C-A	-318	-251	64	-3749	-10656	-4200	-1765	-12640
O-90C-A	56	-61	-39	-2260	1005	-298	1032	-2287
O112C-A	-298	-237	11	-4629	-10336	-3307	-3115	-11851
O135C-A	-75	53	25	1808	-1710	373	1847	-1749
O157C-A	-28	-5	39	777	-596	-594	998	-817
O180C-A	-2	-28	14	-294	-163	-556	332	-789
O202C-A	14	-50	-16	-1472	-11	-446	115	-1597
O225C-A	55	-34	-76	-2486	892	566	985	-2578
O247C-A	351	205	-19	3701	11631	2996	12636	2696
O292C-A	362	-11	242	4681	12253	-3377	13540	3394
O315C-A	72	-68	-25	-2129	1511	-571	1598	-2217
O337C-A	20	-20	-48	-1511	156	380	239	-1594
O180C-L	-5	-31	17	-296	-250	-645	372	-918

Table A.9 (continued)

OUT-OF-PLANE MOMENT LOADING, MYC, ON CYLINDER (60000 IN-LB)

	MICRO-STRAIN			STRESSES			PRIN STRESSES	
ROSETTE	GAGE1	GAGE2	GAGE3	TRANS	LONG	SHEAR	SIGMX	SIGMN
I-0-N-*	17	-17	-29	-1022	218	153	237	-1040
I-22N-A	79	53	50	2174	3036	39	3038	2172
I-45N-A	66	103	112	4669	3371	-118	4679	3360
I-67N-A	154	242	236	10342	7709	76	10344	7707
I-90N-A	207	-442	-516	-21281	-183	981	-138	-21326
I112N-A	168	230	239	10129	8087	-118	10135	8081
I135N-A	65	112	109	4800	3393	39	4801	3392
I157N-A	24	21	30	1085	1040	-119	1184	941
I180N-A	3	-12	0	-253	17	-156	89	-324
I202N-A	-6	-56	-29	-1860	-727	-352	-626	-1960
I225N-A	-53	-134	-58	-4172	-2830	-1010	-2288	-4714
I247N-A	-187	-259	-207	-10046	-8612	-699	-8328	-10330
I292N-A	-163	-198	-233	-9300	-7690	465	-7565	-9425
I315N-A	-58	-85	-122	-4486	-3097	505	-2933	-4650
I337N-A	-15	-29	-55	-1845	-995	349	-870	-1970
O-22N-A	-43	6	3	255	-1211	39	256	-1212
O-45N-A	-43	-92	46	-949	-1568	-1843	610	-3127
O-67N-A	15	-317	-103	-9243	-2330	-2843	-1311	-10262
O-90N-A	101	-63	-26	-2057	2427	-499	2482	-2112
O112N-A	-11	-239	-338	-12658	-4135	1326	-3933	-12860
O135N-A	-42	48	-99	-1071	-1595	1969	653	-3320
O157N-A	-37	14	14	671	-902	0	671	-902
O180N-A	-3	-25	6	-425	-206	-417	116	-746
O202N-A	14	-25	-33	-1301	42	102	50	-1308
O225N-A	-5	51	-71	-424	-292	1628	1271	-1987
O247N-A	0	324	114	9624	2892	2802	10638	1879
O292N-A	29	103	338	9660	3758	-3143	11020	2398
O315N-A	0	-61	73	259	85	-1796	1970	-1626
O337N-A	17	-39	-22	-1363	104	-227	138	-1397
O-0-N-L	-3	-3	3	10	-74	-74	53	-118

Table A.10. In-plane moment loading, M_{ZC}, on cylinder

IN-PLANE MOMENT LOADING, MZC, ON CYLINDER (24000 IN-LB)

	MICRO-STRAIN			STRESSES			PRIN STRESSES	
ROSETTE	GAGE1	GAGE2	GAGE3	TRANS	LONG	SHEAR	SIGMX	SIGMN
I-0-C-A	138	76	70	3057	5047	75	5050	3054
I-0-C-B	112	59	48	2219	4036	150	4049	2207
I-0-C-C	87	45	36	1692	3119	113	3128	1683
I-0-C-D	65	31	25	1159	2284	75	2289	1154
I-0-C-E	48	28	20	995	1729	112	1745	978
I-0-C-F	11	20	14	724	551	75	752	523
I-0-C-G	0	25	17	921	272	112	939	253
I-0-C-H	0	31	22	1160	346	112	1175	331
I-0-C-J	3	33	28	1343	485	74	1349	478
I-0-C-K	3	31	25	1220	446	74	1227	439
I-0-C-L	0	28	19	1038	308	112	1054	291
0-0-C-A	-146	-17	-23	-717	-4581	76	-716	-4583
0-0-C-B	-108	-43	-37	-1637	-3745	-77	-1634	-3748
0-0-C-C	-77	-46	-40	-1798	-2851	-75	-1793	-2857
0-0-C-D	-57	-49	-46	-2007	-2315	-38	-2003	-2319
0-0-C-E	-40	-46	-43	-1901	-1770	-39	-1759	-1911
0-0-C-F	-9	-37	-34	-1559	-725	-38	-723	-1561
0-0-C-G	3	-29	-29	-1259	-293	0	-293	-1259
0-0-C-H	0	-29	-29	-1255	-379	1	-379	-1255
0-0-C-J	-3	-28	-26	-1186	-442	-38	-440	-1188
0-0-C-K	0	-28	-26	-1187	-357	-38	-355	-1189
0-0-C-L	0	-23	-20	-937	-282	-37	-279	-939

Table A.10 (continued)

IN-PLANE MOMENT LOADING, MZC, ON CYLINDER (24000 IN-LB)

	MICRO-STRAIN			STRESSES			PRIN STRESSES	
ROSETTE	GAGE1	GAGE2	GAGE3	TRANS	LONG	SHEAR	SIGMX	SIGMN
I-0-N-B**	0	52	49	2226	668	40	2227	667
I-0-N-C	81	38	32	1438	2864	77	2868	1434
I-0-N-D	61	23	20	883	2090	37	2091	881
I-0-N-E	46	20	14	706	1600	76	1606	700
I-0-N-F	14	9	9	365	543	1	543	365
I-0-N-G	0	12	12	508	150	0	508	150
I-0-N-H	3	14	17	697	294	-38	700	290
I-0-N-J	12	23	23	1012	651	0	1012	651
I-0-N-K	17	29	26	1199	883	36	1203	879
I-0-N-L**	29	35	-204	-3756	-248	3190	1639	-5642
O-0-N-A	-134	-26	-26	-984	-4313	0	-984	-4313
O-0-N-B	-97	-34	-34	-1401	-3328	0	-1401	-3328
O-0-N-C	-70	-38	-35	-1538	-2576	-39	-1537	-2577
O-0-N-D	-47	-41	-38	-1695	-1920	-39	-1688	-1926
O-0-N-E	-29	-41	-38	-1712	-1396	-39	-1391	-1717
C-0-N-F	0	-32	-32	-1423	-434	0	-434	-1423
O-0-N-G	14	-24	-24	-1056	114	0	114	-1056
O-0-N-H	8	-21	-21	-929	-29	2	-29	-929
C-0-N-J	9	-24	-27	-1112	-76	39	-74	-1113
O-0-N-K	14	-29	-29	-1306	38	0	38	-1306

Table A.10 (continued)

IN-PLANE MOMENT LOADING, MZC, ON CYLINDER (24000 IN-LB)

	MICRO-STRAIN			STRESSES			PRIN STRESSES	
ROSETTE	GAGE1	GAGE2	GAGE3	TRANS	LONG	SHEAR	SIGMX	SIGMN
I270C-A	92	-418	-421	-18547	-2808	37	-2808	-18547
I270C-B	92	-315	-349	-14689	-1651	446	-1636	-14705
I270C-C	81	-243	-259	-11120	-914	223	-909	-11125
I270C-D	78	-198	-209	-9035	-372	148	-369	-9037
I270C-E	60	-154	-168	-7149	-350	190	-344	-7154
I270C-F	23	-37	-43	-1780	148	76	151	-1783
I270C-H	-14	46	40	1896	140	76	1899	137
I270C-J	-6	88	80	3698	937	113	3703	932
I270C-K	6	108	111	4818	1616	-38	4819	1616
I270C-L	20	145	137	6180	2452	114	6184	2448
I270C-M	20	151	151	6619	2584	0	6619	2584
O270C-A	182	131	91	4673	6862	530	6983	4551
O270C-B	148	94	77	3586	5511	227	5537	3560
O270C-C	119	65	45	2306	4274	265	4309	2271
O270C-D	94	54	37	1893	3381	229	3416	1859
O270C-E	88	43	26	1401	3061	228	3092	1371
O270C-F	46	17	9	513	1521	114	1534	501
O270C-G	9	20	20	867	516	0	867	516
O270C-H	-14	31	37	1519	28	-76	1523	24
O270C-J	-57	68	66	3007	-810	38	3007	-810
O270C-K	-86	83	88	3854	-1409	-75	3855	-1410
O270C-L	-117	100	100	4513	-2154	0	4513	-2154
O270C-M	-131	105	108	4843	-2483	-38	4843	-2484

Table A.10 (continued)

IN-PLANE MOMENT LOADING, MZC, ON CYLINDER (24000 IN-LB)

	MICRO-STRAIN			STRESSES			PRIN STRESSES	
ROSETTE	GAGE1	GAGE2	GAGE3	TRANS	LONG	SHEAR	SIGMX	SIGMN
I270N-A	-134	-564	-584	-25076	-11557	273	-11551	-25082
I270N-B	-164	-677	-686	-29791	-13847	117	-13846	-29792
I270N-C	-146	-678	-815	-32638	-14175	1828	-13996	-32817
I270N-D	-193	-829	-745	-34381	-16100	-1128	-16031	-34450
I270N-E	-228	-864	-914	-38836	-18488	662	-18466	-38857
I270N-F	-56	-1052	-1061	-46378	-15595	118	-15594	-46378
I270N-G	-56	-878	-796	-36727	-12699	-1100	-12649	-36777
I270N-H	-44	-651	-510	-25470	-8968	-1885	-8756	-25683
I270N-J	-171	-330	-365	-15098	-9658	471	-9617	-15138
I270N-K	-159	-251	-251	-10836	-8026	0	-8026	-10836
I270N-L	-136	-156	-159	-6781	-6102	39	-6100	-6784
I270N-N	-127	-97	-88	-3941	-4984	-118	-3928	-4998
O270N-A	261	118	89	4254	9118	384	9148	4223
O270N-B	353	158	135	6046	12414	307	12429	6031
O270N-C	437	207	167	7725	15419	537	15456	7688
O270N-D	503	259	221	9990	18082	498	18113	9960
O270N-E	566	305	273	12069	20601	420	20622	12049
O270N-F	523	489	500	21152	22036	-154	22062	21127
O270N-G	305	552	549	23853	16292	37	23853	16292
O270N-H	106	517	512	22493	9937	77	22494	9936
O270N-J	-58	340	354	15319	2863	-193	15322	2861
O270N-K	-87	239	230	10408	525	116	10409	524
O270N-L	-84	132	109	5405	-891	307	5420	-906
O270N-N	-84	23	26	1162	-2164	-39	1162	-2165

Table A.10 (continued)

IN-PLANE MOMENT LOADING, MZC, ON CYLINDER (24000 IN-LB)

	MICRO-STRAIN			STRESSES			PRIN STRESSES	
ROSETTE	GAGE1	GAGE2	GAGE3	TRANS	LONG	SHEAR	SIGMX	SIGMN
I-0-C-*	81	67	70	2934	3324	-37	3327	2930
I-22C-A	152	100	92	4045	5762	113	5769	4038
I-45C-A	180	114	163	5902	7178	-648	7450	5631
I-67C-A	386	209	143	7310	13781	877	13897	7193
I-90C-A	74	-415	-426	-18573	-3341	152	-3339	-18574
I112C-A	349	160	212	7790	12809	-687	12902	7697
I135C-A	166	160	120	5979	6771	534	7040	5710
I157C-A	140	103	106	4435	5535	-38	5536	4434
I202C-A	144	98	98	4153	5573	-1	5573	4153
I225C-A	202	139	176	6694	8068	-500	8231	6531
I247C-A	401	205	156	7487	14281	654	14344	7424
I292C-A	404	167	231	8307	14616	-846	14727	8196
I315C-A	185	182	124	6522	7498	769	7921	6099
I337C-A	150	95	104	4212	5766	-115	5774	4203
I180C-L	-4	12	12	511	42	1	511	42
O-22C-A	-168	-17	-26	-759	-5275	116	-756	-5278
O-45C-A	-223	-31	17	-63	-6711	-632	-4	-6770
O-67C-A	-519	-393	-31	-8745	-18180	-4828	-6712	-20213
O-90C-A	215	100	123	4664	7836	-297	7863	4636
O112C-A	-466	-365	-67	-8986	-16662	-3974	-7299	-18349
O135C-A	-195	42	-22	640	-5663	854	754	-5777
O157C-A	-170	-8	-6	-123	-5140	-37	-122	-5141
O180C-A	-137	-17	-8	-404	-4221	-112	-401	-4224
O202C-A	-153	-11	-3	-142	-4646	-112	-140	-4649
O225C-A	-234	-43	28	-62	-7024	-946	64	-7151
O247C-A	-527	-359	-57	-8558	-18364	-4018	-7123	-19800
O292C-A	-524	-31	-367	-8182	-18160	4473	-6471	-19872
O315C-A	-216	26	-34	44	-6480	797	140	-6576
O337C-A	-165	-9	-9	-198	-5015	0	-198	-5015
O180C-L	3	-14	-14	-632	-108	0	-108	-632

Table A.10 (continued)

IN-PLANE MOMENT LOADING, MZC, ON CYLINDER (24000 IN-LB)

	MICRO-STRAIN			STRESSES			PRIN STRESSES	
ROSETTE	GAGE1	GAGE2	GAGE3	TRANS	LONG	SHEAR	SIGMX	SIGMN
I-0-N-*	95	66	63	2749	3683	39	3684	2747
I-22N-A	-171	-41	6	-590	-5305	-628	-507	-5387
I-45N-A	162	148	221	7929	7248	-983	8629	6548
I-67N-A	195	242	398	13859	10001	-2084	14770	9091
I-90N-A	68	-454	-502	-21087	-4291	629	-4267	-21111
I112N-A	201	375	245	13399	10040	1730	14131	9309
I135N-A	171	233	156	8373	7647	1022	9095	6925
I157N-A	139	109	80	3998	5361	393	5466	3893
I180N-A	148	80	89	3535	5487	-118	5494	3528
I202N-A	145	97	115	4511	5692	-236	5737	4465
I225N-A	152	169	230	8613	7133	-816	8974	6772
I247N-A	201	239	356	12852	9892	-1554	13518	9226
I292N-A	166	356	277	13723	9104	1049	13951	8877
I315N-A	143	222	146	7918	6662	1010	8479	6100
I337N-A	131	102	79	3829	5085	311	5158	3756
O-22N-A	-138	-92	20	-1439	-4585	-1497	-840	-5184
O-45N-A	-130	-225	26	-4235	-5167	-3341	-1328	-8073
O-67N-A	-121	-504	-179	-14884	-8100	-4338	-5986	-16999
O-90N-A	314	89	127	4395	10732	-499	10771	4356
O112N-A	-122	-193	-518	-15491	-8317	4318	-6290	-17518
O135N-A	-122	40	-236	-4181	-4925	3675	-859	-8246
O157N-A	-131	31	-65	-609	-4110	1288	-186	-4533
O180N-A	-142	-17	-17	-600	-4449	1	-600	-4449
O202N-A	-137	-77	22	-1060	-4416	-1315	-606	-4870
O225N-A	-120	-222	43	-3809	-4729	-3523	-716	-7822
O247N-A	-128	-520	-208	-15859	-8599	-4167	-6703	-17756
O292N-A	-117	-176	-526	-15313	-8096	4660	-5811	-17598
O315N-A	-101	34	-219	-3970	-4230	3369	-728	-7471
O337N-A	-132	28	-73	-851	-4220	1350	-377	-4694
O-0-N-L	31	-28	-34	-1395	505	75	508	-1398

Table A.11. Axial force loading, F_{XC}, on cylinder

AXIAL FORCE LOADING, FXC, ON CYLINDER (8000 LB)

	MICRO-STRAIN			STRESSES			PRIN STRESSES	
ROSETTE	GAGE1	GAGE2	GAGE3	TRANS	LONG	SHEAR	SIGMX	SIGMN
I-0-C-A	-110	-48	-31	-1623	-3784	-225	-1600	-3807
I-0-C-B	-85	-37	-23	-1220	-2905	-186	-1200	-2925
I-0-C-C	-62	-26	-12	-746	-2089	-187	-721	-2115
I-0-C-D	-42	-20	-9	-586	-1450	-149	-561	-1475
I-0-C-E	-28	-17	-6	-472	-996	-150	-433	-1035
I-0-C-F	0	-17	-6	-510	-162	-150	-106	-566
I-0-C-G	2	-23	-12	-762	-156	-150	-121	-797
I-0-C-H	2	-26	-17	-944	-212	-110	-196	-960
I-0-C-J	-3	-31	-20	-1110	-427	-149	-396	-1141
I-0-C-K	-3	-28	-17	-992	-401	-149	-366	-1028
I-0-C-L	-3	-23	-15	-816	-348	-108	-324	-840
O-0-C-A	111	23	28	998	3626	-74	3629	996
O-0-C-B	74	37	34	1474	2655	35	2657	1473
O-0-C-C	48	37	25	1309	1835	155	1877	1267
O-0-C-D	28	31	31	1335	1245	-2	1335	1245
O-0-C-E	14	25	31	1224	781	-78	1237	768
O-0-C-F	-9	20	20	872	-4	0	872	-4
O-0-C-G	-9	14	14	620	-81	0	620	-81
O-0-C-H	-9	11	14	561	-105	-37	563	-107
O-0-C-J	-9	17	17	742	-45	0	742	-45
O-0-C-K	-9	17	14	689	-63	38	691	-65
O-0-C-L	-12	14	11	568	-180	38	570	-182

Table A.11 (continued)

AXIAL FORCE LOADING, FXC, ON CYLINDER (8000 LB)

	MICRO-STRAIN			STRESSES			PRIN STRESSES	
ROSETTE	GAGE1	GAGE2	GAGE3	TRANS	LONG	SHEAR	SIGMX	SIGMN
I-0-N-B**	0	-29	-30	-1296	-389	2	-389	-1296
I-0-N-C	-61	-18	-15	-649	-2039	-40	-647	-2040
I-0-N-D	-41	-9	-9	-357	-1337	-3	-357	-1337
I-0-N-E	-30	-9	-6	-308	-979	-41	-306	-982
I-0-N-F	-6	-3	-6	-194	-240	40	-171	-263
I-0-N-G	0	-6	-12	-393	-128	76	-108	-414
I-0-N-H	-3	-9	-15	-516	-251	78	-230	-537
I-0-N-J	-9	-12	-18	-641	-466	78	-437	-671
I-0-N-K	-12	-15	-17	-701	-569	32	-562	-708
I-0-N-L**	-23	-18	166	3293	289	-2454	4668	-1086
O-0-N-A	105	37	37	1498	3599	-1	3599	1498
O-0-N-B	74	37	37	1532	2669	0	2669	1532
O-0-N-C	50	38	35	1547	1951	39	1955	1543
O-0-N-D	32	35	35	1500	1411	0	1500	1411
O-0-N-E	17	32	35	1453	958	-39	1456	955
O-0-N-F	0	23	26	1087	319	-39	1089	317
O-0-N-G	-6	14	17	705	29	-39	707	26
O-0-N-H	-3	11	14	570	75	-39	573	72
O-0-N-J	-3	14	14	637	97	0	637	97
O-0-N-K	-12	15	20	779	-126	-78	786	-133

Table A.11 (continued)

AXIAL FORCE LOADING, FXC, ON CYLINDER (8000 LB)

	MICRO-STRAIN			STRESSES			PRIN STRESSES	
ROSETTE	GAGE1	GAGE2	GAGE3	TRANS	LONG	SHEAR	SIGMX	SIGMN
I270C-A	-132	409	342	16668	1047	893	16719	997
I270C-B	-135	328	292	13780	95	483	13797	78
I270C-C	-126	278	226	11214	-419	705	11256	-462
I270C-D	-123	245	189	9674	-794	739	9726	-846
I270C-E	-115	211	162	8324	-939	647	8369	-984
I270C-F	-80	128	80	4656	-1014	646	4729	-1087
I270C-H	-52	68	54	2743	-727	190	2754	-737
I270C-J	-49	48	51	2224	-800	-41	2224	-801
I270C-K	-54	34	40	1680	-1131	-76	1682	-1133
I270C-L	-52	22	28	1171	-1201	-76	1173	-1204
I270C-M	-49	20	28	1107	-1132	-114	1113	-1137
O270C-A	-114	54	-63	-80	-3448	1554	528	-4055
O270C-B	-97	73	-40	838	-2666	1513	1401	-3229
O270C-C	-80	85	-12	1699	-1892	1288	2113	-2307
O270C-D	-66	94	8	2299	-1291	1142	2631	-1624
O270C-E	-63	96	25	2736	-1078	947	2959	-1300
O270C-F	-46	102	62	3671	-279	532	3741	-349
O270C-G	-32	91	71	3594	126	266	3614	105
O270C-H	-17	77	71	3266	458	74	3268	456
O270C-J	0	68	57	2743	812	153	2755	800
O270C-K	14	54	45	2170	1072	116	2182	1060
O270C-L	22	40	34	1590	1150	76	1603	1137
O270C-M	14	40	37	1666	914	38	1668	912

Table A.11 (continued)

AXIAL FORCE LOADING, FXC, ON CYLINDER (8000 LB)

	MICRO-STRAIN			STRESSES			PRIN STRESSES	
ROSETTE	GAGE1	GAGE2	GAGE3	TRANS	LONG	SHEAR	SIGMX	SIGMN
I270N-A	58	494	461	20923	8020	429	20937	8006
I270N-B	84	573	543	24429	9863	390	24439	9852
I270N-C	76	631	651	28092	10699	-275	28096	10695
I270N-D	125	675	596	27786	12096	1052	27856	12026
I270N-E	166	689	730	31012	14292	-545	31030	14274
I270N-F	47	816	869	36986	12506	-707	37006	12485
I270N-G	59	645	648	28359	10270	-39	28359	10270
I270N-H	44	465	409	19178	7073	747	19224	7027
I270N-J	129	241	289	11508	7337	-628	11600	7244
I270N-K	115	185	194	8220	5908	-118	8226	5902
I270N-L	100	118	130	5323	4597	-157	5356	4565
I270N-N	94	76	74	3192	3782	39	3784	3190
O270N-A	-170	75	-69	315	-4995	1915	934	-5614
O270N-B	-239	40	-109	-1252	-7536	1993	-673	-8114
O270N-C	-311	0	-147	-2880	-10182	1954	-2390	-10672
O270N-D	-368	-43	-187	-4651	-12439	1916	-4205	-12885
O270N-E	-428	-89	-224	-6418	-14780	1802	-6046	-15152
O270N-F	-431	-282	-394	-14382	-17258	1495	-13746	-17894
O270N-G	-267	-380	-411	-17088	-13150	422	-13105	-17132
O270N-H	-106	-377	-371	-16318	-8088	-77	-8087	-16318
O270N-J	37	-257	-242	-11010	-2187	-192	-2182	-11014
O270N-K	60	-179	-150	-7301	-382	-384	-361	-7323
O270N-L	57	-98	-72	-3810	578	-346	606	-3837
O270N-N	57	-20	-20	-962	1433	-1	1433	-962

Table A.11 (continued)

AXIAL FORCE LOADING, FXC, ON CYLINDER (8000 LB)

	MICRO-STRAIN			STRESSES			PRIN STRESSES	
ROSETTE	GAGE1	GAGE2	GAGE3	TRANS	LONG	SHEAR	SIGMX	SIGMN
I-0-C-*	-76	-34	-40	-1534	-2743	77	-1529	-2748
I-22C-A	-132	-72	-63	-2827	-4809	-119	-2820	-4816
I-45C-A	-146	-80	-123	-4314	-5684	573	-4106	-5892
I-67C-A	-284	-121	-60	-3666	-9616	-801	-3560	-9722
I-90C-A	-141	369	363	16247	659	76	16248	659
I112C-A	-227	-109	-112	-4612	-8181	36	-4612	-8181
I135C-A	-106	-109	-52	-3421	-4215	-761	-2960	-4676
I157C-A	-118	-52	-40	-1899	-4105	-152	-1888	-4115
I202C-A	-102	-41	-58	-2063	-3665	228	-2031	-3697
I225C-A	-116	-75	-127	-4324	-4775	693	-3821	-5278
I247C-A	-295	-171	-145	-6613	-10839	-347	-6585	-10868
I292C-A	-281	-47	-125	-3457	-9455	1040	-3282	-9631
I315C-A	-142	-119	-84	-4297	-5546	-462	-4145	-5698
I337C-A	-113	-64	-70	-2806	-4231	77	-2802	-4236
I180C-L	-40	-3	-12	-282	-1280	117	-269	-1293
O-22C-A	136	17	39	1078	4418	-299	4444	1052
O-45C-A	187	39	0	641	5788	520	5840	589
O-67C-A	410	357	33	8118	14725	4311	16853	5990
O-90C-A	-134	-45	22	-355	-4134	-891	-156	-4334
O112C-A	309	290	11	6268	11160	3716	13162	4265
O135C-A	131	-6	22	211	3986	-372	4022	175
O157C-A	136	58	28	1735	4610	409	4667	1678
O180C-A	111	55	58	2377	4050	-38	4051	2376
O202C-A	106	16	39	1092	3493	-297	3530	1056
O225C-A	145	14	-17	-234	4274	419	4312	-272
O247C-A	398	284	8	5992	13745	3680	15213	4524
O292C-A	393	40	347	8068	14205	-4097	16255	6018
O315C-A	168	-6	42	617	5214	-644	5302	528
O337C-A	128	20	17	662	4032	38	4032	661
O180C-L	-46	3	8	291	-1289	-76	294	-1292

Table A.11 (continued)

AXIAL FORCE LOADING, FXC, ON CYLINDER (8000 LB)

	MICRO-STRAIN			STRESSES			PRIN STRESSES	
ROSETTE	GAGE1	GAGE2	GAGE3	TRANS	LONG	SHEAR	SIGMX	SIGMN
I-0-N-*	-90	-38	-35	-1501	-3142	-37	-1500	-3143
I-22N-A	138	47	3	940	4433	589	4529	844
I-45N-A	-119	-101	-177	-5975	-5358	1022	-4598	-6734
I-67N-A	-121	-145	-290	-9411	-6459	1929	-5506	-10364
I-90N-A	-109	401	428	18333	2216	-353	18341	2209
I112N-A	-109	-248	-177	-9227	-6049	-944	-5790	-9486
I135N-A	-104	-165	-77	-5214	-4670	-1180	-3731	-6153
I157N-A	-103	-65	-6	-1451	-3540	-785	-1189	-3803
I180N-A	-127	-9	-33	-779	-4045	314	-749	-4075
I202N-A	-89	-30	-74	-2185	-3319	588	-1936	-3569
I225N-A	-85	-114	-146	-5619	-4232	427	-4111	-5740
I247N-A	-143	-222	-269	-10620	-7479	622	-7360	-10738
I292N-A	-88	-239	-140	-8241	-5105	-1321	-4623	-8724
I315N-A	-96	-155	-91	-5288	-4480	-854	-3939	-5829
I337N-A	-97	-67	-50	-2468	-3636	-233	-2423	-3681
O-22N-A	118	80	5	1759	4066	999	4438	1387
O-45N-A	115	193	-6	3980	4644	2650	6983	1641
O-67N-A	98	406	170	12549	6698	3150	13923	5324
O-90N-A	-217	-41	20	-219	-6563	-807	-118	-6664
O112N-A	40	148	364	11193	4549	-2881	12268	3473
O135N-A	99	-12	170	3381	3991	-2425	6130	1242
O157N-A	116	23	62	1738	4010	-530	4128	1620
O180N-A	113	59	62	2545	4164	-36	4165	2544
O202N-A	111	54	9	1251	3690	600	3830	1111
O225N-A	79	142	-34	2276	3060	2349	5050	286
O247N-A	54	401	162	12303	5305	3182	13534	4074
O292N-A	85	182	406	12822	6392	-2993	14000	5214
O315N-A	78	-12	171	3415	3373	-2434	5828	960
O337N-A	101	-9	55	916	3298	-855	3574	640
O-0-N-L	-23	14	20	757	-457	-76	762	-462

Table A.12. In-plane force loading, F_{YC}, on cylinder

IN-PLANE FORCE LOADING, FYC, ON CYLINDER (1000 LB)

	MICRO-STRAIN			STRESSES			PRIN STRESSES	
ROSETTE	GAGE1	GAGE2	GAGE3	TRANS	LONG	SHEAR	SIGMX	SIGMN
I-0-C-A	104	29	12	768	3361	226	3380	749
I-0-C-B	73	14	15	558	2372	-2	2372	558
I-0-C-C	48	9	9	332	1547	-1	1547	332
I-0-C-D	31	6	6	233	1010	-1	1010	233
I-0-C-E	17	6	6	240	592	-1	592	240
I-0-C-F	0	9	9	391	129	1	391	129
I-0-C-G	-2	15	15	645	126	1	645	126
I-0-C-H	3	20	20	868	351	-1	868	351
I-0-C-J	14	22	25	1031	733	-37	1036	728
I-0-C-K	17	23	22	970	805	0	970	805
I-0-C-L	26	23	20	906	1037	34	1045	897
O-0-C-A	-103	-37	-46	-1706	-3594	114	-1699	-3601
O-0-C-B	-66	-49	-43	-1935	-2550	-76	-1925	-2559
O-0-C-C	-43	-43	-37	-1709	-1797	-76	-1665	-1841
O-0-C-D	-29	-37	-37	-1599	-1336	0	-1336	-1599
O-0-C-E	-11	-31	-31	-1367	-753	0	-753	-1367
O-0-C-F	6	-17	-20	-822	-75	38	-73	-823
O-0-C-G	9	-14	-11	-574	85	-38	87	-576
O-0-C-H	3	-17	-17	-756	-141	0	-141	-756
O-0-C-J	9	-20	-17	-822	9	-38	11	-824
O-0-C-K	14	-20	-20	-891	159	0	159	-891
O-0-C-L	28	-11	-11	-531	694	0	694	-531

Table A.12 (continued)

IN-PLANE FORCE LOADING, FYC, ON CYLINDER (1000 LB)

	MICRO-STRAIN			STRESSES			PRIN STRESSES	
ROSETTE	GAGE1	GAGE2	GAGE3	TRANS	LONG	SHEAR	SIGMX	SIGMN
I-0-N-B**	0	12	12	510	153	0	510	153
I-0-N-C	46	6	0	77	1416	77	1421	72
I-0-N-D	29	0	-3	-96	842	39	844	-97
I-0-N-E	15	-3	-3	-144	392	0	392	-144
I-0-N-F	-3	0	0	3	-86	0	3	-86
I-0-N-G	-6	3	3	134	-134	0	134	-134
I-0-N-H	0	9	9	383	115	0	383	115
I-0-N-J	6	12	15	580	360	-39	587	354
I-0-N-K	9	18	20	832	521	-32	835	517
I-0-N-L**	17	27	-172	-3222	-443	2648	1158	-4823
O-0-N-A	-91	-40	-42	-1703	-3233	38	-1702	-3234
O-0-N-B	-59	-37	-40	-1612	-2267	38	-1609	-2269
O-0-N-C	-38	-35	-32	-1441	-1577	-39	-1431	-1587
O-0-N-D	-21	-32	-29	-1333	-1017	-39	-1012	-1337
O-0-N-E	-6	-23	-23	-1026	-486	0	-486	-1026
O-0-N-F	6	-15	-18	-718	-43	39	-41	-720
O-0-N-G	6	-9	-9	-397	52	0	52	-397
O-0-N-H	3	-6	-9	-333	-18	40	-13	-337
O-0-N-J	3	-12	-12	-522	-72	0	-72	-522
C-0-N-K	9	-15	-18	-719	43	39	45	-721

Table A.12 (continued)

IN-PLANE FORCE LOADING, FYC, ON CYLINDER (1000 LB)

	MICRO-STRAIN			STRESSES			PRIN STRESSES	
ROSETTE	GAGE1	GAGE2	GAGE3	TRANS	LONG	SHEAR	SIGMX	SIGMN
I270C-A	73	-332	-376	-15633	-2501	594	-2474	-15659
I270C-B	73	-239	-323	-12438	-1542	1115	-1429	-12551
I270C-C	65	-175	-251	-9439	-896	1004	-779	-9555
I270C-D	62	-136	-209	-7655	-447	969	-319	-7783
I270C-E	46	-94	-174	-5943	-414	1064	-216	-6141
I270C-F	11	-11	-60	-1580	-132	646	115	-1826
I270C-H	-20	34	37	1589	-122	-38	1590	-123
I270C-J	-11	51	83	2959	545	-418	3029	475
I270C-K	0	74	103	3887	1166	-380	3939	1114
I270C-L	26	114	120	5112	2304	-76	5115	2302
I270C-M	31	126	128	5545	2605	-38	5546	2605
O270C-A	148	256	-48	4400	5757	4055	9190	968
O270C-B	117	222	-57	3497	4548	3714	7773	272
O270C-C	97	185	-68	2456	3638	3373	6471	-377
O270C-D	82	165	-63	2160	3122	3032	5711	-429
O270C-E	71	139	-65	1547	2597	2728	4851	-706
O270C-F	48	74	-40	699	1664	1520	2776	-413
O270C-G	23	57	-14	915	959	950	1887	-13
O270C-H	0	54	17	1567	470	494	1757	280
O270C-J	-37	74	46	2673	-310	380	2721	-358
O270C-K	-60	86	66	3388	-780	266	3405	-797
O270C-L	-97	88	74	3679	-1805	190	3686	-1812
O270C-M	-117	83	86	3826	-2360	-38	3827	-2360

Table A.12 (continued)

IN-PLANE FORCE LOADING, FYC, ON CYLINDER (1000 LB)

	MICRO-STRAIN			STRESSES			PRIN STRESSES	
ROSETTE	GAGE1	GAGE2	GAGE3	TRANS	LONG	SHEAR	SIGMX	SIGMN
I270N-A	-114	-456	-511	-21115	-9743	739	-9695	-21163
I270N-B	-134	-564	-587	-25141	-11566	311	-11559	-25149
I270N-C	-120	-581	-689	-27783	-11921	1443	-11791	-27913
I270N-D	-155	-716	-625	-29291	-13424	-1207	-13333	-29382
I270N-E	-184	-759	-753	-33043	-15426	-78	-15426	-33044
I270N-F	-53	-969	-840	-39679	-13493	-1721	-13380	-39791
I270N-G	-56	-819	-608	-31290	-11064	-2816	-10680	-31675
I270N-H	-35	-611	-399	-22154	-7707	-2815	-7178	-22684
I270N-J	-135	-291	-294	-12691	-7861	39	-7861	-12691
I270N-K	-129	-220	-208	-9279	-6661	-156	-6652	-9289
I270N-L	-112	-132	-129	-5621	-5035	-39	-5033	-5624
I270N-N	-106	-76	-71	-3112	-4106	-78	-3106	-4112
O270N-A	209	267	-90	3664	7377	4749	10619	422
O270N-B	287	301	-52	5155	10148	4709	12981	2322
O270N-C	347	336	-41	6102	12244	5016	15054	3292
O270N-D	419	379	23	8361	15076	4747	17533	5905
O270N-E	468	407	74	10076	17052	4438	19209	7919
O270N-F	428	497	342	17954	18215	2067	20156	16014
O270N-G	244	497	451	20547	13477	611	20600	13425
O270N-H	80	434	454	19406	8227	-267	19412	8221
O270N-J	-52	259	337	13151	2388	-1036	13250	2289
O270N-K	-84	178	224	8945	176	-614	8988	133
O270N-L	-72	92	106	4441	-831	-192	4448	-838
O270N-N	-75	14	26	964	-1960	-154	972	-1968

Table A.12 (continued)

IN-PLANE FORCE LOADING, FYC, ON CYLINDER (1000 LB)

	MICRO-STRAIN			STRESSES			PRIN STRESSES	
ROSETTE	GAGE1	GAGE2	GAGE3	TRANS	LONG	SHEAR	SIGMX	SIGMN
I-0-C-*	82	9	26	666	2653	-228	2678	641
I-22C-A	106	54	54	2274	3860	0	3860	2274
I-45C-A	115	69	146	4593	4813	-1030	5739	3667
I-67C-A	326	229	249	10148	12836	-267	12862	10122
I-90C-A	54	-401	-315	-15788	-3105	-1144	-3003	-15891
I112C-A	298	23	160	3700	10042	-1831	10533	3209
I135C-A	166	129	140	5732	6701	-153	6724	5708
I157C-A	126	123	123	5272	5361	0	5361	5272
I202C-A	130	121	124	5253	5475	-38	5482	5246
I225C-A	211	156	162	6751	8351	-77	8355	6747
I247C-A	364	156	38	3853	12074	1578	12366	3561
I292C-A	329	240	234	10048	12893	77	12895	10046
I315C-A	121	147	75	4754	5066	962	5885	3935
I337C-A	110	52	52	2165	3942	0	3942	2165
I180C-L	-35	9	3	292	-952	77	297	-957
O-22C-A	-106	-9	-40	-950	-3451	418	-882	-3519
O-45C-A	-145	11	0	402	-4229	147	407	-4233
O-67C-A	-404	-254	44	-4152	-13368	-3972	-2677	-14843
O-90C-A	184	-64	267	4264	6792	-4417	10122	934
O112C-A	-410	-348	-114	-9717	-15204	-3118	-8307	-16614
O135C-A	-184	47	-39	382	-5405	1150	602	-5625
O157C-A	-159	33	5	1027	-4459	371	1052	-4484
O180C-A	-131	17	31	1180	-3577	-186	1188	-3585
O202C-A	-151	0	31	833	-4268	-408	866	-4300
O225C-A	-233	-60	37	-235	-7057	-1290	1	-7292
O247C-A	-486	-361	-105	-9704	-17491	-3410	-8422	-18774
O292C-A	-407	29	-244	-4296	-13487	3637	-3031	-14752
O315C-A	-142	17	0	540	-4095	226	551	-4106
O337C-A	-111	-34	-11	-870	-3581	-303	-837	-3614
O180C-L	-23	-6	-6	-218	-742	0	-218	-742

Table A.12 (continued)

IN-PLANE FORCE LOADING, FYC, ON CYLINDER (1000 LB)

	MICRO-STRAIN			STRESSES			PRIN STRESSES	
ROSETTE	GAGE1	GAGE2	GAGE3	TRANS	LONG	SHEAR	SIGMX	SIGMN
I-0-N-*	90	14	14	536	2847	0	2847	536
I-22N-A	-132	-50	-9	-1149	-4310	-547	-1057	-4402
I-45N-A	111	117	164	6074	5154	-626	6391	4837
I-67N-A	188	317	373	14964	10129	-741	15076	10018
I-90N-A	56	-429	-379	-17828	-3680	-665	-3649	-17859
I112N-A	159	294	100	8476	7302	2584	10539	5239
I135N-A	164	206	147	7565	7203	783	8188	6580
I157N-A	126	117	114	4959	5276	40	5281	4954
I180N-A	126	114	115	4893	5257	-1	5257	4893
I202N-A	132	132	123	5466	5603	116	5669	5400
I225N-A	154	165	221	8315	7108	-736	8663	6760
I247N-A	171	113	290	8677	7741	-2360	10615	5803
I292N-A	157	305	331	13801	8841	-348	13826	8817
I315N-A	96	165	110	5953	4658	735	6285	4326
I337N-A	96	64	35	2060	3488	387	3586	1962
O-22N-A	-101	-58	-9	-1350	-3431	-652	-1162	-3619
O-45N-A	-98	-144	34	-2302	-3632	-2379	-497	-5437
O-67N-A	-49	-412	-101	-11216	-4837	-4143	-2797	-13255
O-90N-A	250	-92	279	3833	8660	-4949	11752	740
O112N-A	-162	-201	-438	-13867	-9018	3147	-7470	-15415
O135N-A	-96	32	-233	-4317	-4183	3524	-726	-7774
O157N-A	-110	63	-62	134	-3275	1666	813	-3954
O180N-A	-139	15	21	928	-3885	-79	929	-3886
O202N-A	-127	-76	50	-443	-3955	-1682	233	-4630
O225N-A	-110	-230	35	-4174	-4563	-3524	-839	-7898
O247N-A	-165	-466	-216	-14802	-9378	-3333	-7792	-16387
O292N-A	-36	-90	-414	-11052	-4405	4320	-2278	-13179
O315N-A	-75	34	-146	-2363	-2969	2397	-250	-5082
O337N-A	-101	-5	-52	-1153	-3367	627	-987	-3532
O-0-N-L	17	-22	-28	-1120	183	76	188	-1124

Table A.13. Out-of-plane force loading, F_{ZC}, on cylinder

OUT-OF-PLANE FORCE LOADING, FZC, ON CYLINDER (1200 LB)

	MICRO-STRAIN			STRESSES			PRIN STRESSES	
ROSETTE	GAGE1	GAGE2	GAGE3	TRANS	LONG	SHEAR	SIGMX	SIGMN
I-0-C-A	3	-20	8	-254	6	-375	273	-521
I-0-C-B	3	-23	25	53	98	-636	712	-561
I-0-C-C	3	-20	22	56	99	-562	639	-485
I-0-C-D	0	-23	22	-5	-4	-599	595	-604
I-0-C-E	3	-23	25	57	98	-637	714	-560
I-0-C-F	3	-23	22	-8	79	-599	637	-565
I-0-C-G	0	-17	22	118	31	-524	600	-452
I-0-C-H	3	-19	23	68	110	-558	647	-470
I-0-C-J	3	-14	20	125	126	-446	571	-320
I-0-C-K	3	-14	17	65	111	-408	497	-321
I-0-C-L	3	-17	17	6	93	-447	499	-399
O-0-C-A	1	23	-22	16	25	607	627	-587
O-0-C-B	-2	21	-17	88	-37	499	529	-478
O-0-C-C	-2	21	-19	33	-53	529	520	-541
O-0-C-D	-2	18	-20	-35	-76	497	442	-553
O-0-C-E	-2	18	-17	30	-53	460	451	-473
O-0-C-F	1	18	-19	-35	5	494	480	-509
O-0-C-G	1	15	-19	-95	-9	457	407	-511
O-0-C-H	1	15	-19	-100	-2	456	407	-509
O-0-C-J	3	20	-20	-3	84	531	573	-492
O-0-C-K	3	17	-20	-66	66	493	497	-497
O-0-C-L	3	20	-23	-66	66	569	573	-573

Table A.13 (continued)

OUT-OF-PLANE FORCE LOADING, FZC, ON CYLINDER (1200 LB)

	MICRO-STRAIN			STRESSES			PRIN STRESSES	
ROSETTE	GAGE1	GAGE2	GAGE3	TRANS	LONG	SHEAR	SIGMX	SIGMN
I-0-N-B	0	-26	23	-83	-25	-655	602	-710
I-0-N-C	2	-26	23	-80	48	-659	646	-678
I-0-N-D	0	-24	23	-19	-16	-622	605	-639
I-0-N-E	-1	-24	23	-21	-22	-621	599	-642
I-0-N-F	3	-23	26	51	95	-656	730	-583
I-0-N-G	0	-26	26	-11	-13	-698	686	-709
I-0-N-H	3	-29	26	-76	55	-735	727	-748
I-0-N-J	0	-24	26	56	6	-662	693	-632
I-0-N-K	-3	-24	29	125	-58	-708	747	-681
I-0-N-L	0	-24	-21	-971	-288	-40	-286	-973
O-0-N-A	-3	23	-20	60	-72	568	566	-578
O-0-N-B	0	17	-17	-6	-7	455	448	-461
O-0-N-C	-6	15	-15	1	-182	390	310	-491
O-0-N-D	-3	12	-15	-69	-114	351	260	-443
O-0-N-E	-3	15	-15	-2	-92	390	346	-440
O-0-N-F	-3	12	-15	-67	-114	351	261	-442
O-0-N-G	0	11	-15	-73	-30	351	300	-403
O-0-N-H	0	11	-12	-18	-19	314	296	-333
O-0-N-J	0	14	-18	-73	-26	430	381	-480
O-0-N-K	0	12	-15	-67	-28	351	304	-400

Table A.13 (continued)

OUT-OF-PLANE FORCE LOADING, FZC, ON CYLINDER (1200 LB)

	MICRO-STRAIN			STRESSES			PRIN STRESSES	
ROSETTE	GAGE1	GAGE2	GAGE3	TRANS	LONG	SHEAR	SIGMX	SIGMN
I270C-A	81	-608	76	-11784	-1102	-9103	4111	-16997
I270C-B	90	-535	101	-9646	-208	-8471	4770	-14624
I270C-C	76	-491	101	-8655	-330	-7877	4416	-13401
I270C-D	62	-432	103	-7290	-340	-7132	4119	-11749
I270C-E	68	-400	82	-7050	-74	-6424	3747	-10871
I270C-F	22	-251	37	-4736	-751	-3840	1582	-7070
I270C-H	-3	-114	-46	-3517	-1150	-912	-839	-3828
I270C-J	-9	-75	-63	-3024	-1176	-156	-1163	-3037
I270C-K	-6	-63	-43	-2323	-877	-266	-829	-2370
I270C-L	8	-46	8	-838	-6	-722	411	-1256
I270C-M	14	-23	40	348	524	-836	1277	-405
O270C-A	28	-233	188	-1032	544	-5613	5424	-5911
O270C-B	40	-211	139	-1607	713	-4664	4359	-5254
O270C-C	46	-182	85	-2177	713	-3565	3115	-4578
O270C-D	46	-154	46	-2427	638	-2655	2171	-3960
O270C-E	54	-131	14	-2624	835	-1934	1700	-3489
O270C-F	66	-66	-80	-3271	988	190	996	-3279
O270C-G	71	-29	-120	-3340	1138	1217	1448	-3649
O270C-H	68	-14	-126	-3149	1110	1483	1576	-3614
O270C-J	54	-20	-94	-2568	856	989	1121	-2833
O270C-K	37	-17	-71	-1985	517	723	711	-2179
O270C-L	9	3	-46	-950	-28	646	305	-1283
O270C-M	-17	26	-26	19	-508	684	489	-978

Table A.13 (continued)

OUT-OF-PLANE FORCE LOADING, FZC, ON CYLINDER (1200 LB)

	MICRO-STRAIN			STRESSES			PRIN STRESSES	
ROSETTE	GAGE1	GAGE2	GAGE3	TRANS	LONG	SHEAR	SIGMX	SIGMN
I270N-A	55	-506	0	-11181	-1700	-6734	1794	-14675
I270N-B	64	-549	-70	-13691	-2189	-6383	652	-16532
I270N-C	44	-567	-129	-15346	-3298	-5842	-931	-17713
I270N-D	26	-567	-246	-17889	-4588	-4281	-3329	-19148
I270N-E	-3	-558	-205	-16769	-5129	-4710	-3462	-18436
I270N-F	-9	-557	-386	-20724	-6480	-2279	-6124	-21080
I270N-G	-38	-315	-377	-15183	-5702	825	-5631	-15254
I270N-H	-62	-136	-283	-9130	-4592	1964	-3861	-9861
I270N-J	-124	-62	-200	-5629	-5402	1847	-3665	-7366
I270N-K	-88	-44	-118	-3463	-3690	982	-2588	-4565
I270N-L	-71	-26	-97	-2642	-2913	943	-1825	-3730
I270N-N	-59	-29	-62	-1941	-2350	432	-1668	-2623
O270N-A	20	-279	224	-1230	230	-6702	6242	-7241
O270N-B	34	-299	299	-46	1014	-7967	8469	-7501
O270N-C	75	-316	379	1302	2627	-9269	11257	-7328
O270N-D	63	-322	417	2010	2495	-9844	12100	-7594
O270N-E	95	-319	460	2986	3735	-10382	13749	-7028
O270N-F	100	-155	517	7848	5369	-8964	15657	-2440
O270N-G	26	-3	411	8938	3453	-5517	12356	35
O270N-H	-29	95	276	8178	1589	-2413	8967	800
O270N-J	-69	112	115	5076	-556	-39	5076	-557
O270N-K	-64	89	52	3165	-956	499	3225	-1016
O270N-L	-38	49	9	1303	-738	538	1436	-871
O270N-N	-20	6	3	206	-549	38	208	-551

Table A.13 (continued)

OUT-OF-PLANE FORCE LOADING, FZC, ON CYLINDER (1200 LB)

	MICRO-STRAIN			STRESSES			PRIN STRESSES	
ROSETTE	GAGE1	GAGE2	GAGE3	TRANS	LONG	SHEAR	SIGMX	SIGMN
I-0-C-*	0	-3	25	492	146	-373	730	-93
I-22C-A	6	-3	29	560	340	-420	884	16
I-45C-A	9	60	74	2948	1142	-191	2968	1122
I-67C-A	117	203	303	11007	6824	-1335	11397	6434
I-90C-A	-109	-163	512	7795	-925	-9003	13438	-6568
I112C-A	-326	-449	-427	-18894	-15460	-305	-15433	-18921
I135C-A	-43	-180	-106	-6245	-3162	-992	-2870	-6536
I157C-A	-17	-66	-23	-1932	-1095	-572	-804	-2222
I202C-A	29	46	90	2952	1752	-577	3184	1519
I225C-A	81	136	199	7275	4609	-847	7521	4363
I247C-A	445	451	428	18809	18988	308	19219	18578
I292C-A	-72	-240	-150	-8490	-4714	-1193	-4368	-8836
I315C-A	3	-38	-43	-1781	-448	77	-443	-1785
I337C-A	0	-20	9	-254	-76	-385	230	-560
I180C-L	0	-29	20	-190	-57	-654	534	-781
O-22C-A	-9	26	-9	386	-141	456	649	-405
O-45C-A	-22	75	0	1683	-157	1006	2126	-600
O-67C-A	-125	134	-19	2659	-2958	2043	3324	-3622
O-90C-A	-8	-178	243	1427	186	-5610	6451	-4838
O112C-A	399	112	11	2267	12648	1338	12818	2097
O135C-A	76	-81	-95	-3934	1085	186	1092	-3941
O157C-A	31	20	-61	-942	646	1078	1190	-1487
O180C-A	-16	50	-42	213	-431	1226	1159	-1377
O202C-A	-53	62	-3	1357	-1173	854	1619	-1434
O225C-A	-114	74	74	3372	-2409	1	3372	-2409
O247C-A	-495	-125	-17	-2589	-15636	-1440	-2432	-15793
O292C-A	74	17	-159	-3211	1258	2351	2267	-4220
O315C-A	6	-6	-63	-1512	-288	759	75	-1875
O337C-A	6	11	-20	-198	107	417	399	-489
O180C-L	0	45	-40	122	34	1137	1216	-1060

Table A.13 (continued)

OUT-OF-PLANE FORCE LOADING, FZC, ON CYLINDER (1200 LB)

	MICRO-STRAIN			STRESSES			PRIN STRESSES	
ROSETTE	GAGE1	GAGE2	GAGE3	TRANS	LONG	SHEAR	SIGMX	SIGMN
I-0-N-*	3	-6	9	60	105	-192	276	-111
I-22N-A	-118	-53	-29	-1681	-4041	-314	-1640	-4082
I-45N-A	39	56	12	1454	1620	590	2133	941
I-67N-A	151	269	210	10357	7629	781	10565	7421
I-90N-A	-50	-145	538	8691	1113	-9089	14749	-4945
I112N-A	-310	-387	-490	-18927	-14977	1377	-14545	-19359
I135N-A	-80	-112	-159	-5876	-4150	630	-3945	-6081
I157N-A	-15	-41	-26	-1471	-881	-198	-820	-1531
I180N-A	15	3	33	770	676	-392	1118	328
I202N-A	39	74	68	3085	2084	83	3092	2077
I225N-A	105	193	114	6620	5141	1050	7165	4596
I247N-A	330	487	438	19965	15882	660	20069	15778
I292N-A	-96	-146	-210	-7715	-5199	855	-4936	-7978
I315N-A	-17	3	-20	-362	-632	310	-158	-835
I337N-A	6	-12	6	-131	140	-233	274	-265
O-22N-A	-20	11	3	332	-510	115	347	-525
O-45N-A	-23	11	49	1348	-294	-500	1488	-434
O-67N-A	-121	-118	49	-1397	-4054	-2227	-133	-5319
O-90N-A	-41	-205	265	1366	-807	-6258	6631	-6072
O112N-A	111	65	449	11171	6673	-5116	14510	3334
O135N-A	37	-108	65	-991	799	-2311	2382	-2574
O157N-A	48	-14	-29	-1001	1137	190	1154	-1018
O180N-A	-18	42	-32	244	-455	988	942	-1153
O202N-A	-63	14	24	903	-1622	-137	911	-1629
O225N-A	-49	-86	102	413	-1341	-2499	2184	-3113
O247N-A	-134	-481	-88	-12361	-7727	-5227	-4326	-15762
O292N-A	116	-89	53	-907	3204	-1894	3944	-1647
O315N-A	14	-37	-20	-1256	41	-225	79	-1294
O337N-A	8	3	-12	-204	188	191	266	-281
O-0-N-L	0	14	-17	-63	-22	411	369	-454

Table A.14. Out-of-plane moment loading, M_{XN}, on nozzle

OUT-OF-PLANE MOMENT LOADING, MXN, CN NOZZLE (10000 IN-LB) W/R

	MICRO-STRAIN			STRESSES			PRIN STRESSES	
ROSETTE	GAGE1	GAGE2	GAGE3	TRANS	LONG	SHEAR	SIGMX	SIGMN
I-O-C-A	-6	-3	16	288	-84	-262	423	-220
I-O-C-B	2	-3	18	328	145	-289	540	-67
I-C-C-C	4	-1	14	284	202	-193	440	45
I-O-C-D	6	-3	16	270	273	-259	530	13
I-C-C-E	6	-3	16	287	275	-259	541	22
I-O-C-F	4	-6	11	109	152	-229	361	-99
I-C-C-G	1	-6	13	160	86	-262	387	-142
I-O-C-H	5	0	12	245	209	-163	391	63
I-O-C-J	5	0	7	145	180	-98	262	63
I-O-C-K	2	-3	12	198	116	-197	358	-44
I-C-C-L	2	0	14	300	147	-194	432	15
O-C-C-A	2	7	7	301	143	2	301	143
O-C-C-B	-3	2	4	139	-54	-37	146	-61
O-O-C-C	-6	-3	4	30	-161	-95	70	-200
O-C-C-D	-5	-6	2	-71	-186	-101	-12	-244
O-O-C-E	-6	-6	2	-75	-191	-100	-17	-248
O-O-C-F	-3	-8	-1	-184	-143	-97	-64	-263
O-O-C-G	-1	-10	2	-189	-76	-164	40	-306
O-C-C-H	-1	-8	2	-131	-66	-129	35	-232
O-O-C-J	-1	-9	1	-166	-91	-128	5	-262
O-C-C-K	-2	-8	-3	-247	-121	-63	-95	-274
O-O-C-L	-4	-8	-3	-242	-178	-65	-138	-282

Table A.14 (continued)

OUT-OF-PLANE MOMENT LOADING, MXN, ON NOZZLE (10000 IN-LB) W/R

	MICRO-STRAIN			STRESSES			PRIN STRESSES	
ROSETTE	GAGE1	GAGE2	GAGE3	TRANS	LONG	SHEAR	SIGMX	SIGMN
I-C-N-B	0	-8	13	106	32	-287	358	-220
I-C-N-C	1	-8	14	121	68	-296	391	-203
I-O-N-D	2	-9	11	51	61	-269	325	-213
I-C-N-E	1	-11	9	-62	11	-266	243	-294
I-O-N-F	2	-8	7	-28	44	-192	203	-187
I-C-N-G	-1	-8	4	-83	-52	-166	100	-235
I-O-N-H	-1	-10	4	-131	-66	-194	98	-295
I-O-N-J	-3	-8	4	-74	-126	-162	64	-264
I-O-N-K	-6	-9	2	-130	-208	-144	-19	-318
I-C-N-L	-7	-13	-71	-1834	-773	777	-363	-2245
C-O-N-A	-2	8	4	268	35	63	284	19
O-O-N-B	-4	8	1	213	-57	95	243	-87
O-C-N-C	-6	4	-3	28	-167	99	70	-208
O-O-N-D	-6	4	-6	-33	-182	130	42	-258
O-O-N-E	-6	4	-6	-26	-173	131	51	-250
O-O-N-F	-3	4	-6	-30	-112	130	65	-207
O-C-N-G	-1	4	-8	-96	-63	162	84	-243
O-O-N-H	-4	4	-9	-117	-158	170	33	-308
O-C-N-J	-3	6	22	622	88	-202	690	21
O-O-N-K	-4	7	-8	-17	-116	196	136	-270

Table A.14 (continued)

OUT-OF-PLANE MOMENT LOADING, MXN, ON NOZZLE (10000 IN-LB) W/R

	MICRO-STRAIN			STRESSES			PRIN STRESSES	
ROSETTE	GAGE1	GAGE2	GAGE3	TRANS	LONG	SHEAR	SIGMX	SIGMN
I270C-A	-82	-153	-82	-5068	-3976	-950	-3427	-5618
I270C-B	-116	-180	-87	-5747	-5216	-1246	-4207	-6755
I270C-C	-178	-155	-69	-4743	-6759	-1148	-4223	-7279
I270C-D	-195	-134	-57	-3971	-7040	-1020	-3663	-7349
I270C-E	-204	-121	-52	-3585	-7204	-912	-3368	-7421
I270C-F	-217	-52	-27	-1509	-6952	-327	-1490	-6972
I270C-H	-162	26	9	957	-4583	228	967	-4592
I270C-J	-75	54	31	1943	-1654	314	1970	-1681
I270C-K	-23	53	36	1986	-89	229	2011	-114
I270C-L	14	28	24	1126	745	65	1137	734
I270C-M	7	-1	-1	-43	183	0	183	-43
O270C-A	-18	62	150	4674	853	-1168	5003	524
O270C-B	35	76	152	4988	2543	-1013	5353	2178
O270C-C	72	87	152	5174	3702	-876	5582	3294
O270C-D	96	94	142	5072	4391	-636	5453	4010
O270C-E	112	103	145	5326	4971	-552	5729	4568
O270C-F	149	118	140	5495	6122	-290	6236	5381
O270C-G	137	120	118	5083	5637	34	5639	5081
O270C-H	108	103	108	4533	4604	-69	4646	4491
O270C-J	40	81	79	3478	2243	36	3479	2242
O270C-K	-6	50	57	2374	541	-92	2379	537
O270C-L	-35	11	18	681	-856	-97	687	-862
O270C-M	-11	-6	-1	-134	-377	-64	-119	-393

Table A.14 (continued)

OUT-OF-PLANE MOMENT LOADING, MXN, ON NOZZLE (10000 IN-LB) W/R

	MICRO-STRAIN			STRESSES			PRIN STRESSES	
ROSETTE	GAGE1	GAGE2	GAGE3	TRANS	LONG	SHEAR	SIGMX	SIGMN
I270N-A	-81	-242	-164	-8840	-5095	-1037	-4827	-9108
I270N-B	-47	-274	-201	-10369	-4525	-973	-4368	-10527
I270N-C	-15	-265	-245	-11175	-3815	-268	-3805	-11185
I270N-D	-13	-313	-245	-12233	-4063	-908	-3963	-12333
I270N-E	-11	-328	-306	-13907	-4493	-293	-4483	-13916
I270N-F	11	-443	-436	-19340	-5461	-100	-5460	-19341
I270N-G	-122	-377	-367	-16225	-8513	-131	-8511	-16227
I270N-H	-178	-262	-210	-10168	-8395	-685	-8162	-10402
I270N-J	-153	-114	-129	-5160	-6148	197	-5122	-6186
I270N-K	-124	-62	-77	-2926	-4592	196	-2904	-4615
I270N-L	-89	-35	-33	-1389	-3096	-32	-1388	-3097
I270N-N	-55	-25	-25	-1050	-1962	-1	-1050	-1962
O270N-A	-115	21	126	3351	-2459	-1391	3667	-2775
O270N-B	-189	6	128	3159	-4718	-1621	3479	-5039
O270N-C	-230	-11	123	2729	-6085	-1782	3076	-6432
O270N-D	-281	-15	119	2575	-7666	-1785	2878	-7969
O270N-E	-313	-23	116	2397	-8678	-1855	2700	-8980
O270N-F	-325	60	153	5048	-8235	-1234	5162	-8349
O270N-G	-289	118	187	7027	-6547	-913	7088	-6608
O270N-H	-259	136	180	7219	-5602	-582	7246	-5628
O270N-J	-224	89	104	4491	-5382	-196	4494	-5386
O270N-K	-195	50	38	2147	-5213	162	2151	-5216
O270N-L	-120	11	-3	313	-3508	194	323	-3518
O270N-N	-59	-3	-3	-80	-1803	-2	-80	-1803

Table A.14 (continued)

OUT-OF-PLANE MOMENT LOADING, MXN, ON NOZZLE (10000 IN-LB) W/R

	MICRO-STRAIN			STRESSES			PRIN STRESSES	
ROSETTE	GAGE1	GAGE2	GAGE3	TRANS	LONG	SHEAR	SIGMX	SIGMN
I-0-C-*	-8	7	16	513	-86	-124	537	-111
I-22C-A	-18	-9	-15	-504	-690	84	-472	-723
I-45C-A	-37	-39	-59	-2125	-1760	263	-1622	-2263
I-67C-A	-172	-252	-116	-7897	-7531	-1820	-5885	-9543
I-90C-A	97	92	175	5749	4637	-1107	6432	3954
I112C-A	-213	-226	-311	-11561	-9871	1131	-9304	-12128
I135C-A	0	-86	-60	-3206	-962	-352	-908	-3260
I157C-A	-31	-18	-16	-705	-1129	-32	-702	-1131
I202C-A	14	18	31	1071	727	-172	1142	656
I225C-A	53	63	97	3472	2625	-457	3672	2426
I247C-A	278	342	227	12178	11980	1532	13614	10544
I292C-A	197	106	256	7741	8237	-1988	9993	5986
I315C-A	41	66	46	2406	1941	262	2523	1823
I337C-A	9	21	17	825	514	66	838	501
I180C-L	3	7	-13	-134	53	266	242	-323
O-22C-A	13	-4	-2	-144	354	-20	354	-145
O-45C-A	45	-15	-30	-1048	1050	194	1068	-1066
O-67C-A	192	46	4	883	6023	553	6082	824
O-90C-A	33	-130	-79	-4629	-395	-680	-288	-4736
O112C-A	263	38	48	1611	8374	-133	8376	1609
O135C-A	68	-23	-30	-1235	1656	95	1659	-1238
O157C-A	26	9	-6	41	790	194	838	-7
O180C-A	-3	4	4	183	-46	-3	183	-46
O202C-A	-28	16	-4	304	-753	261	365	-814
O225C-A	-80	31	28	1374	-1981	41	1375	-1981
O247C-A	-336	-40	-50	-1626	-10558	133	-1624	-10559
O292C-A	-256	-28	-64	-1739	-8211	489	-1703	-8248
O315C-A	-60	26	8	820	-1557	233	842	-1579
O337C-A	-16	6	14	455	-344	-99	467	-356
O180C-L	1	2	-8	-147	-5	129	71	-224

Table A.14 (continued)

OUT-OF-PLANE MOMENT LOADING, MXN, ON NOZZLE (10000 IN-LB) W/R

	MICRO-STRAIN			STRESSES			PRIN STRESSES	
ROSETTE	GAGE1	GAGE2	GAGE3	TRANS	LONG	SHEAR	SIGMX	SIGMN
I-C-N-*	-8	4	16	457	-98	-159	500	-140
I-22N-A	-50	-30	-30	-1279	-1881	0	-1279	-1881
I-45N-A	-52	-50	-40	-1934	-2129	-130	-1869	-2194
I-67N-A	-153	-128	-96	-4758	-6016	-427	-4627	-6147
I-90N-A	27	104	202	6692	2817	-1297	7086	2423
I112N-A	-219	-197	-214	-8795	-9205	228	-8693	-9307
I135N-A	-68	-75	-72	-3160	-2975	-33	-2969	-3165
I157N-A	-26	-16	-9	-511	-924	-89	-492	-943
I180N-A	-3	13	-4	210	-36	221	340	-166
I202N-A	15	24	21	964	751	46	974	742
I225N-A	50	87	61	3196	2460	356	3341	2316
I247N-A	218	237	200	9382	9354	494	9862	8873
I292N-A	144	110	122	4948	5795	-165	5826	4917
I315N-A	38	51	58	2340	1850	-96	2358	1832
I337N-A	8	13	21	746	469	-100	778	436
O-22N-A	9	11	-6	108	298	226	448	-42
O-45N-A	4	40	-28	273	194	904	1138	-671
O-67N-A	33	137	21	3431	2023	1594	4433	1021
O-90N-A	115	-113	-50	-3699	2351	-840	2465	-3814
O112N-A	98	28	247	5936	4707	-2908	8293	2349
O135N-A	38	-40	65	520	1304	-1403	2369	-545
O157N-A	21	-1	9	165	685	-129	715	134
O180N-A	-1	4	6	219	32	-28	223	28
O202N-A	-26	-1	4	98	-739	-64	103	-744
O225N-A	-28	-50	48	-4	-841	-1303	946	-1791
O247N-A	-106	-272	-40	-6745	-5203	-3099	-2781	-9168
O292N-A	-60	-23	-187	-4565	-3171	2184	-1576	-6160
O315N-A	-11	28	-53	-528	-489	1081	572	-1589
O337N-A	-16	16	-2	326	-377	246	404	-454
O-C-N-L	-3	14	-8	140	-63	292	348	-271

Table A.15. In-plane moment loading, M_{ZN}, on nozzle

IN-PLANE MOMENT LOADING, MZN, ON NOZZLE (15000 IN-LB) W/R

	MICRO-STRAIN			STRESSES			PRIN STRESSES	
ROSETTE	GAGE1	GAGE2	GAGE3	TRANS	LONG	SHEAR	SIGMX	SIGMN
I-O-C-A	-232	-42	-2	-709	-7168	-526	-667	-7211
I-O-C-B	-154	-12	-10	-325	-4713	-24	-325	-4713
I-O-C-C	-88	3	5	277	-2561	-27	277	-2561
I-O-C-D	-44	10	9	469	-1177	4	469	-1177
I-O-C-E	-15	11	13	535	-285	-30	536	-287
I-O-C-F	25	2	0	12	740	29	741	11
I-O-C-G	24	-16	-10	-595	536	-69	540	-599
I-O-C-H	6	-14	-14	-623	-10	5	-10	-623
I-O-C-J	-1	-11	-11	-478	-182	1	-182	-478
I-O-C-K	-2	-9	-11	-435	-195	32	-191	-439
I-O-C-L	-7	-6	-7	-290	-298	11	-282	-305
O-O-C-A	228	104	121	4685	8231	-221	8245	4671
O-O-C-B	132	115	104	4658	5353	147	5383	4628
O-O-C-C	71	91	83	3741	3240	109	3764	3218
O-O-C-D	35	83	82	3591	2114	22	3591	2113
O-O-C-E	12	61	59	2630	1151	23	2630	1151
O-O-C-F	-14	30	32	1374	-6	-31	1375	-7
O-O-C-G	-5	12	15	599	39	-35	601	37
O-O-C-H	4	13	8	447	257	69	469	234
O-O-C-J	5	14	9	518	294	68	537	275
O-O-C-K	-3	8	11	418	32	-29	421	30
O-O-C-L	-9	6	8	323	-186	-32	325	-188

Table A.15 (continued)

IN-PLANE MOMENT LOADING, MZN, ON NOZZLE (15000 IN-LB) W/R

	MICRO-STRAIN			STRESSES			PRIN STRESSES	
ROSETTE	GAGE1	GAGE2	GAGE3	TRANS	LONG	SHEAR	SIGMX	SIGMN
I-O-N-B**	0	-9	-13	-487	-146	45	-140	-493
I-O-N-C	-84	3	11	387	-2389	-104	390	-2393
I-O-N-D	-41	9	15	579	-1058	-81	583	-1062
I-O-N-E	-10	9	12	478	-165	-44	481	-168
I-O-N-F	35	1	3	66	1076	-26	1077	66
I-O-N-G	40	-14	-13	-644	998	-7	998	-644
I-O-N-H	30	-18	-18	-838	647	3	647	-838
I-O-N-J	27	-21	-18	-887	549	-31	550	-888
I-O-N-K	28	-22	-12	-778	598	-133	611	-790
I-O-N-L	34	-9	16	132	1070	-331	1175	28
O-O-N-A	204	112	119	4858	7582	-102	7586	4854
O-O-N-B	128	99	105	4341	5152	-70	5158	4335
O-O-N-C	74	89	84	3723	3328	66	3733	3317
O-O-N-D	42	74	74	3195	2218	-2	3195	2218
O-O-N-E	18	59	62	2647	1333	-33	2648	1333
O-O-N-F	-3	32	35	1476	360	-37	1477	359
O-O-N-G	7	17	15	682	401	28	685	398
O-O-N-H	15	13	12	551	620	16	623	547
O-O-N-J	25	17	-45	-637	551	827	975	-1062
O-O-N-K	21	18	16	725	849	32	857	717

Table A.15 (continued)

IN-PLANE MOMENT LOADING, MZN, ON NOZZLE (15000 IN-LB) W/R

	MICRO-STRAIN			STRESSES			PRIN STRESSES	
ROSETTE	GAGE1	GAGE2	GAGE3	TRANS	LONG	SHEAR	SIGMX	SIGMN
I270C-A	7	70	-56	296	311	1677	1980	-1373
I270C-B	10	128	-114	296	379	3216	3553	-2879
I270C-C	12	151	-134	358	475	3803	4220	-3387
I270C-D	18	160	-151	174	580	4153	4535	-3780
I270C-E	5	172	-164	171	197	4474	4658	-4290
I270C-F	7	151	-156	-119	177	4078	4110	-4052
I270C-H	-2	62	-72	-218	-119	1795	1627	-1964
I270C-J	-2	3	-10	-148	-116	174	42	-307
I270C-K	-2	-9	11	50	-35	-259	270	-255
I270C-L	-2	-4	8	77	-46	-164	191	-159
I270C-M	-4	3	3	146	-81	-1	146	-81
O270C-A	-17	422	-430	-153	-560	11354	10999	-11712
O270C-B	-35	397	-410	-249	-1129	10752	10072	-11450
O270C-C	-30	361	-376	-282	-978	9823	9199	-10459
O270C-D	-21	335	-319	359	-518	8711	8643	-8802
O270C-E	-24	278	-298	-432	-845	7674	7038	-8315
O270C-F	2	151	-165	-323	-40	4212	4033	-4395
O270C-G	2	63	-73	-210	-2	1816	1714	-1925
O270C-H	2	12	-14	-40	63	347	362	-339
O270C-J	2	-17	19	45	76	-479	539	-419
O270C-K	1	-11	17	143	61	-378	482	-278
O270C-L	-1	0	5	102	14	-65	137	-20
O270C-M	4	3	3	121	152	1	152	121

Table A.15 (continued)

IN-PLANE MOMENT LOADING, MZN, ON NOZZLE (15000 IN-LB) W/R

	MICRO-STRAIN			STRESSES			PRIN STRESSES	
ROSETTE	GAGE1	GAGE2	GAGE3	TRANS	LONG	SHEAR	SIGMX	SIGMN
I270N-A	22	94	-36	1245	1046	1729	2878	-587
I270N-B	23	53	11	1370	1093	557	1805	658
I270N-C	20	5	59	1386	1026	-731	1959	453
I270N-D	30	-23	50	549	1061	-973	1811	-201
I270N-E	35	-75	137	1327	1439	-2832	4216	-1449
I270N-F	-27	-216	296	1794	-270	-6827	7667	-6142
I270N-G	-17	-221	266	1017	-212	-6495	6926	-6121
I270N-H	24	-184	120	-1426	305	-4059	3590	-4710
I270N-J	40	-36	52	311	1284	-1181	2075	-480
I270N-K	18	-14	20	105	561	-460	847	-181
I270N-L	10	6	18	514	464	-161	652	326
I270N-N	13	18	8	559	551	129	685	426
O270N-A	-13	510	-525	-325	-473	13795	13396	-14194
O270N-B	-13	512	-535	-497	-546	13949	13428	-14471
O270N-C**	-35	500	-567	-1420	-1468	14213	12770	-15657
O270N-D	14	478	-517	-873	161	13260	12915	-13626
O270N-E	1	451	-473	-479	-108	12304	12012	-12599
O270N-F	0	237	-253	-334	-102	6531	6314	-6750
O270N-G	10	60	-63	-66	266	1646	1754	-1554
O270N-H	10	-43	47	70	335	-1196	1406	-1001
O270N-J	10	-107	108	18	298	-2857	3018	-2702
O270N-K	-5	-95	90	-117	-186	-2462	2311	-2613
O270N-L	-3	-53	49	-90	-118	-1363	1259	-1467
O270N-N	-5	-17	15	-53	-177	-426	316	-545

Table A.15 (continued)

IN-PLANE MOMENT LOADING, MZN, ON NOZZLE (15000 IN-LB) W/R

	MICRO-STRAIN			STRESSES			PRIN STRESSES	
ROSETTE	GAGE1	GAGE2	GAGE3	TRANS	LONG	SHEAR	SIGMX	SIGMN
I-0-C-*	-195	4	-37	-515	-5999	537	-463	-6051
I-22C-A	-227	-52	-55	-2091	-7431	38	-2091	-7431
I-45C-A	-217	-42	-11	-933	-6785	-418	-903	-6814
I-67C-A	-85	152	282	9637	327	-1723	9946	19
I-90C-A	28	-98	98	-21	836	-2609	3052	-2237
I112C-A	79	-257	-126	-8506	-193	-1741	157	-8855
I135C-A	0	3	51	1205	362	-639	1549	18
I157C-A	232	57	37	1809	7507	263	7519	1797
I202C-A	233	39	50	1714	7510	-144	7514	1711
I225C-A	251	70	19	1681	8022	685	8095	1608
I247C-A	88	-161	-237	-8850	-7	1011	107	-8964
I292C-A	-110	238	145	8534	-731	1241	8698	-895
I315C-A	-244	-25	-50	-1391	-7747	328	-1374	-7764
I337C-A	-234	-50	-45	-1837	-7583	-64	-1836	-7584
I180C-L	-9	9	8	397	-147	10	397	-147
O-22C-A	228	94	119	4440	8173	-329	8202	4412
O-45C-A	254	140	150	6074	9444	-133	9449	6069
O-67C-A	222	230	308	11584	10135	-1045	12131	9588
O-90C-A	-13	-483	435	-1044	-698	-12238	11368	-13110
O112C-A	-208	-203	-285	-10502	-9376	1100	-8704	-11175
O135C-A	-230	-147	-127	-5754	-8618	-267	-5729	-8643
O157C-A	-245	-125	-108	-4839	-8792	-232	-4825	-8806
O180C-A	-208	-125	-119	-5138	-7782	-73	-5136	-7784
O202C-A	-214	-108	-111	-4577	-7789	33	-4577	-7790
O225C-A	-267	-131	-152	-5941	-9804	278	-5921	-9824
O247C-A	-223	-206	-289	-10626	-9880	1112	-9080	-11426
O292C-A	241	269	244	11022	10542	328	11189	10376
O315C-A	263	164	146	6517	9834	241	9851	6500
O337C-A	234	107	100	4309	8304	95	8307	4307
O180C-L	10	-9	-9	-420	164	-1	164	-420

Table A.15 (continued)

IN-PLANE MOMENT LOADING, MZN, ON NOZZLE (15000 IN-LB) W/R

	MICRO-STRAIN			STRESSES			PRIN STRESSES	
ROSETTE	GAGE1	GAGE2	GAGE3	TRANS	LONG	SHEAR	SIGMX	SIGMN
I-0-N-*	-212	-4	-7	8	-6348	39	8	-6348
I-22N-A	28	25	-66	-935	551	1215	1232	-1616
I-45N-A	-145	44	-211	-3490	-5384	3358	-910	-7964
I-67N-A	27	327	-98	4997	2320	5668	9482	-2165
I-90N-A	25	-73	83	192	814	-2077	2603	-1597
I112N-A	-34	138	-299	-3498	-2057	5812	3079	-8634
I135N-A	174	218	-56	3367	6227	3656	8723	871
I157N-A	191	138	-30	2171	6394	2235	7358	1208
I180N-A	268	24	62	1588	8518	-502	8554	1552
I202N-A	195	-12	149	2798	6703	-2155	7658	1843
I225N-A	120	-29	245	4602	4990	-3650	8451	1141
I247N-A	-12	-303	86	-4745	-1776	-5181	2129	-8650
I292N-A	56	-120	307	4048	2908	-5680	9186	-2231
I315N-A	-103	-201	52	-3172	-4041	-3375	-204	-7009
I337N-A	-175	-126	18	-2181	-5915	-1907	-1379	-6716
O-22N-A	202	158	73	4840	7506	1131	7921	4425
O-45N-A	223	238	107	7326	8885	1743	10014	6196
O-67N-A	326	142	164	6373	11683	-292	11699	6357
O-90N-A	-33	-526	476	-1066	-1303	-13344	12160	-14529
O112N-A	-344	-181	-180	-7562	-12583	-13	-7562	-12583
O135N-A	-232	-119	-266	-8212	-9433	1956	-6773	-10871
O157N-A	-205	-85	-146	-4844	-7611	819	-4619	-7836
O180N-A	-233	-139	-140	-5892	-8753	10	-5892	-8753
O202N-A	-208	-151	-97	-5235	-7822	-720	-5047	-8009
O225N-A	-213	-230	-105	-7113	-8527	-1661	-6015	-9626
O247N-A	-347	-188	-168	-7443	-12646	-264	-7429	-12659
O292N-A	335	215	203	8809	12694	160	12700	8802
O315N-A	209	105	238	7317	8457	-1775	9751	6022
O337N-A	202	79	149	4793	7488	-941	7784	4497
C-0-N-L	29	10	11	440	1012	-8	1012	440

Table A.16. Axial force loading, F_{YN}, on nozzle

AXIAL FORCE LOADING, FYN, CN NOZZLE (4000 LB) W/R

	MICRO-STRAIN			STRESSES			PRIN STRESSES	
ROSETTE	GAGE1	GAGE2	GAGE3	TRANS	LONG	SHEAR	SIGMX	SIGMN
I-0-C-A	-227	-90	-71	-3294	-7810	-261	-3279	-7825
I-0-C-B	-171	-61	-54	-2333	-5834	-98	-2331	-5837
I-0-C-C	-120	-39	-34	-1477	-4036	-65	-1476	-4037
I-0-C-D	-81	-22	-22	-874	-2681	0	-874	-2681
I-0-C-E	-51	-17	-12	-586	-1713	-65	-582	-1717
I-0-C-F	0	-10	-5	-317	-92	-65	-75	-335
I-0-C-G	15	-17	-12	-655	248	-65	253	-660
I-0-C-H	5	-17	-17	-761	-78	0	-78	-761
I-0-C-J	3	-15	-10	-543	-87	-66	-78	-552
I-0-C-K	0	-10	-5	-323	-94	-66	-76	-340
I-0-C-L	3	0	3	55	93	-33	113	36
O-0-C-A	228	44	69	2226	7497	-326	7517	2206
O-0-C-B	152	74	71	3009	5457	33	5457	3009
O-0-C-C	100	69	66	2852	3868	32	3869	2851
O-0-C-D	61	64	73	2947	2722	-130	3006	2663
O-0-C-E	37	54	61	2491	1852	-97	2505	1837
O-0-C-F	-2	32	39	1566	399	-98	1574	391
O-0-C-G	-10	15	20	768	-60	-65	773	-65
O-0-C-H	-2	7	15	490	78	-98	512	56
O-0-C-J	0	3	10	273	86	-98	315	44
O-0-C-K	0	0	5	110	37	-65	148	-1
O-0-C-L	3	-7	-5	-268	-4	-33	0	-272

Table A.16 (continued)

AXIAL FORCE LOADING, FYN, CN NOZZLE (4000 LB) W/R

	MICRO-STRAIN			STRESSES			PRIN STRESSES	
ROSETTE	GAGE1	GAGE2	GAGE3	TRANS	LONG	SHEAR	SIGMX	SIGMN
I-C-N-B**	0	-61	-66	-2782	-835	64	-832	-2784
I-C-N-C	-120	-39	-39	-1578	-4060	1	-1578	-4060
I-O-N-D	-83	-22	-24	-916	-2763	34	-916	-2763
I-C-N-E	-56	-19	-24	-891	-1945	67	-887	-1949
I-O-N-F	-10	-10	-19	-626	-475	130	-400	-701
I-C-N-G	8	-19	-29	-1075	-95	131	-78	-1092
I-O-N-H	0	-27	-37	-1391	-409	130	-393	-1407
I-C-N-J	-17	-32	-41	-1584	-980	130	-953	-1611
I-O-N-K	-19	-31	-37	-1475	-1022	70	-1012	-1486
I-O-N-L**	-37	-27	152	2785	-264	-2376	4084	-1562
O-C-N-A	210	61	76	2781	7142	-195	7150	2772
O-C-N-B	147	66	76	2958	5290	-130	5297	2951
O-O-N-C	101	72	72	3035	3946	0	3946	3035
O-C-N-D	64	67	72	2968	2816	-66	2993	2792
O-O-N-E	37	57	64	2618	1897	-99	2631	1884
O-O-N-F	-5	42	47	1960	443	-66	1962	441
O-O-N-G	-12	27	32	1319	30	-66	1322	27
O-C-N-H	-10	22	27	1102	41	-66	1106	36
O-O-N-J**	-12	22	-31	-187	-423	716	420	-1031
O-O-N-K	-22	22	30	1164	-312	-99	1171	-318

Table A.16 (continued)

AXIAL FORCE LOADING, FYN, CN NOZZLE (4000 LB) W/B

	MICRO-STRAIN			STRESSES			PRIN STRESSES	
ROSETTE	GAGE1	GAGE2	GAGE3	TRANS	LONG	SHEAR	SIGMX	SIGMN
I270C-A	210	276	212	10500	9440	854	10975	8965
I270C-B	261	313	215	11312	11237	1314	12589	9960
I270C-C	355	264	153	8768	13284	1478	13724	8327
I270C-D	377	227	111	7011	13421	1544	13774	6658
I270C-E	383	202	84	5856	13252	1567	13570	5537
I270C-F	381	81	10	1592	11901	948	11987	1506
I270C-H	253	-66	-51	-2847	6736	-196	6740	-2851
I270C-J	89	-99	-65	-3720	1551	-451	1589	-3759
I270C-K	-29	-95	-68	-3561	-1937	-360	-1861	-3638
I270C-L	-161	-61	-56	-2385	-5551	-65	-2384	-5553
I270C-M	-203	-53	-46	-1966	-6680	-98	-1964	-6682
O270C-A	-180	-63	-425	-10523	-8572	4812	-4637	-14458
O270C-B	-232	-73	-432	-10842	-10203	4781	-5731	-15314
O270C-C	-259	-95	-425	-11135	-11098	4390	-6727	-15506
O270C-D	-273	-110	-390	-10688	-11401	3738	-7290	-14800
O270C-E	-288	-141	-393	-11423	-12061	3349	-8378	-15106
O270C-F	-289	-185	-345	-11321	-12069	2137	-9525	-13864
O270C-G	-236	-202	-279	-10312	-10162	1036	-9198	-11276
O270C-H	-175	-180	-236	-8937	-7928	745	-7532	-9332
O270C-J	-39	-131	-146	-6041	-2976	194	-2963	-6053
O270C-K	54	-58	-80	-3100	676	291	698	-3122
O270C-L	161	29	15	790	5052	194	5061	781
O270C-M	185	58	56	2311	6238	32	6238	2310

Table A.16 (continued)

AXIAL FORCE LOADING, FYN, CN NOZZLE (4000 LB) W/R

	MICRO-STRAIN			STRESSES			PRIN STRESSES	
ROSETTE	GAGE1	GAGE2	GAGE3	TRANS	LONG	SHEAR	SIGMX	SIGMN
I270N-A	267	477	401	18993	13696	1008	19178	13511
I270N-B	218	535	484	22159	13179	683	22210	13127
I270N-C	164	518	596	24316	12214	-1040	24405	12125
I270N-D	164	613	565	25709	12632	650	25741	12599
I270N-E	162	626	726	29526	13704	-1334	29637	13592
I270N-F	22	808	1002	39747	12584	-2593	39992	12339
I270N-G	157	697	825	33265	14702	-1706	33421	14546
I270N-H	234	512	500	21977	13606	165	21981	13602
I270N-J	271	268	330	12847	11975	-821	13340	11482
I270N-K	221	185	212	8462	9182	-361	9332	8312
I270N-L	184	121	121	5095	7064	0	7064	5095
I270N-N	153	86	84	3560	5643	33	5644	3559
O270N-A	-88	29	-425	-8589	-5210	6049	-619	-13181
O270N-B	-34	44	-432	-8487	-3567	6342	775	-12830
O270N-C	-12	54	-434	-8351	-2868	6505	1449	-12668
O270N-D	49	34	-425	-8633	-1122	6115	2299	-12053
O270N-E	64	22	-420	-8810	-735	5888	2367	-11912
O270N-F	115	-195	-447	-14233	-825	3350	-35	-15023
O270N-G	171	-349	-442	-17565	-140	1236	-53	-17652
O270N-H	222	-398	-395	-17676	1363	-33	1363	-17676
O270N-J	270	-299	-243	-12219	4440	-746	4474	-12252
O270N-K	263	-209	-122	-7557	5620	-1167	5723	-7659
O270N-L	190	-100	-32	-3093	4770	-908	4874	-3196
O270N-N	146	-19	-12	-851	4129	-97	4130	-853

Table A.16 (continued)

AXIAL FORCE LOADING, FYN, CN NOZZLE (4000 LB) W/R

	MICRO-STRAIN			STRESSES			PRIN STRESSES	
ROSETTE	GAGE1	GAGE2	GAGE3	TRANS	LONG	SHEAR	SIGMX	SIGMN
I-0-C-*	-159	-66	-88	-3208	-5730	293	-3175	-5764
I-22C-A	-227	-110	-117	-4740	-8241	101	-4737	-8244
I-45C-A	-247	-147	-149	-6228	-9275	32	-6227	-9275
I-67C-A	-430	-298	-66	-7528	-15168	-3098	-6430	-16266
I-90C-A	269	294	348	13805	12222	-717	14081	11945
I112C-A	-345	-406	-399	-17299	-15531	-96	-15525	-17304
I135C-A	0	-166	-51	-4774	-1432	-1533	-835	-5371
I157C-A	-205	-32	25	75	-6133	-750	165	-6222
I202C-A	-188	27	-29	165	-5605	753	262	-5702
I225C-A	-154	-66	-171	-5051	-6142	1405	-4089	-7103
I247C-A	-441	-466	-407	-18686	-18836	-784	-17974	-19549
I292C-A	-458	-95	-340	-9074	-16469	3267	-7837	-17706
I315C-A	-247	-159	-154	-6618	-9407	-66	-6616	-9409
I337C-A	-216	-110	-100	-4390	-7783	-131	-4385	-7788
I180C-L	-111	-20	-32	-1002	-3640	162	-992	-3650
O-22C-A	238	58	51	2149	7793	96	7794	2147
O-45C-A	301	71	25	1770	9561	619	9610	1721
O-67C-A	629	367	201	11786	22400	2216	22844	11341
O-90C-A	-210	-443	-51	-10625	-9495	-5215	-4814	-15306
O112C-A	470	162	34	3789	15230	1695	15476	3543
O135C-A	179	32	-15	184	5415	620	5488	112
O157C-A	203	179	86	5587	7771	1239	8330	5028
O180C-A	171	181	188	7934	7521	-97	7955	7499
O202C-A	159	74	157	4884	6240	-1108	6861	4263
O225C-A	186	-17	32	123	5612	-652	5688	47
O247C-A	547	125	39	3002	17322	1139	17412	2912
O292C-A	643	176	332	10465	22417	-2083	22769	10113
O315C-A	276	15	71	1580	8761	-749	8838	1503
O337C-A	222	20	54	1371	7085	-456	7121	1335
O180C-L	-124	10	15	677	-3532	-65	678	-3533

Table A.16 (continued)

AXIAL FORCE LOADING, FYN, CN NOZZLE (4000 LB) W/R

	MICRO-STRAIN			STRESSES			PRIN STRESSES	
ROSETTE	GAGE1	GAGE2	GAGE3	TRANS	LONG	SHEAR	SIGMX	SIGMN
I-0-N-*	-181	-76	-76	-3132	-6378	-1	-3132	-6378
I-22N-A	150	34	-45	-390	4385	1050	4606	-610
I-45N-A	-196	-118	-250	-7864	-8226	1764	-6272	-9818
I-67N-A	-245	-100	-370	-10069	-10373	3591	-6627	-13815
I-90N-A	167	343	400	16140	9846	-751	16228	9758
I112N-A	-299	-387	-409	-17176	-14124	294	-14096	-17204
I135N-A	-145	-228	-76	-6518	-6293	-2025	-4378	-8434
I157N-A	-164	-88	91	236	-4855	-2385	1179	-5797
I180N-A	-252	76	25	2488	-6827	686	2539	-6877
I202N-A	-159	71	-96	-360	-4886	2222	548	-5794
I225N-A	-101	-106	-205	-6720	-5056	1312	-4334	-7442
I247N-A	-311	-422	-397	-17645	-14613	-328	-14578	-17680
I292N-A	-215	-350	-128	-10274	-9521	-2955	-6919	-12876
I315N-A	-165	-229	-106	-7192	-7116	-1641	-5512	-8795
I337N-A	-178	-141	-74	-4525	-6688	-886	-4209	-7005
O-22N-A	195	158	3	3321	6840	2075	7801	2360
O-45N-A	178	285	3	6120	7170	3761	10443	2847
O-67N-A	304	516	200	15395	13748	4215	18866	10277
O-90N-A	-175	-421	0	-9054	-7968	-5610	-2875	-14147
O112N-A	123	86	493	12593	7460	-5420	16024	4029
O135N-A	174	-17	201	3861	6391	-2907	8296	1956
O157N-A	199	128	118	5180	7522	130	7529	5173
O180N-A	197	199	204	8641	8490	-67	8666	8464
O202N-A	192	113	111	4720	7167	25	7167	4720
O225N-A	143	162	-27	2821	5125	2515	6739	1207
O247N-A	145	498	98	12945	8232	5325	16411	4766
O292N-A	305	204	550	16229	14005	-4605	19855	10380
O315N-A	136	-5	264	5544	5734	-3579	9220	2059
O337N-A	180	-7	131	2519	6157	-1841	6926	1750
O-0-N-L	-42	17	27	1024	-946	-131	1033	-955

ORNL-5021
NRC-1, -5

INTERNAL DISTRIBUTION

1. R. L. Battiste
2. M. Bender
3. J. J. Blass
4-6. S. E. Bolt
7. R. H. Bryan
8-11. J. W. Bryson
12. J. H. Butler
13. J. P. Callahan
14. C. J. Claffey
15. J. A. Clinard
16. C. W. Collins
17-18. J. M. Corum
19. W. B. Cottrell
20. J. S. Crowell
21. F. L. Culler
22. R. W. Derby
23. W. G. Dodge
24. G. G. Fee
25. M. H. Fontana
26. W. R. Gall
27. R. H. Gallagher (consultant)
28. M. J. Goglia
29-30. W. L. Greenstreet
31-35. R. C. Gwaltney
36. W. O. Harms
37. R. F. Hibbs
38. H. W. Hoffman
39. P. R. Kasten
40. K. C. Liu
41. R. N. Lyon
42. R. E. MacPherson
43. W. J. McAfee
44. W. J. McCarthy, Jr.
45. H. C. McCurdy
46. J. G. Merkle
47-61. S. E. Moore
62. F. M. O'Hara (consultant)
63. T. W. Pickel
64. H. Postma
65. C. E. Pugh
66. M. Richardson
67. D. N. Robinson
68. R. A. Schmidt
69. M. R. Sheldon
70. J. E. Smith
71. I. Spiewak
72. W. C. T. Stoddart
73. J. J. Taylor
74. D. B. Trauger
75. G. D. Whitman
76. W. J. Wilcox
77. G. T. Yahr
78. ORNL Patent Office
79-81. Central Research Library
82. Document Reference Section
83-88. Laboratory Records Department
89. Laboratory Records, ORNL RC

Subcontractors

90-91. E. C. Rodabaugh, Battelle-Columbus Laboratories, Columbus, OH 43201

EXTERNAL DISTRIBUTION

92-93. Director, Division of Reactor Research and Development, ERDA, Washington, DC 20545
94-101. Director, Office of Nuclear Regulatory Research, NRC, Washington, DC 20555
102. Director, Reactor Division, ERDA, ORO
103. Research and Technical Support Division, ERDA, ORO
104-184. Design Criteria for Piping and Nozzles Program Distribution
185-444. Given distribution as shown under categories NRC-1 and NRC-5 (25 copies – NTIS)

☆ U.S. GOVERNMENT PRINTING OFFICE: 1975-748-189/108